Seismological Studies of Upper-Crustal Structure in the Vicinity of the Girvan-Ballantrae Area, SW Scotland.

By

DHIA AL-MANSOURI

Thesis submitted in fulfilment of the degree of Doctor of Philosophy (by research) in the Faculty of Science, Department of Geology, University of Glasgow.

January, 1986.

To my wife NIDHAL and daughters NOOR & FARAH,

without whose support, love and encouragement

this work would not have been possible.

C O N T E N T S

LIST OF FIGURES

LIST OF TABLES

ACKNOWLEDGEMENTS

My first acknowledgement has to be to my supervisors, Drs. J. Hall and D.W. Powell for their meticulous interest, guidance, advice and assistance during the course of this study. Their constructive criticism of the manuscript and that of Dr J. Doody is profoundly appreciated.

I wish to thank Professors D. Bowes and B. Leake for providing facilities to undertake this research.

I am grateful also to Dr. J. Floyd for providing the greywacke samples and Dr. B. J. Bluck for useful comments at various stages of the work. Dr. C.M. Graham of the Experimental Petrology Unit, University of Edinburgh was very helpful in the use of high-pressure system.

Successful completion of this thesis would not be possible without the assistance of Messrs. R. Morrison, R.T. Cumberland, D. MacLean, K. Roberts and E. Speirs. The enthusiastic assistance from Mr. G. Gordon; his willing help in the field, equipment improvement and kind suggestions is deeply appreciated.

I am grateful to Messrs. K. Davidson, P. Tsoumakos and Miss. E. Syba for their useful and enthusiastic discussions.

Mr Goodwin; the Lt. Commander of HMS. Neptune (Clyde Submarine Base), receives my thanks for punctual firing of the Portobello marine shot.

I thank the thirty colleagues who took part in recording the Royal Navy shot, especially L. Fernandes, P. Nicholson, P. Bradshaw, R. Hanna and E. Elias.

My thanks are also due to Messrs. J. Wilson (Manager of Hillhouse Quarry), J. McBain, (Benbain NCB site manager), the manager of the Dalmellington Forestry Commission and all the landowners for their assistance and patience in granting access to their property.

I thank my mother and all members of my family for their support throughout the period of my study.

I acknowledge with thanks, receipt of a Research Studentship from the Ministry of Higher Education and Scientific Research - IRAQ.

SUMMARY

The geology of the Midland Valley and the Southern Uplands is outlined with special reference to the Ballantrae ophiolite complex which crops out close to the boundary between them. In this study, several seismic refraction profiles, with different azimuths, were recorded across the complex and the surrounding regions. These lines constitute a network, covering the south-western part of Scotland, for the investigation of the areal extension of the complex at depth.

Laboratory velocity measurements were carried out, at confining pressures of up to 200 bars, upon samples of the Ballantrae complex and greywackes of the Northern Belt of the Southern Uplands. Serpentinite is found to have the lowest velocity in the Ballantrae complex (circa 4.0 km/sec) and gabbro has velocities as high as 6.3 km/sec at 200 bars. At the same pressure, the greywackes have an average velocity of 5.7 km/sec. These determinations were used to constrain the interpretation of near surface velocities in the study area. High-pressure velocity measurements (up to 5 kbar) on two greywacke samples suggest that some mafic greywackes could have velocities of $>$6.0 km/sec. The high velocities, previously interpreted as crystalline basement, could be a characteristic of the Northern Belt mafic greywackes.

The velocity-depth structure of the Ballantrae complex has been inferred from measurements directly on the complex by applying time-term and Wiechert-Herglotz-Bateman (WHB) analysis. The seismic structure below the complex is similar to that of "basement" incorporated in ray-tracing modelling on the wider net of profiles. This implies that the basement may be the same below the complex as around it. Basement is shallowest (1.7 - 2.0 km) under the Ballantrae complex and the Craighead Inlier, with P-wave velocity of 6.0 km/sec, which increases

rapidly to 6·35 - 6·40 km/sec at a depth of 6 km. It extends from the Midland Valley underneath the Northern Belt of the Southern Uplands at about 1·8 - 2·3 km and deepens with an unknown dip under the Central and Southern Belts, giving way to thicker overlying Lower Palaeozoic sediments.

No conclusive statement on the thickness or extent of the complex can be made. However, a study of recorded S-waves yielded a Poisson's Ratio of 0·31. Combining this result with two-dimensional gravity modelling across the area suggests that the gabbroic components of the Ballantrae complex constitute the basement in the area covering a triangle between Troon (N), Loch Doon (SE) and Portobello (SW). These gabbroic rocks are predicted to be partially hydrated on the basis of a P-wave volocity of only 6·35 - 6·40 km/sec at 6 km depth. The basement may be regionally extensive though the correlation of the seismic refraction line (Colmonell line) where the S-wave velocity is determined with an aeromagnetic anomaly might suggest its restriction to a strip parallel to the Southern Uplands Fault.

Travel-time delays of about 0·2 sec are associated with the Southern Uplands, Kerse Loch and Stinchar Faults. The geological and geophysical possibilities that can generate such delays are reviewed. From reversed recording on one of the profiles, the delay is attributed to vertical zones of low velocity rocks in the fault zone, postulated to be either serpentinite or sheared, fractured rocks.

CHAPTER ONE

Introduction (Geology of the Study Area and Previous Geophysical Work)

1.1 Introduction

The study area is the south-western parts of both the Midland Valley and the Southern Uplands of Scotland (fig 1.1).

The Midland Valley lies between two Caledonian fold belts: the Southern Highlands to the north and the Southern Uplands to the south. The bounding faults, the Highland Boundary and the Southern Uplands Faults are typical of old faults reactivated through a younger cover.

The earliest movement of the Southern Uplands fault may have been Old Red Sandstone or Silurian at the earliest and it is made up of three discontinuous segments, slightly offset from one another. The south-west segment forms the Glen App Fault, the central sector is the Southern Uplands Fault, and in the north-east (beyond fig 1.1) lies the Lammermuir Fault. These fractures form the southern margin of the Midland Valley and the general impression from the Upper Palaeozoic rocks to the north is of downthrow in that direction.

The Midland Valley outcrop comprises rocks mainly of Upper Palaeozoic age (table 1.1) which are now disposed in a rather complex syncline, subjected to much faulting.

The Southern Uplands (mainly Lower Palaeozoic outcrop) contains mainly greywacke, siltstone and shale of Upper Ordovician (Nb) and Silurian age (Cb & Sb) which rest on the Arenig foundation of spilite, black-shale and radiolarian chert. All these rocks are

Fig 1.1 Geological Map of S.W Scotland

Locations: A: Ayr, B: Ballantrae, Ba: Barr, BH: Burrow Head, C: Colmonell, CB: (offshore): Culzean Bay, CB: Central Belt, CC: Cairnsmore of Carspnairn, CF: Cairnsmore of Fleet, CG: Criffel granite, Cn: Craighead Inlier, D: Dalmellington, Dh: Distinkhorn, Dy: Dailly, FC: Firth of Clyde, G: Girvan, HA: Heads of Ayr, LG: Loch Doon Granite, Ln: Lesmahagow Inlier, LR: Loch Ryan, M: Muirkirk, Mb: Maybole, Md: Maiden, Mn: Mauchline, N: New Cumnock, NB: Northern Belt, P: Patna, Pb: Portobello, S: Stranraer, SB: Southern Belt, SF: Solway Firth, SG: Spango Grano-diorite, Sq: Sanquhar, St: Straiton, T:Troon, Tb: Turnberry.

Faults: GAF: Glen App Fault, KF: Kingledorse Fault, KLF: Kerse Loch Fault, SF: Stinchar Fault, StF: Straiton Fault, SUF: Southern Uplands Fault.

Key Abbreviations: CARB: Carboniferous, Dev. Intrus: Devonian Intrusions, L.Palz: Lower Palaeozoic, Lst: Limestone, O.R.S: Old Red Sandstone.

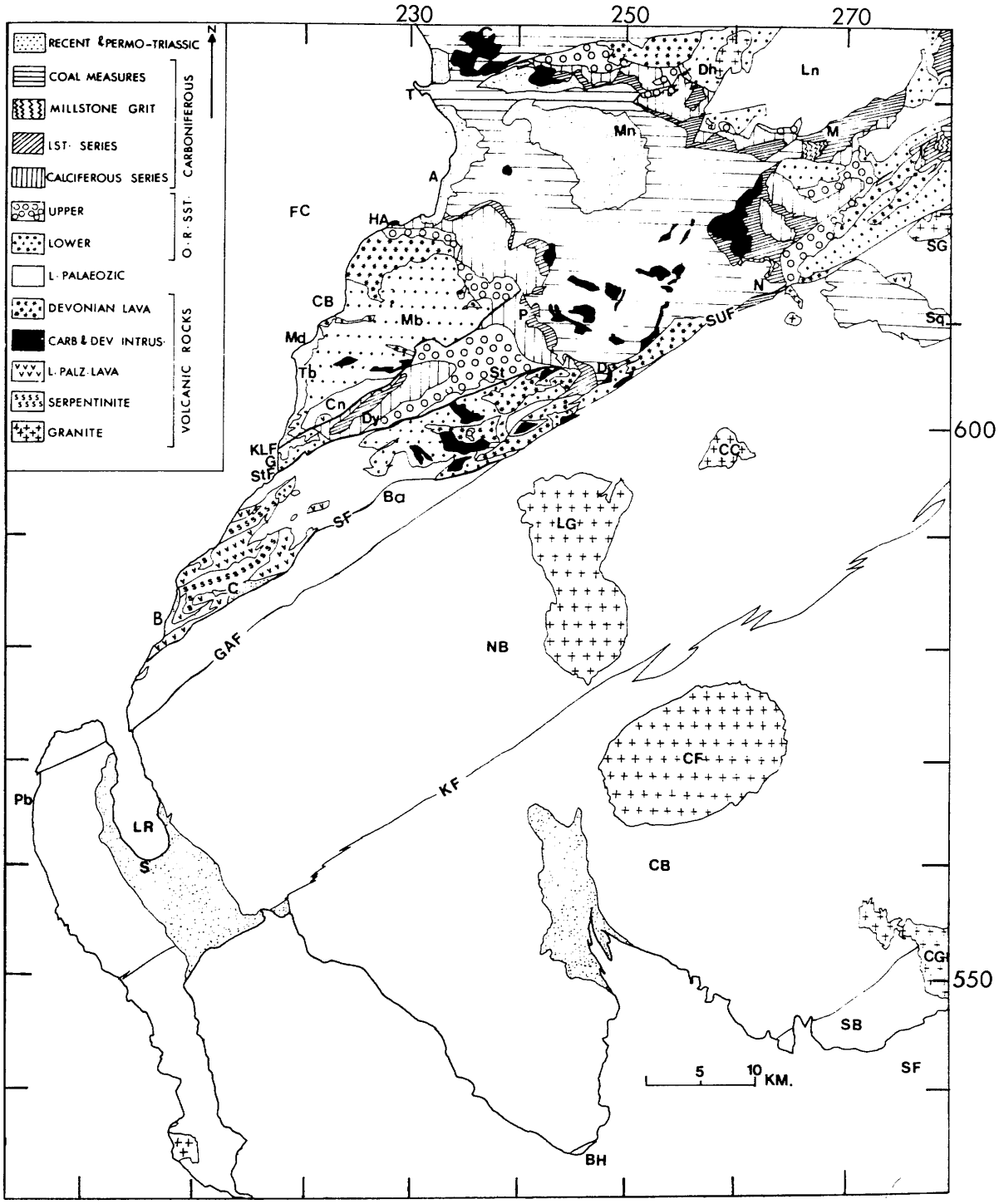

Fig 1.1 Geological Map of S.W Scotland.

System	Main Exposures: Midland Valley	Main Exposures: Southern Uplands	Lithology	Maximum Thickness (m).	Intrusive Igneous Rocks	Contemporaneous Igneous Rocks	Main Structural Events
Permo-Triassic	Mauchline basin	Stranraer basin	Sandstone, basal volcanics	≈750	Volcanic rocks and plugs.	Lavas & Tuffs.	Steep faulting in the Midland Valley.
Carboniferous	Most of the Midland Valley	Sanquhar	Sandstone, mudstone, siltstone, coals, marine limestone, ironstone, seatclays, shales, cementstone, cornstone, lavas and tuffs.	1,000 - 2,000 at any one place in the Midland Valley. 3,500 in the Southern Uplands (Sanquhar).	Alkaline basic sills (some of basaltic type), dykes and volcanic necks.	Basalt lava.	Development of narrow graben basins defined by faults.
Upper Old Red Sandstone	Narrow belt (Heads of Ayr to Straiton)	Narrow irregular belt from the N2 to Solway Firth	Conglomerate, sandstone, marls and cornstone.	1,000 in the Midland Valley (no more than 150m in study area). 200 in the Southern Uplands, east of the study area.			Faulting and relatively gentle folding with uplift in the Midland Valley.
Lower Old Red Sandstone	Southern margin	Two N-NW trending belts	Conglomerates, sandstone, mudstone, breccia, shales, siltstone, agglomerates, lavas and basalts. Mainly greywacke - conglomerate in the Southern Uplands.	9,000 ? (no more than 2,000 in the study area). 600 in the Southern Uplands (east of the study area).	Volcanic sills, necks and major plutons, (eg. Loch Doon granite in the Southern Uplands and Distinkhorn in the Midland Valley).	Andesitic lava.	Contemporaneous normal faults giving rise to fault scarps and rift valleys.
Silurian	Several inliers (eg. Craighead, Lesmahagow)	Most of the Central Belt	Greywackes, shales, mudstone, red sandstone, conglomerate, thin limestone and cherts.	2,200?in the Midland Valley (1,200? at Girvan - Craighead). Unknown in the Southern Uplands	Serpentine, Gabbro, dyke or sheet complex.	Spilitic lavas and tuffs.	Accretion of the Southern Uplands, folding, thrusting, wrench faulting.
Ordovician	Girvan - Ballantrae area	Northern belt and most of the Southern Uplands		?			Emplacement of Ballantrae Ophiolite.

Table 1.1 Geological succession, rock type,thicknesses and main structural events.

complexely folded and faulted but have suffered little metamorphism, and McKerrow et al (1977) have proposed that they are part of an accretionary prism formed on the landward edge of a northerly subducting plate.

On the southern margin of the Midland Valley, the basic and ultrabasic rocks of the Ballantrae Ophiolite Complex are the Arenig foundation and represent remnants of an older obducted plate. They form the basement to the northward overstepping Caradocian sediments of the Girvan district. The complex is one of the important tectonic elements in understanding the Palaeogeography of the area, and whether it is local or has lateral extensions under the Northern Belt of the Southern Uplands remains a moot point.

The geological succession in the study area is discussed in this chapter, along with a summary of previous geophysical interpretations.

1.2 Geological Succession

See table (1.1).

Aspects of the geology which bear on the problem studied in this thesis, are outlined in this section in a stratigraphical manner.

1.2.1 Permian

The Permo-Triassic rocks of Scotland were formed at a time of major regression (withdrawal of Carboniferous sea to the south). They are found in isolated and largely unfossilferous outcrops.

In the Midland Valley, these are represented by the Ballantrae Breccias (small outcrop on shore), and about 700m of sandstone and basalt are lying in the

Mauchline Basin, north-east of the area studied.

In the Southern Uplands, geophysical work indicates that the Stranraer Basin closes northwards, and is asymmetrical with thickness of up to 1·2 km of breccia and sandstone, at the south-eastern margin of Loch Ryan (Lovell in Craig 1983).

In the Firth of Clyde, sediments of this age cover most, or possibly all of the western part, and also much of the eastern half where it oversteps Upper Palaeozoic rocks to rest on Lower Palaeozoic, south-west from Girvan (McLean and Deegan 1978).

1.2.2 Carboniferous

Faults like the Kerse Loch Fault are very well known for their control on Carboniferous sedimentation. Rocks of this age occupy the greater part of the Midland Valley with fewer outcrops in the Southern Uplands. The subdivisions are:

Coal Measures mainly coal, shale, sandstone and seat-clay. MacGregor (1960), redesignated this group into Upper and Lower and Middle Coal Measures. At most places the coal-bearing sequence follows conformably on Passage Group. Few data are available on the variation in thickness of the Lower and Middle Measures, with a maximum thickness of 420m occuring in South Ayrshire near Dalmellington. The Upper Coal Measures are thickest in Mauchline Basin (up to 550m).

Across the Southern Uplands Fault in Sanquhar, Upper Carboniferous rocks overlie Ordovocian greywakes and are folded into a gentle syncline with a NW-SE trend. The total thickness of the Carboniferous rocks known is approximately 500m.

Passage Group in Ayrshire, it is complicated by volcanism. North-west of the Kerse Loch Fault, the volcanic rocks consist mainly of lavas reaching a maximum thickness of over 150m at Troon. The lavas are overlapped by Lower Coal Measures and rest on Upper Limestone strata (Richey et al 1930).

South-east of the Kerse Loch Fault the lavas give way to a sedimentary sequence 128m thick, originally termed "Millstone Grit" by Eyles et al (1949). The total thickness of sediments ranges from 125m at Dalmellington, to a few metres at Troon.

Upper Limestone Group it contains a number of thick beds of shale, four to eight limestones and a few thin coals. It ranges in thickness from 200m at Patna in south Ayrshire, to 90m at Dalry (19 km north of Troon) in the north.

A thin layer, about 10m, of rocks presumed to belong to this group is present at the south-east of the Sanquhar Basin. This basin suggests southerly downthrow at this part of the Southern Uplands Fault.

Limestone Coal Group consists of alternating sandstones and shales, with subordinate coals and ironstones. It shows signs of attenuation towards the west margin of the Midland Valley. It is 77m thick at Machrihanish in Kintyre, and less than 90m in Dailly (vertical section in Limestone Coal Group, p265, in Craig 1983).

Lower Limestone Coal Group mainly shales and limestones. In Ayrshire it is no where more than 30m thick, with abrupt variations across lines of major north-easterly disturbance.

In the Heads of Ayr, a vent of pyroclastic rocks with ultrabasic fragments is emplaced in gently-

dipping sediments at the end of Calciferous Sandstone times. It is the deeply eroded remnant of a volcano which was in existence at that time (Whyte 1961). From Iherzolite fragments and peridotite xenoliths in the vent, Whyte indicated the presence of an ultrabasic layer at depth, both during the volcanism and the later period of intrusion.

Calciferous Sandstone Measures mainly shales and argillaceous dolomite. In Ayrshire, the measures are thickest in the south-west around Dailly and Straiton; where they amount to over 560m in a section recorded by Freshney (1961, fig 1.2).

The base of the measures is indistinguishable from the underlying Upper Old Red Sandstone sediments, therefore, Carboniferous and Upper Old Red rocks are considered as one seismic unit in this study.

1.2.3 Upper Old Red Sandstone

It consists of sandstone, marls, conglomerates and beds of cornstone which laid down unconformably on an irregular surface of older sediments and lavas.

In the Southern Uplands, it crops out in the eastern borders (fig 1.3) and rests on an irregular landscape of Lower Old Red Sandstone and Lower Palaeozoic rocks.

It is thickest in the west of the Midland Valley where it may reach over 1 km (Bluck 1978). In Ayrshire, the thickness ranges from 100m near Ayr to over 300m near Straiton.

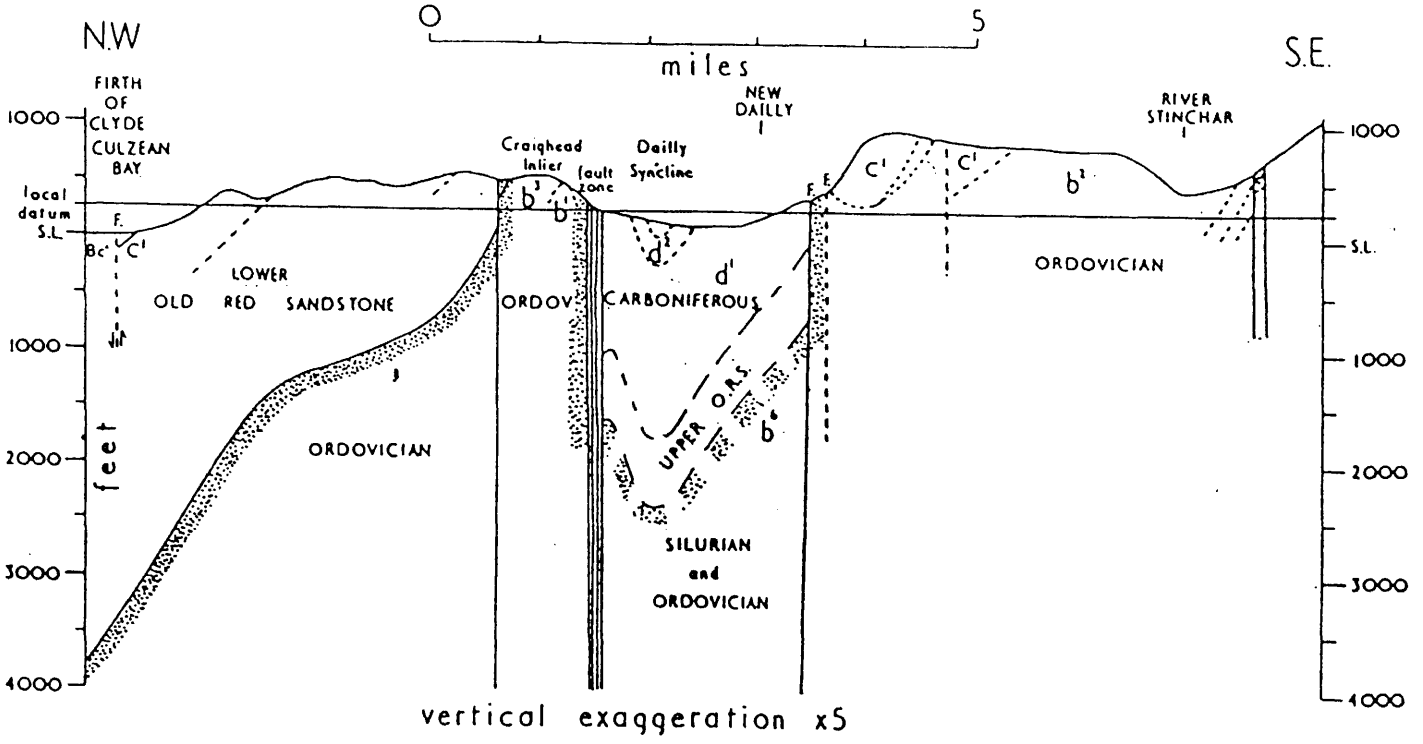

Fig 1.2 Geological section across the Kerse Loch Fault zone at the north-eastern end of the Dailly coalfield (after McLean 1966)

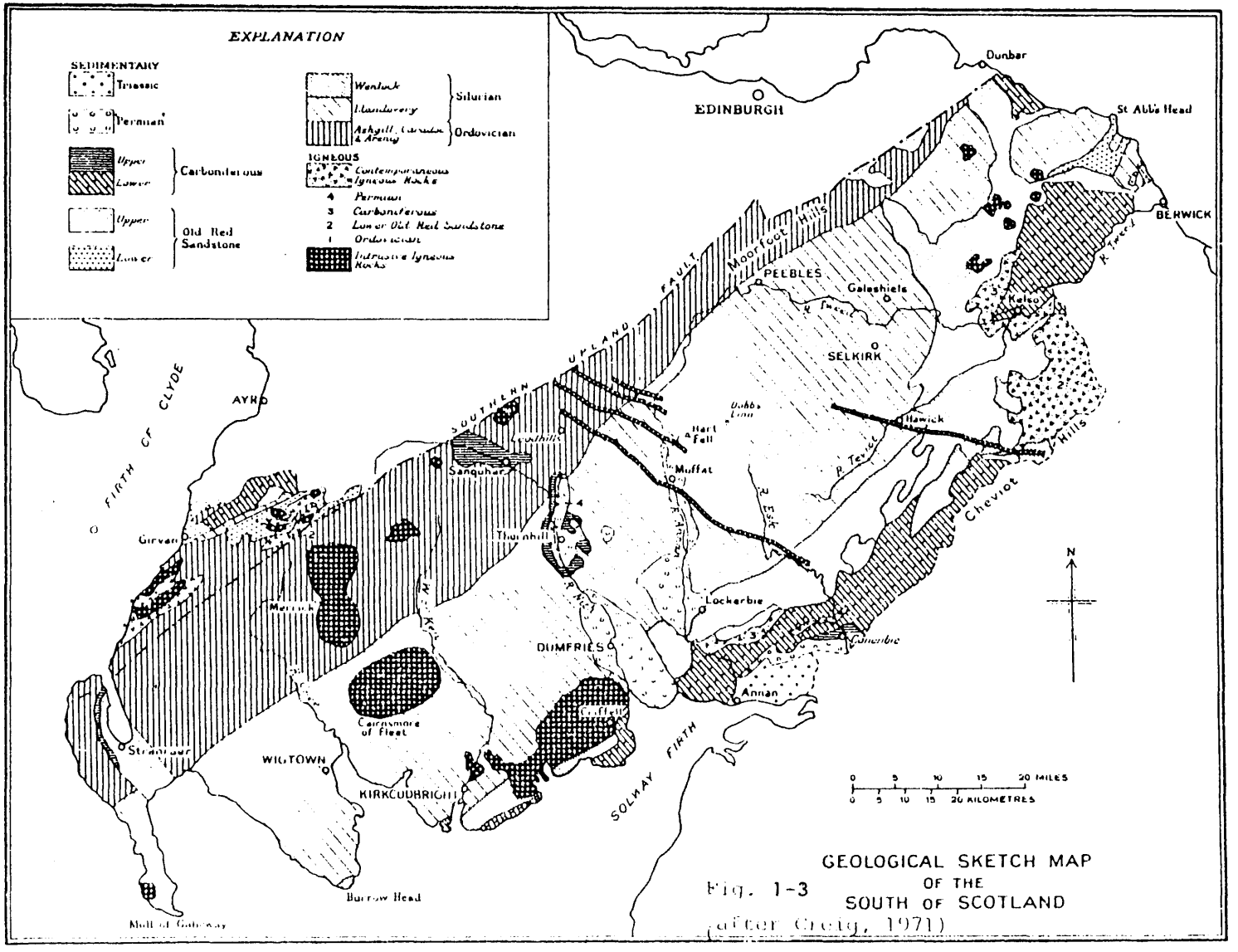

Fig. 1-3 GEOLOGICAL SKETCH MAP OF THE SOUTH OF SCOTLAND (after Craig, 1971)

The narrow, generally fault-bounded, outcrops in South Ayrshire (Eyles and others 1949) fall into two groups:- a western group extending from the coast at the Heads of Ayr south-eastwards to the Kerse Loch Fault, and then south into the area around Straiton; and an eastern group around Muirkirk (fig 1.1).

Upper Old Red is characterised by much faulting and relatively gentle folding with uplift in the Midland Valley. It rests with marked unconformity on older rocks, and volcanic rocks are absent in this period. Both the Southern Uplands Fault at New Cumnock, and the Straiton Fault appear to have undergone considerable movements before deposition of the Upper Old Red Sandstone.

1.2.4 Lower Old Red Sandstone

In Lower Old Red Sandstone times the topography of the Scottish area was largely controlled by contemporaneous normal faults, giving rise to major fault scarps and rift valleys. By far the greatest amount of deposition took place within the Midland Valley Rift which, it is deduced, contained two major parallel river valleys (fig 1.4) flowing to the south-west, with intervening volcanic uplands. The terrestrial sediments of Old Red Sandstone accumulated in alluvial fans, on the floodplains of braided and meandering rivers, and in shallow lakes along the foot of the emerging Caledonian mountains.

Distinctive conglomerates, lavas and sandstones rest unconformably on a group of Silurian rocks in the southern Midland Valley in the Pentland Hills and at Girvan, although they may be conformable with the Silurian at Lesmahagow.

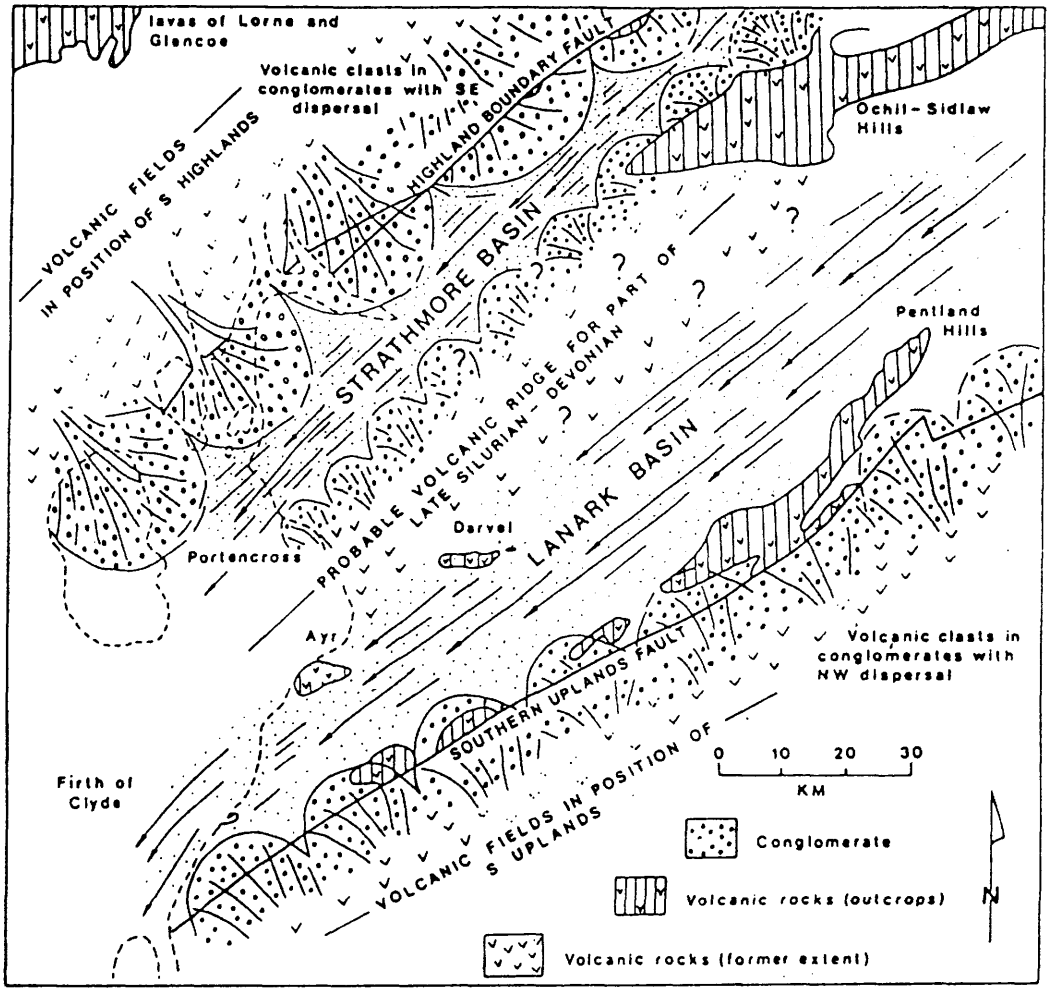

Fig 1.4 Palaeogeography of Late Silurian- Early Devonian of W Midland Valley.(after Bluck 1983)

Thick conglomerates with lava cherts and with a south-east dispersal lie adjacent to the Highland Boundary Fault. Similar relationship occurs along the Southern Uplands Fault with conglomerates lying alongside the fault, having a north-west dispersal (fig 1.4). Both these relationships imply lava fields north of the Highland Boundary Fault and south of the Southern Uplands Fault, providing substantial source of volcanic detritus.

In the Midland Valley, the southern outcrop is discontinious and dissected by sub-parallel north-east trending faults. In the Maybole area, the lower sedimentary group is up to 1·2 km thick. The overlying volcanic rocks form the Carrick Hills as well as two smaller coastal outcrops at Culzean Castle and Maidens (Geikie 1897, Tyrrel 1914). In the Carrick Hills, the volcanic sequence is 300m to 450m thick and consists of olivine-basalts, augite and andesites (Eyles et al 1949). The sequence in the Dalmellington area is similar to that of Maybole, but it is much more disturbed by faulting. The sedimentary group may be up to 700m thick and the overlying volcanic group consists of nearly 600m of olivine-basalt. South of Girvan, a small outlier of Old Red Sandstone appears to be the remains of a valley infilling.

In the eastern part of the Southern Uplands (fig 1.4), greywacke-conglomerate, red feldspathic sandstones and a volcanic succession, are ascribed to this age.

A feature of the volcanic rocks within the study area, is their association with an extensive suite of contemporaneous minor intrusions, which include sheets and laccoliths of felsite and quartz porphyry, and sills and dykes of biotite-porphyrite, plagiophyre, kersentite, pyroxene-porphyrite, quartz-dolerite and basalt.

At a late radiometric ages available of the Caledonian orogeny, granite bosses were intruded in the Southern Uplands. Large granite complexes of Loch Doon, Cairnsmore of Carsphairn and Cairnsmore of Fleet occupy much of the Southern Uplands with the small Distinkhorn intrusion in the Midland Valley (fig 1.1). The Loch Doon mass was formed by three phases of intrusion, successively more acid in composition (Gardiner and Reynolds 1931). Norite represents the first phase, tonalite the second (occupies much of the present outcrop), and the final phase is granite. The plutonic boss of grandiorite and diorite forming the Distinkhorn in east Ayrshire, cuts the lower sediments and is probably the same age as the Lower Old Red Sandstone volcanic group.

Geophysical results indicate that the Old Red Sandstone crops out off the coast near Turnberry and in an inlier between there and south-east of Arran. It is probably absent, apart from small patches preserved in the area lying more than 6 km to the south of Ailsa Craig.

No detailed stratigraphic correlations have been established in the Lower Old Red Sandstone of the Southern Midland Valley (Mykura in Craig 1983). The Lower Old Red Sandstone rests conformably on Silurian rocks in the Lesmahagow area but oversteps south-westwards to overlie ordovician with a basal unconformity.

1.2.5 Lower Palaeozoic

Such rocks are found in small inliers in the Midland Valley and over much of the Southern Uplands (fig 1.1 and 1.5). Sedimentary facies and structure invite comparison with modern trenches and subduction zones, and lead to the interpretation of the

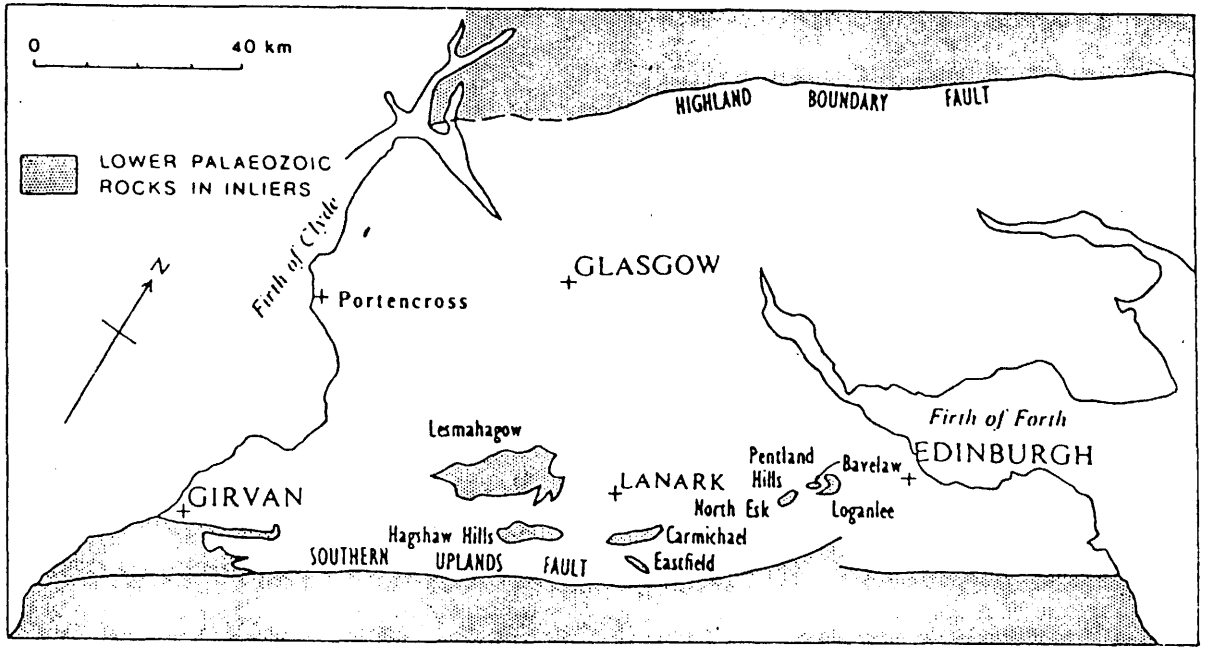

Fig 1.5 Sketch map showing the Lower Palaeozoic inliers in the southern part of the Midland Valley.(after Walton 1983)

Southern Uplands as an accretionary prism; a model promoted vigirously by McKerrow and his co-workers (McKerrow et al 1977, Leggett et al 1979). On this model the fault blocks of the Southern Uplands are successive thrust masses formed from trench sediments (fig 1.6). Sedimentation and deformation proceeded simultaneously, the earlier, inner sequences being deformed and thrust up to establish the source for subsequent sediment. The appearance of Silurian Cockburnland is simply the expression of deformation leading to the formation of an emergent trench-slope break; the Midland Valley inliers then become examples of upper-slope basins.

Ordivician and Silurian conglomerates of the Midland Valley and the Southern Uplands share a suite of quartzite, basic-ultrabasic and granitic clasts (Bluck 1983). This implies a similarity in provenance which argues against lateral displacement of the Midland Valley relative to the Southern Uplands. Bluck stated that the source of the Silurian conglomerates is unlikely to be found in the Ordivician rocks of the Southern Uplands. With the evidence for a missing fore-arc sequence in Ordivician times, he inferred the accretionary prism was not in its present position during the Silurian, and that the Midland Valley basement extended beneath the Southern Uplands to the region where Wenlockian trench deposits now outcrop (Southern Belt). On this model, the accreted Southern Uplands was thrust in from SE over the projected Midland Valley and the Girvan fore-arc sequence (fig 1.7).

Silurian rocks are in contact with Ordivician; south of Girvan, on the coast and inland to the south of Girvan Water. The main outcrop is separated from the Craighead anticlinal inlier to the north, by the Kerse Loch Fault along the Girvan Water (fig 1.8).

a

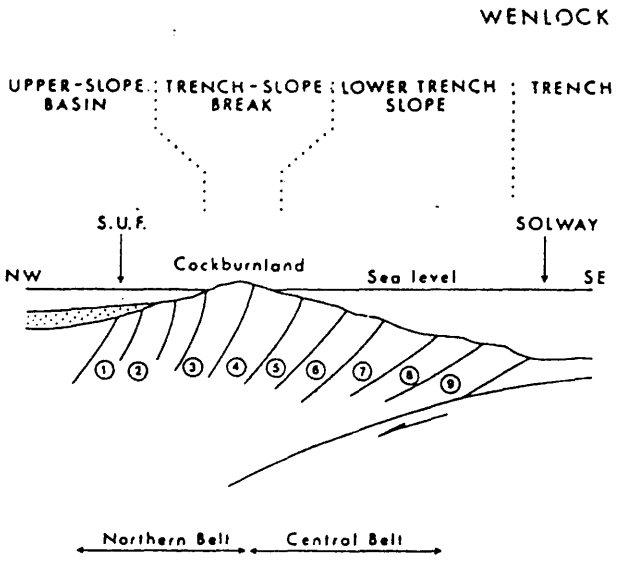

b

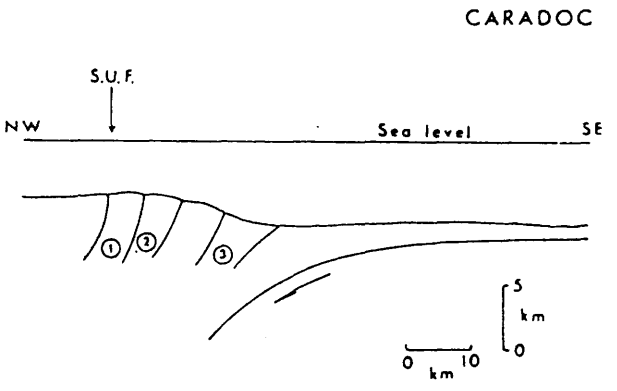

Fig.1–6 The Southern Uplands area as an accretionary prism in a. Caradoc and b. Wenlock times.

The numbers refer to the tracts, indicated on the map belowseparated from one another by major faults. The Upper Slope basin is indicated in Wenlock times as below sea-level; this is the case at Girvan though elsewhere in the Midland Valley the area was emergent. S.U.F. Southern Uplands Fault (from McKerrow *et al.* 1977, Leggett *et al.* 1979).

Faults

DF	Drumblair	GBF	Gillespie Burn
EVT	Ettrick Valley Thrust	KT	Killantringan Thrust
FL	Fardingmullach Line	LL	Leadhills Line
GF	Grassfield	PT	Pibble Thrust
GAF	Glen App	RL	Riccarton Line

Localities

Cr	Craigmichan Scaurs	P	Portpatrick
K	Kirkcudbright	St	Stranraer

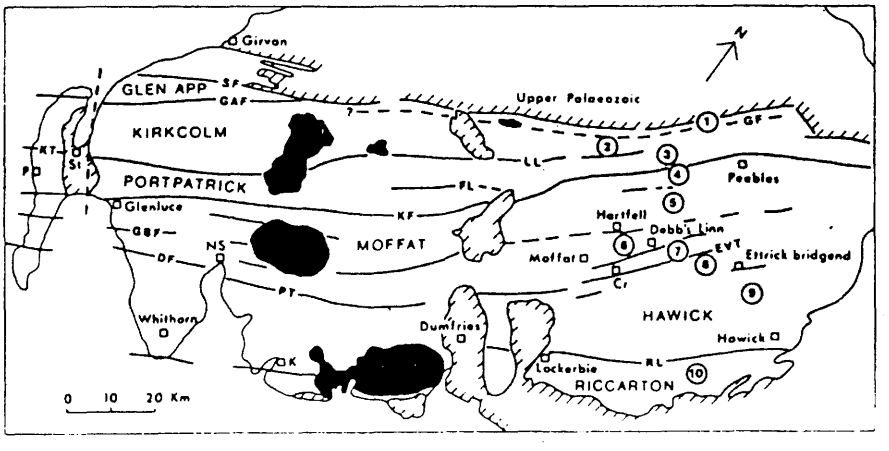

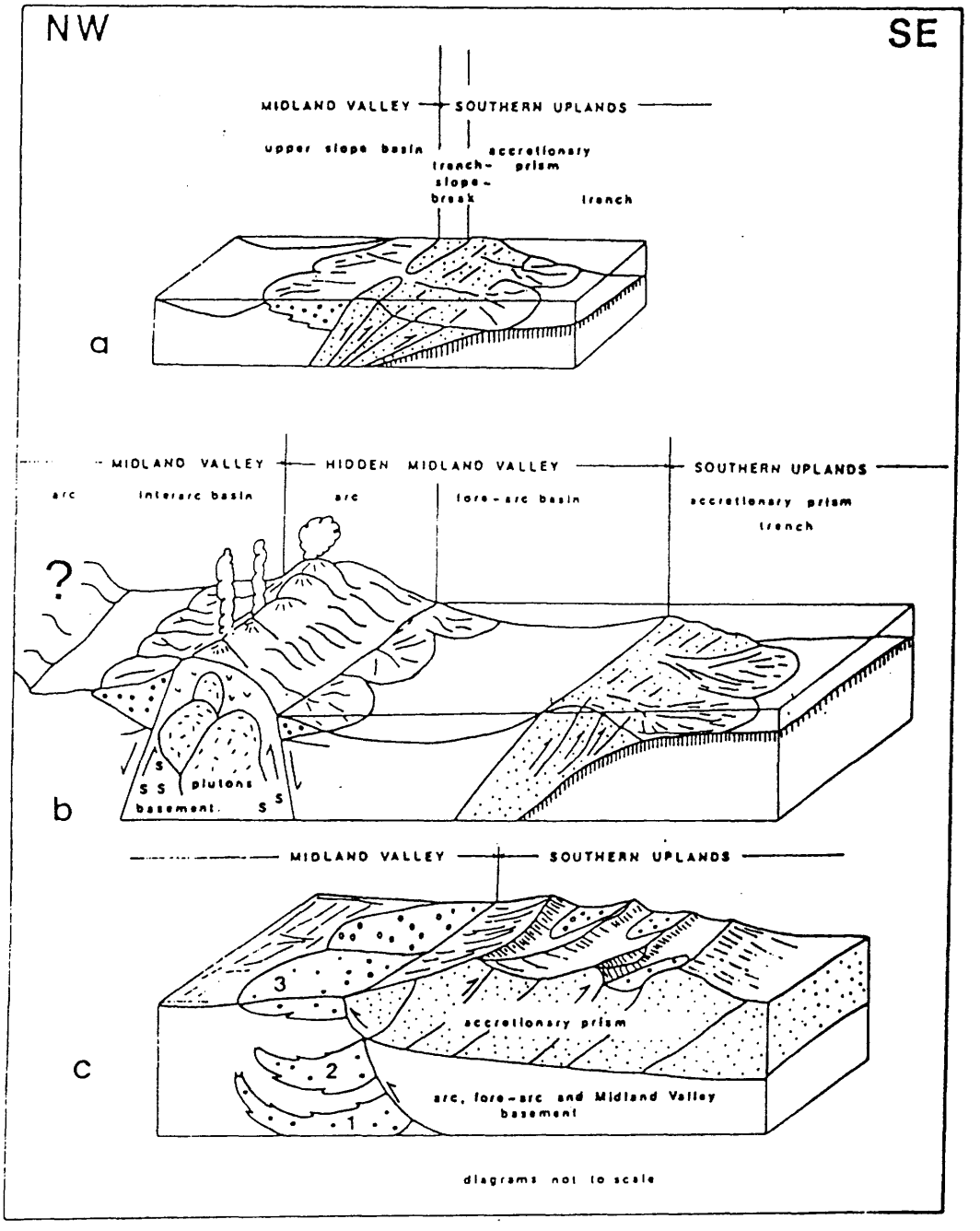

Fig 1.7 a)Midland Valley as fore-arcbasin with trench-slope-break and upper-slope basin. b)Inter-arc basin, missing fore-arc basin(beneath Southern Uplands). c)Overthrusting of accretionary prism:1"igneous conglomerate"2"quartzite conglomerate"3"greywacke conglomerate". (after Bluck 1983)

Fig. 1–8. Silurian successions at Girvan and Craighead (after Cocks & Toghill 1973). Inset-sketch map showing Silurian outcrops in Girvan area.

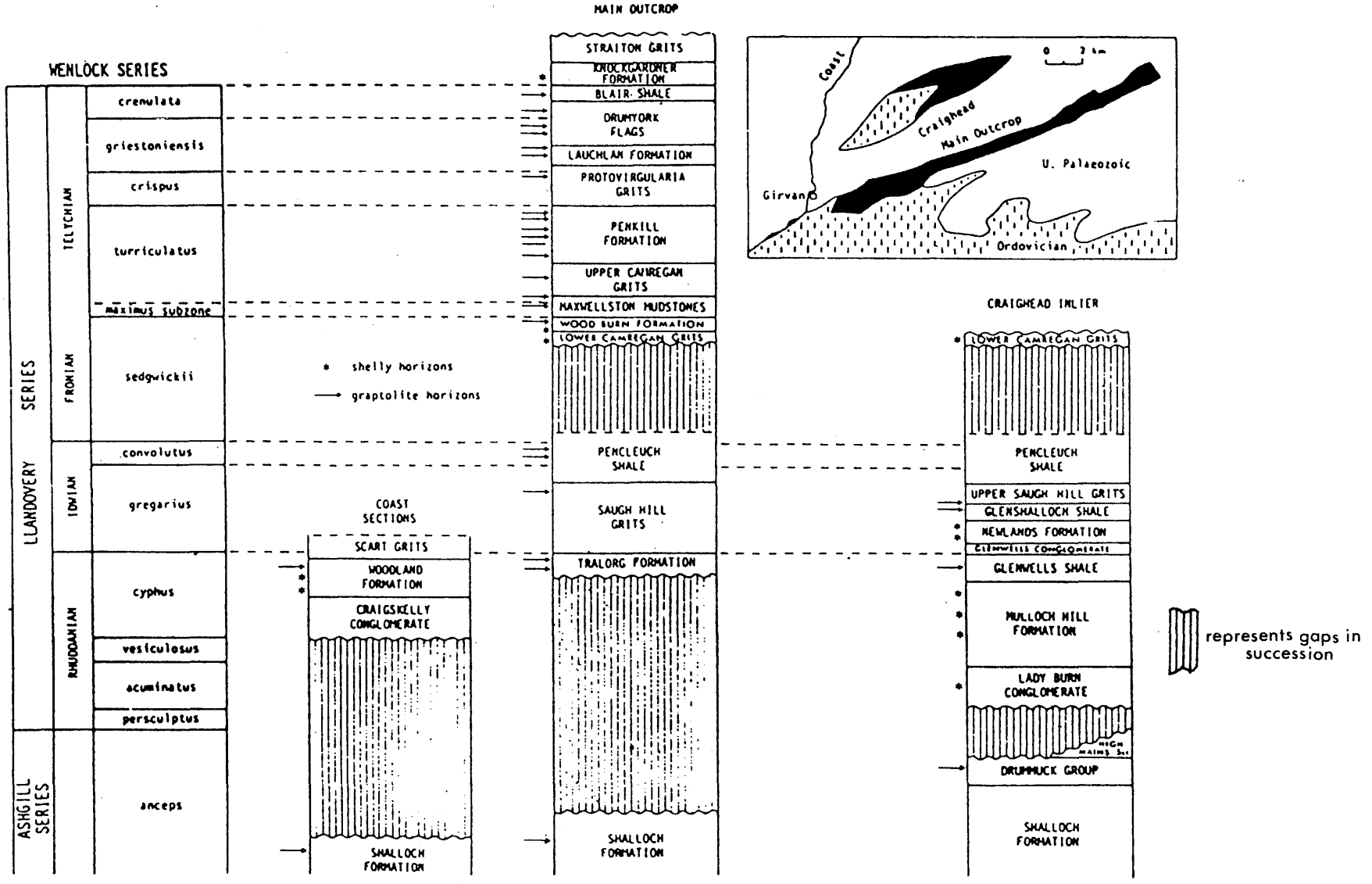

The Central Belt (fig 1.1) is defined by the boundary of the Silurian with the Ordivician rocks to the north, and by the Wenlock rocks in the south. The northern part of the belt is occupied by greywacke sequences; the rest is comprised of shales, conglomerates, grits and greywackes (Pringle 1935). The boundary between the top Ordivician and Silurian has been faulted (Kingledores Fault fig 1.1).

Ordivician sequences younger than Arenig occur in three main areas; Girvan, including the Craighead inlier, the Northern Belt and small isolated inliers in the Central Belt. The sequence in Girvan has many of the features of the Southern Uplands, although it operated as a different basin during the Silurian. Movement along the Southern Uplands Fault during Ordovician is still uncertain (B J Bluck, personal communications 1985) and evidence of movement of the faults in south-west Scotland during Lower Palaeozoic time is poor (Kelling 1961).

The uppermost Ordovician beds are found in Craighead inlier. Here the Drummuck Formation is mainly mudstone above a basal conglomerate. The succession at Craighead is important in its lower members including the Craighead Limestone, which lies unconformably on Ballantrae volcanics and cherts (Arenig).

South-west, towards the Stinchar Valley, the Ardmillan and the Upper Barr Group represent Ashgillian and Caradocian times. The Lower Ardmillan series is composed of:-

A. Shalloch Formation: fine grained, laminated sandstones.
B. Whitehouse Beds: 200m of shale, sandstone and limestone members.
C. Ardwell Formation: some 1·5 km of mudstones with

thin sandy bands.

D. Balcatchie Formation: at the base of the Ardmillan Group. Mainly mudstone with some sandy and conglomeritic lenses (fig 1.9).

The sequence of the Barr series is transgressive with younger rocks overlapping the earlier in a northerly direction (fig 1.10). The arrangement from top to bottom in the Barr Series is as follows (fig 1.9):

A. Benan Conglomerate: shows large changes in thickness (max. is 640m) due to overstep over a topographically variable Arenig basement and partly due to channeling which has sometimes removed all the Superstes Mudstones bringing the conglomerate to rest on the Stinchar Limestone. In the north-west of the area near the coast, it is on top of the Ballantrae Complex (Walton in Craig 1983).
B. Superstes Mudstones: mainly siltstones and mudstones.
C. Stinchar Limestones: interbedded with shales.
D. Confinis Flags: shales and mudstones.
E. Kirkland Conglomerate: ophiolitic clasts in sandy matrix.

Although there is some variation in conglomerate composition within the Kirkland and Benan conglomerates, the earliest (Kirkland) contains mainly basic and ultrabasic clasts, but with some granitic, porphyritic and metamorphic rock fragments. The younger Benan conglomerate have a predominance of granite in the coarser sizes and basic and ultrabasic rocks in the finer sizes. This suggests the unroofing of a major igneous complex (Bluck 1983). Longman et al (1979) reported the presence of boulders of metaquartzite, amphibolite and sheared granite in the northerly derived Ordivician conglomerates with southerly derived Silurian conglomerates of the southern Midland Valley. They pointed that this evidence supports the existence of

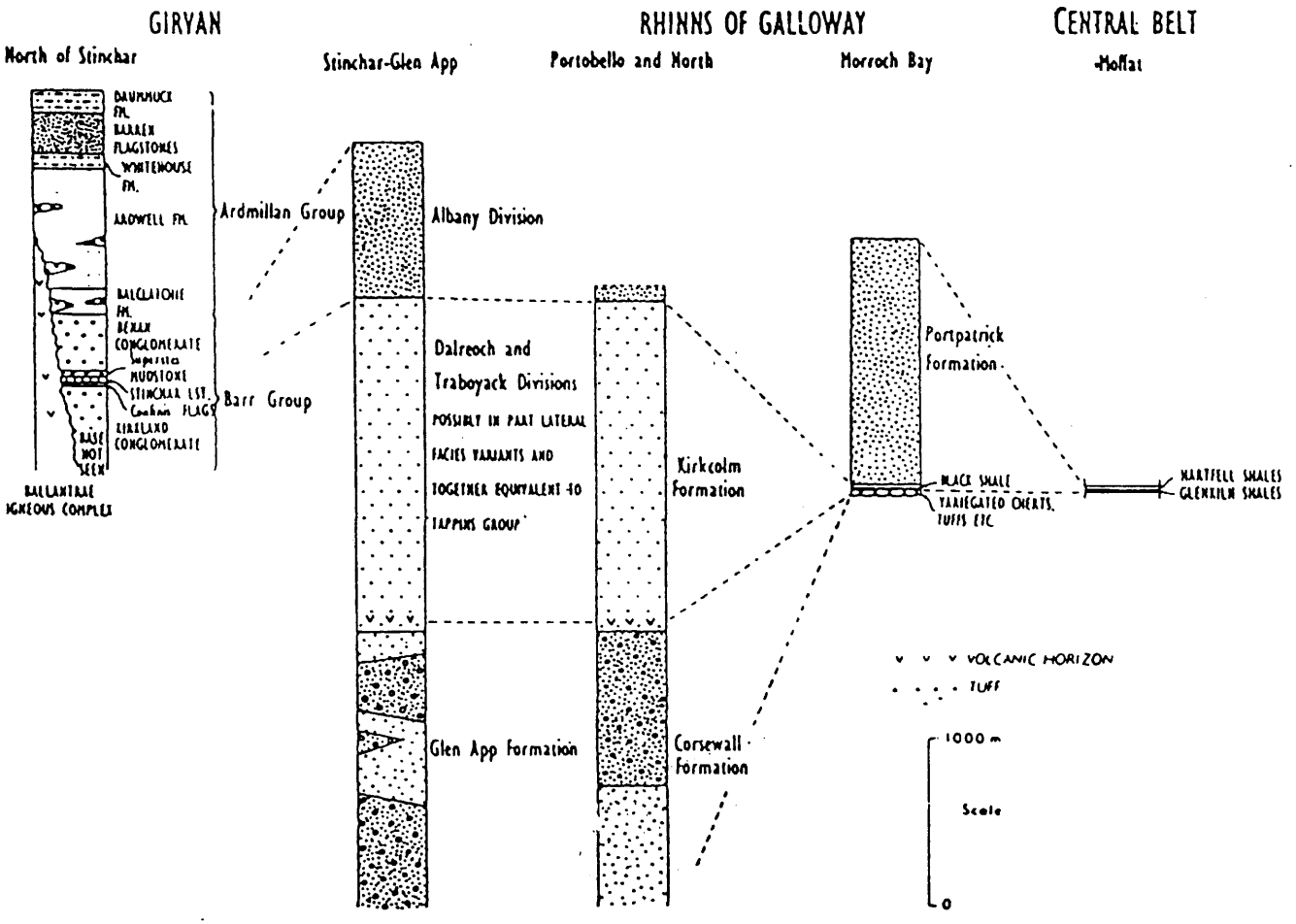

Fig.1-9. Ordovician successions across the northern half of the Southern Uplands.

(after Walton 1983)

Fig.1-10 Geological sketch map of the Girvan area (after Williams 1962). Stippled ornament within Lower Ardmillan Group represents Conglomeratic horizons.

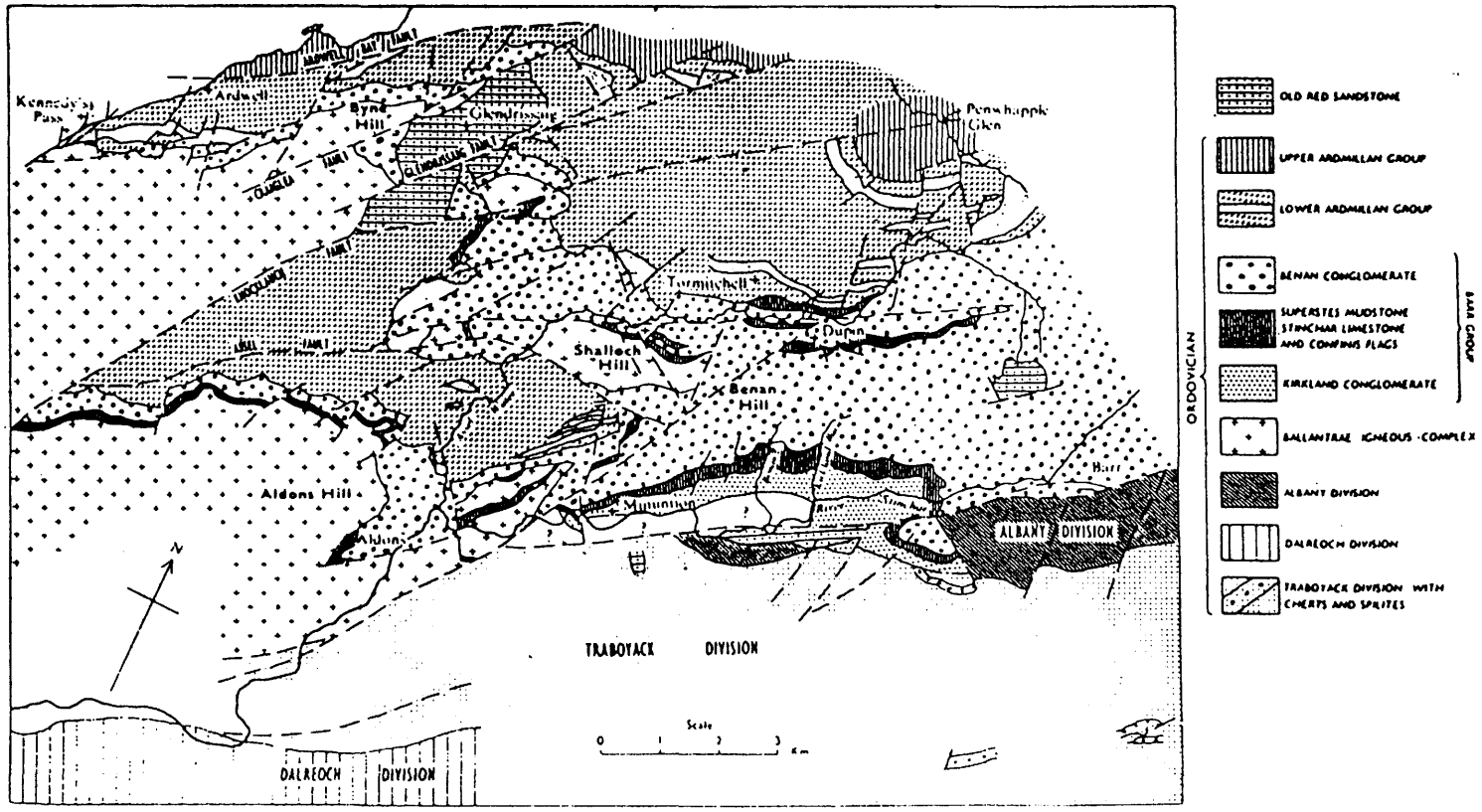

Precambrian basement under the Midland Valley.

The Lower Barr sequence seems to extend into the Llandelio (Williams 1972).

The early Ordovician Ophiolites are separated from the greywackes of the Southern Uplands by the Stinchar Fault. Thick sequences of greywackes, shales and mudstones occur to the south of the Stinchar Fault, which may perhaps represent the westerly continuation of the Southern Uplands Fault (Leggett et al 1979).

Peach and Horne (1899) read the succession as:

Glen App Conglomerate	Age equivalence	Benan Conglomerate
Tappins Group	Age equivalence	Superstes Mudstones
Mudstones and Cherts conformable on Arenig Cherts	Age equivalence	Stinchar Limestone Group

In place of the Tappins Group, Williams (1962) recognised three divisions:

A. The Albany: resembles the Ardwell Formation in lithology.
B. The Traboyak: mudstones with spilites and cherts.
C. The Dalreoch: greywackes, siltstones and mudstones.

The last two may be lateral facies variants. On the coast, they pass down conformably into the Glen App Conglomerate (fig 1.11).

A similar sequence to that of the south of Stinchar occurs along the strike in the Rhinns of Galloway, where Kelling (1961) separated a lower Corsewall divisions of conglomerates. In both areas, the minerals and/or rock fragments of greywackes and

Fig. 1.11. Ordovician successions in the Northern Belt, from the Rhinns of Galloway along strike to Nithsdale (after Floyd 1975). a. Rhinns of Galloway. b. Loch Ryan east. c. Nithsdale.

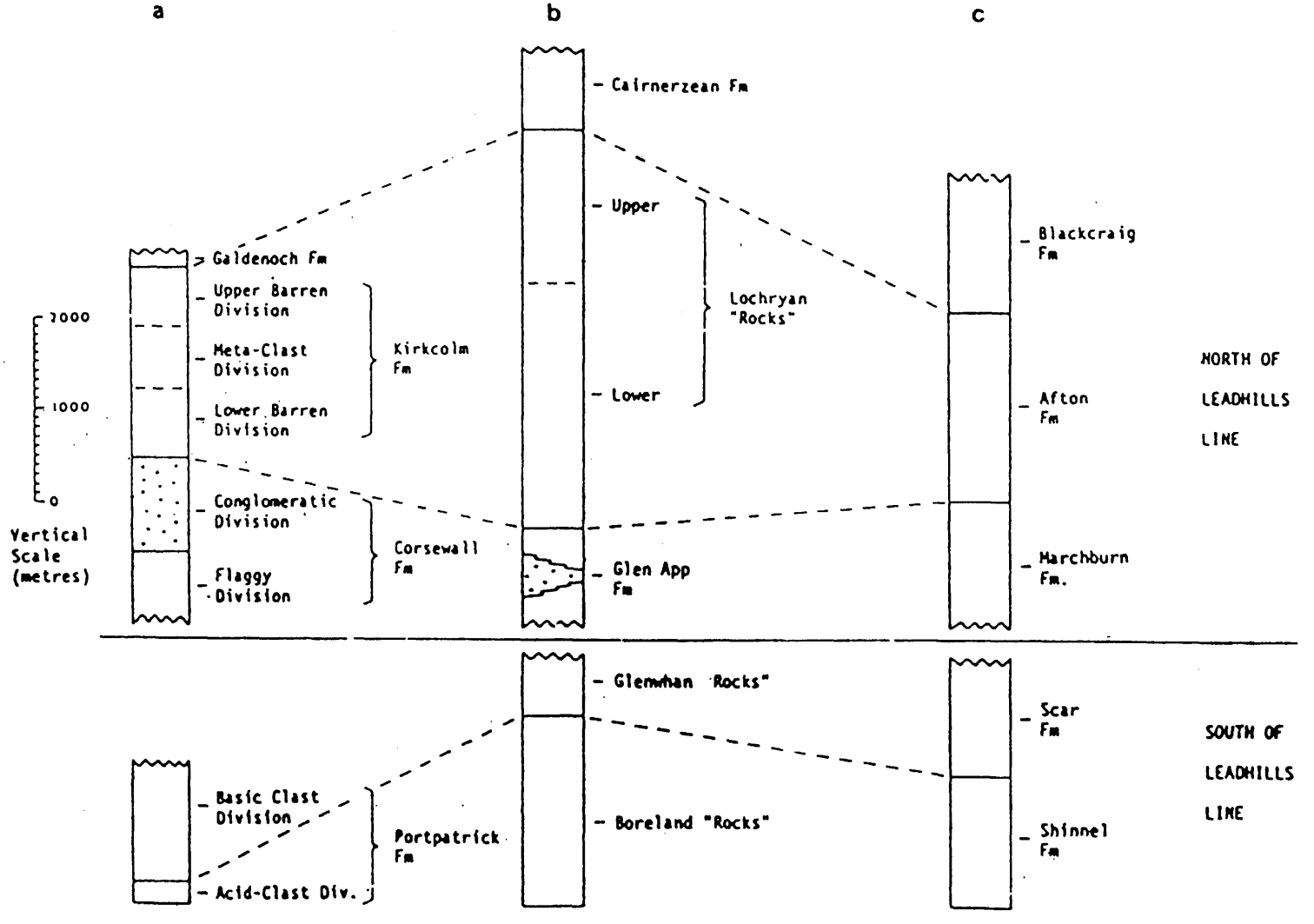

conglomerates are basic, thus serving to distinguish these beds from the Dalreoch rocks.

The predominantly greywacke sequences continue in the Northern Belt. In addition to the Corsewall Formation found to the north of Glen App Fault, in the Rhinns, Kelling recognised three main divisions; the Galdenoch, Kirkcolm and Portpatrick (fig 1.11). The Kirkcolm make up the northern part of the Belt with two small areas of the Galdenoch, while the Portpatrick sequences occupy the southern half, up to the Silurian boundary.

Along the strike, formations corresponding to these in the Rhinns have been traced to Moorfoot Hills south of Edinburgh.

Volcanic episodes, usually with cherts, are of various ages in the Northern Belt. Arenig volcanics are undoubtedly basal to the greywacke sequence at Raven Gill, elsewhere pillow basalts and cherts may be underlain by greywackes, as in Glen App area and along the Southern Uplands Fault near New Cumnock.

1.2.6 Cambrian and Early Ordovician (Arengian)

The Girvan-Ballantrae area in south Ayrshire exposes under the transgressive base of the Barr Series (fig 1.9), early Ordovician rocks; the Ballantrae Igneous Complex (fig 1.12).

The complex forms a typical ophiolite assemblage including the Steinmann Trinity of serpentinite, pillow lavas and cherts. Serpentenite make up approximately half of the outcrop area and predominates two belts; Northern and Southern. The main rock type forming the serpentinite was a peridotite. In the

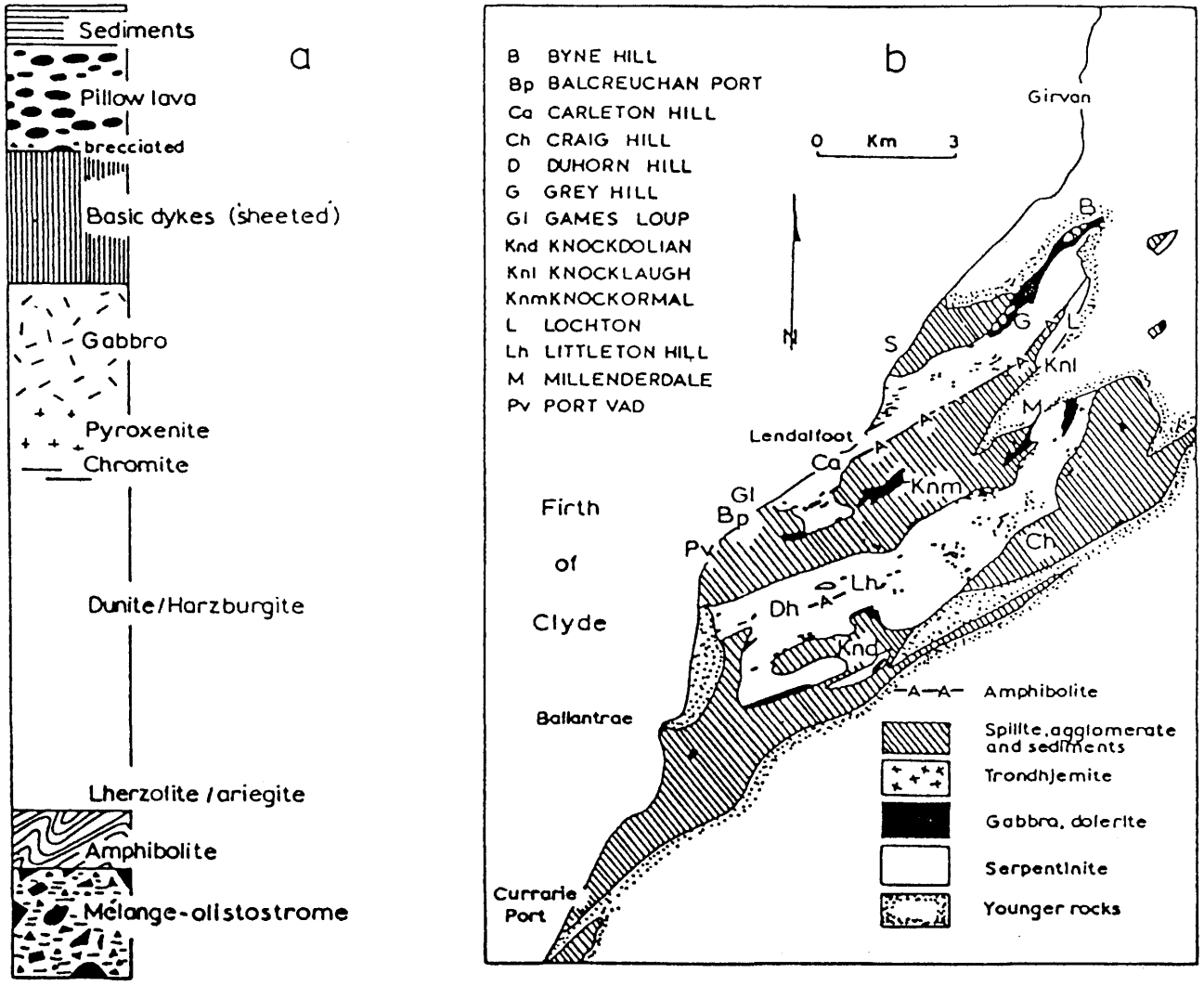

Fig.1.12 (a) section of an ideal ophiolite; (b) simplified map of the Ballantrae Complex.

(after Bluck 1978)

basal (southern) part of the northern serpentinite belt, lherzolites have layers of abundant clinopyroxene and orthopyroxenes. In a similar position at Laigh Knocklauch, coarse bronzitites also represent pyroxenite cumulates. Another distinctive rock at this locality is garnet ariegite, with garnet, pyroxene, amphibole and spinel. Micro-probe analyses of the pyroxenes, amphiboles and garnet show them to have relatively iron-rich compositions (Church & Gayer 1973). The mineral compositions are very similar to those of the amphibolite aureole at Trout River, Western Newfoundland. Church and Gayer inferred from the similarity in petrography, chemistry, and above all geologic disposition, that the amphibolites occuring at the base of ultramafic sequences in Western Newfoundland and Ballantrae, have the same origin. Unfoliated gabbros which pass through a dioritic composition into trondjemite form the north-west margin of the northern serpentinite belt. An intrusive mass near Millenderdale has been claimed as a sheeted-dyke complex (Dewey 1974, Bluck 1978). The main rock-type is a foliated gabbro with a NW-SE trend.

The volcanic rocks comprise lavas, agglomerates and tuffs. They are massive or pillowed. Both porphyritic and non-porphyritic basalts are found (Balsillie 1932). On Mains Hill, near Ballantrae, a coarse-grained agglomerate has masses large enough to be lava flows and it has very close resemblance to the Bail Hill mass in the Northern Belt. It seems to be significant in representing an important source for the succeeding greywackes.

The sedimentary rocks, associated with the Ballantrae Igneous Complex are mostly cherts, conglomerates (previously identified as agglomerates) and black shales. The clasts reported from the conglomerates include all rock types making up the igneous complex:

serpentinite, gabbro, dolerite, pyroxenite, granulite, spilite, amphibolite, glaucophane schist, epidote schist, chert and black shale. In addition, there are blocks of limestone and greywacke (Church and Gayer 1973).

The Ballantrae Complex, although containing most of the components of an ophiolite, has an unproven sequence (Bluck 1978). It has been greatly disturbed by post-emplacement Caledonian deformation (fig 1.13).

The area underwent six significant metamorphic stages: Blueschist facies regional metamorphism, thermal (ocean-ridge) metamorphism, spilitisation (ocean-floor) metamorphism, metamorphism during obduction (dynamo-thermal aureole), serpentinisation and rodingitisation (post-obduction metamorphism) and finally burial metamorphism (Smellie 1984).

1.2.7 Origin of the Ballantrae Ophiolite & Tectonic Setting of the Area

Wilson (1966) indicated a probability that an early Ordovician proto-Atlantic ocean had existed until shortly before the end of the Ordovician. The bases of Wilson's suggestion were, 1, that the proto-Atlantic (Iapetus) was bounded by an "American Continent" which included most of Scotland and northern Ireland, and a "Europe" which included the rest of Britain, 2, that it closed in late Ordovician times to form a single continent. It began to open again during the late Mesozoic but along a different suture to form our present day Atlantic.

Dewey (1969, 1971) extended the hypothesis and suggested that Scotland, north of the Southern Uplands and the northern part of Ireland had been on the plate edge of a north-western American continent. The

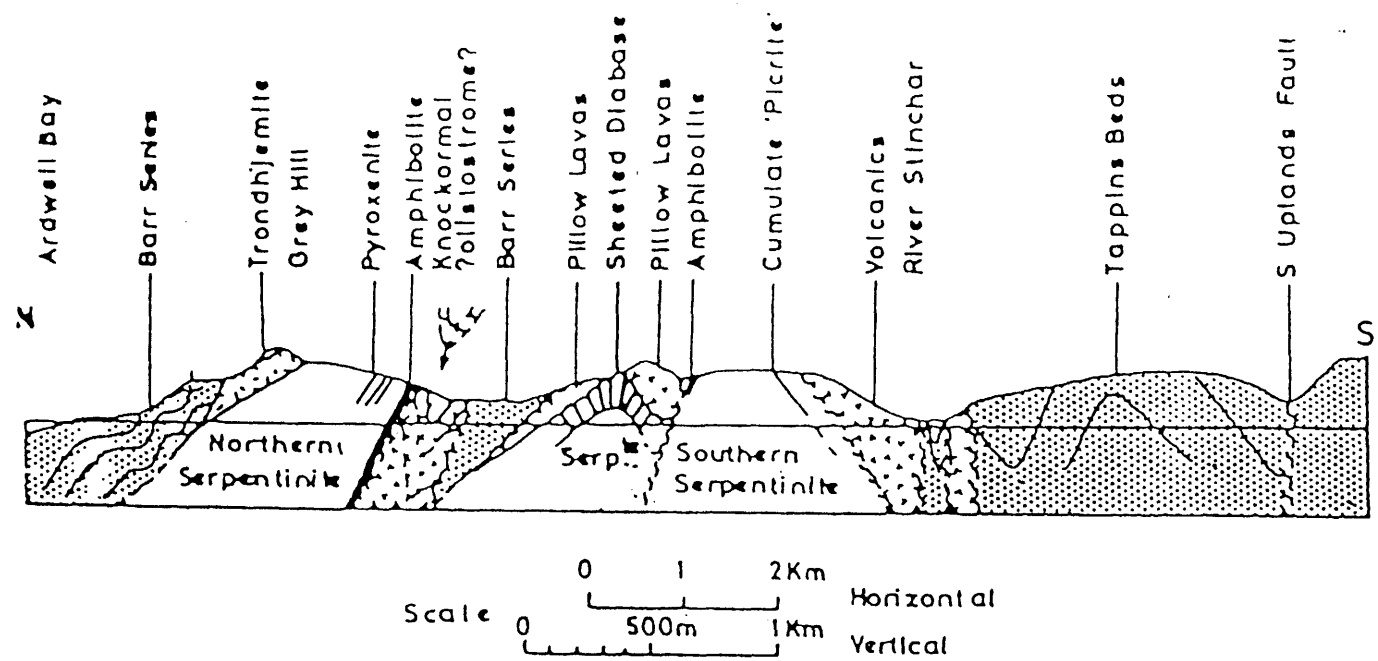

Fig 1.13 Geological section illustrating the structure of the Ballantrae region.(after Church&Gayer 1973)

Midland Valley was considered to be a continental margin, transitional between continental and oceanic crust, and composed largely of sediments resting on Dalradian and mantle wedges. South of this, the Girvan-Ballantrae ophiolite region was interpreted as an upthrust relic of an ancient northward-dipping Benioff zone composed of oceanic crust and mantle with a marginal basin origin. The "Southern Uplands" was believed to have been the final remnant of the proto-Atlantic ocean and was composed of oceanic crust. The "European" continent to the south, was believed to be similarly bounded by earlier and later Benioff zones, here dipping south-eastwards beneath the island arc of Wales and the Lake District (fig 1.14a).

Church and Gayer (1973) concluded that the Ballantrae ophiolite could be equated with those in northern Newfoundland. In this respect, the tectonic setting of the Midland Valley and the Southern Uplands emerge as one of the important points of speculation which divides opinion about the nature and history of the Caledonian orogeny.

Many workers (eg Leggett 1980) endorsed Dewey's model by taking the view that the Midland Valley was a fore-arc basin dividing the accretionary prism to the south from a basement-arc terrain to the north and that the Southern Uplands Fault approximates to site of a former northerly dipping subduction zone. Others hold an alternative view (eg Moseley 1977, Longman 1980, Bluck et al 1980) by seeing the Midland Valley, at least for part of its history, as an arc which supplied detritus to the basins to the immediate south (fig 1.14d).

The interpretation of the origin of the Ballantrae complex ranges from a simple ocean-crust sequence (Lambert & McKerrow 1976), to an island-arc pile (Lewis & Bloxam 1977). Bluck et al (1980) and Hamilton et al

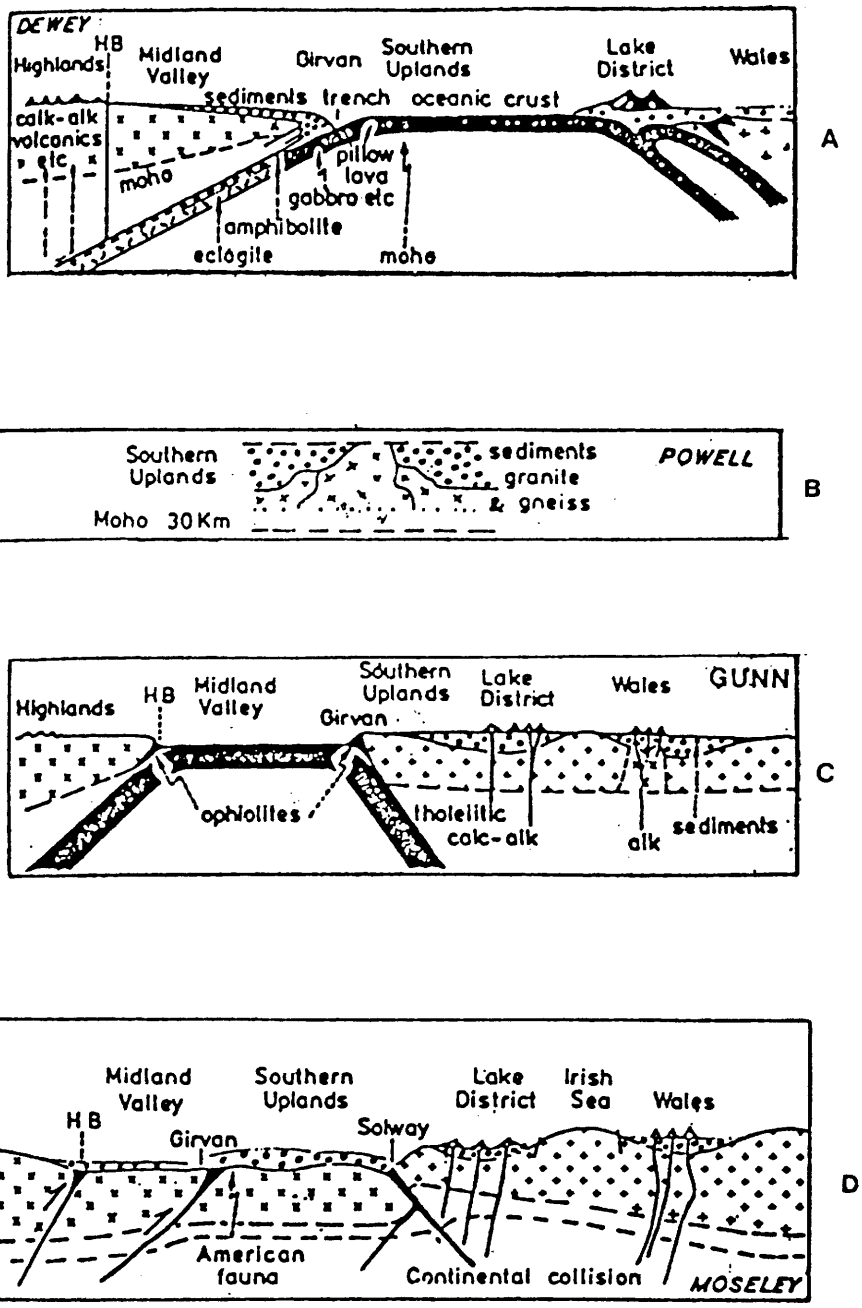

Fig 1.14 Summaries of some of the hypotheses to explain the closing of the proto-Atlantic ocean(Iapetus). HB:Highland Bordrs.

(1984) interpreted the complex as representing tectonic fragments of an island arc - marginal basin assemblage which was thrust (obducted) onto the continental mass, now beneath the Midland Valley. Subsequent work by Bluck (1984) indicates that this island arc - marginal basin assemblage was thrust onto the products of earlier subduction, and the whole complex obducted onto a continental mass. The obduction event was succeeded by dyke intrusions which cut the rocks of the thermal aureole (Holub et al 1984).

1.3 Previous Geophysical Work

Geophysicists' contributions to the solution of geological problems in the Midland Valley and the Southern Uplands regions, has been condensed in the last decade. Crustal models were defined on the bases of gravity, magnetic and seismic studies. Interpretations of particular interest as well as those which could be related to this study are discussed below.

1.3.1 Magnetic and Gravity Surveys

A. McLean (1966), made a semidetailed gravity survey of Ayrshire. Some of his geological conclusions are:

1. The synclines at Dailly, Kerseloch and Dalleagles (fig 1.15) are probably sags on the downthrown sides of the Kerse Loch and Southern Uplands Faults, which were initiated before deposition of the Upper Old Red Sandstone, and moved again as essentially normal faults in Hercynian stages.

2. Resolution of the anomalies at Kerseloch is complicated by igneous intrusions and other

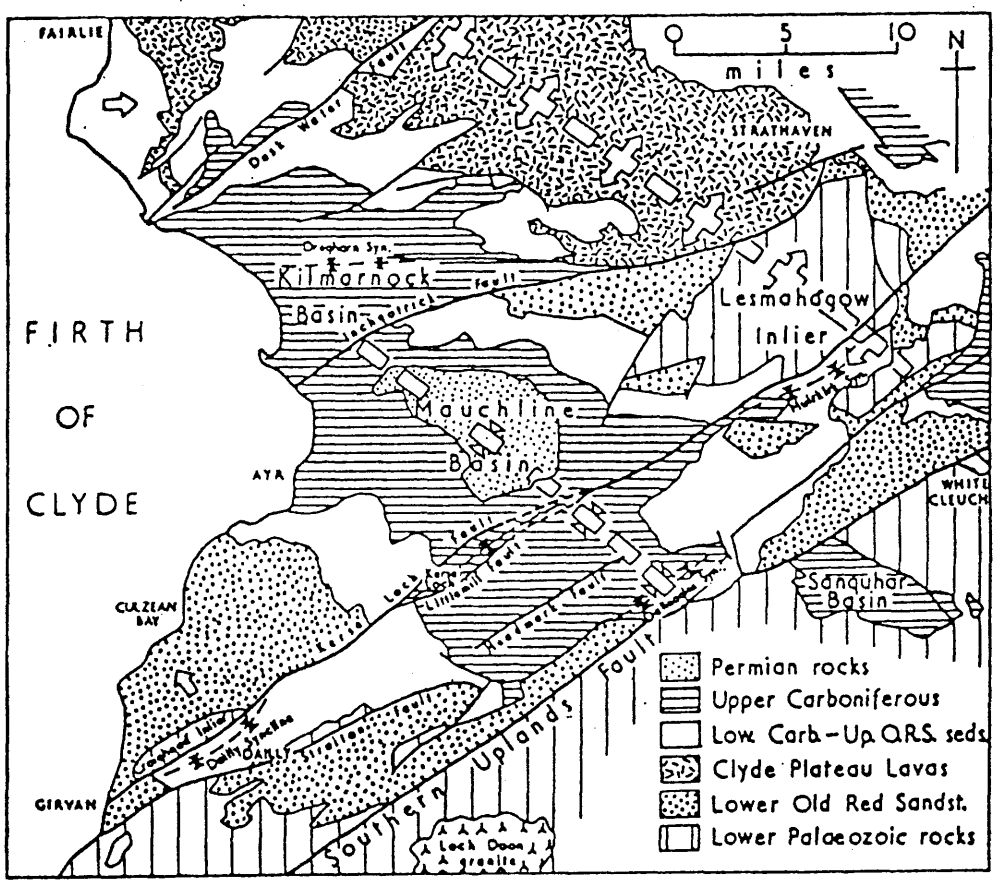

Fig 1.15—Generalized geological map of Ayrshire and its surroundings (after the Geological Survey) showing the more importa post-Carboniferous structures. The axes of the principal folds and the regional dips in the Upper Old Red Sandstone, and Carbonifero rocks, and the New Red Sandstone are indicated.

(after McLean 1966)

dense shallow masses, but the results favour an increased thickness of Upper Old Red Sandstone and Carboniferous rocks in the down-faulted block.

3. The Kerse Loch Fault, SW of Dailly, and the sub-parallel Straiton Fault, both end against or trail into a structural high NNE. - SSW. This structure is apparently continuous from the core of Arenig rocks at Byne Hill, SW of Girvan, to the Arenig outcrops of Craighead and beyond.

B. Analysis of regional gravity field across the western part of the Midland Valley (McLean & Qureshi 1966) reveals that the crust here could be 5 km thinner than under the Grampians and Southern Uplands, where it is referred to be thickened by Dalradian and Lower Palaeozoic rocks less dense than those below. The regional Bouguer anomalies in the area exhibit a westerly rise in gravity (fig 1.16).

C. From aeromagnetic anomalies (fig 1.17) and high gravity (fig 1.18) over the western part of the Southern Uplands (Galloway), Powell (1970) modelled a dense Lewisian basement under the Lower Palaeozoic sediments. Strong magnetic "highs" over the Ballantrae Igneous Complex are due mainly to serpentinite which contains secondary magnetite derived from olivine. Powell attributed the extension of the high magnetic eastward, as far as Dalmellington, to red and purple greywackes derived from the complex and deposited along the southern flank against active fault scarps.

D. Powell (1971) had criticized the conclusions of Dewey that the Southern Uplands could represent a remnant of the proto-Atlantic ocean. He referred to a number of different geophysical investigations,

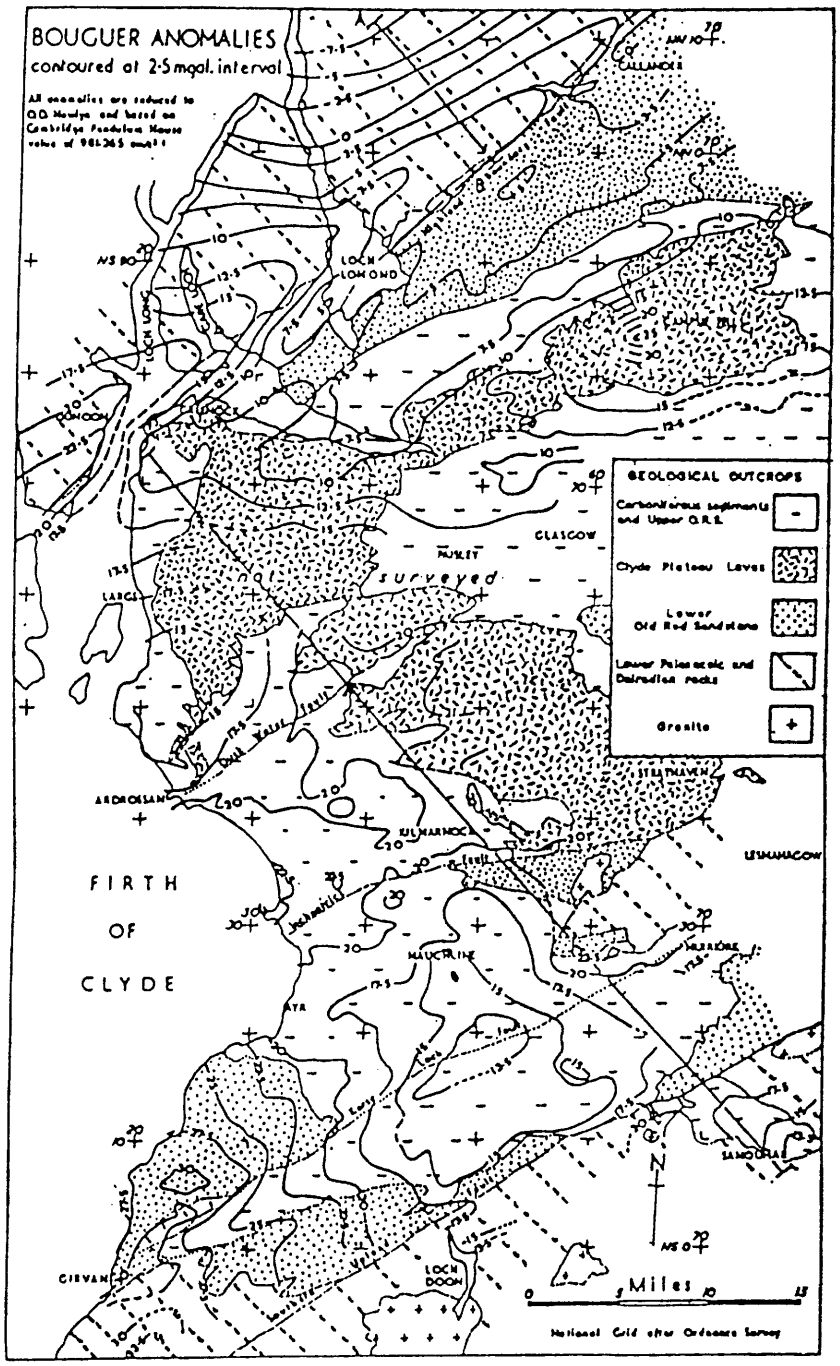

Fig 1.16—Bouguer anomalies map of the western Midland Valley and its environs, showing generalized geological outcrops.

(after McLean&Qureshi 1966)

Fig 1.17 Aeromagnetic anomalies over parts of western Scotland based on Institute of Geological Sciences map sheets 7, 8, 10, 11, 12 and 13 at 1:250,000 scale, flown at 1000 ft mean ground clearance. Thick contours at 50 gamma intervals; fine contours, where shown, at 10 gamma intervals. Magnetic minima are stippled. Some peak values are numbered in 100 gamma units. Principal National Grid lines are numbered and parts of the coastline are shown by oblique lines.

Bh—Barrhill; Bt—Ballantrae; Bn—Binsey; Bu—Bute; Da—Dalmellington; Is—Islay; I.o.M.—Isle of Man; K—Kintyre; L—Lanark; M.o.G.—Mull of Galloway; N.C.—New Cumnock; N.G.—New Galloway; N.I.—Northern Ireland; R—Ramsay; W—Whitehaven.

Inset Map

C.F.—Cromarty Firth; C.W.—Cape Wrath; D.F.—Dornoch Firth; Er—Loch Eriboll; Ew—Loch Ewe; Sh—Loch Shin; St—Point of Stoer; To—Upper Loch Torridon

(after Powell 1970)

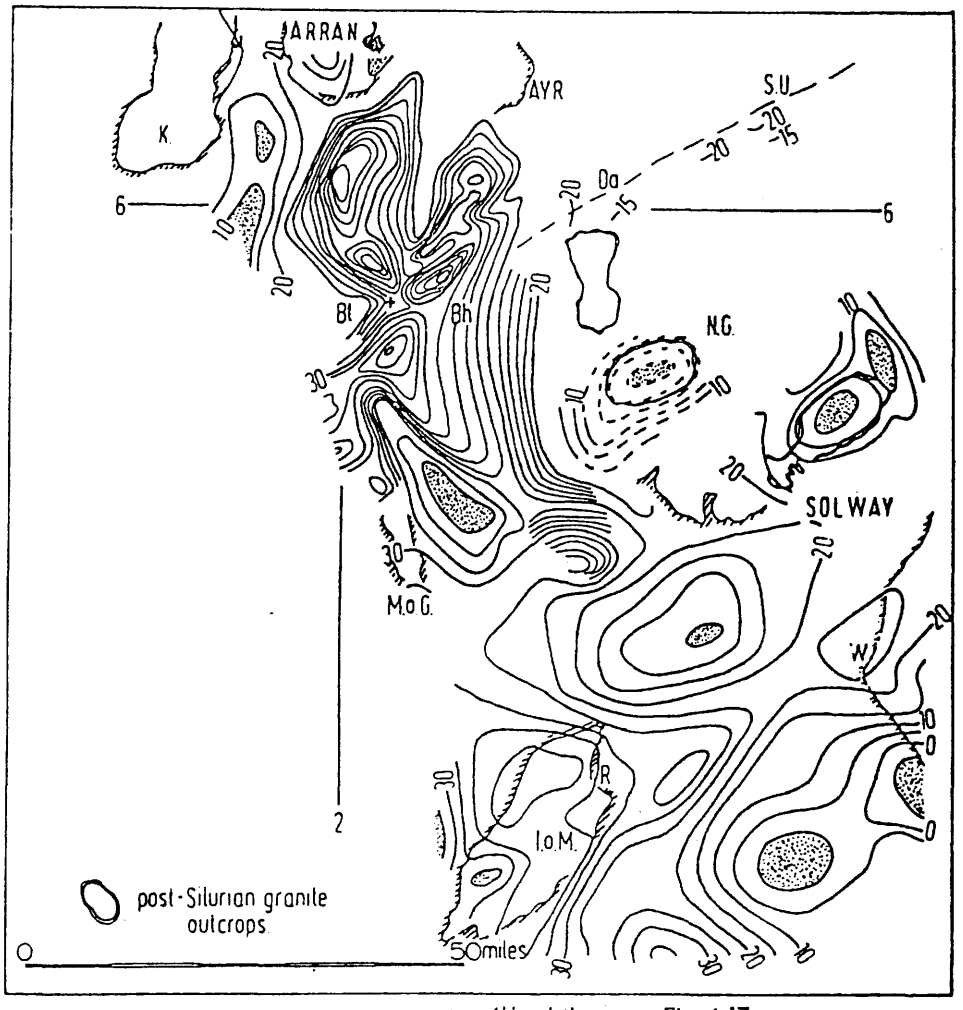

Fig 1.18. Bouguer gravity of south-west Scotland . *Abbreviations as on Fig . 1.17*
Thick contours at 5 mgal intervals; fine contours, where shown, at 1 mgal intervals. Gravity minima are stippled.

(after Powell 1970)

magnetic, seismic, resistivity and gravity, all of which combined to provide powerful evidence that there was as much as 30 km of continental crust in the region. His model (fig 1.14b) shows that the Lower Palaeozoic sediments and the Caledonian granites extend to depths of about 12-15 km. Underneath these the pre-Palaeozoic basement is taken to consist of high-grade schists and gneisses, probably Lewisian.

E. Gunn (1973), using existing aeromagnetic data, suggested that the Midland Valley is a "remnant" of the proto-Atlantic ocean, with the Highland Boundary and Southern Uplands Faults marking the position of diverging Benioff zones. Sediments eroded from the flanking continental areas of the Highlands and the Southern Uplands rest directly on oceanic crust (fig 1.14c).

F. Elbatrouk (1975) and Lagios & Hipkin (1979), from regional interpretations of Bouguer anomalies in the Southern Uplands, suggested that the granite plutons are concealed at depth as a single massive batholith along the Caledonian trend.

G. Powell (1978a) made a magnetic study along the LISPB seismic refraction line, and inferred that any granulites under the Midland Valley are less magnetic than their counterpart in the NW Highlands.

H. Following detailed magnetic and gravity survey over the ophiolites of the Girvan area, Powell (1978b) gave a probable distribution of these rocks but no final conclusions about their origin. A shallow ultrabasic body under the southern Serpentinite Belt, suggested by him, was expected to be detected by seismic refraction measurements (profiles of $\simeq$ 1 km).

Powell states that the results were inconclusive even in revealing the velocities expected for the exposed rock units. Recorded velocities were 4·0 - 5·0 km/sec. up to 1 km range.

I. From a magnetotelluric study in southern Scotland, Jones and Hutton (1978 part 1) indicated marked lateral variations in conductivity structure across the region. The authors took the interpretation further (see part II), to conclude that there is a conducting zone under the Midland Valley at a depth greater than 12 km, and that the crust under the Southern Uplands is mainly resistive. They stated that the conductivity variations beneath eastern Canada can be strongly correlated with those beneath the Midland Valley and the Southern Uplands, and proposed that the Iapetus suture-zone in Britain is now represented by the Southern Uplands.

J. Hutton et al (1980) presented results of two dimensional modelling of both magnetotelluric and geomagnetic response function, obtained along a traverse which follows roughly the course of LISPB. They indicated that sharp changes in depth of seismic boundaries, for example, at Great Glen, Highland Boundary and Southern Uplands faults, have their counterparts in the electrical model.

K. Hall (1980) integrated Hutton et al model with NASP and LISPB results to conclude that the Caledonian crust contain lateral and vertical changes in physical properties that can be related to surface geology.

1.3.2 Seismic Investigations

A. Agger & Carpenter (1964-65), in their crustal

studies in the vicinity of Eskdalemuir, analysed records of shots fired in the Irish Sea, and which were received at EKA (a seismological array of continuous operation). They obtained a mean velocity of 6·09 ± 0·06 for first arrivals from ranges $<$130 km. The nature of the experiment excludes details about the shallow structure.

B. Jacob (1969) analysed apparent velocities of local events recorded at EKA; the seismic array as noted above. Most of the events were quarry blasts. The analysis indicated a gradual increase in velocity from 5·54 km/sec at the surface to 5·94 km/sec at 12 km at which depth the velocity jumps to 6·4 km/sec.

C. Grampin et al (1970) studied explosions and natural events recorded on a permanent radio-linked short period seismometer network (LOWNET). The network is operating with nine stations scattered in the Midland Valley. A three layer model is represented by their time travel diagram. An assumed thin top layer with P-velocity of 3·0 km/sec followed by a middle layer, 5·4 km thick with 5·65 km/sec velocity which is overtaken by a velocity of 6·45 km/sec beyond ranges of 50 km.

D. In a review of seismic studies around the British Isles, Willmore (1973) concluded that the Moho shallows toward the west.

E. After the North Atlantic Seismic Project (NASP 1972), Smith & Bott (1975) derived the following model for crustal structure beneath the Caledonian foreland. 1. sedimentary layer of variable velocity and not present everywhere. 2. a thin upper crustal layer with estimated velocity of 6·10 km/sec interpreted as either Lewisian rocks of lower metamorphic grade or Caledonian belt metamorphic rocks and varies in

thickness up to 10 km. 3. an undulating refractor of estimated P-velocity of 6·48 occurs at variable depth between 2 and 16 km and identified as granulite facies Lewisian basement rocks.

F. In 1974, the Lithospheric Seismic Profile in Britain (LISPB) was completed. It is a reversed 1000 km seismic refraction line across Britain (Bamford et al 1976). LISPB crossed the eastern half of the Midland Valley and the Southern Uplands on a NS line (fig 1.19a). Their P-wave velocity structure is shown in fig 1.19b. Under the Midland Valley, the model is:

1. A velocity of 4·5 - 5·0 km/sec for a surface layer of upper Palaeozoic sediments, to a depth of 2-3 kms. The layer is shown continuous across the Southern Uplands where rocks of Lower Palaeozoic outcrop (cracked shallow Lower Palaeozoic rocks). LISPB is not designed to detail surface layers.

2. 5·8 - 6·0 km/sec for Lower Palaeozoic sediments, to a depth of 7-8 kms. This layer interpreted by analogy with the Southern Uplands segment between these velocity limits.

3. 6·4 km/sec for an inferred crystalline basement underlying the sedimentary sequence. This layer has been compared with NASP granulite facies Lewisian basement (see previous section E). The model for the Southern Uplands is still three layered:

1. A top superficial layer of 5·0 km/sec ($<$2·5 km thickness), and not a distinct geological unit being the Lower Palaeozoic outcrop.
2. An upper crustal sequence contains material of 5·8 - 6·0 km/sec to depths greater than 10km.

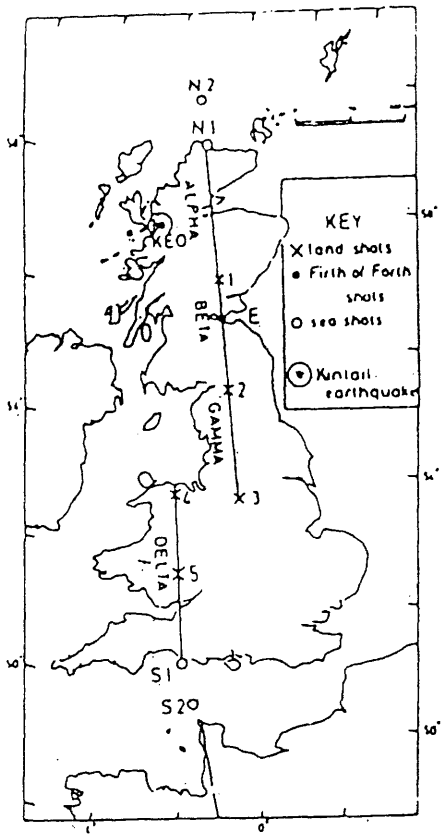

(A) Location of LISPB shots and profile, Northern Britain.

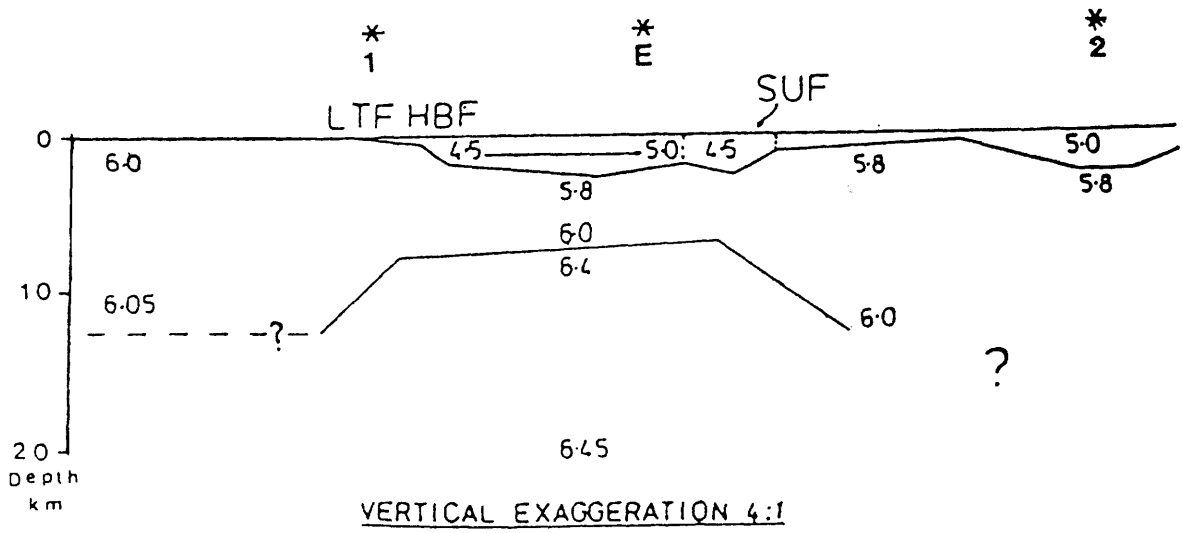

Fig. (1.19) (B) P-wave velocity distributions and upper crustal structure Midland Valley, Southern Upland and Highlands. (After Bamford et al, 1977).

3. Mid crustal rocks with Vp=6·3 km/sec to an undefined depth.

According to Bamford et al (1978), the granulite Lewisian basement extends from Caledonian foreland into the Midland Valley, but appears to terminate at the Southern Uplands Fault.

G. El-Isa (1977) analysed observations of quarry blasts and other seismic sources at EKA and the Broughton array (BTN), which is located on the Northern Belt of the Southern Uplands. He noticed higher apparent velocities from sources along strike (parallel to S.U.F.) at EKA and in the Midland Valley to the north and west, but low apparent velocities (5·6 - 5·8 km/sec) from sources at similar ranges (25-50 km) to the north and east. El-Isa concluded that P-wave velocities within the Lower Palaeozoic rocks of Scotland around EKA increase with depth and vary with azimuth.

H. In order to add to the understanding of the physical properties and structure of the crust and upper mantle in Northern Britain, Assumpcao and Bamford (1978) presented data on the distribution of Poisson's ratio (σ) in the region. LISPB Poisson's ratios are generally close to the conventional 0·25 except for layer 1 in the Southern Uplands (σ = 0·231) and layer 2 under the Midland Valley (σ = 0·224). These low values of σ were said, by the authors, to indicate some anomalous properties of the layers, possibly to confirm the region of the Southern Uplands Fault as a major point of interest.

I. Warner et al (1982) gave a brief interpretation of the Southern Uplands Seismic Profile (SUSP). It is

a reversed 120 km seismic refraction line along the Northern Belt, from Dunbar to Sanquhar in the Southern Uplands. They derived a three layer upper crust model for the Northern Belt (fig 1.20):-

1. Lower Palaeozoic greywackes extend from the surface to a depth of no more than 1 km, with velocities of 5·75 - 5·80 km/sec.

2. A refractor with velocity of 6·0 km/sec, which is suggested to be an igneous or metamorphic body.

3. At depths of 2 - 3·8 km, another refractor with velocity of 6·32 km/sec.

J. From field and laboratory velocity measurement on Lower Palaeozoic greywackes, Adesanya (1982) concluded that the high velocity observed in the Southern Uplands ($>$6·0 km/sec), are not Palaeozoic greywackes but crystalline rocks.

K. Hall et al (1983) have recently used seismic data from SUSP, BTN, EKA and LISPB, to propose that the Southern Uplands contain crystalline rocks of continental affinity at shallow depths (1 - 5 kms). They suggest that the high velocity crust of the Midland Valley (6·0 km/sec) continues south of the Southern Uplands Fault but deepens rapidly to the south-east of SUSP and BTN. They infer that the same basement underlies EKA as a block (10-20 km wide), and another block is to underlie LISPB shot 2 in the Southern Belt till the boundary of the Central Belt in the Southern Uplands (fig 1.21a). Their re-interpretation of LISPB shots E and 2 is shown in fig 1.21b.

L. Shallow and deep structure interpretation of the

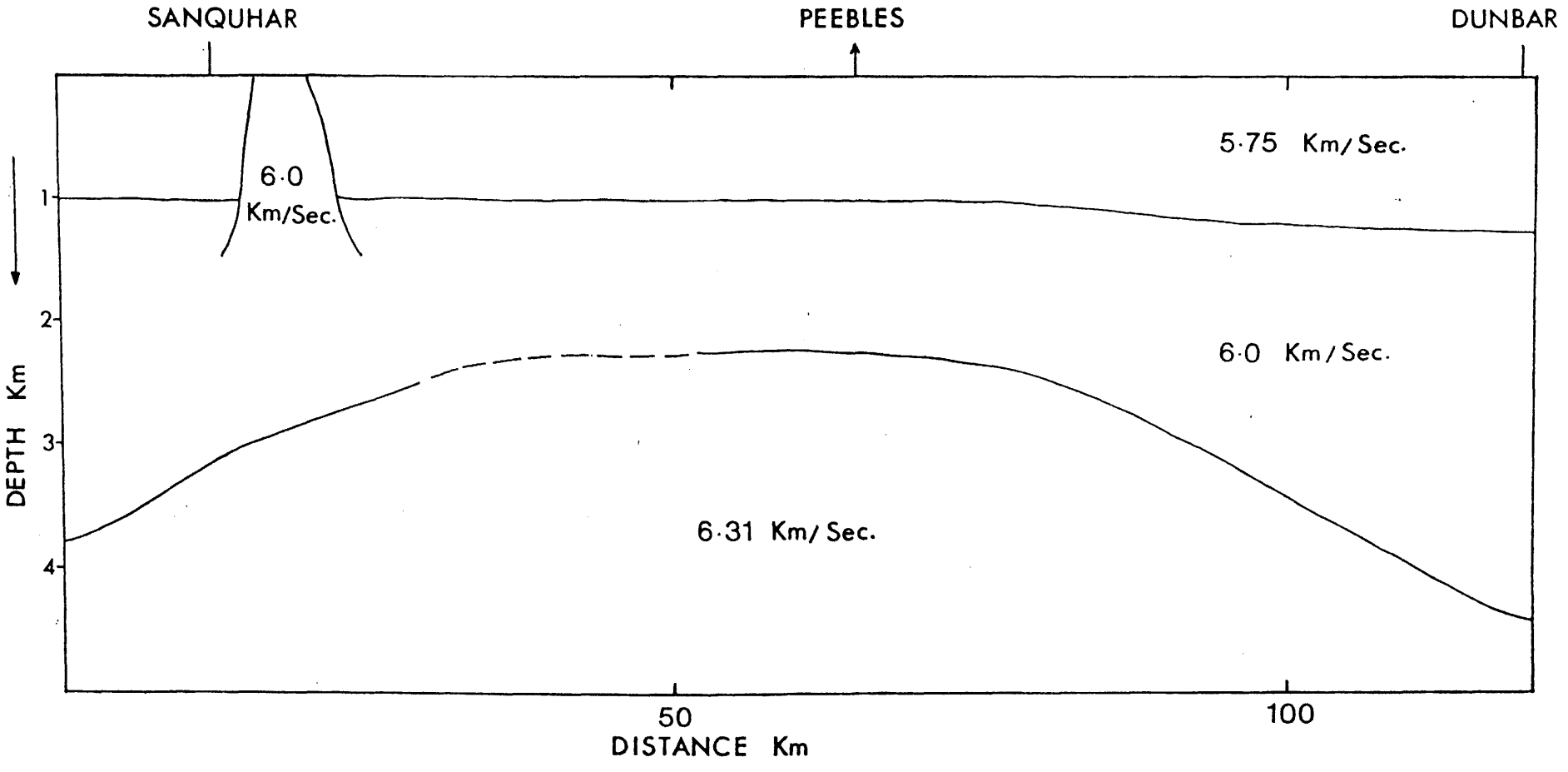

Fig 1.20 Upper crustal velocity structure along the SUSP line as presented by M.Warner in UKGA-6 conference 1982.

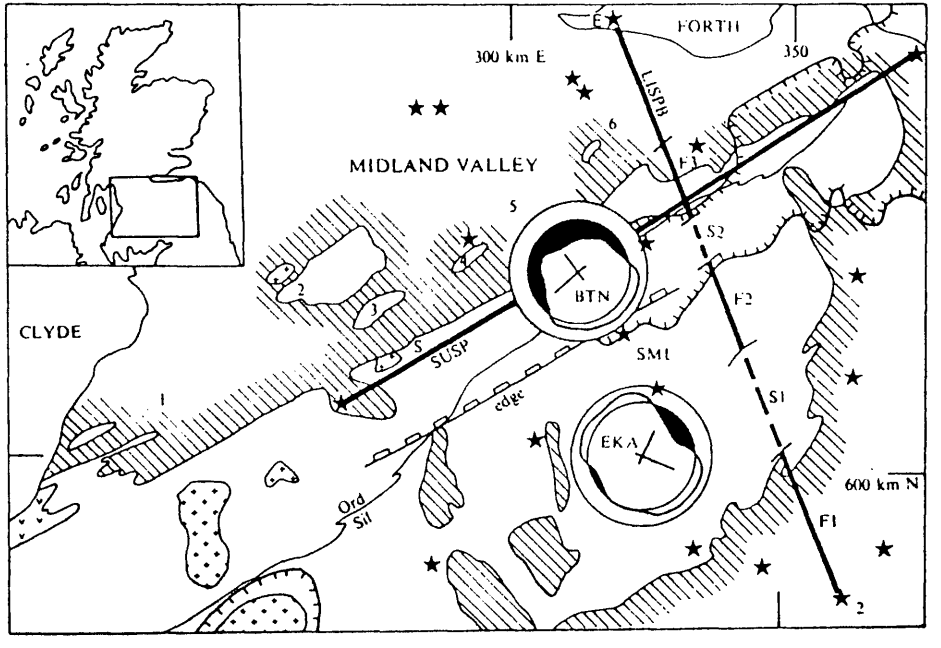

Fig.1.21a Map of the Southern Uplands of Scotland. Area of Lower Palaeozoic rocks is limited by shading. plusses indicate late granites, V indicates Ballantrae igneous complex. Lower Palaeozoic inliers within the Midland Valley are Straiton, Girvan (1), Lesmahagow (2), Hagshaw (3), Carmichael (4), Tinto (5), North Esk (6). Inliers 2–4 are used to define basin edge (line with castellation). A line is drawn to separate Ordovician (Ord) and Silurian (Sil) outcrops. The area within which Bouguer gravity is negative is bounded by line with edging on negative side. On the LISPB profile, E and 2 identify shot positions and F1–3, S1–2, locate high- and low-velocity blocks SUSP is the Southern Uplands Seismic Profile. Seismological arrays at Eskdalemuir (EKA) and Broughton (BTN) were used to observe seismic events at the black stars. Polar plots are of apparent velocity versus direction to source with scale rings at 5.5 km s^{-1} (outer) and 6.0 km s^{-1} (inner), so that black area defines sector in which velocity is greater than 6 km s^{-1}. The Spango granodiorite is marked S, and St Mary's Loch is at SML. Inset shows location of area.

(after Hall et al 1983)

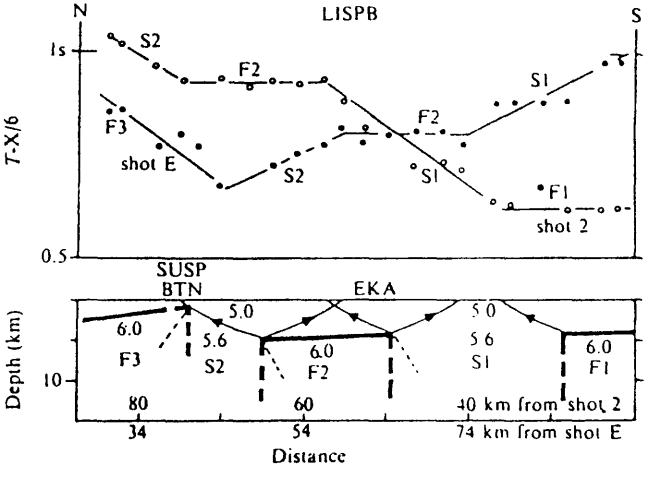

Fig.1.21b Time–distance plot of LISPB data across the Southern Uplands from shots E and 2, using a reduction velocity of 6 km s^{-1} in plotting time. The structural model shows a velocity distribution containing fast (F) and slow (S) blocks which give rise to the corresponding segments of the plots, with offsets shown by arrowed ray-paths.

Western Isles - North Channel deep seismic reflection line (WINCH), is provided by Hall et al (1984). "WINCH" runs through the North Channel across the extension of the Midland Valley and into the Firth of Clyde. Hall et al. stated that no margins to the Midland Valley were observed equivalent to bounding faults on land. They supposed that the Midland Valley basement continues below the Southern Uplands since no contrast in seismic character on either side of the projected Southern Uplands Fault was noticed.

M. More information on the range of distribution of P-wave velocities in the Palaeozoic sedimentary sequence in the Midland Valley were provided by Sola (1985) and Davidson (1985). Their investigation area is the central and southern Midland Valley. Velocity groups recognised by them as Carboniferous and Upper Old Red Sandstone, with Vp=3·0-3·37 km/sec and higher velocities of 4·0-5·5 km/sec for Lower Old Red Sandstone and Lower Palaeozoic sediments. Fig 1.22 shows the interpretation of Davidson et al (1984) of an 80 km E-W seismic refraction line (Troon-Broughton), in which the Palaeozoic sedimentary sequence can be traced to a common boundary at around 3 km. Beneath the sedimentary sequence, they recognised an undulatory refractor characterized by a P-wave velocity of 6·0-6·1 km/sec, which was interpreted to represent quartz-feldspathic gneisses. By this, they revised LISPB layer 2 to be a structure on the crystalline basement. A north-south section (fig 1.23) from the Highland Boundary Fault across the Bathgate area to Carmichael Fault near the Southern Uplands Fault, represents the main conclusions of Sola (1985). Across the Southern Uplands Faults, the SUSP velocities are integrated in this section.

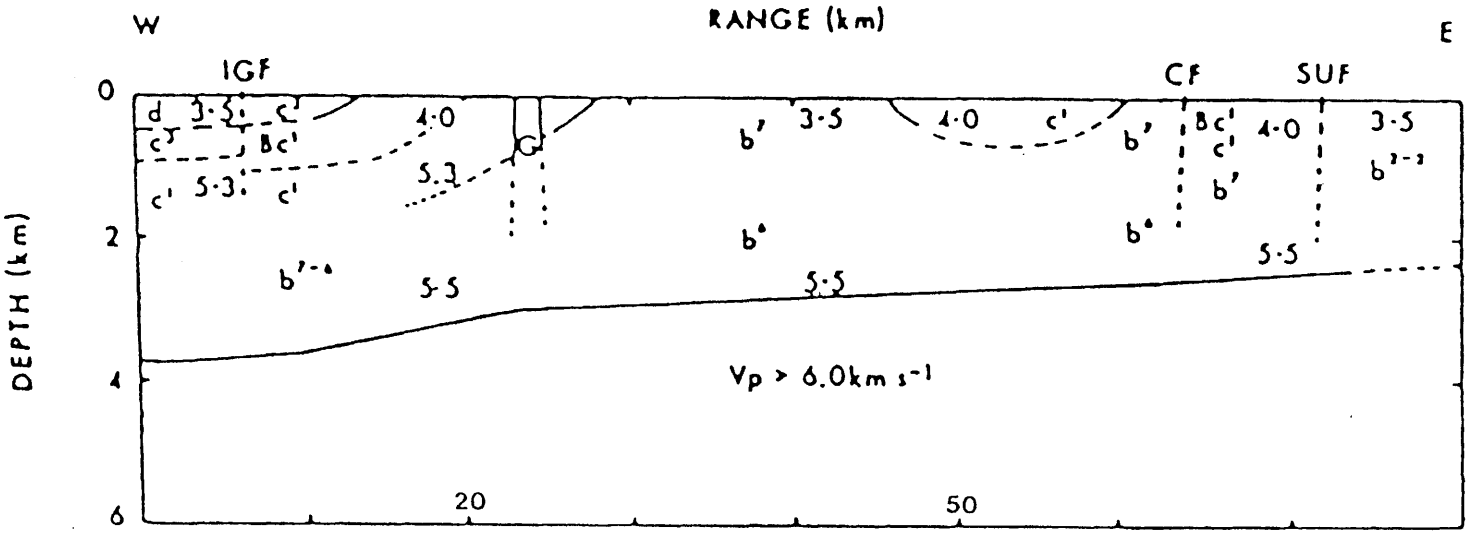

Fig 1.22 Derived interpretation from the Hillhouse-Broughton Line. (after Davidson et al 1984)
CF:Carmichael Fault, IGF:Inchgotrick Fault, SUF:Southern Uplands Fault.
b:Lower Palaeozoic, Bc1:Lower Old Red Sandstone lavas, c1:Lower Old Red Sandstone,
c3:Upper Old Red Sandstone, d:Carboniferous, G:Distinkhorn granite.

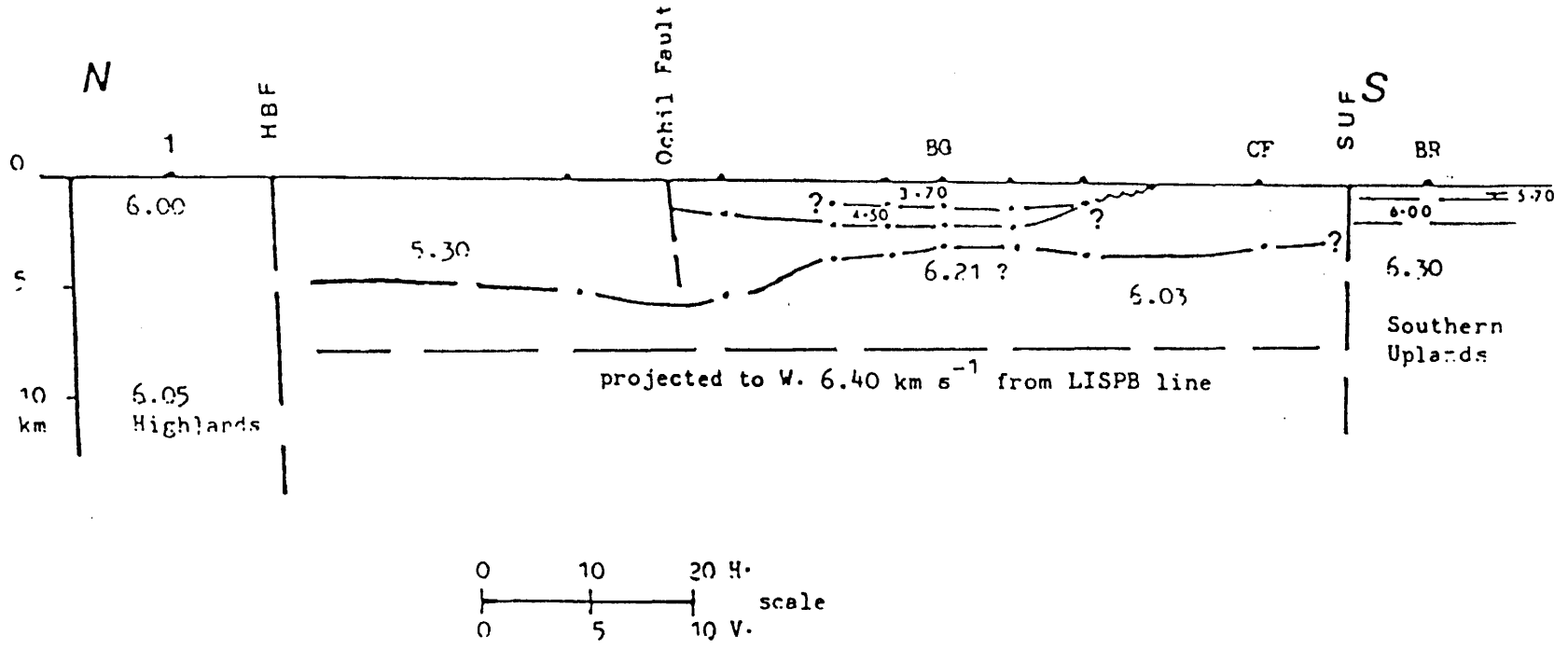

Fig 1.23 Derived seismic interpretation across the Bathgate area in the Midland Valley. (after Sola 1985) BG:Bathgate, CF:Carmichael Fault, BR:Broughton, HBF:Highland Boundary Fault, SUF:Southern Uplands Fault.

1.4 Review of Previous Geophysical Aspects

McLean and Qureshi (1966) derived their crustal model for Scotland depending on gravity coverage then available, and which did not include all gravity data from the Highlands and the Southern Uplands (see section B in 1.3.1). With a complete gravity coverage of northern Britain now available, it seems that the gravity gradients do not closely relate to the boundary faults defining the Midland Valley .

Consequently, LISPB discrimination between the Midland Valley and the Southern Uplands could be questioned on the same basis as well as the following facts:-

1. With shotpoints at least several tens of kilometres apart and recording units on average 3 km apart, the LISPB data can make little contribution to knowledge of the uppermost layers (the top 2-3 km). This could produce a misleading image for solution of deeper problems, such as whether the Midland Valley 6·4 km/sec layer is the same or different from the Southern Uplands 6·3 km/sec.

2. LISPB was recorded across the strike, therefore, seismic measurements parallel or near enough to the trend of the geological strike, would produce better estimates for the seismic layering. Of these are, Sola (1985) and Davidson (1985) who revised LISPB layer 2 from 5·8-6·0 km/sec Lower Palaeozoic sediments to down and up-dip on a 6·0-6·1 km/sec crystalline basement, as well as SUSP, which crosses LISPB with a completely different velocity structure of shallow high velocities comparable to those in the Midland Valley.

3. Bamford (1979) favours the view that the 6·3 km/sec

layer is distinct from the 6·4 km/sec to the north of the Southern Uplands Fault, although he states that it is possible that the velocity variations are within the range that might be expected from a single rock unit due to different metamorphic grade, micro-cracking, anistropy, etc. LISPB does not provide definite evidence to this question. The time-distance graph for LISPB shot E-Southward, shows an apparent velocity of 6·4 - 6·5 km/sec, extending across the Southern Uplands Fault (fig 1.24a). Sola (1985) has ray-traced this part of LISPB by combining his results with SUSP model (fig 1.24b).

Bamford (1979) considered LISPB 6·4 km/sec as an extension of the 6·48 km/sec of the Caledonian foreland (granulite-facies Lewisanian basement), although it is not recognised for certain between the Great Glen and Highland Boundary Faults. In the Southern Uplands, he did not identify the rock type associated with the interpreted 6·3 km/sec different basement. There are few clues as to the nature of the underlying basement in both the Midland Valley and the Southern Uplands. A certain amount of information and inference can be derived from the occurence of crustal xenoliths within Carboniferous vents which suggest a similarity in crustal composition between the Midland Valley and the Southern Uplands (Upton et al 1983).

There is accumulative geophysical evidence supporting the view of an unbroken basement for the Midland Valley and the Southern Uplands, at least under the Northern Belt which LISPB did not exclude by saying that the basement boundary under the Southern Uplands Fault may dip at quite a low angle (Powell 1970, 1971; Warner 1982; Hall et al 1983, 1984; Davidson et al 1984; Sola 1985; Davidson 1985).

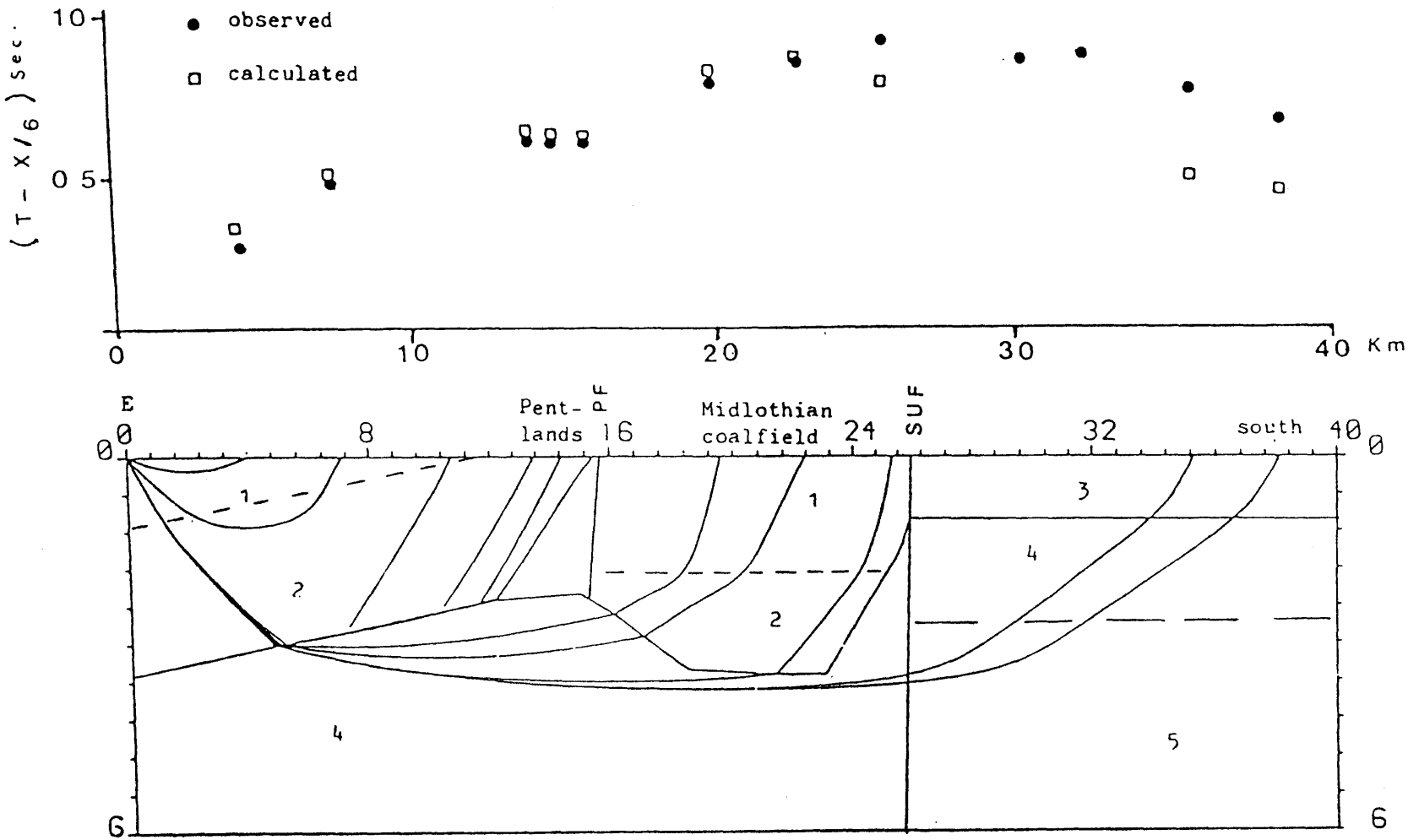

Fig.1.24 LISPB line from shot E - south. (A) Reduced T-X/6 graph shows the observed and calculated travel times. (B) Ray-tracing model for LISPB (from shot E - south)
1 Carobinferous rocks 2 Lower Old Red Sandstone 3 Lower Palaeozoic
4 a_o refractor 5 6.30 km s^{-1} refractor

(after Sola 1985)

The Ballantrae ophiolite on the boundary between the Midland Valley and the Southern Uplands constitutes the basement for the Lower Palaeozoic succession in the Girvan District. This succession in turn resembles the succession in the Southern Uplands Northern Belt (see 1.2.5), therefore, the ophiolites might constitute a basement for the Northern Belt. The occurence of ultrabasic rocks in the Heads of Ayr vent (see 1.2.2) could involve a northerly extension of the ophiolites underneath it.

1.5 Aims of the Present Investigation

The present work is an extension of the continuing investigation of the upper crustal structure in the Midland Valley and the Southern Uplands, with particular emphasis on the Ballantrae ophiolite complex at the boundary between them.

The objects of this thesis are threefold:-

1. To determine the range of p-velocities attributive to the Ballantrae ophiolite complex, and hence to provide more conclusive information on the nature of the crystalline basement(s) in the study area.

2. To investigate the areal extensions of the ophiolites in the Midland Valley and the Southern Uplands.

3. The previous two points could be better achieved by having the velocity distribution of the surrounding and/or overlapping rocks. Then, it is one of the objects to have velocity measurements on such rocks.

CHAPTER TWO

Data Acquisition, Processing and Presentation

2.1 Introduction

The acquisition of the seismic refraction data used to attempt to solve the problems outlined at the end of Chapter 1 took place over a number of years. The seismic sources used included shots fired as parts of other seismic experiments, quarry-blasts, and a single dedicated shot. The seismic refraction data were acquired as follows:

	Year	Source	Recording	Section
1.	1979	WISE	Lendalfoot Array	2.2
2.	1982	CSSP	Galloway Line	2.3.3A
3.	1983	Hillhouse Quarry	Girvan Line	2.3.3B
4.	1984	Hillhouse Quarry	Loch Doon Line	2.3.3C
5.	1984-85	Benbain Open Cast	Colmonell Line	2.3.3D
6.	1985	Rough Hill Open Cast	West Ayrshire (fan shooting)	2.3.3E
7.	1985	Navy Shot (off Corsewall Point)	Portobello-Troon Line (reversal of Girvan Line)	2.3.3F

Seismic data studied in this thesis fall into

two categories in relation to the writer's involvement, which began in 1980:-

A. Pre-existing, but uninterpreted data. These include marine shots (explosive & airguns) of the Western Isles Seismic Experiment (WISE), and some land shots, all recorded on the Lendalfoot Array in 1979 (fig 2.1, 2.2 and tables 1-3 of appendix 1).

B. Subsequently acquired data which can be summarised as:

   1. Laboratory velocity measurements of samples from the Ballantrae ophiolite suite and greywackes from the Southern Uplands. These results are presented in appendix 3 and will be discussed in chapter 3.

   2. Field velocity measurements by means of refraction profiles 40-65 km long, recorded across the study area (tables 4-9 of appendix 1).

It should be noted that in order to simplify the description and discussion of the data, names were ascribed to shots and recording stations according to the nearest locality. This chapter is devoted to the presentation and discussion of data acquisition, and to the methods used in enhancing the signal-to-noise ratio of the data of part (A) above. The pre-existing data will be discussed in section 2.2 and subsequent data acquired in this research will be discussed in section 2.3.

2.2 The Western Isles Seismic Experiment and the Lendalfoot Array

An eight station seismic array, sited on the Ballantrae Ophiolite Complex and adjacent Lower

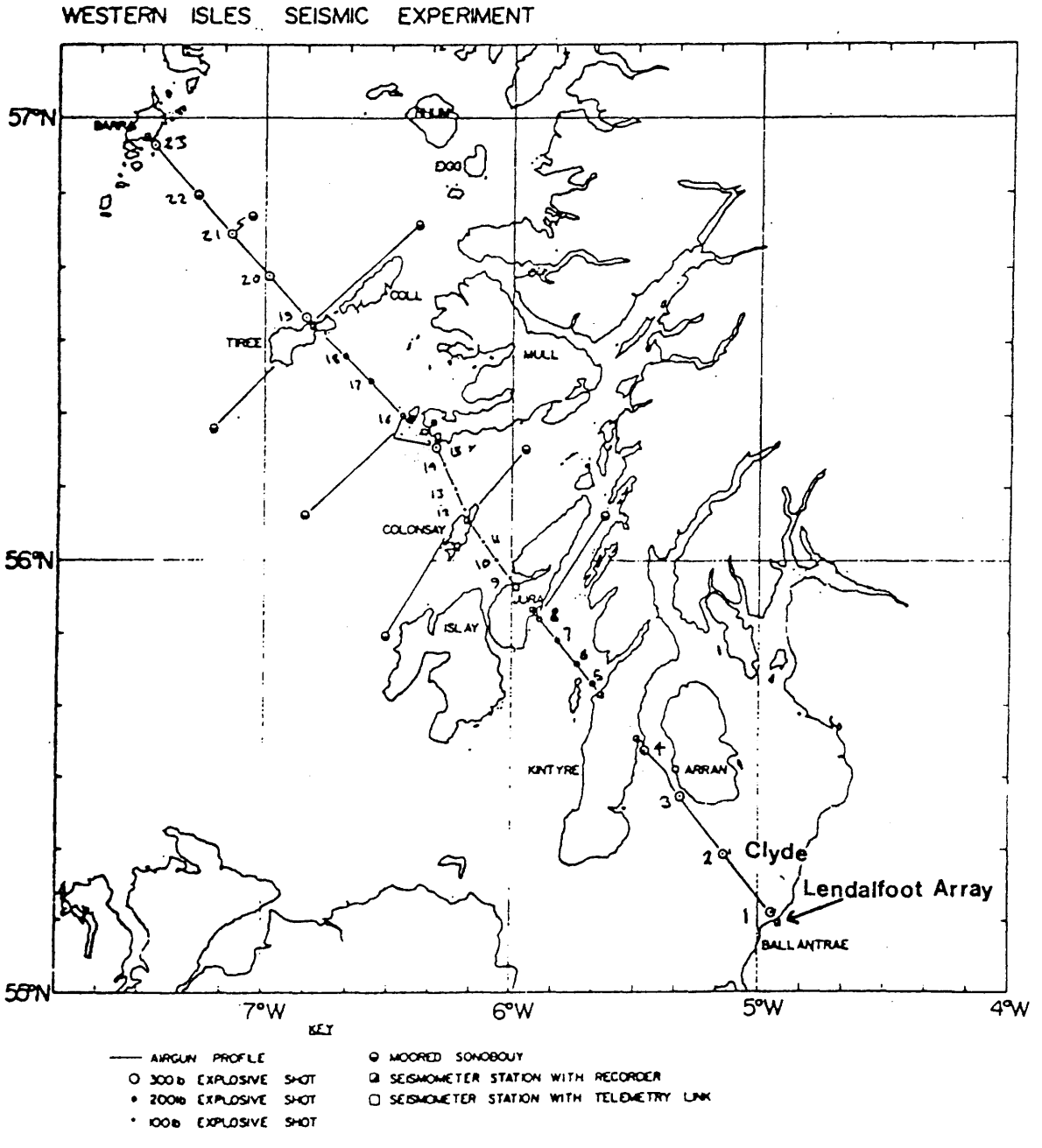

Fig 2.1 Layout of the Western Isles Seismic Experiment in refrence to the Lendalfoot Array.

Palaeozoic sediments, was in operation during the Western Isles Seismic Experiment (WISE) in November 1979, and recorded a line of marine explosive shots from the Clyde to Barra, and an air-gun line in the Clyde (fig 2.1).

The recording array was formed by two lines of vertical seismometers at 2 km spacings convergent on the Lendalfoot shore station. One line was in-line with the WISE shot line, across the local geological strike; the other was parallel to strike (fig 2.2). The Clyde air-gun shots presented a range of azimuths and offsets into the array. Three land shots were fired at receiver stations and three more on the landward extensions of the lines (to 5 km offsets). The intent was that such a pattern of shots would permit the calculation of change in velocity with depth to several kilometres below the array.

2.2.1 WISE Data

Analogue records adequate for picking arrival times, were made up of all the land and marine explosive shots received at the Lendalfoot array. Such records were not prepared for the air-gun shots, as it was thought that the amount of data to be examined required the use of a computer. The air-gun data were digitised, and computer expanded-time records were prepared after applying a number of sophisticated filtering techniques (see section 2.2.1) to improve the first arrivals.

The WISE data extracted from the Lendalfoot array are as follows:

A. Land shots: all six shots were recorded successfully on most of the seismometers. Table 1 of appendix 1

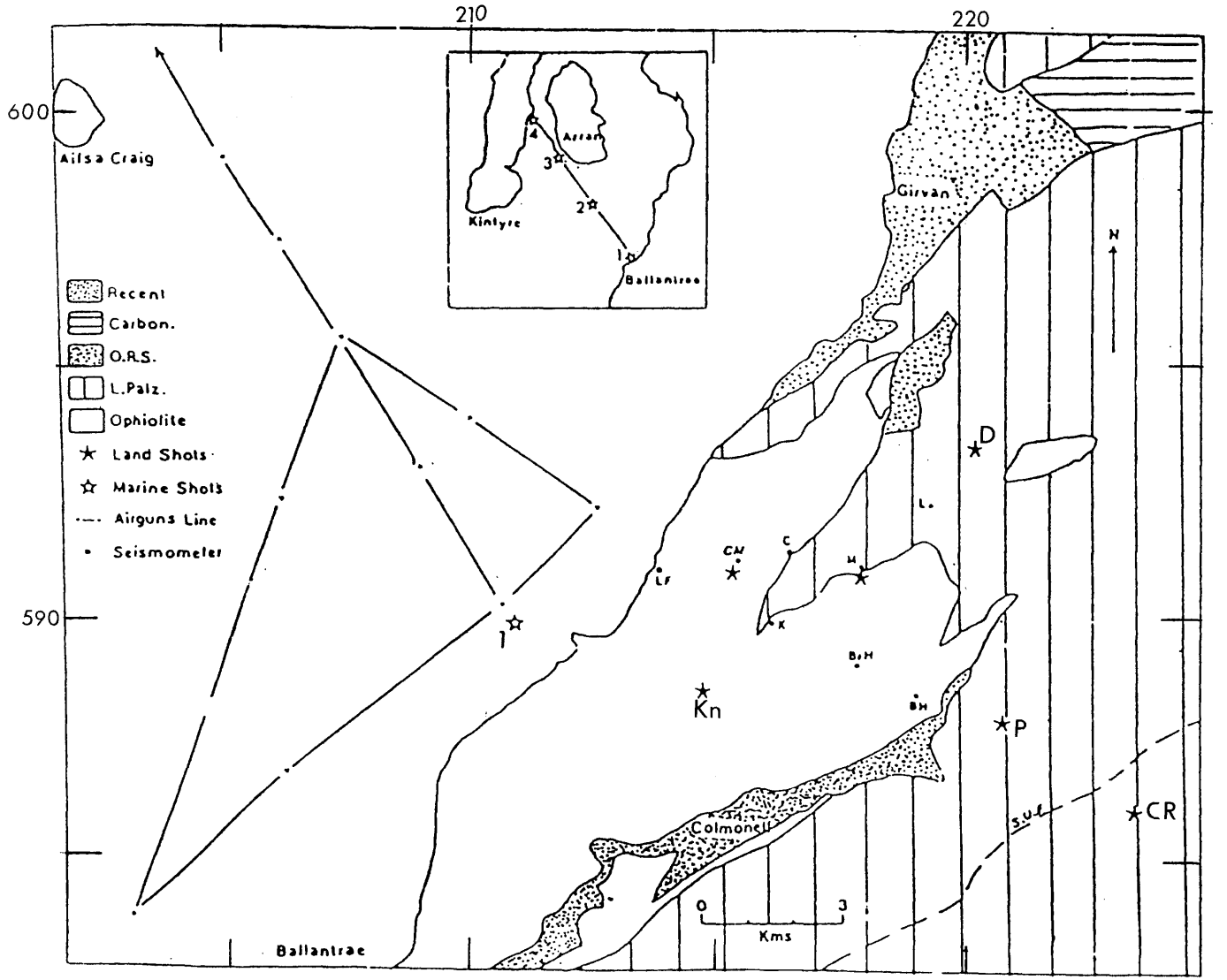

ORS:LOld Red Sandstone

L.Palz: Lower Palaeozoic

SUF :Southern Uplands Fault

Land Shots
CM – cundry mains
CR – craigconnachie
D – dinvin
Kn – knockormal
M – millenderdale
P – pinnmore

Fig 2.2 Geological map of the Girvan district showing the Lendalfoot Array and some WISE shots.

is a list of the time-distance relationships for shot-seismometer pairs. Blank time columns are a result of either the signal being obscured by a high noise level, or a seismometer did not record that particular shot. The shots make different azimuths with ranges between 0·1 - 10 km into the array, with an extra seismometer (Pinbraid Bridge) recording two shots only. Short ranges provide information on the near surface velocities of the present rock types. Comparable ranges in different directions give an idea on any lateral variation in velocity. This could be seen on fig 1 appendix 2, which represents a reduced time-distance graph of each shot received on the array. Marked differences in the arrival times could be noticed on the Millenderdale shot (ranges of 2·2 and 2·5 km), Knockormal shot (ranges of 3·3 and 3·4 km) and Cundry Mains shot (ranges of 4·4 and 4·5 km).

B. Marine explosive shots: WISE marine shots 1,2,3 & 4 recorded at the Lendalfoot array (table 2 appendix 1) give four discrete clusters on the reduced time-distance graph (fig 2 appendix 2). Therefore, a continuous picture of the apparent velocity depends upon considerable interpolation. High apparent velocities ($>$ 6·4 km/sec) are observed on each of the last three clusters. The four shots could be aligned with the across-strike recording arm of the array, and high apparent velocities ($\geqslant$6·4 km/sec) are obvious in fig 2.3.

C. Air-gun shots: only air-guns fired within 14 km of the Lendalfoot array could be evaluated after the computer analysis. These shots were very closely spaced (200m apart) and representative shots at different ranges are listed in table 3 appendix 1. Currarie and Millenderdale seismometers did not record the air-gun shots. At other stations

Numbers refer to seismometers involved from the Lendalfoot array (see table 2 appendix 1).

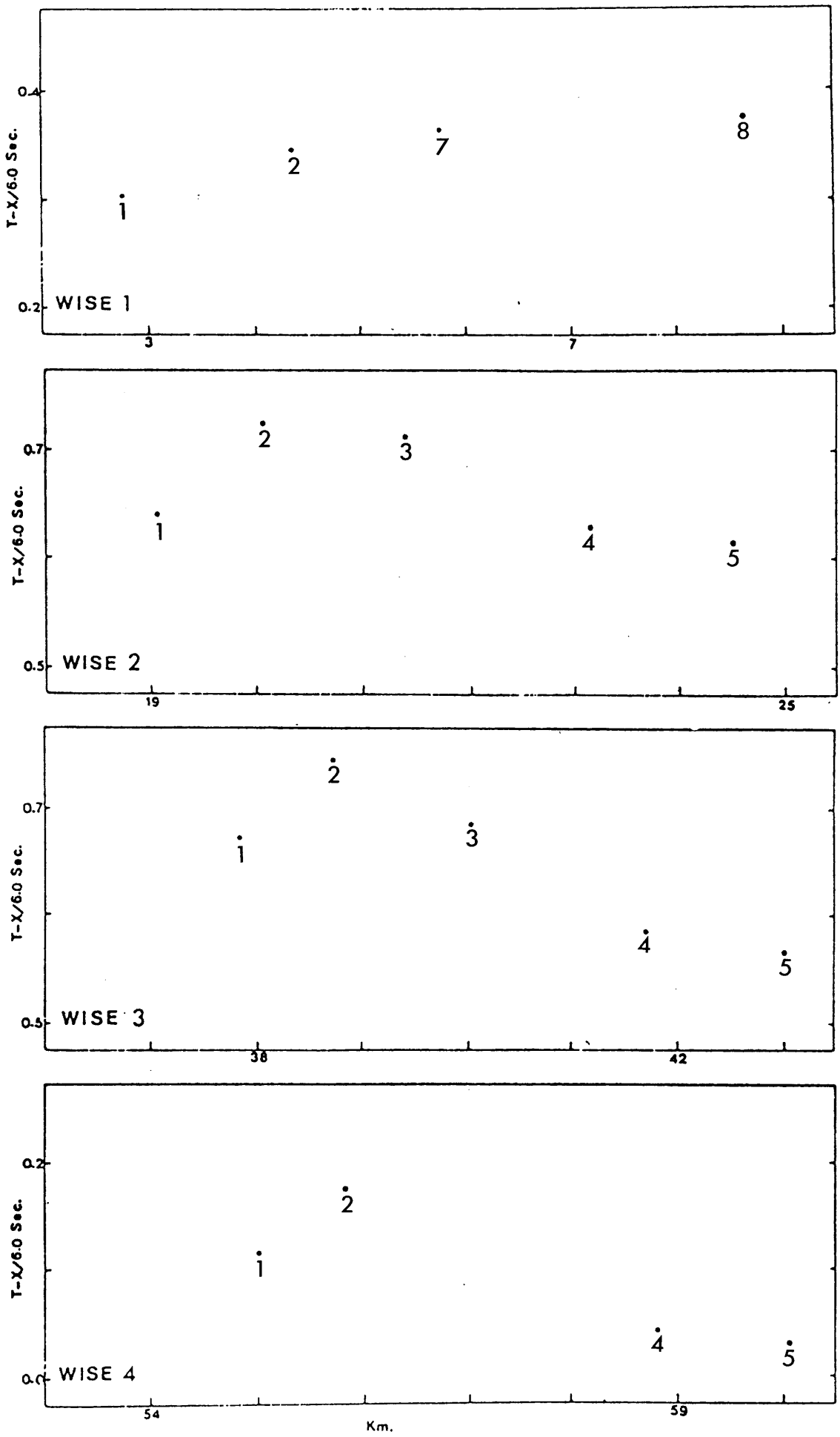

Fig 2.3 Reduced time distance plots of first arrivals from the WISE explosive shots recorded on the across-strike arm of the the Lendalfoot Array.

occasional shots were observed by high background noise levels.

A reduced time-distance plot of five selected air-gun shots in alignment with the across-strike recording arm shows a continuous increase of apparent velocity with range, and different delay times under the shots (fig 3 appendix 2). The apparent velocity approaches 6·0 km/sec at ranges of 8-10 km.

2.2.2 Digitisation of the WISE Air-gun Data

The large number of air-gun shots and the use of advanced techniques (see 2.2.4) to enhance the P-wave signals, prompted the digitisation of the air-gun data. The Lendalfoot data were digitised by Durham University at the British Geological Survey, Edinburgh. Channel relationships between analogue and digitised data are shown in table 2.1.

First Tape		Channel	Second Tape
Int. Clock		1	Int. Clock
Flutter Channel		2	Flutter Channel
Letterpin		3	Cundry Mains
Bargain Hill		4	Knockbain
Lendalfoot	H. Long	5	Currarie
	Vertical	6	Millenderdale
	H. Transv.	7	Breaker Hill
M.S.F.		8	M.S.F

Table 2.1 Channel number on digitised tapes and its relation to analogue recording.

A sampling rate of 64 samples/sec was used, since this was the maximum possible for the recording speed used for WISE. Occasional corruption of the radio signal and internal clock caused problems during the digitisation process, since the computer program that controls the digitisation relies on being able to read the time code. This was overcome by using a manual digitisation operation and starting and stopping the tape at the points about the region to be digitised.

2.2.3 Processing of the Air-gun Data

The digital conversion of the air-gun data is schemed in fig 2.4. To run the data on the ICL 2976 computer at Glasgow University (known as GVME), it was first transcribed by a compatible format by the Data Transfer Service of the University Computer Centre. Conversion of the large number of air-gun data files from binary to character format would have cost considerable expense to the Computer Centre. To half these expenses, the Lendalfoot digitised data were transferred directly to the GVME in their binary format (fig 2.5a), and then program "CHARACTERVAR" was used to decode binary integers into characters. The program calls the subroutine CV which was kindly provided by Dr R MacKenzie of the Computer Service. The character data (fig 2.5b) are then passed through program "TRANSLATE" to decode into actual numbers (the amplitude coefficients, fig 2.5c).

The plotting program "DRAW" has been adopted to display the data in absolute or reduced time-distance sections (Ali 1983). The program provides a comprehensive choice of processing in the time domain and written to allow processing with a wide choice of filters. Necessary adaptations were made by the author to suit the WISE Geostore data.

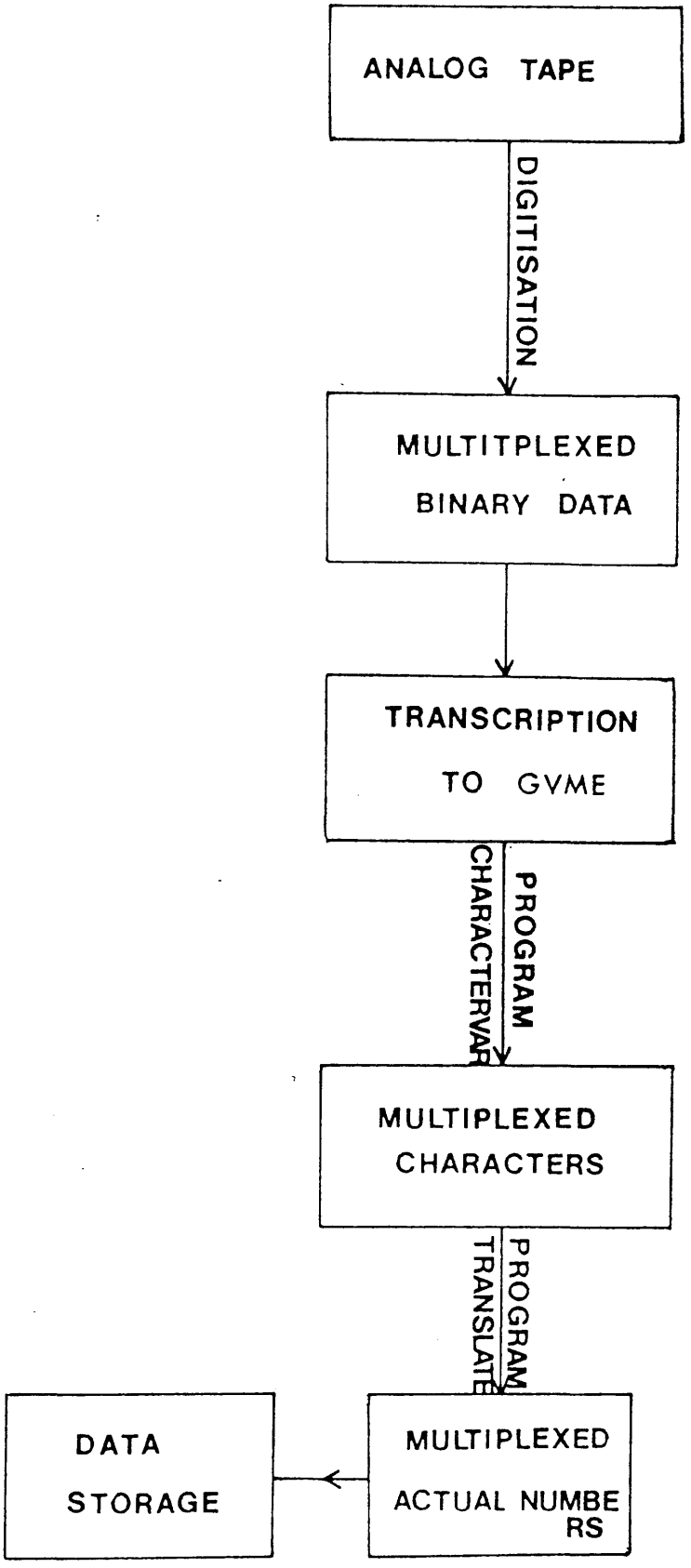

Fig 2.4 Diagram showing the main steps of digitising the analogue air-gun data.

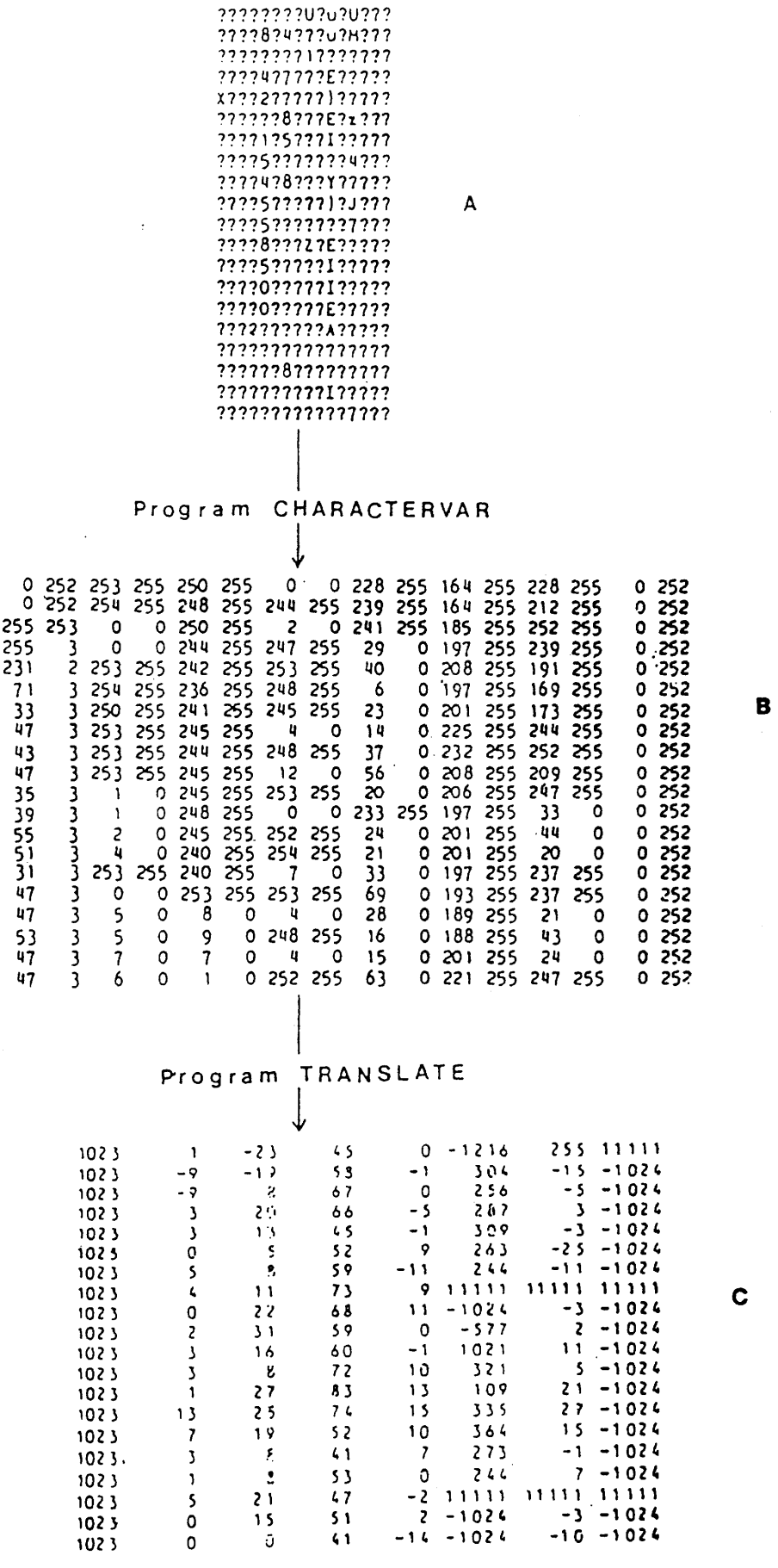

Fig 2.5 Showing the steps of processing the digitised data into real numbers.

A:Binary data B:Character data C:Real numbers

A plot of the nearest air-gun shots to the Lendalfoot station (fig 2.6) has shown that the seismograms and the time channel are dominated by abnormal high amplitude spikes. Initially, they were thought of as being generated by a faulty Geostore recording set or a damaged tape. Whilst revising the data files, the sporious big numbers (eg, 11111 in fig 2.5c) were found to be not a feature of the original data, but were generated by unbalanced subroutines within the software upon GVME which catalogued files on magnetic tapes. Dr P Rosenberg has amended the subroutines, and the whole data files were recatalogued.

2.2.4 Filtering Techniques Used on the Air-gun Data

The air-gun profile provided only a limited amount of data that could be picked by eye (fig 2.7). It can be clearly seen from the records that on most of the traces, the signal-to-noise ratio is very low, and on many the signal cannot be seen at all. To improve the data quality, the main steps followed by Durham University in processing other WISE air-gun data, were adopted. These are different band-pass filters, cross-correlation and predictive deconvolution techniques. Subroutines to perform these operations were obtained from Durham University and adapted for use on GVME within the program DRAW.

The object of a band-pass filter is to transmit a required frequency band and to attenuate frequencies outside this pass-band. Two kinds of band-pass filters were applied:

A. Robinson's band-pass filter (Robinson 1966): gives complete transmission of the pass-band and steep attenuation outside (fig 2.8a). The poor effect of this filter on the air-gun data is shown in fig 2.9.

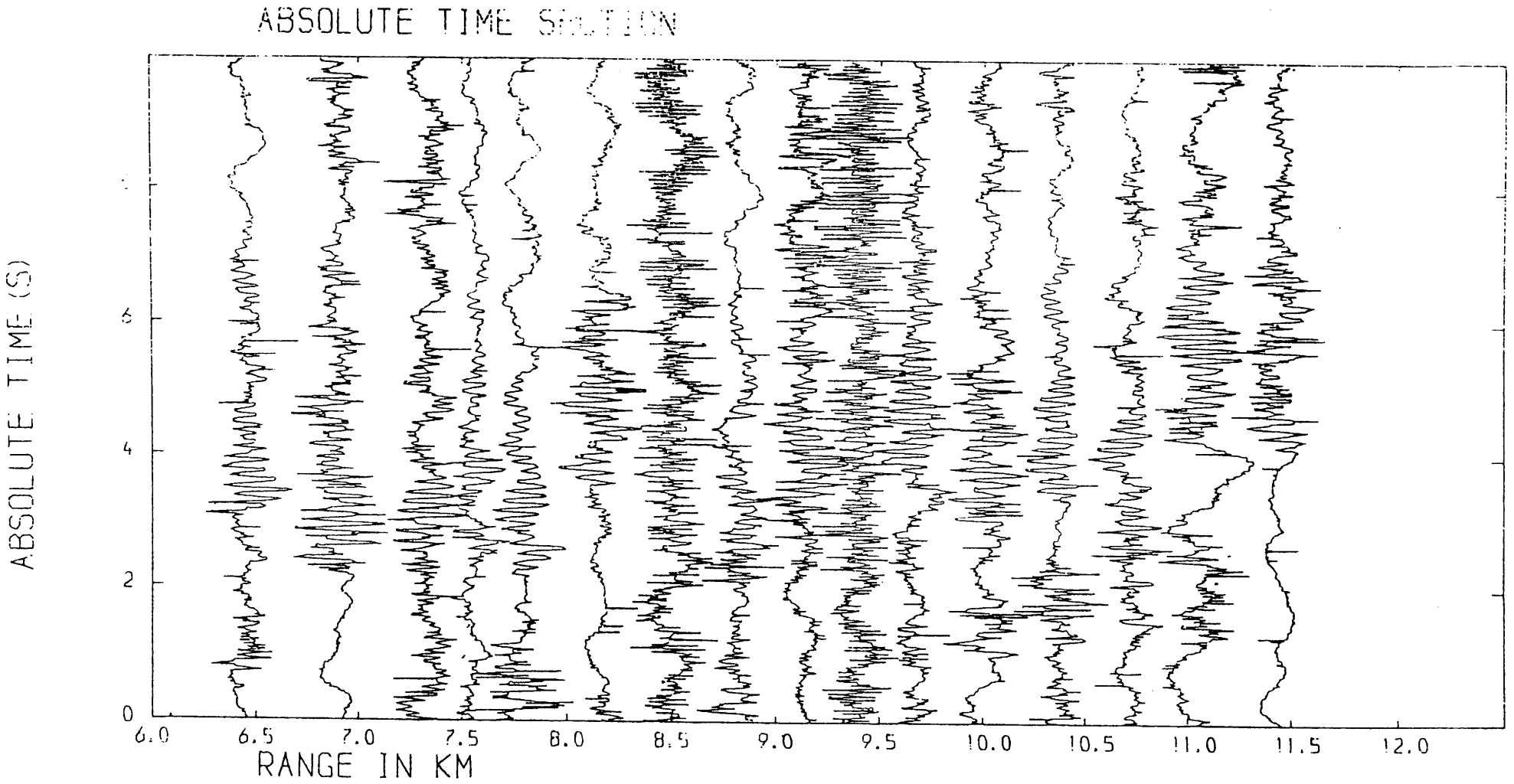

Fig 2.6 Air-gun shots recorded on the lendalfoot seismometer showing spiky high amplitudes on all the traces

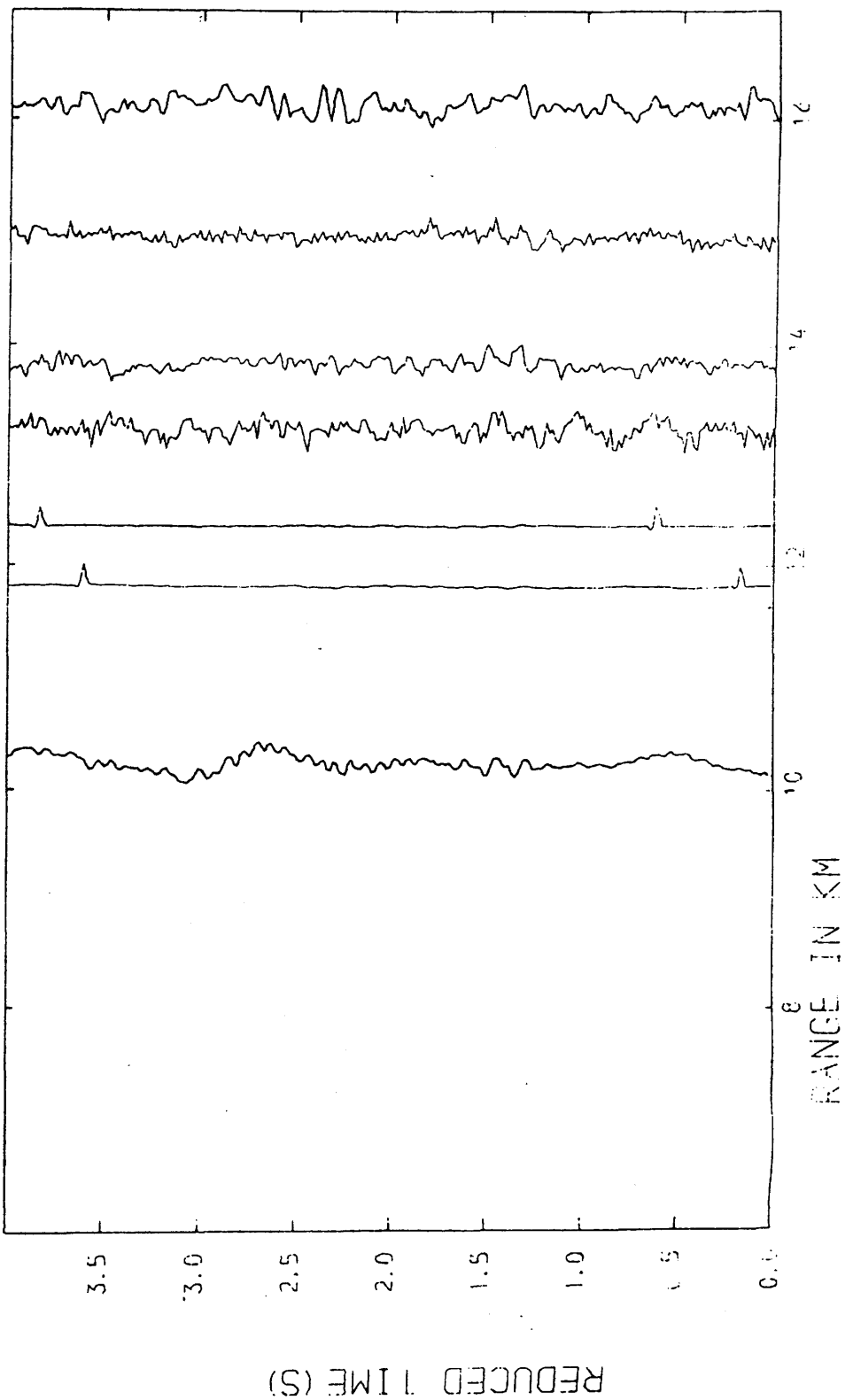

Fig 2.7 Air-gun shot no.222 recorded on the Lendalfoot Array.

Note that the 2nd & 3rd seismometers are faulty.

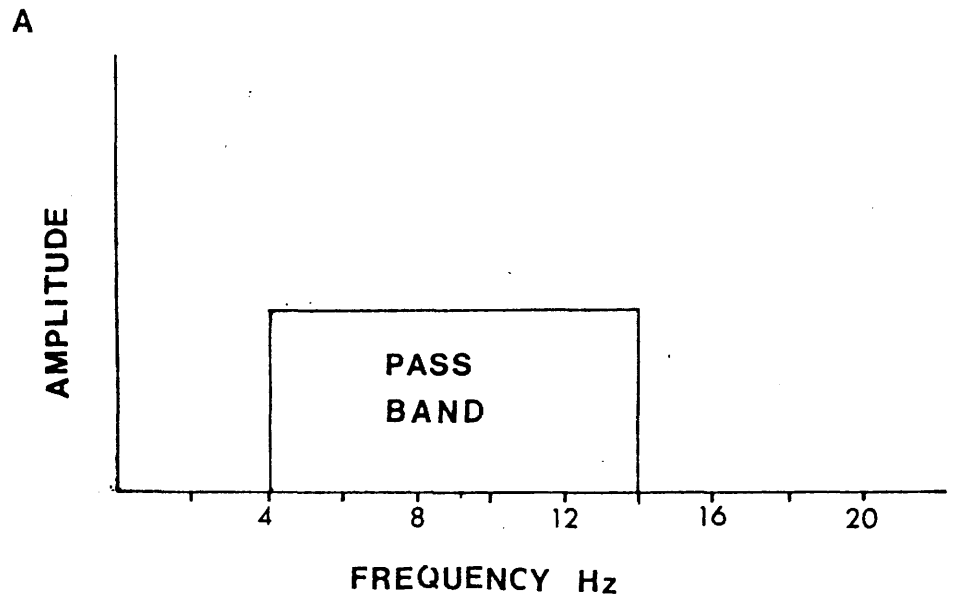

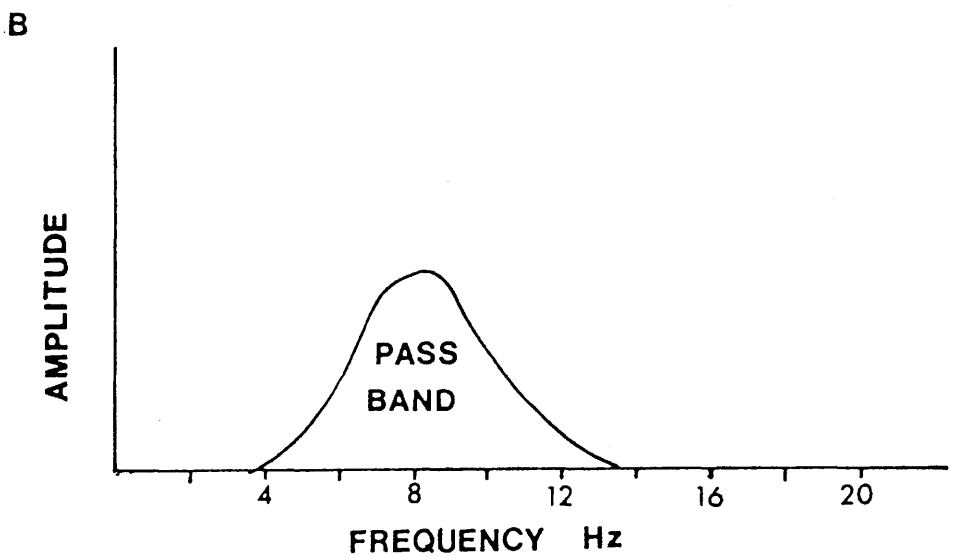

Fig 2.8 Illustration of the differences between the Robinson (A)and the Hanning(B)band-pass filters.

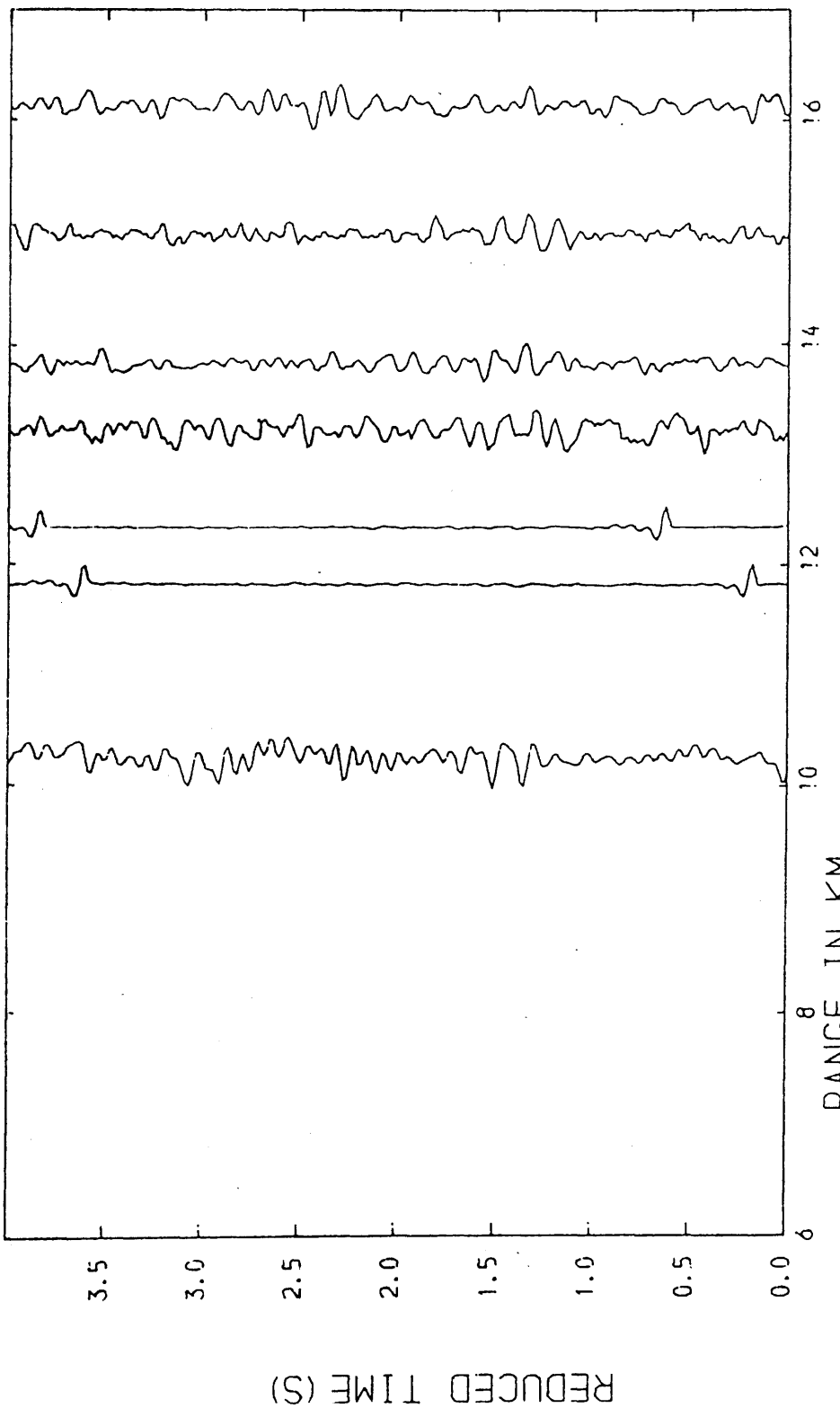

Fig 2.9 Reduced time-distance graph of the air-gun shot shown in fig 2.7 after applying 4-13Hz Robinson band-pass filter.

B. Hanning band-pass filter (Blackman & Tukey 1958): shows a distinctive feature of gradual roll-off on either side of the central frequency within the pass-band (fig 2.8b). Improved resolution can be expected in case of appropriate adjustment of central frequency of the filter with central frequency of the signal. P-wave signals of the air-gun shots occupy a low frequency range, and with reference to some shots recorded on the Lendalfoot seismometer (fig 2.10), it is observed that central frequencies lie between 7-9 Hz, so the filter cut-off frequencies were designed to be 4-12 Hz. This filter proved to be more effective in attenuating the noise (fig 2.11).

After the initial processing, it was expected that the onset might be picked reliably on an increased number of records. The maximum range of good arrivals did not exceed 12-14 km. It was hoped that the arrival could then be found on the poorer traces by use of cross-correlation.

Cross-correlation filtering as applied to seismic data, has been described by Jones and Morrison, (1954), Schneider and Backus (1969) and Kanasewich (1981). Briefly, cross-correlation filtering consists of searching a trace for the occurence of an expected wave form by the mathematical (or electrical) operation of cross-correlating the trace with the expected wave form (Smith 1958). The estimate of the signal was obtained by adding the windowed first arrivals on the Lendalfoot array, from a near air-gun shot, and finding the average. The position of addition was determined by finding the position of maximum cross-correlation between the traces. The average wave form was then correlated with traces of farther shots and the position of maximum correlation was deemed to be that of the onset of the signal. This filter did not give significant improvement in signal quality, since the cross-correlation of the noise and

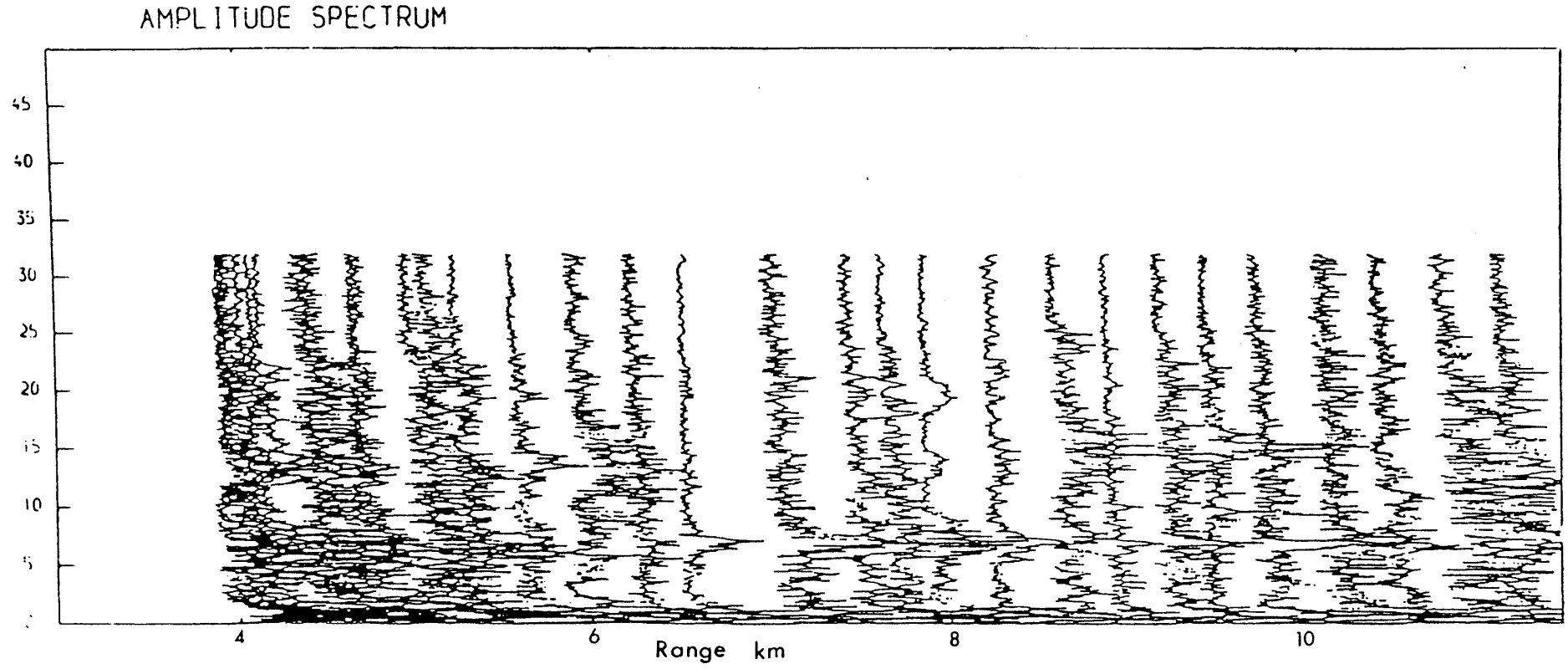

Fig 2.10 P-wave frequency analysis for air-gun shots recorded on the lendalfoot seismometer. Peak frequencies are 7-9 Hz.

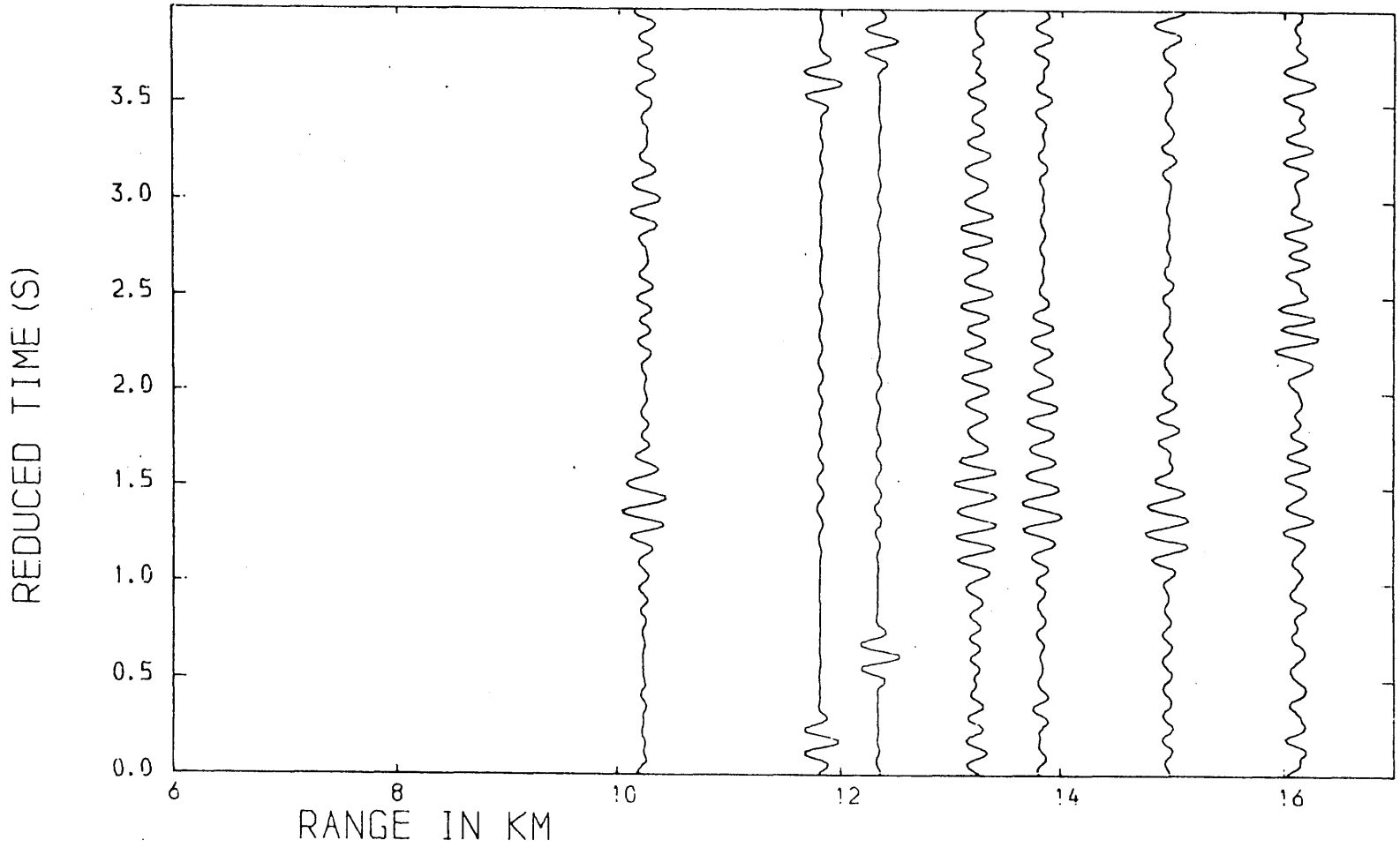

Fig 2.11 4-13 Hz Hanning band-pass filter applied on air-gun shot shown in fig 2.7.

the signal was as high as the autocorrelation of the signal. The effect of this filter is shown in fig 2.12. One of the problems was that the number of cycles of the wavetrain varied from trace to trace, so if correlation was attempted in such a situation, then an incorrect position for the onset of the signal may have resulted. Warren (1981) suggested that predictive deconvolution could be used to truncate the signal and leave the same number of cycles on each trace to give a distinctive character to the signal for its detection by matched filtering. Summers (1982) has shown that the use of predictive deconvolution is inappropriate in that the air-gun data do not conform to the assumptions upon which the technique is based. It was not developed for enhancing signals immersed in noise of equal or greater amplitude.

2.3 Field Velocity Measurement

2.3.1 Instrumentation

The system used to collect seismic data was the Glasgow F.M. seismic instrument, designed and constructed by Mr G Gordon in the Geology Department, to the specification of Dr J Hall.

The field-system comprised of 7 recording instruments (now 50 sets) with integral amplifier/ modulator and tuned radio receiver to record MSF time signals from Rugby. The recorders have a remote-start mechanism and electronic clock that allows them to be deployed up to 24 hours, before a recording window. Using a C120 tape, the maximum recording period is one hour. In this system, the seismic signal is pre-amplified and 60 Hz low-pass filtered. The signal is then presented to two independent variable gain amplifiers that have a set gain difference of 18 dB. The 'A' amplifier has a

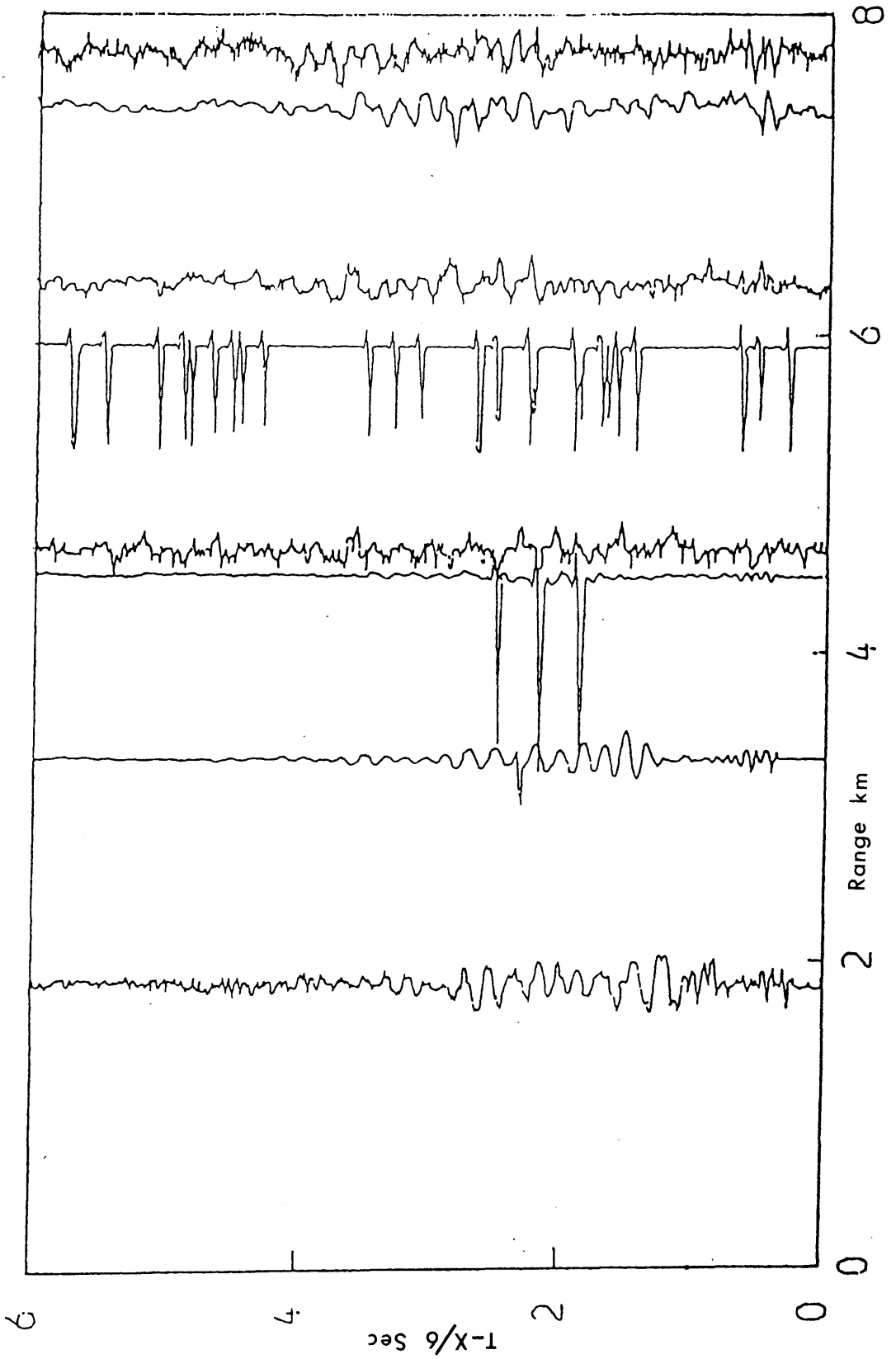

Fig 2.12a Air-gun shot no.220 recorded on the Lendalfoot Array.

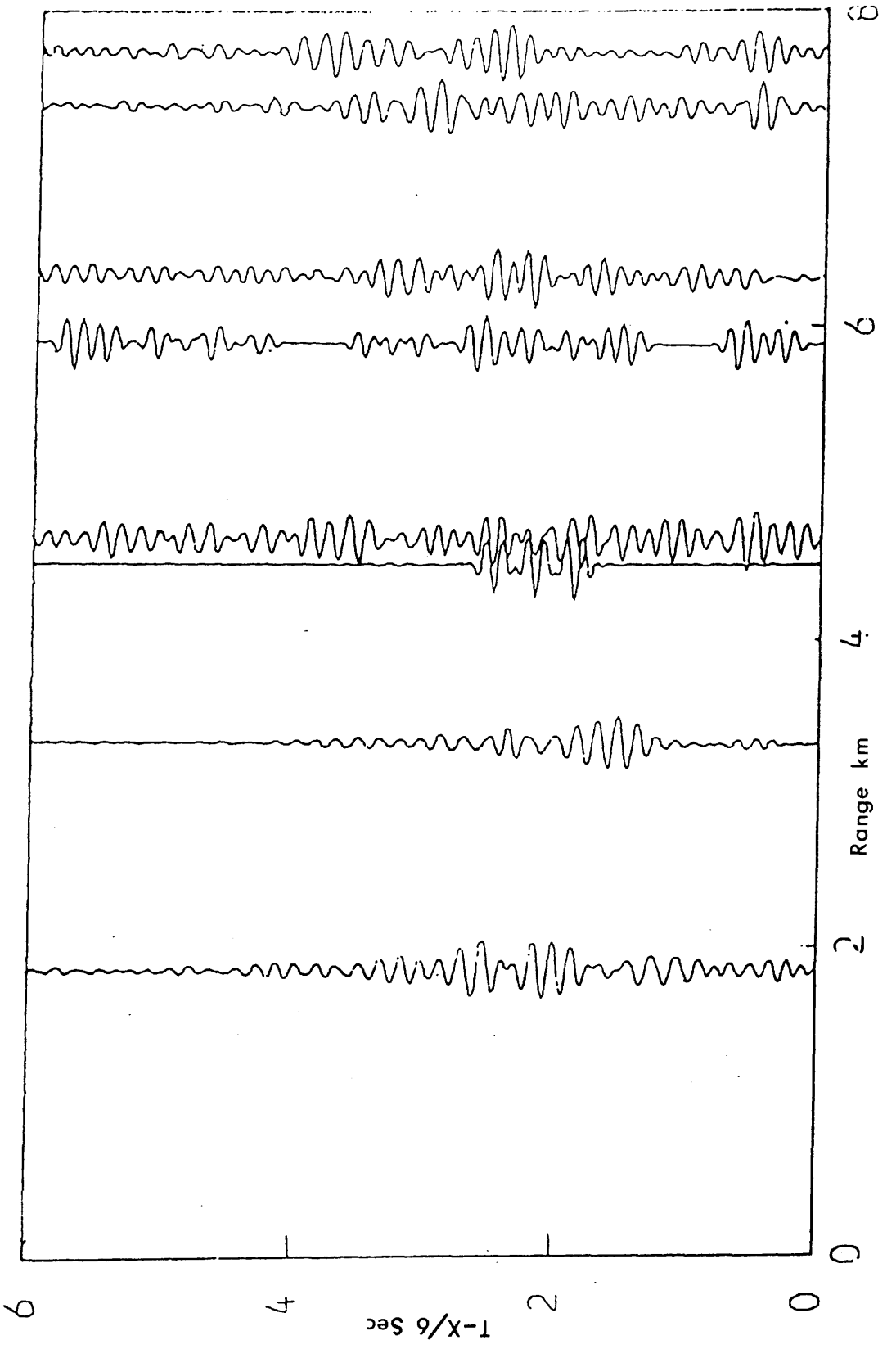

Fig 2.12b 4-12 Hanning band-pass filter applied on shot 220.

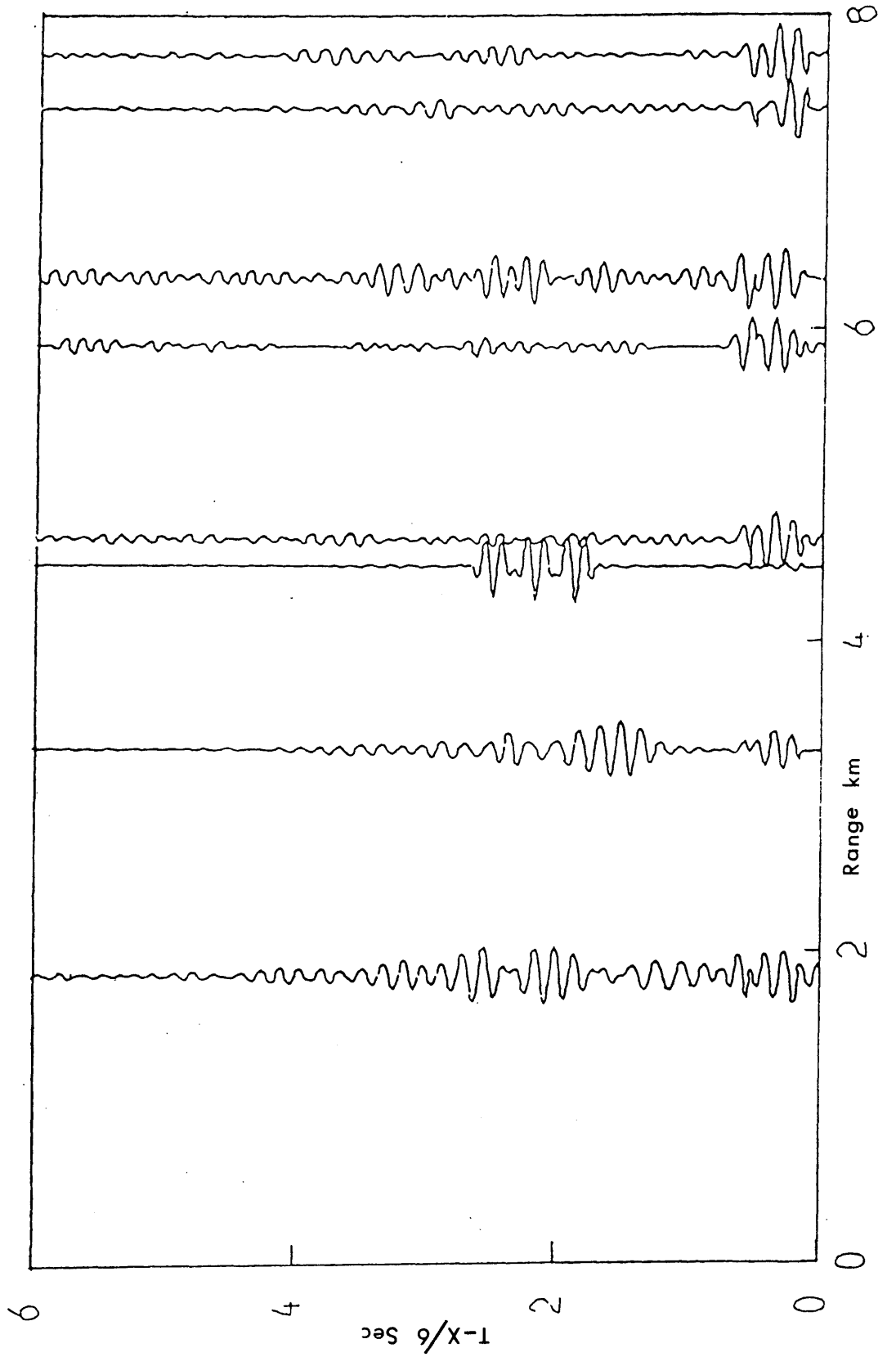

Fig 2.12c Cross-correlation of the data of fig 2.12b with a selected waveform.

gain range of 82 - 112 dB in 6 dB steps and the "B" amplifier a gain range of 64 - 96dB (fig 2.13).

A frequency modulation system is used so that a bandwidth of 2-60 Hz can be recorded on standard magnetic tape. In F.M. system the carrier frequency deviation is directly proportional to the frequency and amplitude of the seismic signal. A carrier frequency of 3 kHz was used as this ideal for tape recording. The maximum amplitude for the seismic signal after amplification is 8V peak-to-peak and this produces a deviation of $\pm$ 80% of the carrier signal.

At maximum gain the dynamic range is amplifier limited to 52 dB increasing directly with gain reduction until limited to about 60 dB by modulator/demodulator noise.

A tuned-radio receiver is built into each seismic recorder. When the 60 kHz MSF signal transmitted from Rugby is present, the output from the radio is a square wave in synchronisation with the transmitted time code (fig 2.14). This square wave signal is used to gate a 3 kHz oscillator to produce tone bursts that can be recorded on the same tape as the seismic signal. On playback, the time signal can be decoded and displayed in digital form so that events can easily be located on the tape.

The playback system consists of a cassette player, demodulator, filters and ultra-violet recorder. The cassette player reproduces the F.M. signals free of instrument noise and then it is amplified and clipped to provide a suitable signal for demodulation. The demodulator has a buffered input and is followed by a low-pass filter to remove any residual F.M. signal from the demodulated seismic signal. Filtering used was between 4-20 Hz. The filtered demodulated signal can now be

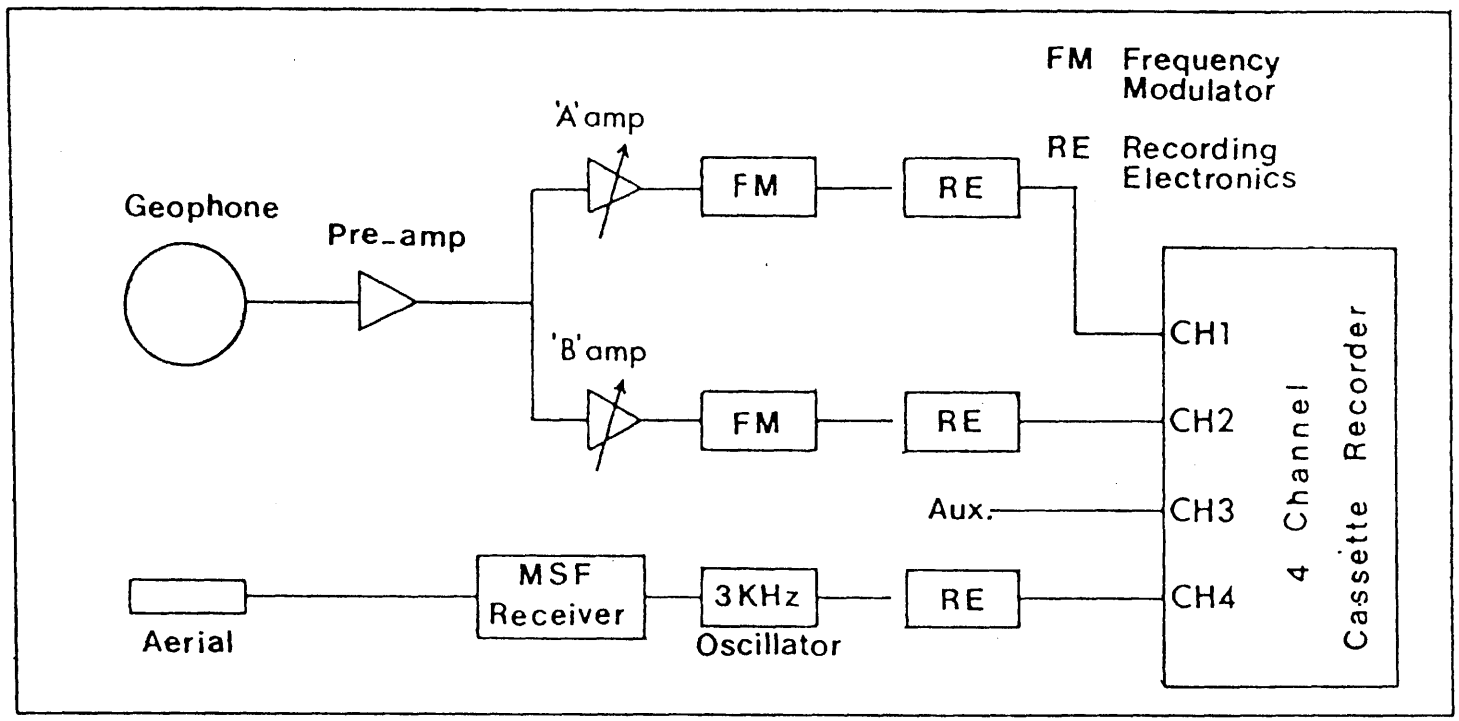

Fig 2.13 Block diagram showing the complete recording arrangement.

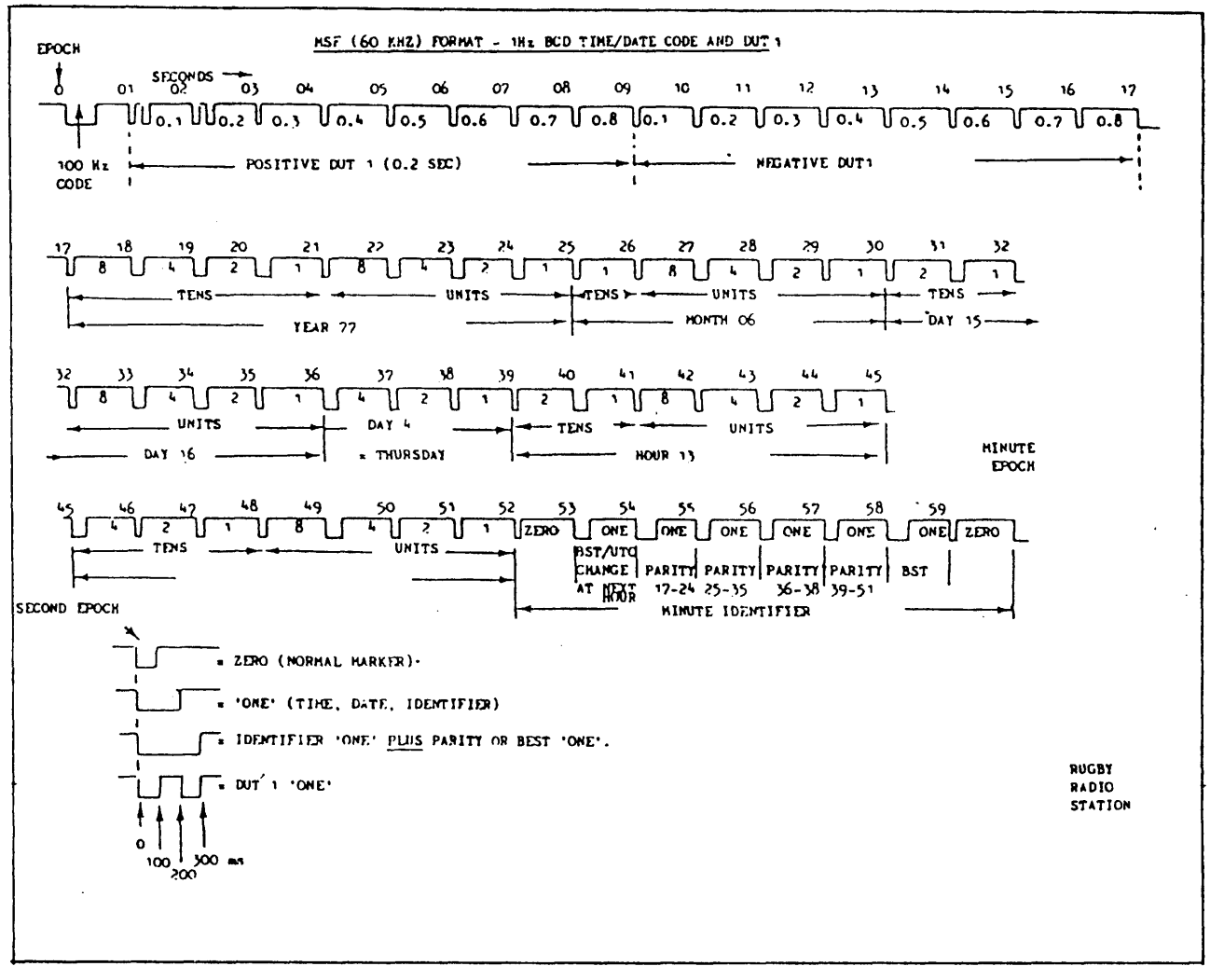

Fig 2.14 Shows MSF slow code.

amplified for driving the galvanometers on a UV recorder series with a selected speed. The galvo-amplifier can amplify the seismic signals over the range of 0·01v/cm to 20v/cm, and a hard copy of the seismic traces can be obtained.

2.3.2 Fixing a Recording Site

Seismometers at sites near to the quarry can be planted or buried into the ground if rock outcrop is not available. As the distance between the shot and seismometer increases the need for fixing the seismometer on rocks becomes crucial, since the seismic energy would be expected to be more attenuated with range.

Quarry blasts were recorded on buried seismometers up to a range of 15 - 20 km. Beyond this range, the arriving energy is too weak to be detected unless the seismometer is on rock. Finding a rock is not always easy, especially in South Ayrshire where the land is thoroughly cultivated. Dip and strike arrows on solid geological maps, as well as drift maps helped in locating rock sites. Such sites were used up to $\pm$ 1-2 km on either side of the intended seismic profiles. Most of the rock exposures have no sizeable joints or fractures within which the seismometer spike could be located. Cracks are invariably either larger or smaller than the optimum wanted, or do not allow vertical mounting of the geophone. The conventional method is either to widen narrow cracks using a chisel and hammer, or to narrow the width of them by forcing wood or metal wedges around the seismometer spike. This may not always be successful, but if so, to occupy many sites on a firing day would be prolonged.

A new simple technique to overcome this

problem was designed by Mr G Gordon during the course of this study, which can be summarized as follows:

A seismometer mounting tripod is made in light alloy to replace the conventional seismometer spike. The tripod mount can then easily be located on most outcrops and adjusted to ensure that the seismometer is vertical. Close-coupling to the rock is achieved by waxing the mount to the rock using an engineering material, wax type A-46 from Brunner Machine Tools Ltd. A small gas blow-lamp is used as a heat-source to melt the wax over the feet of the tripod onto the rock. This method of mounting the seismometer was found to be effective even on wet rock, but it is necessary to remove dust and loose material from the rock surface to ensure firm coupling.

At the conclusion of the survey, the seismometer can be unscrewed from the tripod mount leaving the tripod on the rock to be used on another occasion. Sites prepared in this way have been re-occupied over a two year period with good results.

2.3.3 Recorded Seismic Refraction Lines

Six seismic refraction profiles were recorded during the course of this study (fig 2.15). The layout and the spacing between the recording stations was dictated by the locations of the source of energy, and the access and availability of rock sites for recording.

A. Galloway Line:

This line was recorded by placing seven recording stations across the Galloway region, to record explosive shots M5-M12 (fig 2.16) of the

Fig 2.15 Network of the recorded profiles in relation to Fig 1.1

A: Ayr, AC: Ailsa Craig, B: Ballantrae, Bb: Benbain open-cast, BH: Burrow Head, D: Dalmellington, FC: Firth of Clyde, G: Girvan, HA: Heads of Ayr, HQ: Hillhouse Quarry, K: Kirkoswald, Kb: Kirkcudbright, LD: Loch Doon, LR: Loch Ryan, Mb: Maybole, Mn: Mauchline, N: Newton Stewart, P: Patna, Pb: Portobello, RH: Rough Hill open-cast, S: Stranraer, Sq: Sanquhar, St: Straiton, SUF: Southern Uplands Fault, W: Wigton.

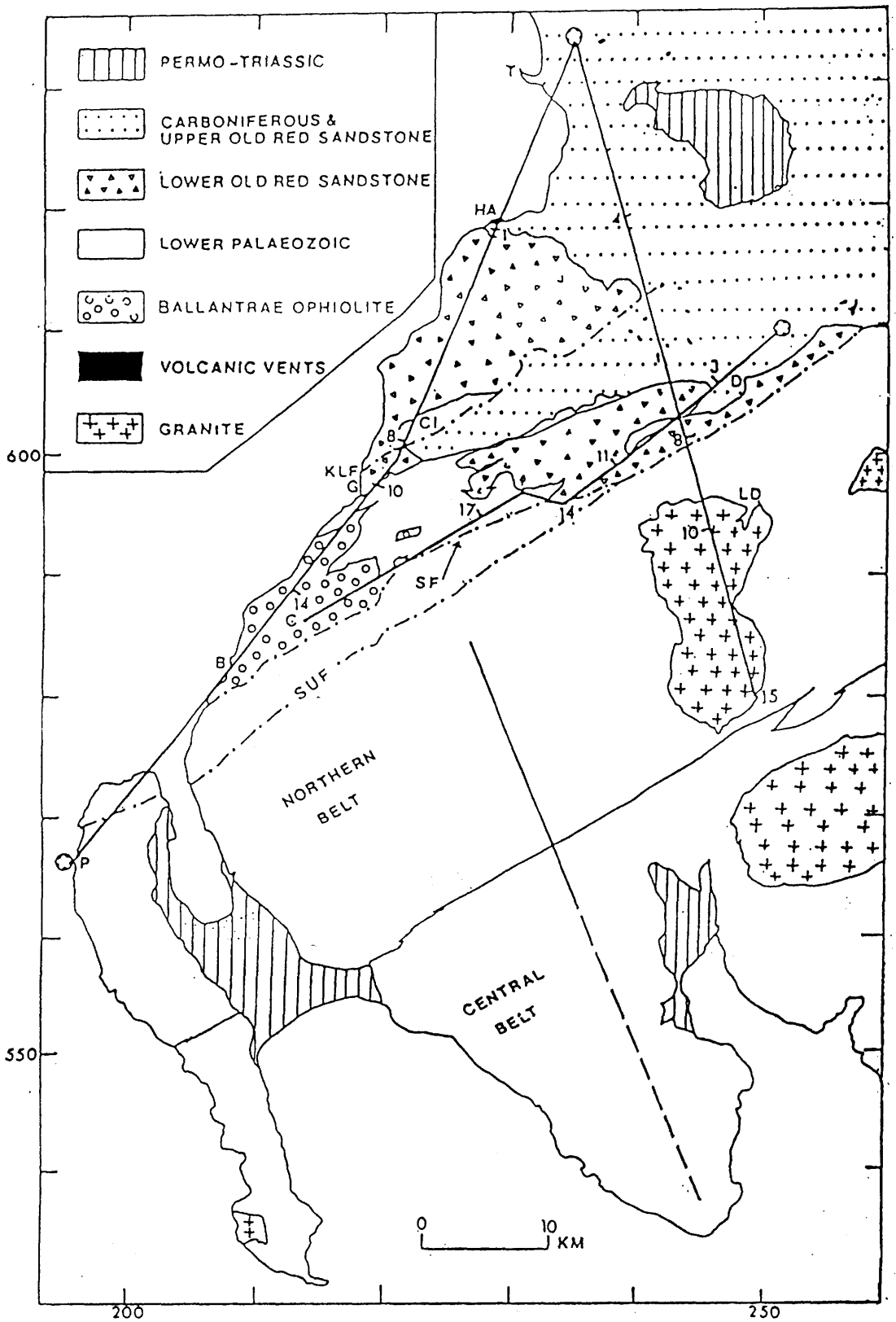

Fig 2.15a Network of the recorded profiles in relation to the geology.

B: Ballantrae, CI:Craighead Inlier, D: Dalmellington, G: Girvan, HA: Heads of Ayr, KLF: Kerse Loch Fault, LD: Loch Doon, P: Portobello, SF: Stinchar Fault, SUF: Southern Uplands Fault, T: Troon.

Numbers indicate seismometer stations listed in appendix 1.

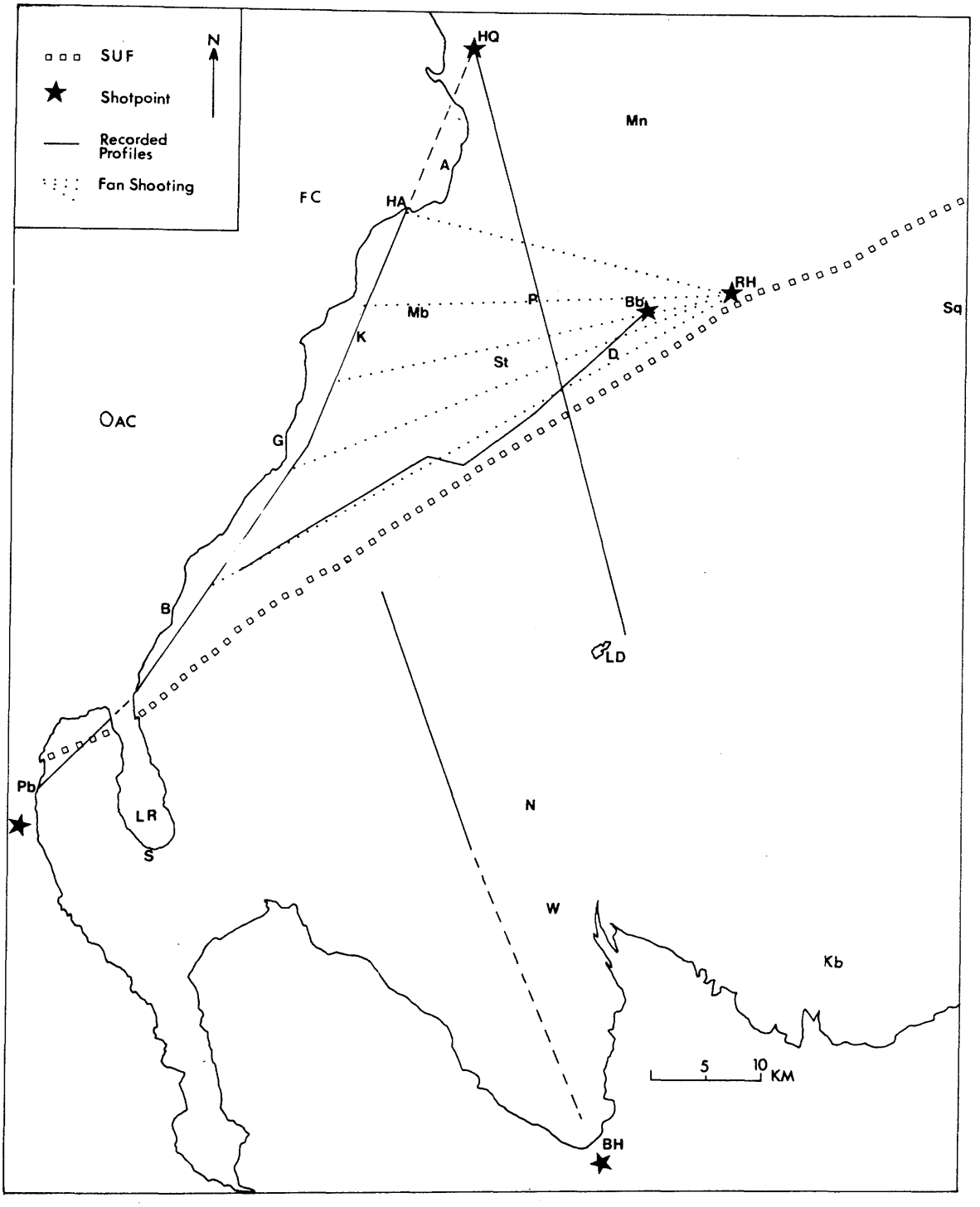

Fig 2.15b Network of the recorded profiles as shown in 2.15a with illustration of fan-shooting.
For abbreviations, see page 83.

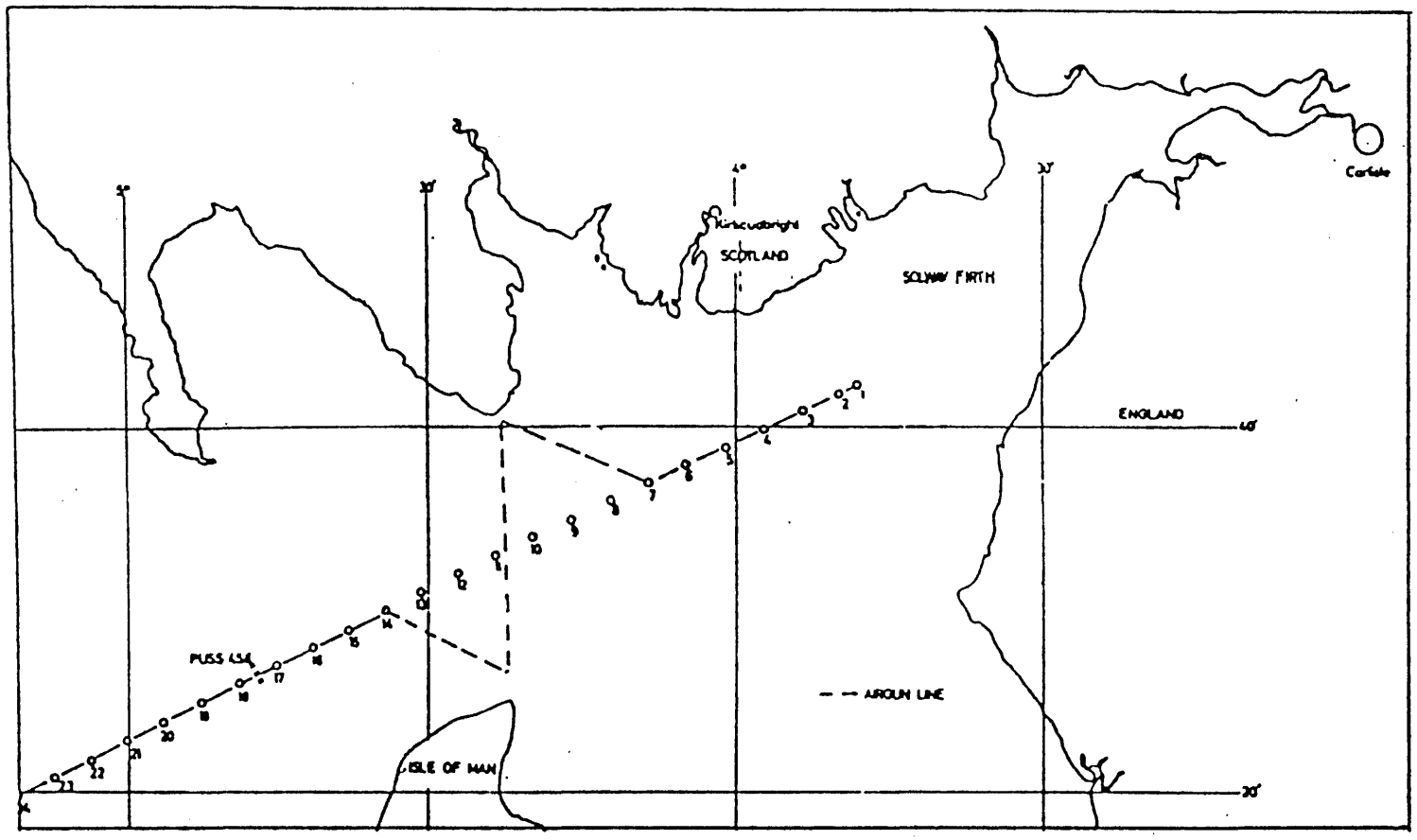

Fig 2.16 Layout of the Caledonian Suture Seismic Project showing explosive shots along the air-gun line.

B. Girvan Line (Hillhouse Quarry - Ballantrae)

Commercial quarries in the study area are scanty and the only one available in the Girvan district (Tormitchell), blasts infrequently and has not enough range to record across the ophiolite outcrop. Hillhouse Quarry (Troon) was used to record two seismic refraction lines across the area. One line was 64 km long, although the first 16 km were covered by the Firth of Clyde (fig 2.4), therefore, the first recording station was at the Heads of Ayr, a distance of 17 km. Seventeen recording stations were sited on Lower Old Red Sandstone and Lower Palaeozoic outcrops, with an azimuth $\simeq 235°$, and the last 25 km cover the ophiolite outcrop. Time-distance relationships are listed in table 5 appendix 1.

The reduced time-distance graph (fig 5 appendix 2) starts with a high apparent velocity (6·4 km/sec) over the Lower Old Red Sandstone, followed by a delay of $\simeq 0·2$ sec at 35 km range at the Kerse Loch Fault. The high apparent velocity is observed again over the ophiolite outcrop.

C. Loch Doon Line (Hillhouse Quarry - Loch Dee)

This line was recorded in order to have more control on the Carboniferous rocks which were not covered by the previous line, and to investigate the velocity structure across the Southern Uplands Fault and the Loch Doon Granite. It was approximately 55 km long, trending perpendicular to the local geological strike with an azimuth of 127°. Fifteen stations were recorded between the quarry and Loch Dee at the south end of the Loch Doon pluton. Carboniferous outcrops of the Midland Valley occupy the first 30 km of the profile; the rest of the

profile traversed Lower Old Red Sandstone and Lower Palaeozoic outcrops.

The reduced time-distance graph (fig 6 appendix 2) resembles that of the previous line since a high apparent velocity (6·4 km/sec) starts at a comparable range (20 km), followed by a delay of about 0·1 sec, again at 35 km (at the Southern Uplands Fault). The high apparent velocity is then repeated followed by an obvious deceleration over the outcrop of the pluton. Time-distance relationships are listed in table 6 appendix 1.

D. Colmonell Line (Benbain Opencast - Ballantrae)

The National Coal Board open-cast at Benbain, 3 km NE of Dalmellington, was the source used to build up this seismic refraction profile. The line is 45 km and is parallel to the local geological strike just north of the Southern Uplands Fault. The line is formed of twenty three seismometers spaced at about 2 km intervals. It crosses Carboniferous and Lower Old Red Sandstone rocks, and then steps north-west (to the north of the Stinchar Fault) before resuming the south-westerly trend, crossing Lower Palaeozoic outcrops and ending on the Ballantrae ophiolite (fig 2.4).

Frequent shifting of the blast position prompted frequent updating of the origin time and the Grid Reference of the blast (see table 7 appendix 1). The main objectives for recording this line are, firstly, to investigate the nature of the delay which has occured on the two previous lines, secondly, traverse the ophiolites in along strike, and thirdly, the line is parallel to SUSP, which was recorded along the Northern Belt of the Southern Uplands, and therefore, a comparison between the two areas can be

made.

Fig 7 (appendix 2) shows high apparent velocity (6·3 km/sec) starting at 12-20 km. A delay of 0·27 sec follows and then the high apparent velocity continues with evident acceleration on the ophiolite outcrop.

E. Portobello-Troon Line (Reversal of Girvan Line)

This line is literally a reversal of the Hillhouse Quarry - Ballantrae line. The same sites were reoccupied with some new ones inbetween, to minimize the spacing. The original line was extended south-eastward, across Loch Ryan to record an offshore blast ($\simeq$ 2 km SE of Portobello), fired by the Royal Navy on 7th June 1985.

The reduced time-distance graph (fig 8 appendix 2) shows an apparent velocity of 6·0 km/sec starting over the ophiolite outcrop, although the arrival is affected by consecutive delays and accelerations. A delay of $\simeq$ 0·16 sec occurs at a distance of 39 km (Fauldribon Station), followed by a marked acceleration culminating at Craighead Quarry station (47 km). The 6·0 km/sec apparent velocity starts again over the Lower Old Red Sandstone outcrops, but is delayed by about 0·1 sec, in relation to the arrival at Craighead Quarry station. A high apparent velocity (6·4 km/sec) takes over at 50 km range till the Heads of Ayr. Information on the time-distance relationships are found in table 8 appendix 1.

The origin time of the blast was not recorded on board the ship as it was assumed that it could be interpreted from the regional geology (see chapter 4).

F. West Ayrshire (Fan Shooting)

Whilst occupying the recording sites of the previous line (in West Ayrshire), a blast at Rough Hill NCB open-cast (Dalleagles) was recorded on most of the stations. The reduced time-distance graph (fig 9 appendix 2) shows a continuous increase of velocity with range, reaching a maximum observed velocity of 6·6 km/sec. The arrival at Fauldribon station suffered a delay of 0·4 sec relative to adjacent stations (see interpretation in chapter 4). Time-distance relationships are listed in table 9 appendix 1.

2.4 Shot-Station Distances

Land shots and recorder sites were easily positioned using large scale ordinance survey maps (1:10560), with an error estimation of ± 20m. The NCB shot positions were provided by their own surveyors.

The location of WISE marine explosive shots was provided by Decca fixes, which could be plotted on a Decca lattice, to calculate the grid reference. Due to the large number of air-gun shots involved, however, this could not be done for the air-guns and an automatic method of processing was preferable. The Decca fixes first had to be corrected for fixed and variable errors. Variable errors are caused by interference between the direct radio signals from the Decca stations and the signals reaching the ship by way of a "Skywave" refraction path. In general, their effect is small and can, therefore, be ignored. The fixed error is due to the distortion of Decca signals passing over ground of low electrical conductivity. Since the distortion does not alter, it is possible to correct the error. The fixed errors for the region were available in a manual

provided by Decca and correction was achieved by adding and subtracting them from the readings. A Hewlett - Packard program (Bacon 1978) was acquired with the input consisting of corrected Decca main chain fixes along the ship's track, and the output in latitude and longitude and/or UTM grid co-ordinates.

The distances between shot and station pairs were calculated by applying Pythagoras Theorem after converting all the co-ordinates to national grid co-ordinates.

2.5 Picking of First Arrivals, Data Quality and Error Estimates

For the purpose of picking P-wave arrivals from the WISE air-gun shots, the data were subjected to a 4-12 Hz Hanning band-pass filter, and presented using a reduction velocity of 6·0 km/sec and an expanded time scale. The most crucial point of Hanning band-pass filtering is the generation of ringing effect about the onset, due to large and slowly decaying side lobes of the filter, and is a major source of confusion in identification of onsets, and needs special care in picking.

Paper records direct from the analogue tapes were made for the WISE marine and land explosive shots and all the subsequently acquired data using a paper speed of 10 cm/recorded sec. This is quite adequate for picking arrival times.

The Hillhouse Quarry and Benbain NCB open-cast refraction lines were built up using many blasts with different depths and charges, and different gain settings for the recording sets. Therefore, no amplitude range relationship could be clearly studied. However, it could be shown on the Girvan line (Hillhouse -

Ballantrae line), that the last four seismograms have a relatively lower signal-to-noise ratio (fig 10 appendix 2).

A sudden attenuation of the amplitude occurs on the delayed segment on the Benbain-Ballantrae line (fig 12 appendix 2).

It could be stated that seismograms on the Portobello-Troon line display the best quality of recorded data, which is probably related to the size of the blast and the effectiveness of marine shots in comparison to commercial quarry blasts.

The main components of error affecting the travel time accuracy are:

1. Picking of onset time which could be in the range of $\pm$ 0·02 second.
2. Irregularities in speed of paper feed on the UV recorder result in different spacings between MSF second pulses. This makes it difficult to interpolate the precise onset of the second pulse, and the incurring error is estimated to be $\pm$ 0·007 second.
3. The uncertainty in locating the shotpoints is estimated to be $\pm$ 30 metres, which gives an error of $\pm$ 0·006 second.

Therefore, the overall accuracy of travel times is calculated to be $\pm$ 0·02 seconds.

2.6 Conclusions

The set of data presented in this thesis involves several seismic refraction profiles recorded across the Ballantrae ophiolite from all directions: east, west, north and south. It is characterized by

two main features:

1. A delay of 0·2 - 0·26 sec occuring at different geographical and geological localities.

2. High apparent velocities (> 6·0 km/sec) recorded at short ranges (19-20 km) with the minimum at Lendalfoot Array (8-10 km). This is significantly different from LISPB ranges for such velocities (> 50 km).

Such high velocities are typical of crystalline basement. These velocities and their variation with azimuth should bear on the problems and aims mentioned in chapter 1.

CHAPTER THREE

Laboratory Velocity Measurements

3.1 Introduction

Laboratory measurements of the velocities of elastic waves in rocks are needed to allow interpretation of velocities determined from field refraction measurements. Unless the depth extent of formations in the field are known, it is not possible to resolve velocity increase due to crack closure on the one hand, from that due to change in rock type on the other. The laboratory measurements over a range of confining pressure provide a basis for this resolution.

A low pressure steel vessel (available in the Department) was used to measure P-wave velocities across representative rock units of the Ballantrae ophiolite and selected greywacke samples from the Northern Belt of the Southern Uplands in Scotland.

Such measurements (even though only to 200 bar) should help give a better picture of the near surface velocity distribution in the Southern Uplands and the Girvan-Ballantrae area, and impose certain constraints on the various lithologies at depth, that are to be interpreted from the refraction profiles.

3.2 Rock Sampling and Core Preparation

By studying Geological Survey of Scotland Map sheet 7, it was possible to pick out outcrop sites of the major ophiolite rock units. Considerable help in finding suitable sites was gained from personal communication with Dr B J Bluck.

Greywacke samples from the Northern Belt were kindly provided by Dr J Floyd, who grouped them into five formations according to petrographical criteria: Marchburn, Afton, Scar, Shinnel and Blackcraig (Floyd 1982).

Once in the laboratory, cylindrical cores were obtained from each sample using a diamond bit, the diameter 25·4mm being selected to match the transducer size. Each core was trimmed using a "Buehler Isomet" low-speed saw, to avoid the induction of cracks caused by faster cutting. Cutting cores this way leaves two parallel faces which do not require any grinding, but only a brief handlap with 400 grade carborundum to produce a satisfactory finish.

For clear observation of the compressional arrival, the length to diameter ratio (L/D) should be less than about 5 (Anderson & Lieberman 1968), because as L/D increases, more of the initial compressional energy is destroyed by boundary reflection and eventually Vp reduces into the noise level. Lengths of specimens range from 27·6 to 58·8mm and were measured by a micrometer screw gauge at several points on each core with standard deviations of about 0·004 to 0·02mm. The greywacke cores were numbered in the same method used by Floyd (1982).

3.3 Saturation of Samples

The presence of water in pores and microcracks of rocks is common in the earth. It constitutes one of the environmental factors that must be considered when in-situ seismic velocities are investigated. It is, therefore, necessary to measure velocities in saturated or dry samples according to the likely condition of the rocks in-situ. At confining pressures up to 200 bar, the rocks are unlikely to be waterfree, so our measurements were confined to saturated samples only.

Samples were placed in water in an evacuated dessicator. The air in the dessicator was removed using a vacuum pump and left in this condition for approximately eight hours, to ensure tnat the samples were fully saturated.

3.4 Density Measurement

Measurement of density is useful, since seismic velocity is strongly dependent on density and mineral composition. Based on Archimedes' principle, densities of all the core samples were determined by measuring three parameters: weight of dry sample in air (W), weight of saturated sample in air (WS) and weight of saturated sample in water (WW). Weighing of dry cores was achieved after the samples had been over-dried at 110°c for 24 hours. Bulk densities, porosities and grain densities were calculated from the following formulae (Holmes 1930):

$$\text{Saturated bulk density } \rho_{bw} = \frac{WS}{WS - WW}$$

$$\text{Porosity } \phi = \frac{WS - W}{WS - WW} \times 100\%$$

$$\text{Grain density } \rho_g = \frac{W}{W - WW}$$

3.5 Method and Instumentation

Velocities are measured by Birch's method (Birch 1960); the pulse transmission technique. This is based on the measurement of the travel time of a high frequency acoustic pulse across the specimen. Each core is placed between 1 MHZ barium titanate ceramic trans-

ducers (set 003), activated by a Velonex 345 high voltage pulse generator. Grease was used as a coupling agent between the faces of the specimen and the transducers.

Prior to the actual measurement of velocity through the samples, the core-transducers assembly was swathed by plastic tubing to prevent the pressure medium (hydraulic oil) from penetrating the sample at higher pressure. 40-mesh copper gauze was placed between the core and the jacket to provide void space into which pore water from the sample could drain during compression. The mesh was soldered tightly around the core to prevent the heated plastic jacket from forcing it off.

The transmission time is measured by matching the onset of the pulse transmitted through the specimen, with that of a pulse transmitted simultaneously through a variable-length mercury delay line. The matching is done on a dual-trace oscilloscope. Pressure is generated by a hand-pump with a Bourdon gauge mounted above it. Velocity readings were taken at 20-30 bar intervals up to a maximum confining pressure of 200 bars, at room temperature.

The velocity of propagation through the sample is simply obtained from the length of the mercury column (L Hg), Vp in mercury (V Hg = 1·453mm/μsec) and the length of the sample (L rock):

$$V_{rock} = L_{rock} \cdot V_{Hg} / L_{Hg}$$

Electronic and transducer delays make the recorded time longer than the actual transit-time through the specimen, therefore, calibration of the mercury delay line is essential. The zero-setting of the delay line was determined by finding the settings that would correspond to the first arrivals, through steel samples of lengths

ranging from 25 to 60mm, and extrapolating to zero-length (Birch 1960). Calibration values have to be subtracted from the length of the mercury column required in the onset matching. As a precautionary measure to ensure that the mercury column was functioning in its normal manner, calibration was repeated periodically (fig 3.1).

3.6 Results and their Implications

The results of laboratory seismic velocity measurements are given in table 3.1 and 3.2. Velocities listed are the mean of measurements during increasing and decreasing pressure cycles. At higher pressures, there is a better transducer-rock contact, so that the first arrival is more easily detected because of its higher amplitude and frequency. In many cases, an accurate reading could not be taken below a pressure of 20 bars.

Accuracy of the measurement depends on the quality of the signal, the calibration values of the mercury delay line, parallelism of the core faces and the reading of the confining pressure. Repetitive measurements on some samples with different sets of transducers (ie. different calibration values), give an overall error estimate of $\pm$ 0·08 km/sec.

3.6.1 The Ophiolite Samples

All of the graphs (appendix 3a) show a gradual increase of velocity with increasing pressure. The average increase of velocity over the full range of pressure (0-200 bar) is 0·18 $\pm$ 0·10 (0·3 km/sec/km). The chert shows a slight increase of 0·03 km/sec (0·05 km/sec/km), whereas in foliated gabbro, it is highest at 0·25 km/sec (0·42 km/sec/km).

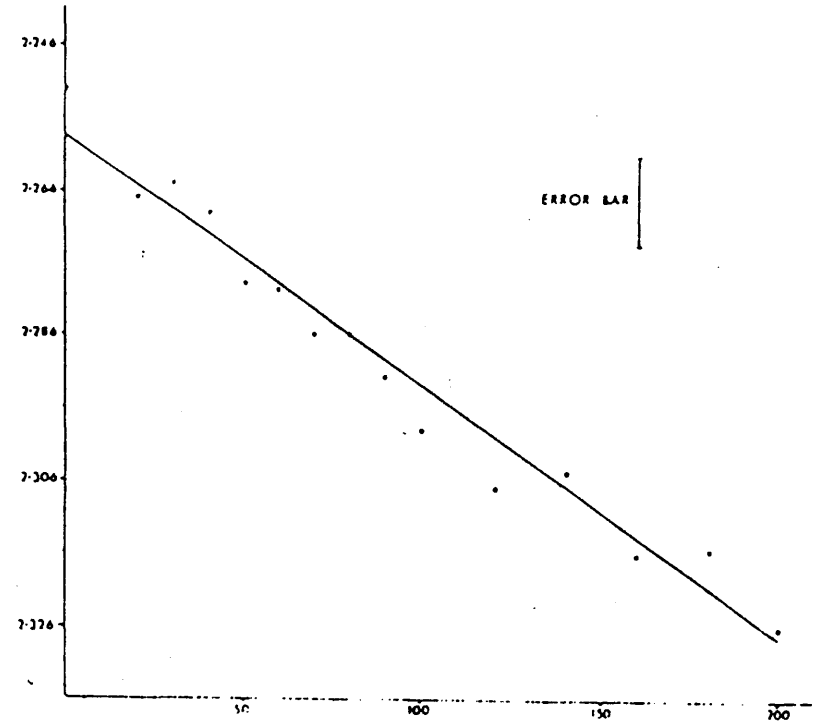

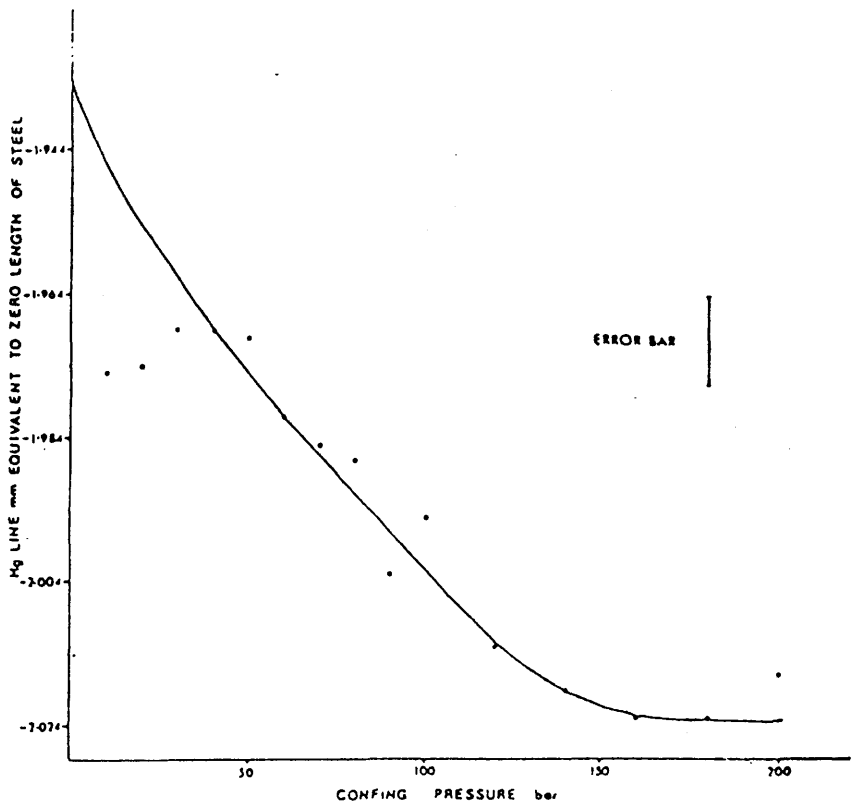

Fig 3.1 Zero-length delays for P-wave velocity measurements

Both graphs are for two different sets of transducers.

Core No.	confining pressure(bars) Atmos. 1 bar	10	20	50	80	100	140	160	180	200
Gr 1	5·57	5·57	5·60	5·62	5·64	5·66	5·68	5·69	5·70	5·71
Gr 2	-	5·16	5·22	5·39	5·44	5·47	5·51	5·55	5·57	5·58
Gr 3	5·42	5·47	5·47	5·50	5·54	5·55	5·57	5·57	5·58	5·58
G 1	5·36	5·48	5·51	5·55	5·59	5·60	5·63	5·63	5·64	5·64
G 2	5·97	6·04	6·06	6·06	6·08	6·09	6·10	6·11	6·11	6·12
D	5·63	5·64	5·66	5·67	5·68	5·68	5·68	5·69	5·69	5·69
S 1	-	4·62	4·63	4·65	4·66	4·67	4·68	4·68	4·69	4·69
S 2	4·57	4·63	4·66	4·69	4·72	4·73	4·74	4·75	4·76	4·76
CH	5·59	5·61	5·61	5·61	5·61	5·61	5·61	5·61	5·62	5·62
FG 1	-	-	6·37	6·52	6·56	6·58	6·64	6·64	6·67	6·67
FG 2	6·50	6·51	6·53	6·61	6·64	6·65	6·68	6·68	6·70	6·70
SP.LV	-	-	5·24	5·28	5·32	5·34	5·35	5·36	5·37	5·37

Table3.1P-wave velocities in the main components of the Ballantrae ophiolite complex. Gr:Granite,G:Gabbro,D:Dolerite,S:Serpentinite,CH:Chert,FG:Foliated Gabbro,SP.LV:Spilitic Lava.

Core No.	Atmos. 1 bar	20	50	80	100	160	200
N621	5·77	5·90	5·92	5·93	5·93	5·94	5·94
AX192	5·56	5·61	5·65	5·66	5·68	5·70	5·71
AX297	5·28	5·40	5·43	5·43	5·43	5·44	5·44
AX309	5·23	5·40	5·43	5·45	5·45	5·46	5·46
L526	5·29	5·48	5·49	5·51	5·51	-	5·51
AX201	5·30	5·60	5·61	5·62	5·62	5·63	5·63
AX565	5·70	5·73	5·76	5·77	5·77	5·79	5·79
L588	5·18	5·29	5·34	5·36	5·38	5·39	5·40
AX3	5·72	5·75	5·77	5·79	5·79	5·80	5·80
AX270	5·39	5·58	5·62	5·62	5·62	5·63	5·63
DTIA290	5·41	5·76	5·78	5·80	5·80	5·80	5·81
AX473	5·62	5·70	5·72	5·73	5·73	5·74	5·74
AX532	5·73	5·82	5·84	5·84	5·85	5·85	5·87
AX534	5·67	5·70	5·73	5·75	5·76	5·77	5·78
AX644	5·58	5·73	5·75	5·77	5·77	5·77	5·78
AX664	5·20	5·38	5·43	5·46	5·47	5·48	5·48
AX862	-	5·75	5·76	5·76	5·76	5·76	5·76
AX863	-	5·60	5·61	5·62	5·62	5·62	5·62
AX159	-	5·84	5·86	5·87	5·87	5·87	5·87
AX160	-	5·96	5·97	5·97	5·97	5·98	5·98
AX871	-	5·69	5·70	5·70	5·70	5·70	5·71
AX873	-	5·63	5·63	5·63	5·63	5·64	5·64
AX205	-	5·81	5·83	5·83	5·83	5·84	5·85
AX856	-	5·65	5·66	5·67	5·67	5·67	5·67
AX755	-	5·86	5·86	5·86	5·87	5·88	5·88
AX659	-	5·85	5·85	5·85	5·86	5·86	5·86
AX781	-	5·76	5·81	5·82	5·82	5·82	5·83
AX861	-	5·86	5·87	5·87	5·87	5·87	5·87
AX851	-	5·45	5·46	5·47	5·48	5·50	5·52
AX847	-	5·38	5·38	5·38	5·38	5·39	5·39
AX849	-	5·56	5·57	5·59	5·59	5·59	5·59
AX604	-	5·77	5·78	5·78	5·78	5·79	5·79
AX981	-	5·59	5·60	5·61	5·61	5·62	5·63
AX983	-	5·90	5·90	5·90	5·91	5·92	5·93
AX989	-	5·75	5·76	5·77	5·77	5·77	5·78
AX990	-	5·94	5·96	5·97	5·97	5·97	5·98
AX753	-	5·72	5·73	5·74	5·74	5·74	5·74

Table 3.2 P-wave velocities in greywackes from the Northern Belt of the Southern Uplands.

Gabbro from Millenderdale showed some foliation in the field, therefore, anisotropy was investigated using two cores cut at right angles to one another: FG1 $\perp$ to the banding and FG2 // to it. The difference in velocity across the two cores at 200 bar is 0·03 km/sec, showing that the rock is almost isotropic.

Locality, porosity and density of each core is listed in table 3.3. Fig 3.2 shows the correlation between bulk density and the velocity at 200 bar. A straight line is applied to the data by linear regression and the scatter in the data points yields a correlation coefficient of 0·84, so that 70% of the variation in Vp can be accounted for by variation with bulk density. Foliated gabbros have the highest density and velocity values, whereas serpentinites have the lowest values. A difference of 0·5 km/sec in the velocity of the two gabbro samples is related to the fact that one of them is more serpentinised and so gave lower velocity and density values. The three granite samples exhibit very similar densities and velocities, and the chert sample is embraced within their field on the graph. The calculated density for the spilitic lava is slightly higher than that recorded by Christensen (1966; 2·70 - 2·74), although its velocity (5·37 km/sec) is within his range (4·85 - 5·74).

Several investigators have made laboratory measurements on different ophiolite samples at elevated pressures. Table 3.4 represents a summary of some of their results and the values listed in table 3.1 compare well with them. It can be seen from both tables that serpentinite has lower velocities than the rest of the ophiolite components, therefore, any seismic refraction profile across the Ballantrae complex would not yield smooth velocity segments, because of the likely mixture of serpentinite in adjacent rocks; each unit thick

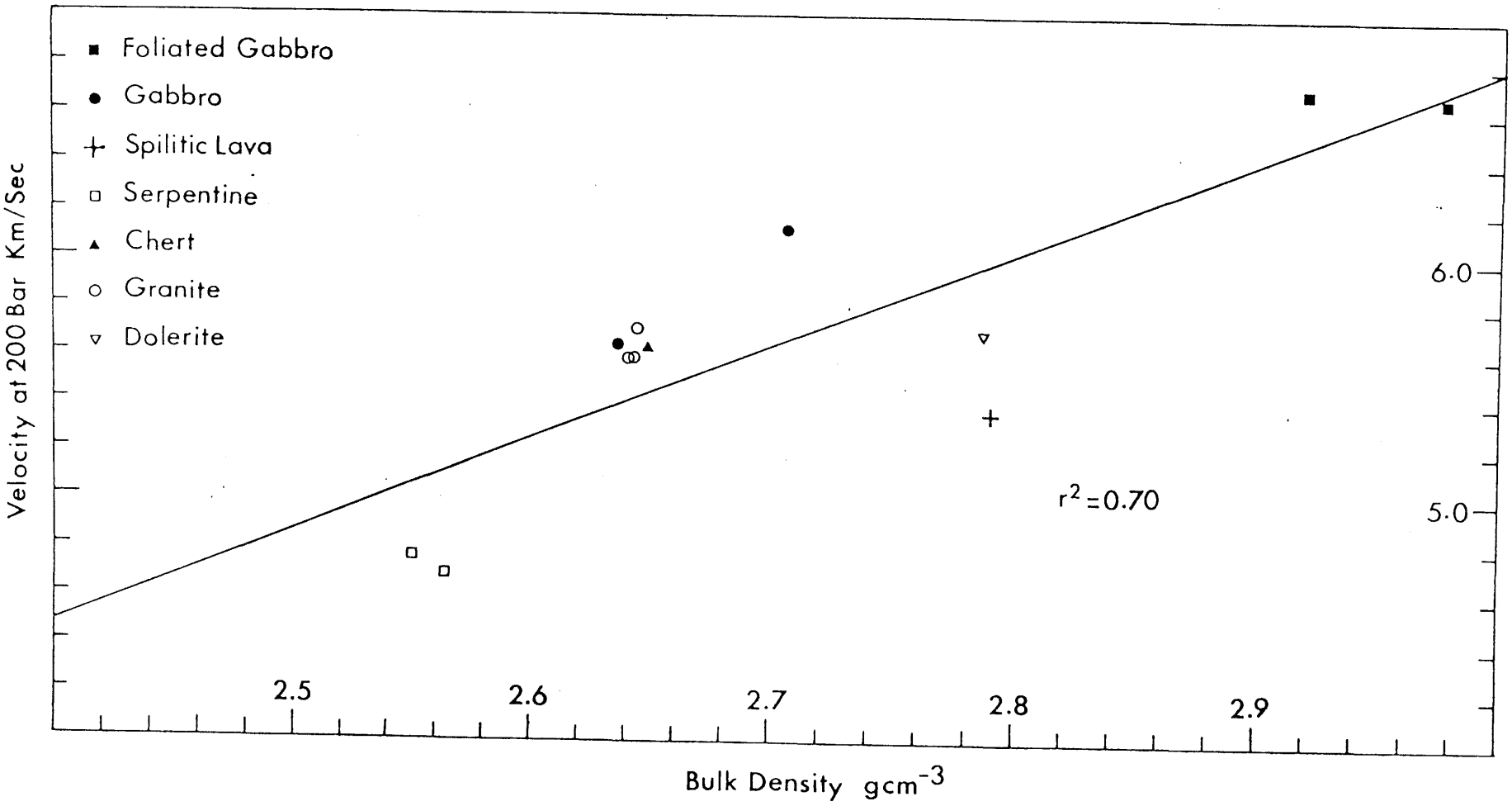

Fig 3.2 Illustration of the relationship between P-wave velocity and bulk density of the main components of the Ballantrae ophiolite complex.

Sample No.	Locality	Vel. km/sec 200 bar	Density	Porosity	Grain Density
S1	Knocklaugh	4·69	2·564	0·040	2·629
S2	Byne Hill	4·76	2·551	0·043	2·621
FG 1	Millenderdale	6·67	2·975	0·006	2·987
FG 2	Millenderdale	6·70	2·918	0·003	2·924
Gr 1	Byne Hill	5·71	2·644	0·008	2·658
Gr 2	Byne Hill	5·58	2·639	0·009	2·653
Gr 3	Byne Hill	5·58	2·639	0·010	2·656
G1	Byne Hill	5·64	2·635	0·010	2·651
G2	Byne Hill	6·12	2·706	0·001	2·707
CH	Bennane Lee	5·62	2·647	0·003	2·651
D	Lendalfoot	5·69	2·786	0·002	2·790
SP.LV	Kennedy Pass	5·37	2·790	0·022	2·831

Table 3.3 Localities,P-wave velocities and other physical properties of the main components of the Ballantrae ophiolite complex. Abbreviations as in table 3.1.

Rock Type	Pressure (bar)	Velocity km/sec	Density gm/cm^3	Reference
Serpentinite	200	4·89 - 6·44	2·513 - 2·665	Christensen 1978
	200	4·20	2·520	Christensen 1966
	10 - 10,000	4·23 - 5·57	2·467 - 2·546	Christensen 1972
	10 - 10,000	4·70 - 6·82	2·601 - 2·710	Birch 1960,1961
Spilite	200	4·85 - 5·74	2·704 - 2·738	Christensen 1978
Gabbro	200	6·63 - 7·16	2·835 - 3·013	Christensen 1978
	10 - 10,000	5·80 - 7·23	2·931 - 3·054	Birch 1960,1961
	600 - 4,000	6·94 - 7·05	2·830 - 2·880	Salisbury & Christensen 1978
	500 - 3,000	6·78 - 7·47	2·880 - 3·010	Christensen 1982
	1,500	6·10 - 7·80	2·900 - 3·200	Peterson et al 1974
Metagabbro	600 - 4,000	6·30 - 7·06	2·810 - 2·950	Salisbury & Christensen 1978
	200	6·07 - 7·08	2·721 - 3·070	Christensen 1978
	500 - 3,000	6·38 - 6·75	2·620 - 2·890	Christensen 1982
Granite	10 - 10,000	3·80 - 6·57	2·619 - 2·679	Birch 1960, 1961
	200	5·77 - 6·14	2·609 - 2·636	Hughes & Maurette 1956
Trondhjemite	200	6·00 - 6·11	2·648 - 2·731	Christensen 1978
	1,300	6·06	2·570	Salisbury & Christensen 1978
Dolerite	1,500	6·10 - 6·90	2·800 - 3·000	Peterson et al 1974
	500 - 3,000	6·10 - 6·96	2·760 - 2·930	Christensen 1982
	600 - 4,000	6·43 - 6·79	2·840 - 2·960	Salisoury & Christensen 1978
Basalt	600 - 4,000	5.67 - 6·22	2·720 - 2·880	Salisbury & Christensen 1978
	500 - 3,000	5·28 - 5·74	2·960 - 2·850	Christensen 1982
	10	4·90 - 5·40	----	Nichols et al 1980
Diabase	200	5·95	2·857	Christensen 1978
	10 - 10,000	6·14 - 6·93	2·964 - 3·012	Birch 1960,1961
Amphibolite	10 - 10,000	6·89 - 7·35	3·120	Birch 1960,1961
	600 - 4,000	7·06 - 7·38	2·960 - 3·010	Salisbury & Christensen 1978
	10 - 10,000	5·50 - 7·22	3·030 - 3·040	Christensen 1965
	500 - 3,000	6·78 - 6·84	2·960 - 3·010	Christensen 1982
Pyroxenite	200	7·73 - 7·74	3·209 - 3·267	Christensen 1978
	10 - 10,000	6·80 - 8·01	3·247	Birch 1960,1961
	2,400	7·640	3·230	Salisbury & Christensen 1978

Table 3.4 Summary of some laboratory velocity measurements on different ophiolite samples.

enough to affect the travel times. Velocities in chert, granite and spilite are indistinguishable, and velocities well over 6·0 km/sec in the field are expected to be due to gabbro, or a mixture of dolerite and gabbro.

3.6.2 The Greywacke Samples

The P-wave velocity as a function of elevating pressure up to 200 bar, across 37 greywacke samples from the Northern Belt in the Southern Uplands, is given in table 3.2 and appendix 3b. Density and porosity were measured for all the available greywacke samples (67) listed in table 3.5.

Density values range from 2·68 to 2·88 Mg/m^3. Adesanya (1982), obtained a density of 2·69 ± 0·04 Mg/m^3 for Lower Palaeozoic greywackes from the Girvan district (more acidic than those of the Northern Belt). McLean (1961b), calculated a mean of 2·75 ± 0·05 for the Lower Palaeozoic greywackes of Ayrshire. Bott and Masson-Smith (1960) measured the density of 63 Silurian greywacke samples from the Southern Uplands, and derived a mean of 2·71 ± 0·06 Mg/m^3. The author obtained a mean density of 2·73 ± 0·04 Mg/m^3.

The density effect on the measured velocities is shown in fig 3.3a, which suggests that about 32% of variation of velocity can be accounted for by correlation with density, and it goes down to 26% when grain density is considered instead of bulk density (fig 3.3b).

Fig 3.4 shows the correlation between the reciprocal of the measured velocity or transit time and porosity. The correlation coefficient implies that 64% of the velocity variation is due to the porosity effect, and it can be postulated from the equation of the best

Sample No.	Locality	Formation	Vel. km/sec 200 bar	Density	Porosity	Grain Density
N621	Over Cairn, New Cumnock	Marchburn	5·94	2·812	0·181	2·815
AX862	Turkey Hill, Haggis Rock	"	5·76	2·721	0·340	2·726
AX863	Turkey Hill, Coulter	"	5·62	2·737	0·558	2·746
DTIA290	Friog Gas Trench	Pyroxenous Group	5·81	2·753	0·491	2·726
AX473	Raesnow Quarry	"	5·74	2·758	0·388	2·764
AX532	Hazelbank Quarry	"	5·87	2·751	0·257	2·755
AX659	Quarry, N Side of A701	"	5·86	2·744	0·207	2·747
AX781	Badlieu Quarry	"	5·83	2·790	0·317	2·796
L526	Glenimshaw Burn, Mennock	Scar	5·55	2·708	0·509	2·717
AX201	Grains Burn Camps	"	5·63	2·710	0·472	2·718
AX565	Broadlaw Road cutting	"	5·79	2·731	0·224	2·735
AX160	Culter Water	"	5·98	2·772	0·325	2·778
AX159	Culter Water, roadside	Scar	5·87	2·769	0·271	2·774
AX871	Misbet Burn	"	5·71	2·746	0·302	2·751
AX873	Misbet Burn	"	5·64	2·759	0·726	2·772
AX205	Kings Beck, Coulter Water	"	5·85	2·791	0·345	2·797
AX856	Fair Burn, Cowgill	"	5·67	2·793	0·254	2·797
AX753	Dreva Hill Broughton	Shinnel ?	5·74	2·709	0·260	2·713
L568	Lime Clench	Shinnel	5·40	2·715	0·828	2·730
AX3	Bowbeat Burn	"	5·80	2·682	0·268	2·687
AX270	Burnsands Burn	"	5·63	2·691	0·621	2·701
AX534	Cramalt Road Section	Intermed	5·78	2·708	0·397	2·714
AX644	Menzian	"	5·78	2·720	0·322	2·725
AX664	Menzian	"	5·48	2·708	0·497	2·717

Table 3.5 Localities,P-wave velocities and other physical properties of greywackes from the Northern Belt of the Southern Uplands.

Sample No.	Locality	Formation	Vel. km/sec 200 bar	Density	Porosity	Grain Densit
AX866	Wool Gill, Gair Gill, Coulter	Marchburn		2·724	0·616	
AX657	Quarry, Tweedsmuir	Pyroxenous		2·708	0·166	
AX973	Cross Water, Barrhill	Afton		2·717	0·217	
AX974	High Altercannoch Quarry, Barrhill	"		2·725	0·233	
AX975	Cross Water, Barrhill	"		2·721	0·257	
AX976	Pollgowan Burn, Barrhill	"		2·712	0·104	
AX977	Loch Naninie Quarry, Barrhill	"		2·713	0·314	
AX979	Cross Water, Barrhill	"		2·715	0·143	
AX980	"	"		2·701	0·361	
AX981	"	"	5·63	2·810	0·541	
AX982	Pollgowan Burn, Laggish, Barrhill	"		2·707	0·109	
AX983	Forestry Quarry, 3 km SW of Barrhill	Afton	5·93	2·860	0·267	2·865
AX851	Powskein Burn, Earlshaugh	Intermed.	5·52	2·685	0·480	2·693
AX847	Whitehope Burn, Earlshaugh	"	5·39	2·687	0·588	2·697
AX849	Aunanhead Hill, Devil's Beef Tub	"	5·59	2·696	0·257	2·708
AX604	Talla Linn, Tweedsmuir	"	5·79	2·697	0·149	2·698
AX790	Fingland Burn, Tweedsmuir	Pyroxenous ?		2·747	0·199	
AX835	Muckle Powskein Burn, Badlieu	"		2·710	0·253	
AX842	Priest Burn, Tweedhope Foot	Intermed.		2·690	0·474	
AX844	Kirkhope Burn, Manor Water	Px/Int. ?		2·720	0·178	
AX857	Shank Houp, Cowgill	Afton		2·720	0·224	
AX858	"	"		2·717	0·475	
AX864	Snaip Hill, Coulter	Marchburn ?		2·721	0·712	
AX865	Cowgill, Coulter	MB/Af ?		2·711	0·533	

Table 3.5 continued

Sample No.	Locality	Formation	Vel. km/sec 200 bar	Density	Porosity	Grain Density
AX984	Pollgowan Burn, Barrhill	Afton		2·756	0·311	
AX985	1km NW Knockycoid Barrhill	"		2·734	0·145	
AX986	Pollgowan Burn Bridge, Barrhill	"		2·695	0·413	
AX987	B7027 Kirkcalla, Barrhill	"		2·721	0·493	
AX988	100m SE of Bridge Knowe, Barrhill	Scar		2·756	0·160	
AX989	Glassoch Bridge	Scar ?	5·78	2·722	0·040	2·723
AX990	A714, 0·5km NW of Barrhill	Afton	5·98	2·876	0·241	2·880
AX991	Pollgowan Burn, Barrhill	"		2·717	0·248	
AX993	Dochroyle, Barrhill	Afton		2·731	0·213	
AX998	1·7km SE of Knock-ycoid, Barrhill	"		2·729	0·142	
AX1000	Blair Hill Wood Quarry, Barrhill	"		2·722	0·387	
AX1501	Laggan, Barrhill	"		2·710	0·350	
AX755	A701 Stanhope	Skimmel	5·88	2·713	0·218	2·717
AX1507	Alty Burn, Barrhill	Afton		2·710	0·277	
AX192	"	"	5·71	2·731	0·458	2·739
AX297	"	"	5·44	2·720	0·754	2·733
AX309	"	"	5·46	2·716	0·788	2·729

Table 3.5 continued

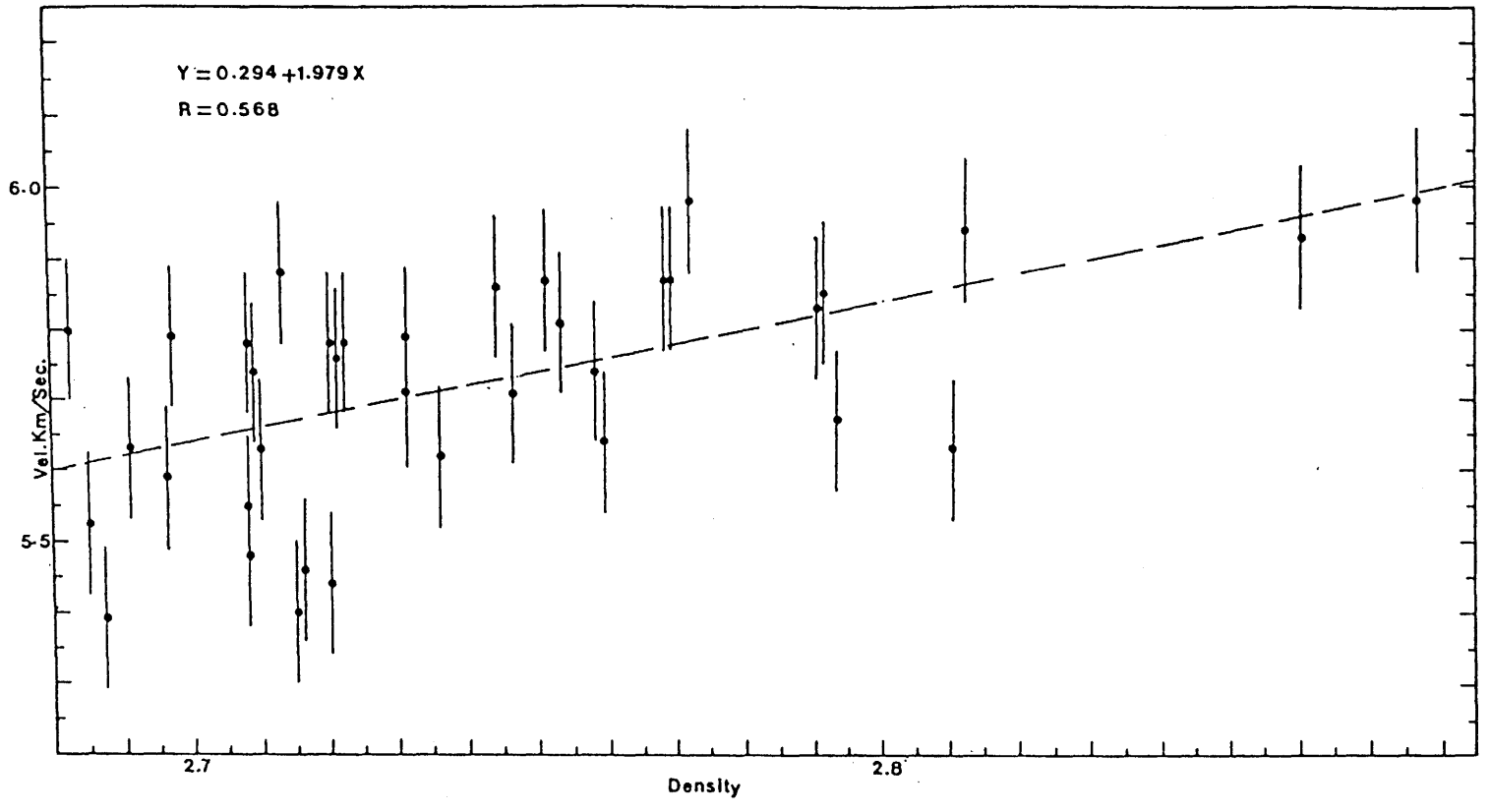

Fig 3.3a Illustration of the relationship between bulk-density and the measured velocities across the Northern Belt greywackies.

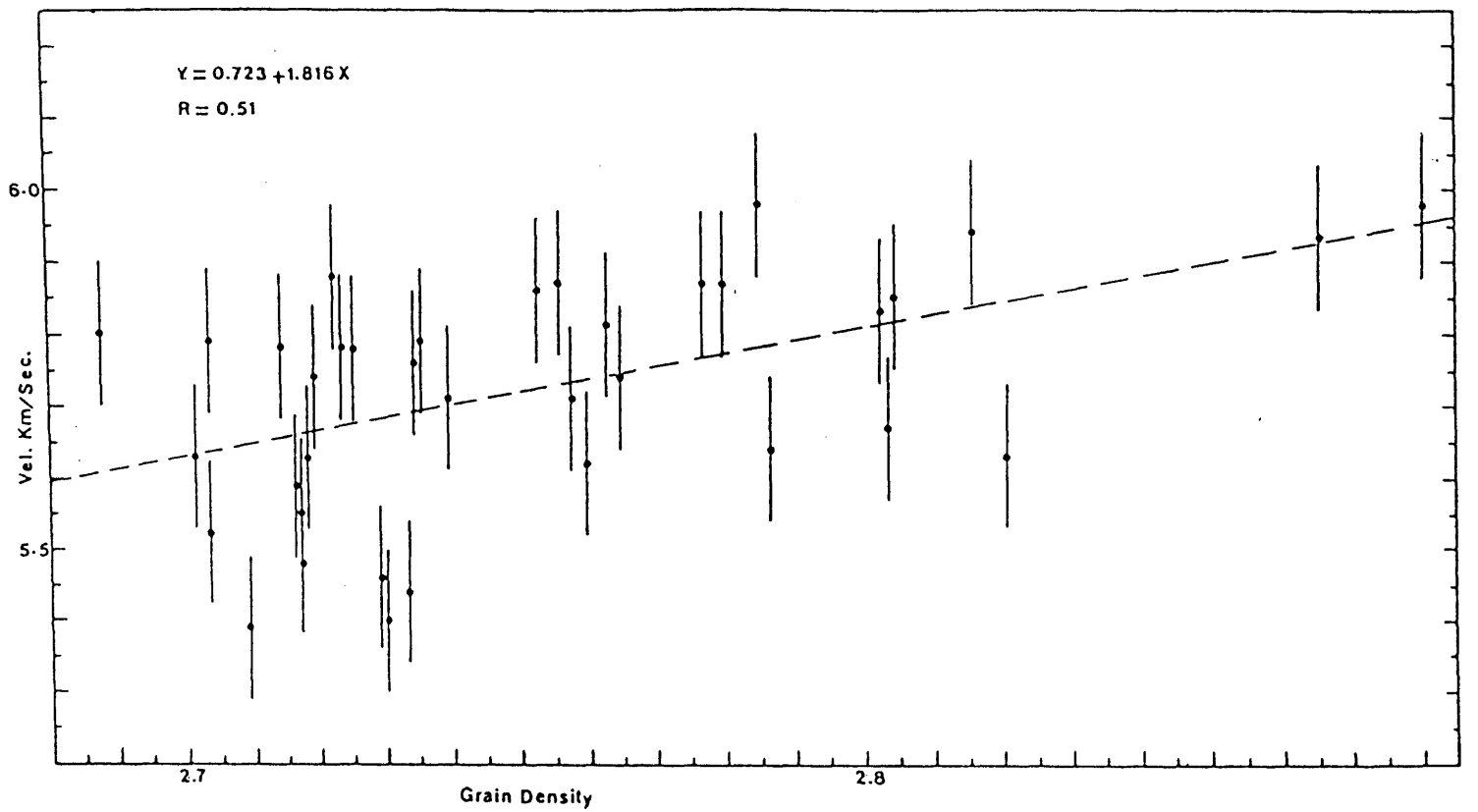

Fig 3.3b Illustration of the relationship between grain-density and the measured velocities across the Northern Belt greywackies.

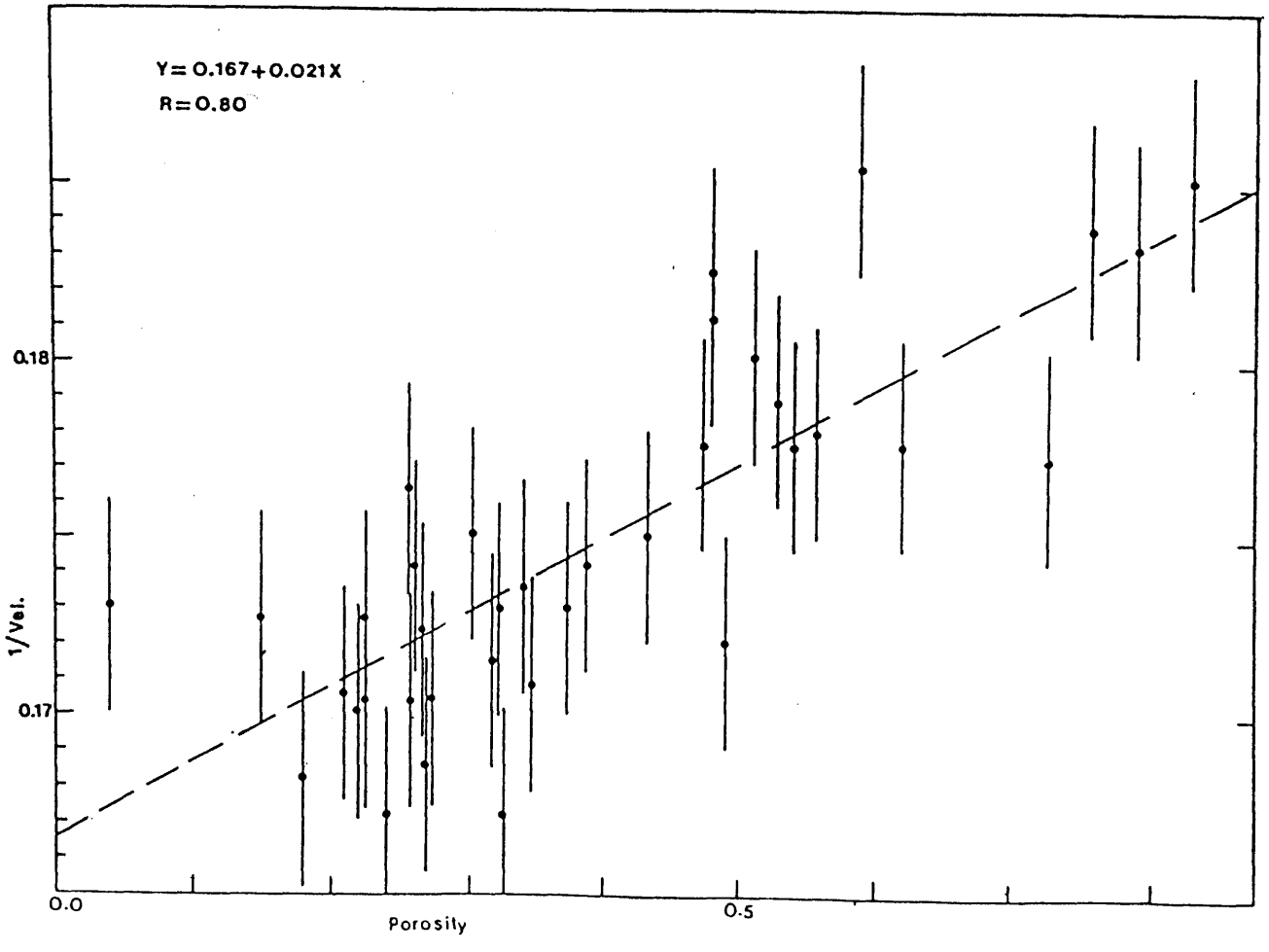

Fig 3.4 The relatiomship between porosity and P-wave velocity of the Northern Belt greywackes.

fit line: Y= 0·167 + 0·021X, that the velocity expected for a crack-free greywacke is 5·99 km/sec ($^{1}/_{0·167}$). This is similar to the maximum velocity value proposed by Adesanya (1982), where he concluded that velocities above 6 km/sec will represent lithologies other than greywackes (crystalline rocks), in the Southern Uplands.

As the velocity across some of the samples approaches 6·0 km/sec (see table 3.2) at the maximum applied pressure (200 bar), the question arises: Is velocity through the Northern Belt greywackes liable to exceed the 6·0 km/sec at higher pressures?

The high pressure vessels of the Experimental Petrology Unit of Edinburgh University were used to measure velocities with increasing confining pressure up to 5 kbar. After deriving new calibration values for the mercury delay line (fig 3.5), only two samples (N621, AX201) were run successfully. Whilst preparing the third sample, the vessel screw-lid failed and hence further measurements could not be taken. More safety precautions and improved sample-transducer design are needed for high pressure measurement in Edinburgh. A full description of the system is found in Adesanya (1982).

High pressure results are shown in fig 3.6. Sample AX201 reaches a maximum velocity of 6·01 km/sec at 5 kbar confining pressure, while the second sample, N621 achieves a velocity as high as 6·29 km/sec at the same pressure. The Edinburgh data for N621 does not correlate satisfactorily with the Glasgow measurements of the same specimen, though the measurements of AX201 do match. This suggests that either the Edinburgh data or the Glasgow data are unreliable. Since the low pressure data from Glasgow were repeatable with different transducers, it is more likely that the Edinburgh data are unreliable, but this is not yet confirmed. However, since some of the low pressure measurements do approach 6 km/sec at only 200 bars, it is likely that velocities over 6 km/sec will be achieved in some mafic greywackes at shallow depth.

Warner (1982), from refraction measurements along the Northern Belt (SUSP, see 1.3.2), interpreted a 6·0 km/sec velocity segment as arrivals from a crystalline basement underlying the sediments there. His

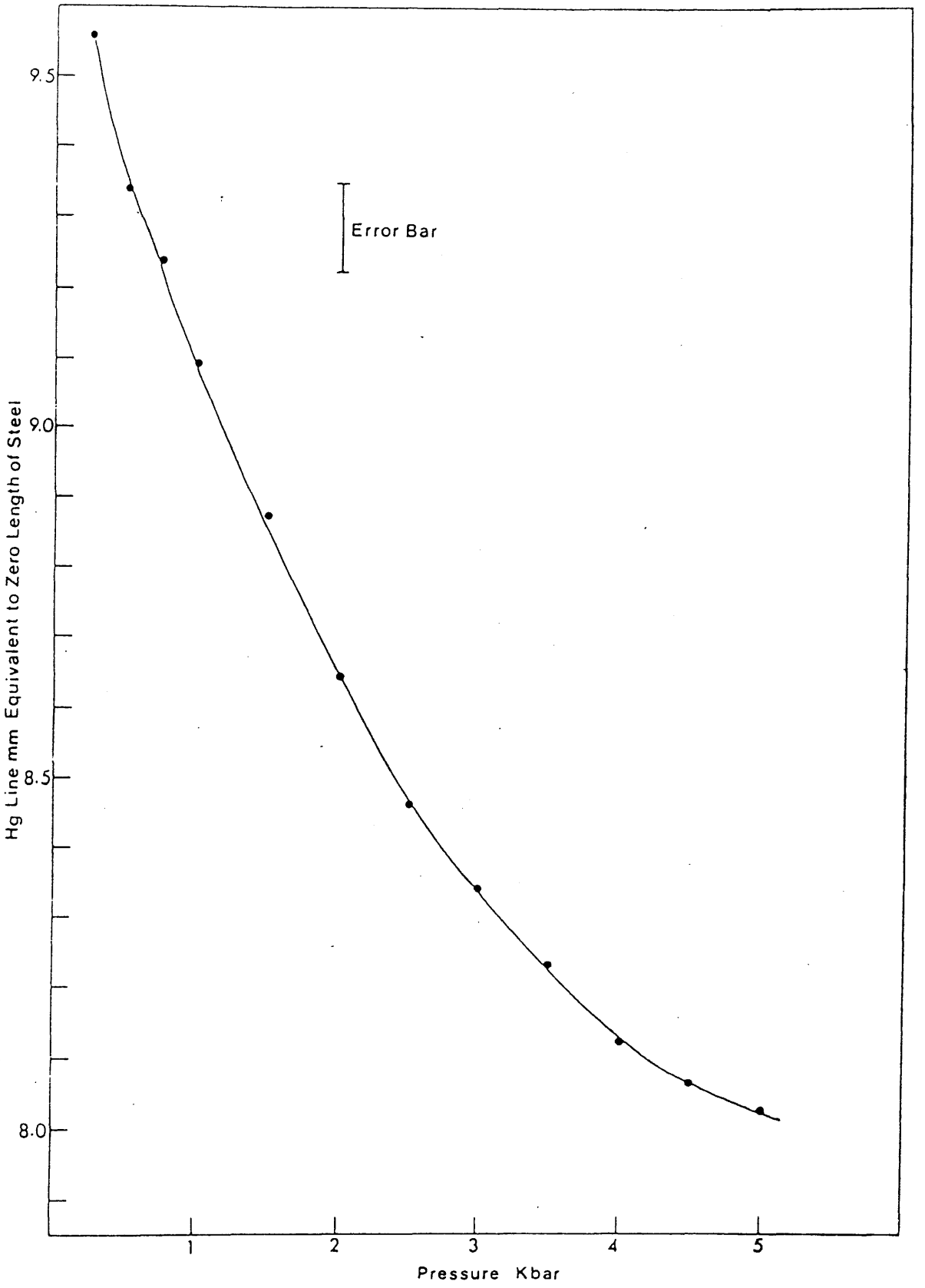

Fig 3.5 Zero-length delays for P-wave velocity measurements at high confining pressures.

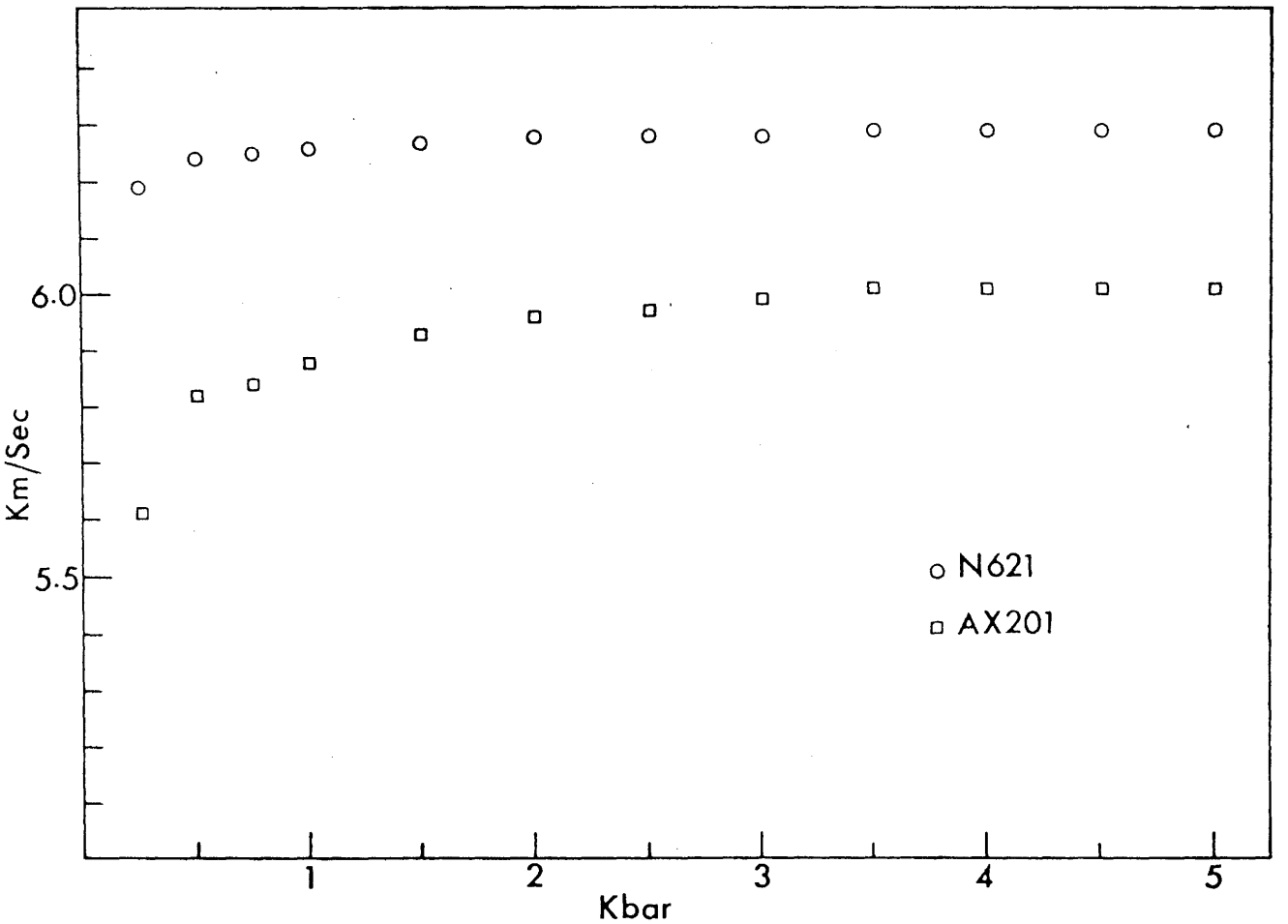

Fig 3.6 High-pressure P-wave velocity across two greywacke samples from the Northern Belt.

interpretation followed Adesanya's conclusions mentioned before. Having the high pressure velocities above, it seems possible to envisage that Warner's high velocity might be through the Northern Belt greywackes.

Owing to data and instrumental limitations, it cannot necessarily be assumed that measurements made in the laboratory are directly applicable to the interpretation of velocity data obtained under field conditions. Further high pressure velocity measurement especially across those samples showing high velocities at 200 bar, are essential for firm conclusions concerning the Northern Belt velocities.

In addition to pressure, density and porosity discussed above, another important factor affecting elastic wave velocities in rocks, is the mineral composition. Point-counting of seven of the examined samples was made available by Dr J Floyd (table 3.6), and correlation of some of the dominant minerals with the velocities measured, is shown in fig 3.7. It is possible to postulate that the velocities measured, are almost independent of the feldspars content, where, on the other hand, quartz and basic minerals and rock fragments can reduce and increase the velocity respectively.

From the percentage proportion of each mineral, an aggregate velocity could be predicted for the crack-free rock, using crack-free P-wave velocities (of each mineral);

$$Vp = 1/ \sum_{j=1}^{n} (Wj/Vj)$$

where Wj is the fractional volume of the rock occupied by the jth mineral (of n), of which the 'effective' velocity is Vj (Hall & Al Haddad 1979).

Sample No.	Formation	Q	F	FM	B	A	M	S	MX
AX 192	Afton	339	118	1	69	1	1	-	471
L 588	Shinnel	452	100	-	14	-	28	-	406
DTIA 290	Pyroxenous	241	214	14	48	6	3	11	463
L 526	Scar	124	744	-	2	-	2	-	128
AX 159	Scar	91	219	65	260	14	1	-	350
AX 160	Scar	85	191	69	291	32	7	13	312
AX 205	Scar	48	167	73	414	15	1	1	281

Q: Quartz
F: Feldspars
FM: Ferromagnesian Minerals
B: Basic Igneous Rock Fragments
A: Acidic Igneous Rock Fragments
M: Metamorphic Rock Fragments
S: Sedimentary Rock Fragments
MX: Matrix

Table 3.6 Point-counting in seven greywacke samples.

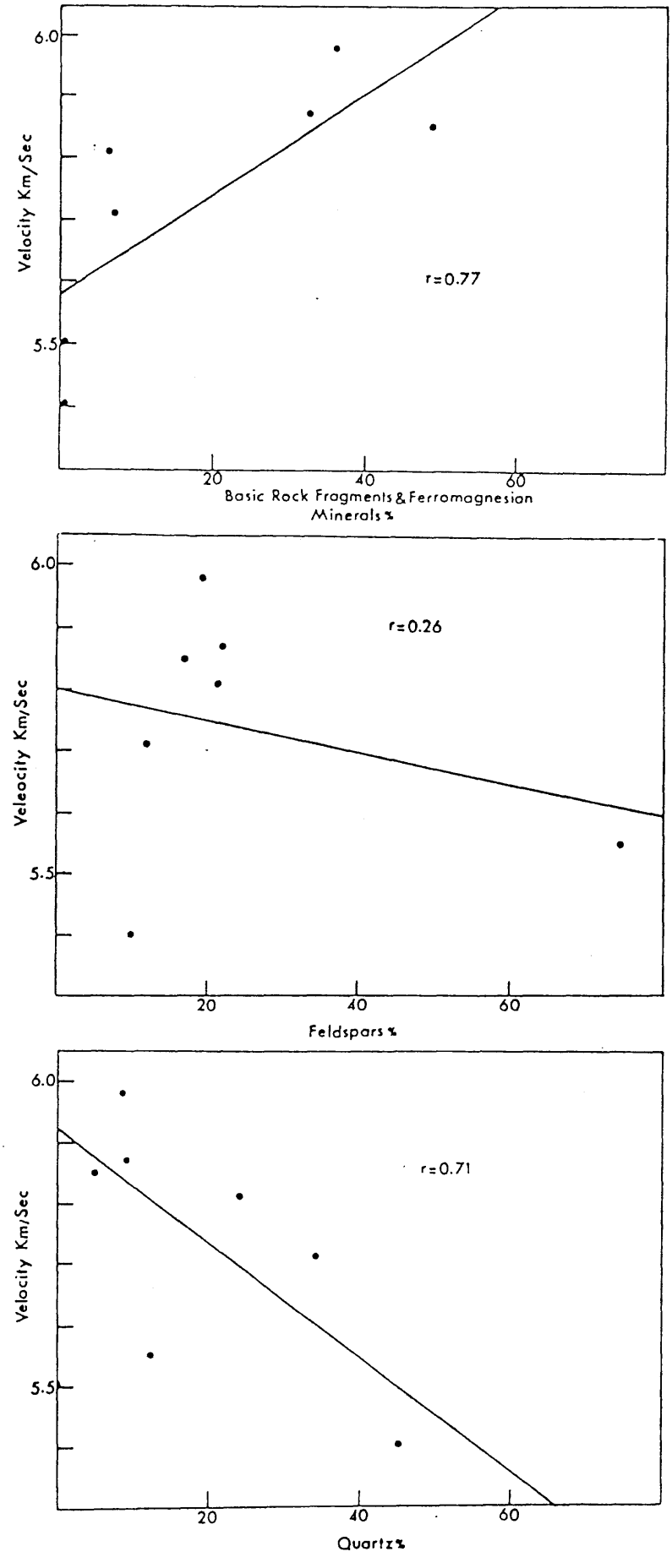

Fig 3.7 Illustration of the relationship between P-wave velocity and the major minerals of table 3.6.

With the indiscriminated broad terms of table 3.6 (eg. matrix, feldspars, rock fragments...), some averaging is expected before calculating the aggregate velocity. According to Floyd (1975), the feldspars are plagioclase (albite or andesine). Ferromagnesian minerals are pyroxene and amphibole with the presence of biotite, muscovite and chlorite. He described the basic igneous rock fragments in the Northern Belt greywackes as: gabbro, diorite, dolerite, keratophyre, andesite, spilite, serpentinite and porphyrite. The acidic rocks are granite, grano-diorite, quartz-porphyry, ryodacite, rhyolite and quartz-keratophyre. The metamorphic rock fragments are low-medium grade, eg. phyllite, epidozite, quartzite, schists and the sedimentary fragments are, greywacke, siltstone, shale, chert and limestone. From the available geophysical literature (especially Christensen 1982), the velocities assigned to each group are as follows: quartz = 6·10 km/sec; feldspars = 6·44 km/sec; basic igneous rock fragments and ferromagnesian minerals = 6·30 km/sec and metamorphic, sedimentary and acidic igneous rock fragments = 5·80 km/sec.

The selection of the proper matrix velocity to be used in the aggregate velocity determination is highly dependent on its composition. The matrix of the Northern Belt greywackes is highly compacted shale or slate (B J Bluck, personal communication). An estimated density value for the matrix can add to the understanding of the matrix composition. This was achieved by assigning a density of 2·65 Mg/m^3 for quartz, 3·00 Mg/m^3 for basic minerals and rock fragments and 3·00 Mg/m^3 for the rest of the components in table 3.6:

$$\rho = \rho A.\ A\% + \rho B.\ B\% + \rho matrix.\ matrix\% + \ldots etc.$$

Where ρ is the measured density of each sample (table 3.5) and A% is the fractional proportion of mineral A

which has a density of ρ_A. A density of 2·818 ± 0·164 Mg/m^3 was derived from seven equations. Powell (1956) obtained 2·68 - 2·83 Mg/m^3 with a mean of 2·77 ± 0·05 Mg/m^3 for Ordovician shales, sandstones and slates from Wales. Anderson & Lieberman (1968) quoted densities as high as 3·07 Mg/m^3 for shale and slate. Considering the matrix as slate and shale, an averaging velocity of 5·6 km/sec is taken from Christensen & Salisbury 1972, Christensen 1965, Wyllie et al 1956 and Birch 1960. The aggregate velocity for the seven samples in table 3.6 is calculated (see table 3.7), according to the above estimations.

The predicted velocities correlate very well with the measured grain density, if the feldspathic greywacke sample (L526) is not taken into account (fig 3.8a). The predicted velocity for sample L526 reduces the correlation coefficient considerably (fig 3.8b). This supports the previous conclusion that the velocities are almost independent of feldspars content. It is still possible that this feldspathic sample contains feldspars other than plagioclase (with lower velocities), therefore, the predicted velocity could be considered as an over-estimation.

The calculated velocities are expected to be higher than those measured at 200 bar confining pressure, because they represent crack-free greywackes. If this is true, then a good correlation would be expected between the velocity difference (ΔV= predicted-measured) and the porosity values (fig 3.9a). Fig 3.9b shows how the correlation is completely lost when sample L526 was included.

3.7 Conclusions

1. In the Ballantrae ophiolite, serpentinite, spilitic lava, chert and granite have a range of velocities

Sample No.	Velocity km/sec at 200 bar	Predicted velocity km/sec	ΔV
AX 192	5·71	5·90	0·19
L 588	5·40	5·91	0·51
DTIA 290	5·81	5·93	0·12
L 526	5·55	6·27	0·72
AX 159	5·87	6·04	0·17
AX 160	5·98	6·04	0·06
AX 205	5·85	6·08	0·23

Table 3.7 Measured and calculated P-wave velocities for the greywacke samples of table 3.6, and the difference between them.

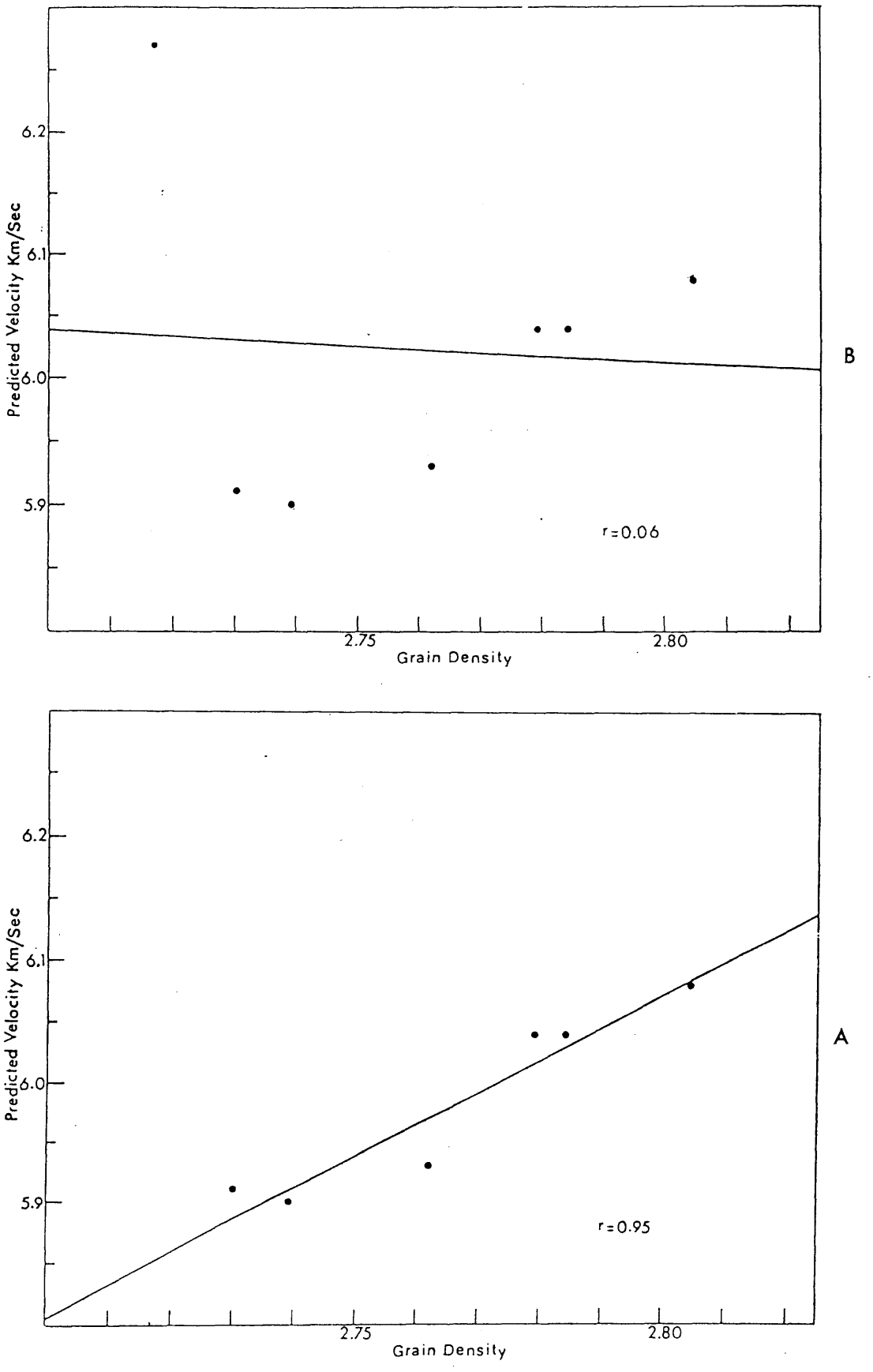

Fig 3.8 Relationship between grain density and calculated velocity for the greywacke s of table 3.8.A)Excluding sample L526.B)Includig L526.

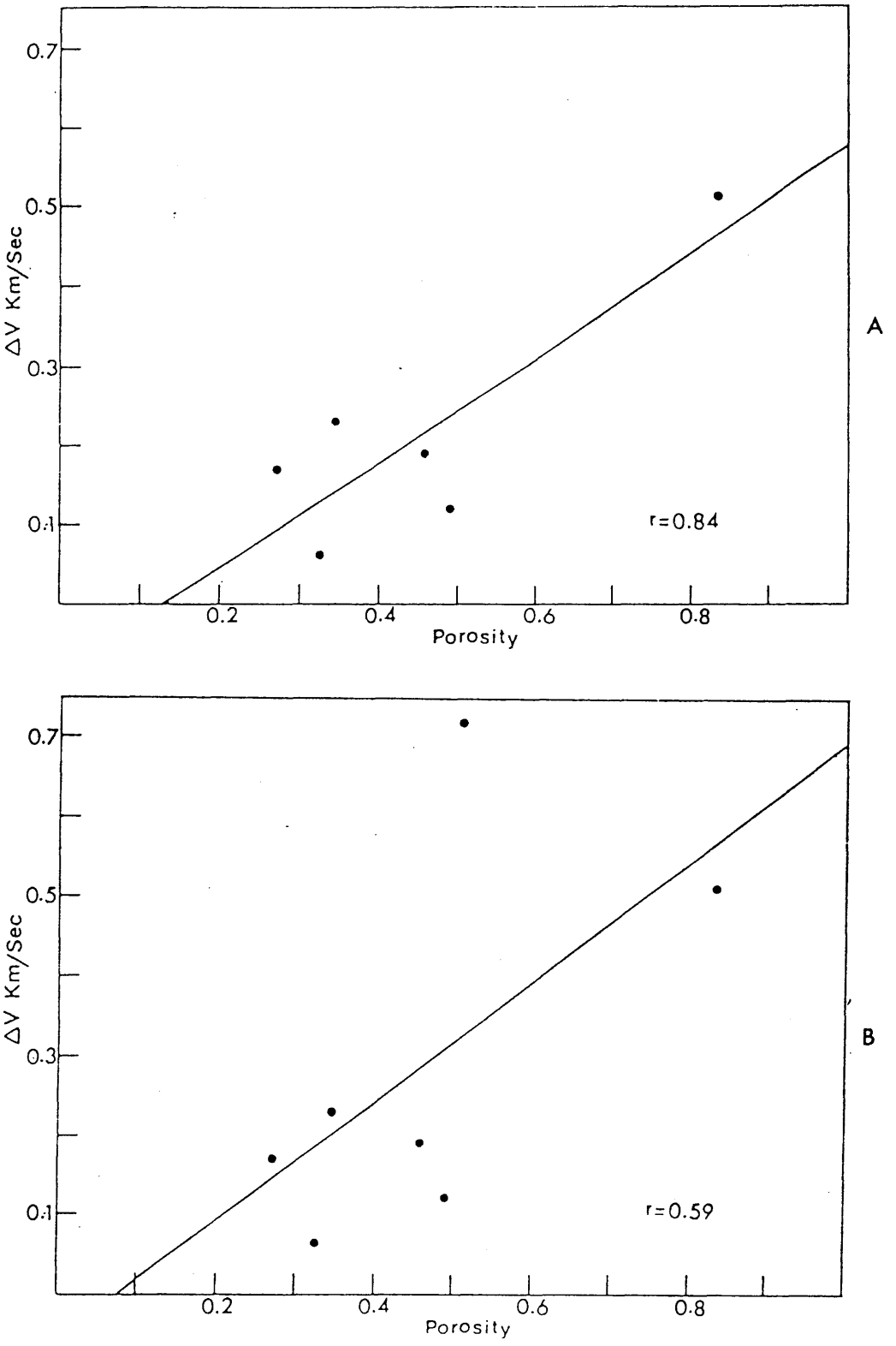

Fig 3.9 Relationship between porosity and the measured and calculated velocity difference.A)Excluding sample L526.B)Including L526.

from 4·0 to 5·7 km/sec. They are much lower than those measured for dolerite and gabbro in the same suite. Accordingly, any velocity in the field higher than 6·0 km/sec is expected to be for gabbroic rocks or a mixture of gabbro and dolerite.

2. Velocities across the Northern Belt greywackes are higher than those of similar rocks in the Girvan district. Some very mafic greywackes reach over 6·0 km/sec.

These velocities are highly dependent on the percentage of basic minerals and quartz but are less dependent on the feldspar content. Average Northern Belt greywacke is likely to have a velocity of 5·7 km/sec at 200 bars (equivalent to a depth of about 1000 m).

CHAPTER FOUR

Field-derived Velocities Associated with Geological Formations and the Seismic Interpretation

4.1 Introduction

Refraction interpretation is often based on first arrivals, primarily because these provide the most readily determined travel times. From a knowledge of the velocities of geological formations in the area, one attempts to reconstruct the paths of the seismic waves. This depends mainly on analysis of the T-X graphs. Each interpretational method is in turn constrained by certain conditions.

There are three main seismic and geological units in the study area (Carboniferous and Upper Old Red Sandstone, Lower Old Red Sandstone and Lower Palaeozoic and Crystalline Basement). The recorded seismic profiles (presented in chapter 2) provide direct and indirect measurements of each of these units. The apparent velocities encompassed on each line may be summarised as follows:

Profile	Carboniferous and Upper Old Red Sandstone 3·6-4·2 km/sec	Lower Old Red Sandstone and Lower Palaeozoic 5·0-5·8 km/sec	Crystalline Basement 6·0-6·4 km/sec
Lendalfoot Array	Continuous increase of velocity with range, 5·0 - 6·1 km/sec		
Galloway line	-	5·77 km/sec	-
Girvan line	-	-	6·44 km/sec, 6·55 km/sec

Profile	Carboniferous and Upper Old Red Sandstone 3·6-4·2 km/sec	Lower Old Red Sandstone and Lower Palaeozoic 5·0-5·8 km/sec	Crystalline Basement 6·0-6·4 km/sec
Portobello-Troon line	-	5·31 km/sec	6·0 km/sec, 6·4 km/sec
Loch Doon line	3·62 km/sec	5·57 km/sec	6·39 km/sec, 6·55 km/sec
Colmonell line	4·04 km/sec	5·06 km/sec	6·28 km/sec, 7·08 km/sec

All of the recorded profiles provided high velocities (>6·0 km/sec) which are likely to be from crystalline basement, except the Galloway profile. This chapter is devoted to the analysis of the T-X graphs, velocities of geological formations as well as the methods applied in interpreting the data sets.

4.2 Velocities of Geological Formations

Velocities of those rocks likely to be present in the study area are discussed in detail in this section to provide a basis for better understanding of the T-X graphs.

4.2.1 Carboniferous

Direct measurements on Carboniferous rocks are obtainable on the first parts of the Loch Doon and Colmonell lines, where the energy sources are located in a Carboniferous dolerite sill and Productive Coal Measures respectively (fig 2.1). The velocity recorded on the Loch Doon line is 3·62 $\pm$ 0·04 km/sec. Results from the WHB integral (fig 4.1) show a surface velocity

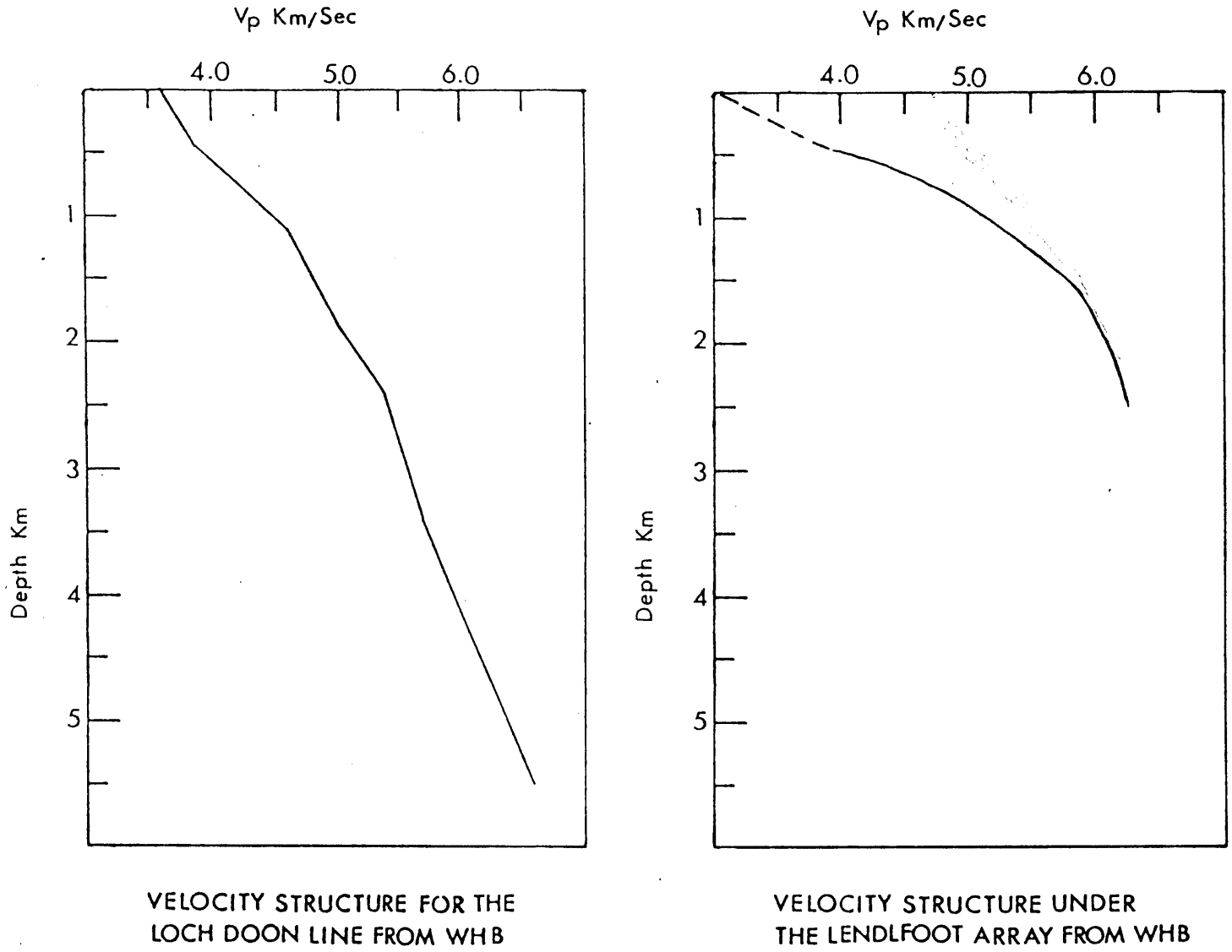

Fig 4.1 Velocity-structure under the Loch Doon line and the Ballantrae ophiolite complex.

of 3·61 km/sec, increasing to 3·88 km/sec at about 500m depth. A thickness of 780m is obtained for the Carboniferous and Upper Old Red Sandstone by planar-layer interpretation which is similar to that estimated by McLean (1966), where he fixed a thickness of 800m for Carboniferous and Upper Old Red Sandstone in his gravity interpretation in the area.

On the Colmonell line, the recorded velocity is 4·04 km/sec, with the WHB integral results in a velocity of 3·91 - 4·15 km/sec over a range of depth 0·0 to 800m. By planar-layer interpretation, a thickness of 900m is achieved.

Hall (1970 and 1978a), from refraction measurements in the western Midland Valley and Firth of Clyde quoted velocities of 3·61 $\pm$ 0·10 km/sec and 3·80 $\pm$ 0·05 km/sec for Carboniferous sediments respectively. Allsop (1974) gives a velocity of 3·78 $\pm$ 0·32 km/sec from borehole velocity-log in Carboniferous sediments (in East Lothian: Spilmersford No.17 borehole). Sola (1985) derived a velocity of 3·63 $\pm$ 0·08 km/sec at a mean depth of 0·5 km for the same sediments in the central Midland Valley.

The Carboniferous velocity on the Colmonell line is higher than that expected for the Coal Measures, where the NCB open-cast and the receivers are sited. The measured velocity is even higher than that for Lower Limestone Group (3·57 - 3·96 km/sec) quoted by Hall (1970), furthermore, the geological section shows that no Lower Limestone Group exist in the area (see fig 1.1). The velocity value may match with those of Carboniferous lava but again none of it exists in the southern Midland Valley. A hidden sill is a possible cause of such high velocity.

4.2.2 Upper Old Red Sandstone

The recorded seismic profiles provide no direct measurements on this geological unit. Hall (1970) derived hammer-line velocities of 2·0 - 4·0 km/sec for the Upper Old Red Sandstone. Sola (1985), from density, porosity and velocity relationships, estimated a velocity of 3·70 - 4·10 km/sec for the Upper Old Red Sandstone in the Midland Valley.

Seismically, the Upper Old Red Sandstone has been considered here as part of the Carboniferous velocity group with which it is conformable.

4.2.3 Lower Old Red Sandstone

The apparent velocity of the second segment is 5·57 $\pm$ 0·07 km/sec on the Loch Doon line and 5·06 $\pm$ 0·06 km/sec on the Colmonell line (fig 4.2). None of the profiles distinguish Lower Old Red Sandstone from Lower Palaeozoic rocks in terms of velocity. Davidson (1985) and Sola (1985) indicated that velocities in Lower Old Red Sandstone and Lower Palaeozoic overlap at depths between 1 and 3 km, and that neither of the two groups will exceed 5·75 km/sec at depths less than 5 km.

The uneven distribution of Carboniferous rocks around the Benbain Open-Cast source precludes valid WHB analysis of underlying Lower Old Red Sandstone. Such analysis is more valid for the northern end of the Loch Doon line where Carboniferous of moderately uniform thickness extends 30 km south of Hillhouse quarry. By applying the WHB integral $Z(V) = \frac{1}{\pi} \int_0^{\Delta} \text{Cosh}^{-1} \left(V \frac{dt}{dx}\right) dx$ (where $\frac{1}{V} = \left(\frac{dt}{dx}\right)$ and $X = \Delta$, see Grant & West 1965), the derived velocity-

Numbers represent seismometer stations shown on fig 2.15a (see table 6 appendix 1 for station names).

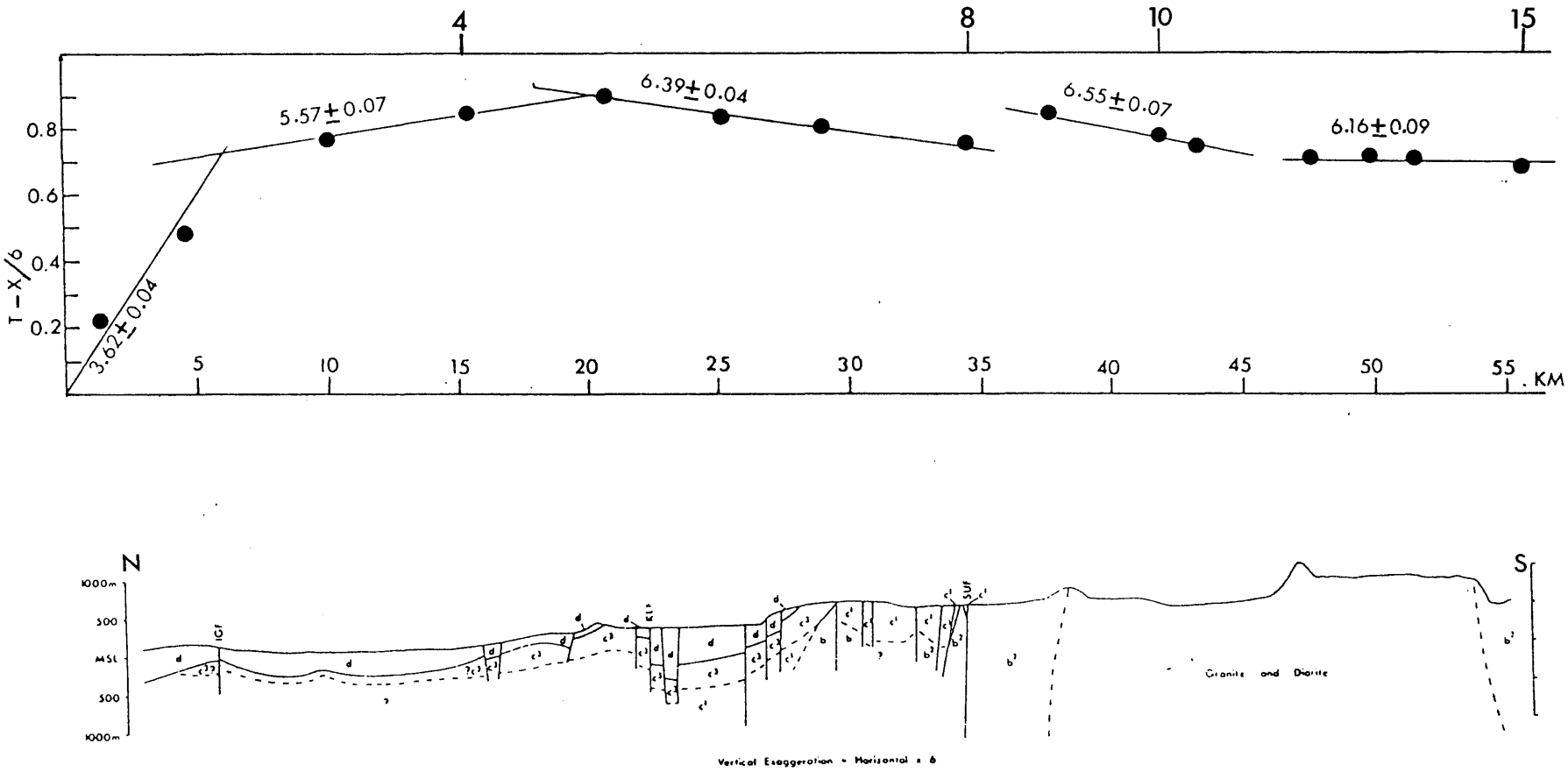

Fig 4.2a Loch Doon line-reduced time-distance plot of first arrivals with cross section based on geological evidence. b:Lower Palaeozoic,c:Lower Old Red Sandstone,d:Carboniferous, IGF:Inchgotrick Fault, KLF:Kese Loch Fault,SUF:Southern Uplands Fault.

Numbers represent seismometer stations shown on fig 2.15a (see table 7 appendix 1 for station names).

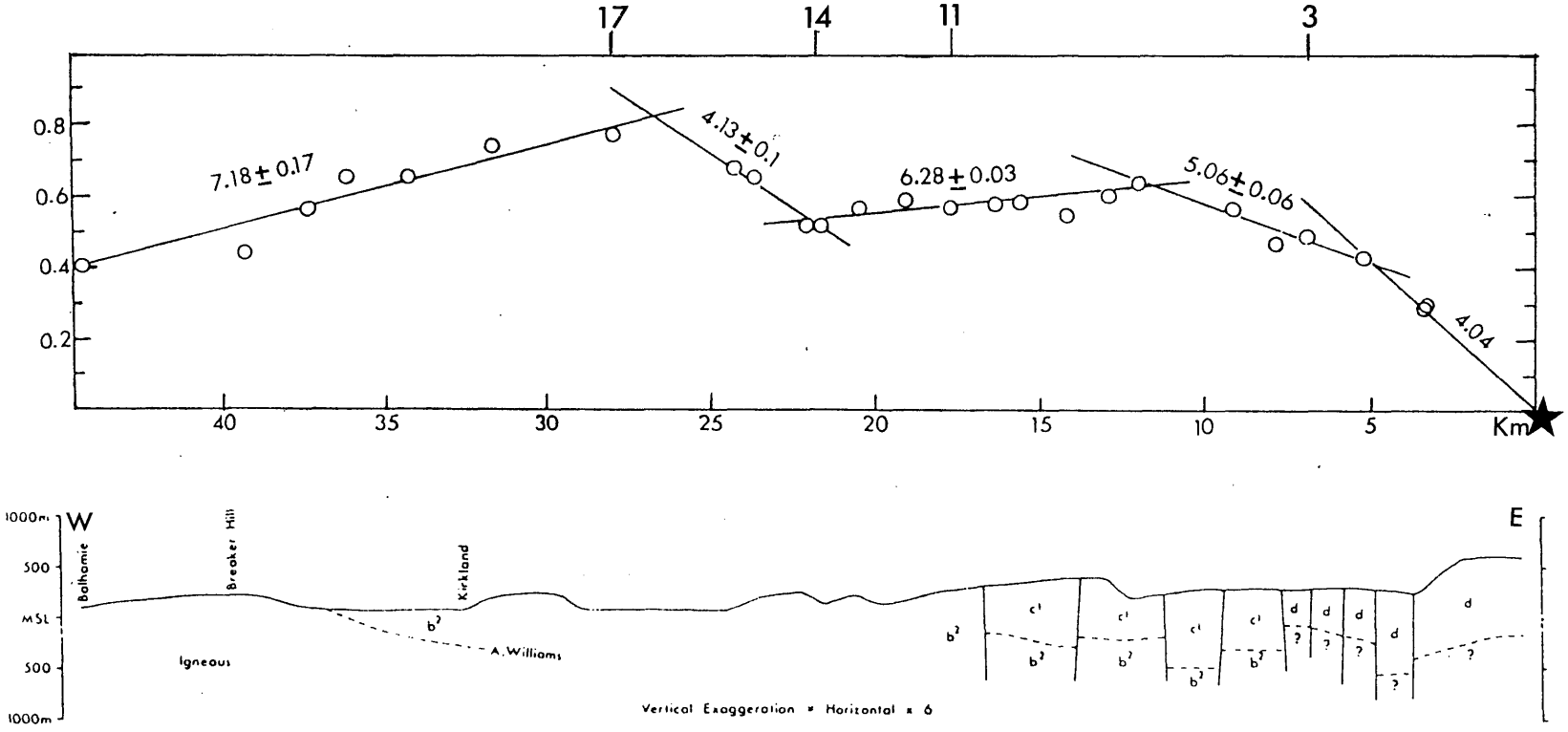

Fig4.2b Colmonell line-reduced time-distance plot of first arrivals with cross section based on geological evidence.Abbreviations as in fig 4.2a

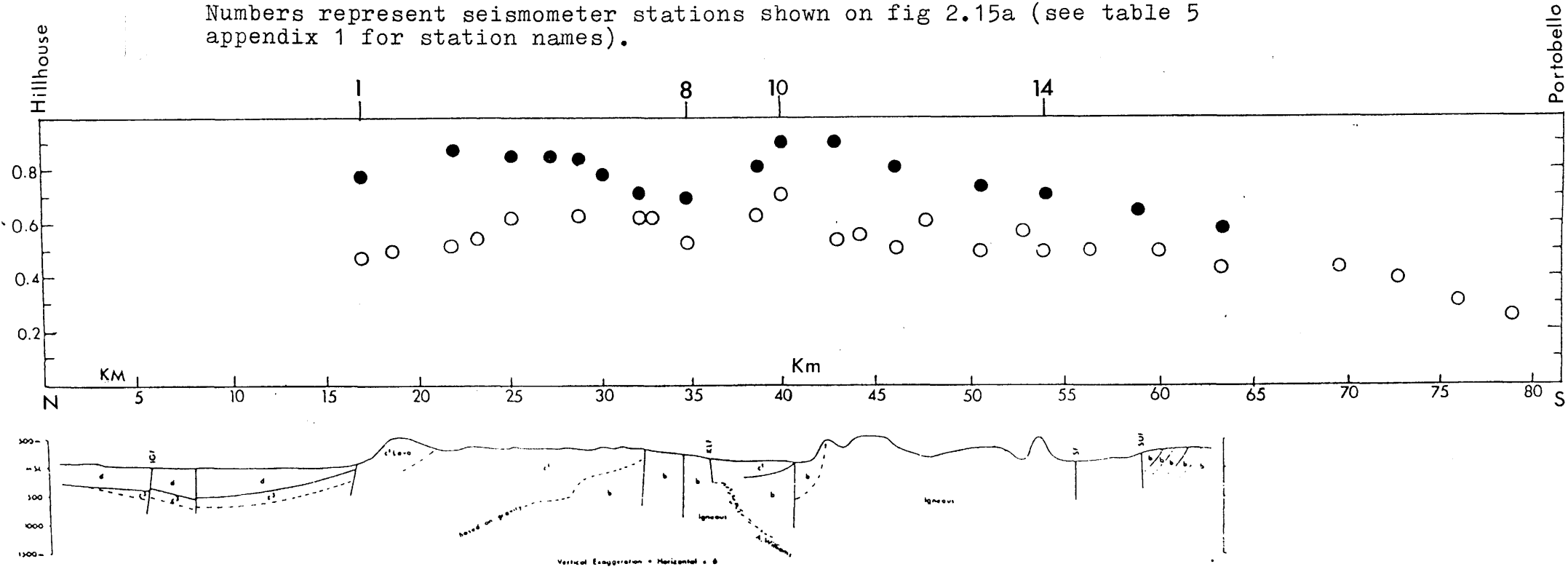

Fig 4.2c Girvan line-reduced time-distance plot of first arrivals with cross section based on geological evidence. SF:Stinchar Fault,other abbreviations as in fig 4.2a. ○ Recording from Portobello shot. ● Recrding from Hillhouse Quarry.

depth structure is shown in fig 4.1. Carboniferous velocities could be traced to a depth of about 900m (as mentioned in 4.2.1), then the velocity increases to 4·6 km/sec at 1·1 km depth, and steadily increases to reach 5·75 km/sec at 3·4 km depth where the velocity markedly increases to above 6·0 km/sec.

Hall (1970) indicated a surface velocity of 4·0 km/sec for Lower Old Red Sandstone. Davidson (1985), from direct refraction measurements in the Southern Midland Valley obtained a velocity of 4·2 - 5·0 km/sec to 1 km depth, but he indicates that these values are higher than those expected, due to a number of sills in the area (K Davidson, personal communication).

4.2.4 Silurian and Ordovician

New direct measurements on Lower Palaeozoic outcrops have been made on the Galloway line and Portobello-Troon line (fig 2.1). A velocity of 5·31 ± 0·04 km/sec is recorded for the Lower Palaeozoic rocks on the Portobello-Troon line (fig 4.2c), from the Rhinns of Galloway to the Stinchar Fault. In the Southern Uplands, close (10 km range) shots into EKA show an increase in velocity from 4·5 to 5·6 km/sec within a km from the surface (El-Isa 1977). This extends back to the surface a velocity of 5·8 km/sec, achieved by inversion of apparent velocities from more distant shots in various azimuths (Jacob 1969). Travel times across the Southern Uplands on LISPB (shot E and 2 into segment Beta) are the basis for the 5·8 - 6·0 km/sec Lower Palaeozoic layer to over 10 km depth on that model (Bamford 1977, 1978). Higher along strike velocities on SUSP and into EKA suggest that the previous deep velocity projections are averages across unresolved structure (Hall et al 1983). The Lower Palaeozoic

interpretation of the same layer, 5·8 - 6·0 km/sec, under the Midland Valley in the LISPB model was questioned by Sola (1985) and Davidson (1985) on the same basis. Davidson (1985) did not question the geometrical interpretation of the LISPB refractor, but he disproved its geological interpretation as being due to Lower Palaeozoic sediments. He concluded that this refractor must be due to a quartz-feldspar rich crystalline rock (either igneous, metamorphic or a mixture of both).

The Lower Palaeozoic velocity on the Galloway line is not different from that of LISPB (5·76 ± 0·04), at ranges of 40-67 km. In order to investigate the shallow velocity structure along this line, time and location of one of the nearest air-gun shots to the recording sites (fig 2.1b) were acquired from Durham University. This particular shot was recorded on most of the recording stations (appendix 1 table 10) and gives a velocity of 5·77 ± 0·03 km/sec, over a range of 13-37 km across the Southern Uplands. This means that there is no change in the 5·77 km/sec velocity along the Galloway line (13 - 67 km), and it suggests a great thickness of Lower Palaeozoic sediments in this area.

4.2.5 Crystalline Rocks

There is very little exposure of 'basement' in the Midland Valley, though numerous Carboniferous vents include xenoliths of basement rocks (eg, magnesian peridotites, Fe-rich ultramafics, basic pyroxene granulites, quartzofeldspathic granulites and gneisses, miscellaneous rocks of presumed igneous origin, see Upton et al 1984). Thus the only field seismological data on basement velocities is derived from measurements across the Ballantrae Complex, discussed overleaf. In a wider regional context the following points are relevant.

The travel-times on LISPB across the Dalradian outcrop have been modelled by a layer with velocities rising very slowly with depth to about 6·05 km/sec at approximately 10 km. Another potential crystalline outcrop, the Lewisian basement complex in NW Scotland, was studied by Hall 1978. He raytraced a velocity of 6·0 km/sec at 1 km depth for the northern belt amphibolite-facies quartzo-feldspathic gneisses, and 6·5 km/sec for the granulite facies at the same depth. Similar velocities were achieved from laboratory measurements on the same rocks by Hall and Simmons, 1979. Adesanya (1982), derived laboratory measured velocity values under different confining pressures for a granodiorite sample from the Southern Uplands. His values are about 6·0 km/sec at 3 km depth.

4.3 Velocity Structure at the Lendalfoot Array

First arrivals of shots at comparable ranges (land shots, air-guns and WISE explosive shot No. 1, fig 2.2) have been subjected to time-term analysis (Willmore & Bancroft 1960). This method assumes that the travel-time data between a system of shots and stations for a single refractor of velocity V, but varying depth can be fitted by a series of equations of the type;

$$tij = \Delta ij/V + ai + bj$$

where Δij is the shot-station distance and the time-terms ai and bj are the delays introduced by the overlying layers at shot and station respectively. The observational equations can be solved by least-squares for the unknown velocity and time-terms provided that 1, there are more equations than unknowns, and 2, at least one shot point and station have a common position (otherwise the equations are singular).

To carry out the analysis, the author used

a computer program written by Mechie (1980). Condition 2, was satisfied since 3 of the land shots were fired at seismometer positions (see fig 2.2). The total number of equations is 113 for 29 sites: 9 seismometers, 6 land shots, 13 air-gun shots and the first marine explosive shot (fig 2.1). The ranges involved are $<$15 km. The average time-term for the 15 land sites is 0·11 sec, and for the 14 marine sites is 0·35 sec, with a refractor velocity of 5·19 km/sec. The standard error of the solution is 0·04 sec.

A WHB analysis of variable velocity under the array is obtained by inversion of a mean T-X curve drawn through a series of airgun shot-recorder T-X curves (fig 4.3), shifted in time to allow for variable delay under the shots (see fig 3 appendix 2). The result shows a continuous increase of velocity with depth (fig 4.1), reaching 6 km/sec at a depth of 1·75 km and increases to 6·21 km/sec at 2·10 km depth.

Attempts to incorporate more distant WISE shots (eg, shots 2.3.4 running NW across the Firth of Clyde) are unhelpful since there is insufficient data to resolve the shot location delay from the refractor velocity.

The land shots (fig 4.4) make a range of azimuths into the Lendalfoot array, crossing different lithological units. The average velocity in general increases with range, but there are noticeable exceptions. The Millenderdale shot has an average velocity of 5·93 km/sec to the Knockbain seismometer, across the lava outcrop, and 4·82 km/sec at a similar range along the southern serpentinite belt to the Breaker Hill seismometer (fig 4.4). The Dinvin shot has its lowest average velocity at the furthest seismometer (Lendalfoot)

Air-gun shots involved are 248△, 252○, 256□, 262◇ and 267▽ recorded on the across strike arm of the Lendalfoot array (seismometers: Lendalfoot, Cundry Mains, Knockbain., Breaker Hill and Bargain Hill).

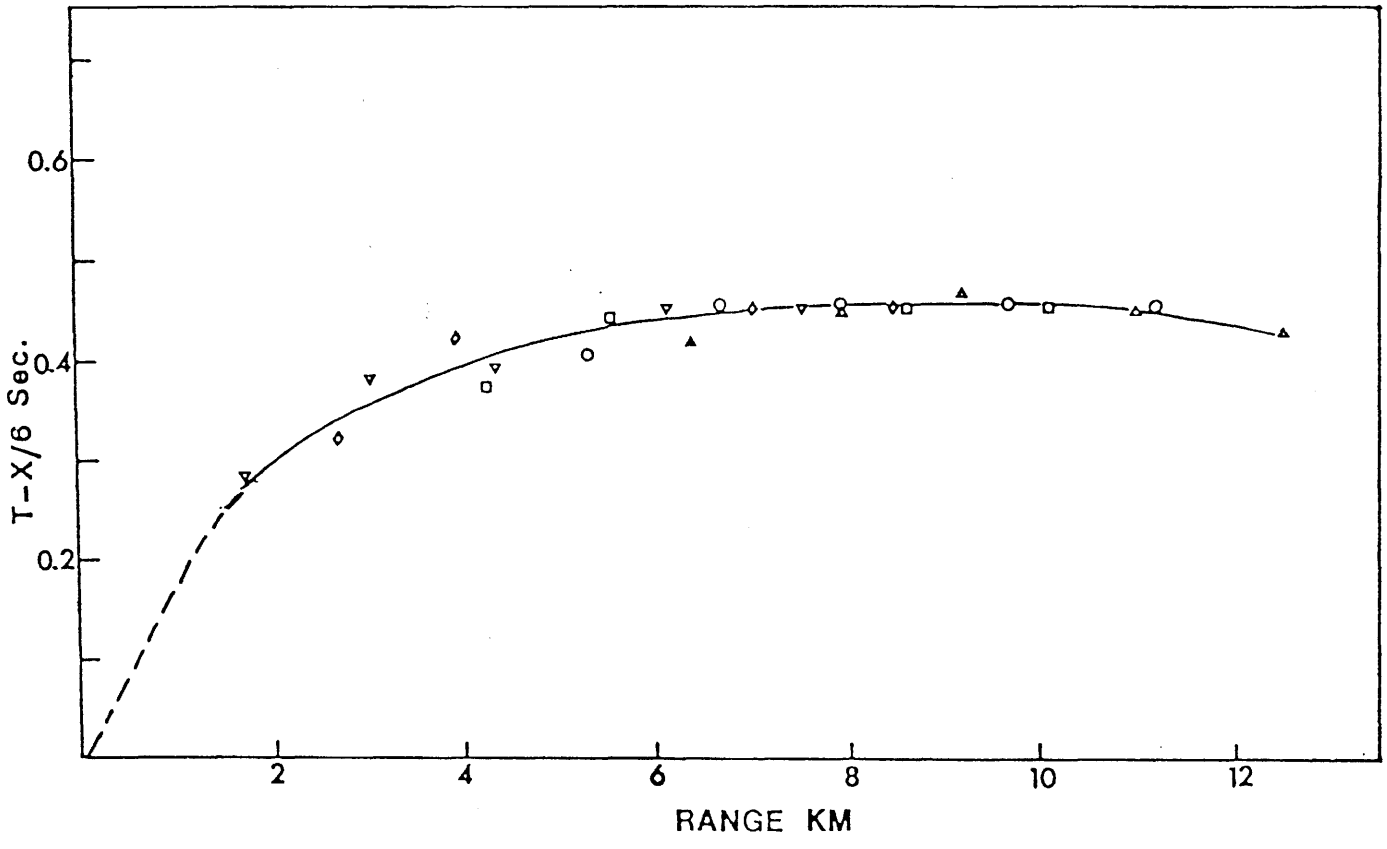

Fig4.3 Reduced T-X plot of first arrivals of airgun shots on the Lendalfoot array.

Each symbol represents one shot, each shot shifted in time to allow for variable delay.

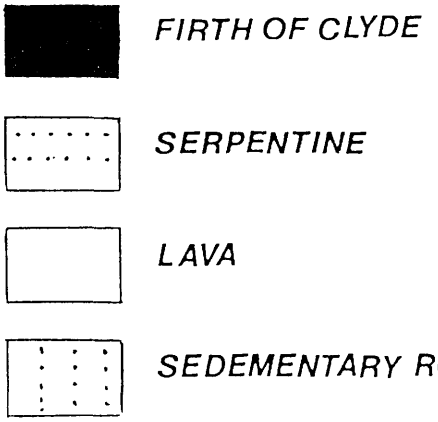

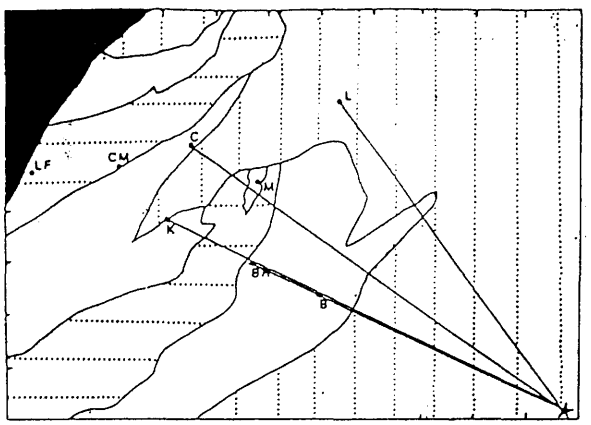

Craigconnachie Shot

Station	Average Vel. km/sec
LF	---
L	5.42
C	5.27
K	5.46
B	5.22
Br	5.60
P	---

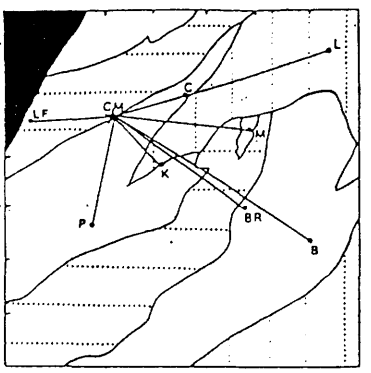

Cundry Mains Shot

Station	Average Vel. km/sec
LF	3.48
L	4.18
C	3.81
K	3.32
B	4.63
Br	4.33
P	4.01
M	3.84

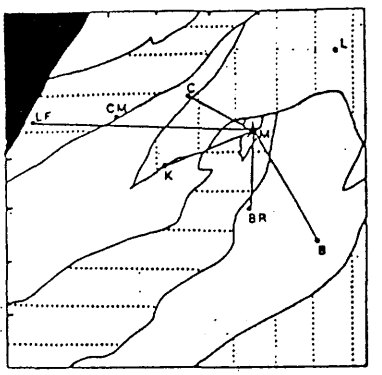

Millenderdale Shot

Station	Average Vel. km/sec
LF	4.38
L	----
C	4.62
K	5.93
B	5.21
Br	4.82
P	----
M	----

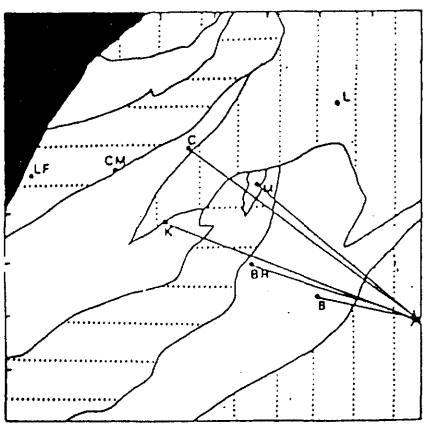

Pinmore Shot

Station	Average Vel. km/sec
LF	----
L	----
C	5.12
K	5.04
B	4.80
Br	4.91
P	---
M	5.10

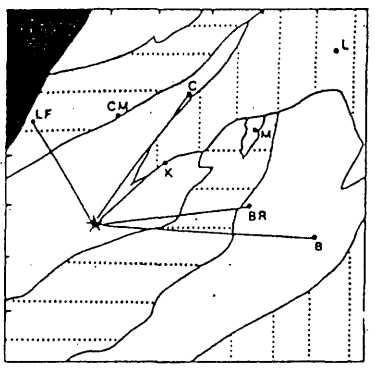

Knockormal Shot

Station	Average Vel. km/sec
LF	4.33
L	---
C	4.16
K	4.27
B	4.74
Br	5.28
P	----
M	----

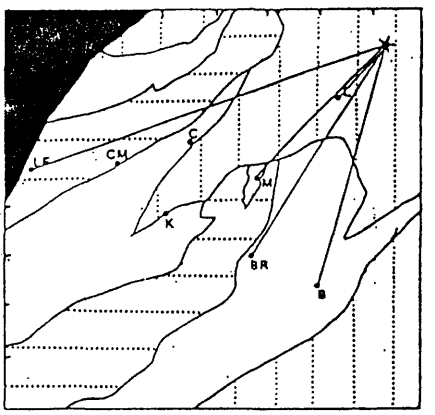

Dinvin Shot

Station	Average Vel. km/sec
LF	4.62
L	4.09
C	----
K	----
B	5.12
Br	5.02

Fig4.4 WISE land shots-average velocities in relation to the Lendalfoot array. For abbreviated seismometer sites see table 2.1.

along the southern serpentinite belt. These could be explained on the basis that there are slow and fast paths across the ophiolite (as was concluded in chapter 3); the slowest is the longest for the wave to travel along the serpentinised rocks. Serpentine is not the only reason for low velocities, as fracturing (open near the surface) is a strong feature of the Ballantrae ophiolite and is expected to lower the velocities. Evidence supporting this, is that the scatter in fig 1 appendix 2 affects points mostly at ≤ 4 km range. Furthermore, LISPB considered the fracture effect by having a top layer of 5·0 km/sec in the Southern Uplands, where Lower Palaeozoic rocks are outcroping. El-Isa (1977), from shots of 10 km ranges into EKA showed an increase of velocity from 4·5 to 5·6 km/sec, for the same reason.

For all the land shots recorded on the Lendalfoot array, interval velocities (pairs of seismometers or shot-seismometer) were plotted against range. Velocities between the Breaker Hill and Bargain Hill seismometers are much higher than those between other pairs of seismometers. By taking the log of the station distances, linear regression is possible and the data could be represented as

$$V = Vo + a \log X$$

Fig 4.5 shows that the surface velocity (Vo) is 4·21 km/sec and the constant (a) is equal to 1·3. The velocities between Breaker Hill and Bargain Hill stations are well above the standard deviation of the points from the best fit line. These two seismometers are situated on the gravity culmination in the area (fig 4.6a) and the high velocities confirm Powell's conclusion (1978) of the existence of a shallow ultrabasic body (velocity $>6{\cdot}0$ km/sec) under the southern serpentinite belt of the Ballantrae ophiolite (fig 4.6b).

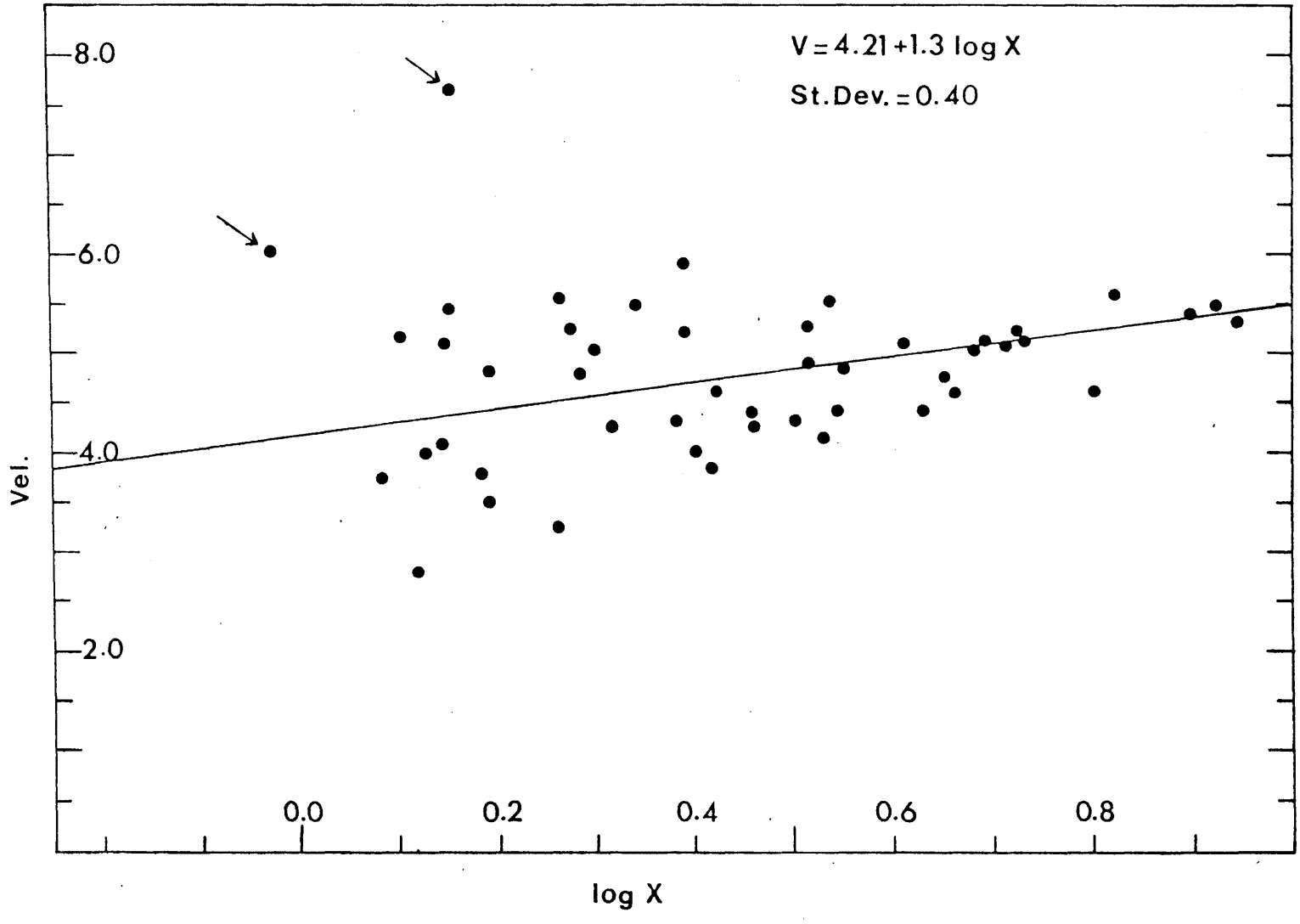

Fig4.5 Plot of interval velocities against logX for land shots recorded on the Lendalfoot arra

Arrows point to high velocities between Breaker hill&Bargain hill seismometers

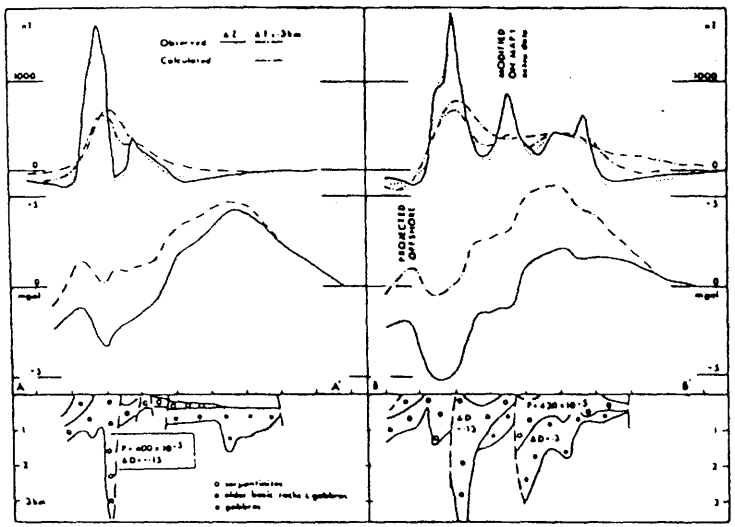

Fig4.6b Observed and calculated magnetic and gravity anomalies along profiles A and B shown in Fig.4a. The pseudo-gravity effect of the serpentinite has been added to the residual gravity profile (solid line) to produce the profile on which the dense body is modelled. P = polarisation contrast in cgs; △D = density contrast in gm/cc.

(after Powell 1978)

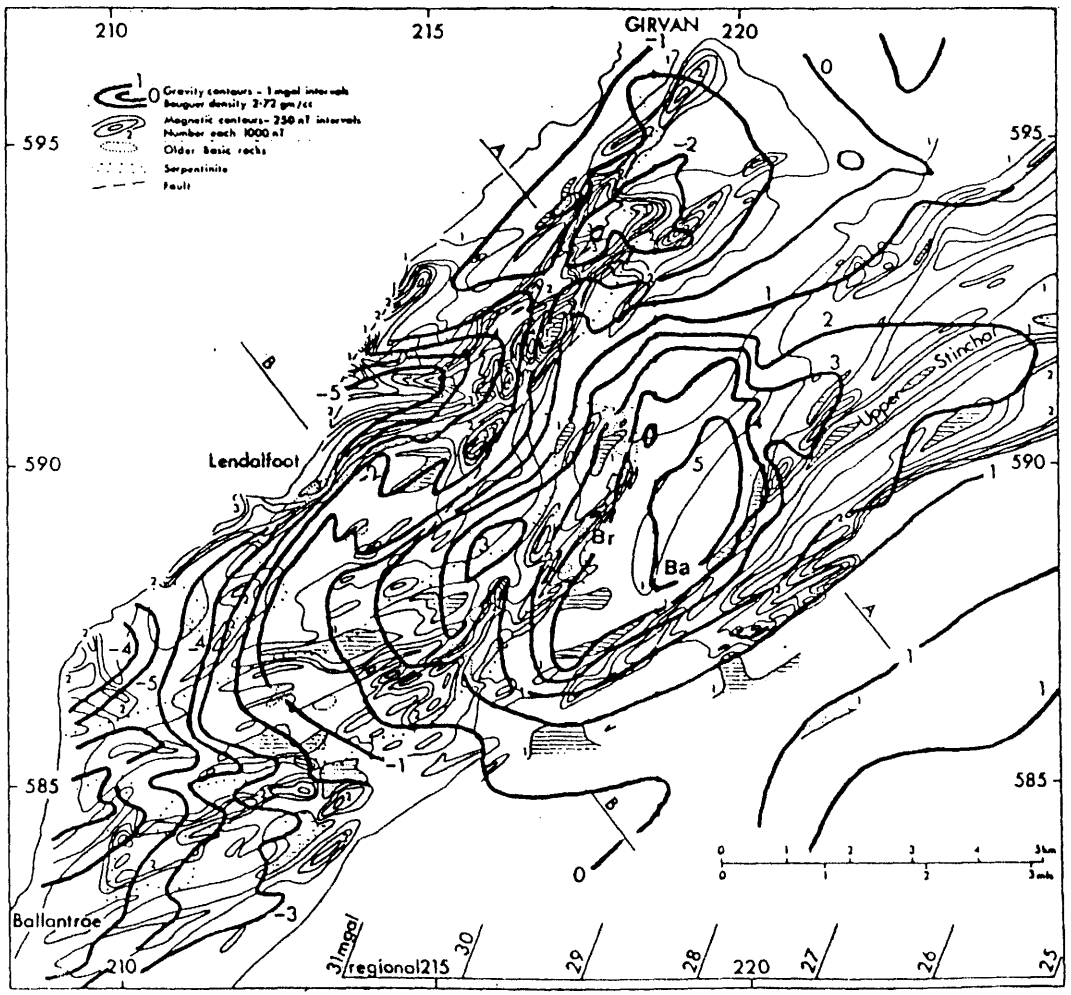

Fig4 6a Map of residual Bouguer gravity and vertical component magnetic anomalies of the Ballantrae region; lines of section refer to figure b.

Ba: Bargain hill Br: Breaker hill

4.4 The Delay Modelling

A delay of 0·20 - 0·27 sec has affected the central parts of the Girvan line, Loch Doon line and the Colmonell line (see chapter 2 and fig 4.2). The seismic and geological possibilities that can cause such a feature are discussed in this section. Three models were envisaged to cause the delay. The reversal of the Girvan line (Portobello-Troon line) will be discussed later in this chapter, after elaborating on the dimensional possibilities of each model.

4.4.1 Basement Step

Occurence of the delay at Kerse Loch Fault (Girvan line, fig 4.2c) and the Southern Uplands Fault (Loch Doon line, fig 4.2a) produces the possibility that these faults may cause a step in the basement, down-throwing lower velocity rocks to the south (fig 4.7a). Taking the upper layer velocity (Vo) as 5·3 km/sec and the basement velocity (V_1) as 6·4 km/sec, the throw Z_T can be determined from the difference between the intercept times of the two linear segments

$$Z_T = (Ti2 - Ti1) \frac{V1\ Vo}{\sqrt{V1_2 - Vo_2}} \quad \text{(see Dobrin 1976)}$$

The throw is calculated to be 0·8 - 1·0 km. The facts which may argue against this model are: (1) the down-throw of lower velocity rocks to the south is against the geological outcrop likelihood, where older rocks crop out southwards (see fig 1.1, though inversion is common across these faults to the NE of this area). (2) The shallowness of the basement on the Colmonell line (fig 4.2b), which is situated at the south of the Midland Valley, provides further evidence against this model.

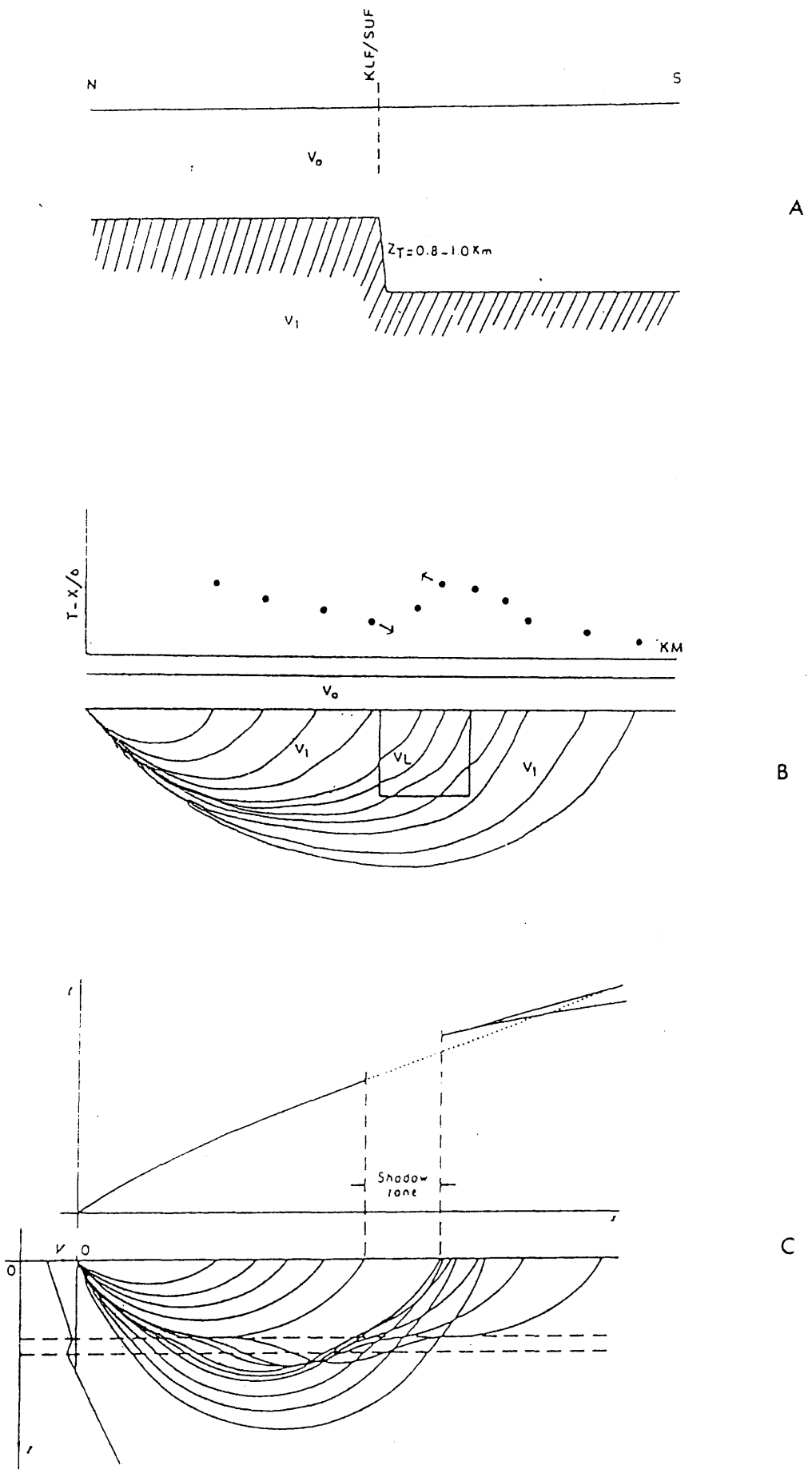

Fig 4.7 Illustration of some sources of seismic delay.

A)A step in the basement B)Shear zone

C)Low-velocity layer at depth.

4.4.2 Fractured Rocks in a Fault Zone

This model involves lateral changes in the velocity structure where sheared or fractured rocks in a fault zone can cause the delay by having rocks of higher velocity on either side (fig 4.7b). The apparent velocity (VA) is approximately equal to the true velocity of the slow zone, but must be greater than the velocity of overlying formations. This apparent velocity is a value which might be reduced by closer spacing of recording stations, corresponding in position to a narrower lower velocity zone which would produce the same nett delay as that modelled with actual spacing (see arrows on fig 4.7b).

Rays passing underneath the low velocity zone will be delay-free, and will continue the trend of the T-X graph for those rays arriving at the surface before the low velocity zone.

4.4.3 Velocity Inversion with Depth

The occurence of a low velocity zone at depth (fig 4.7c) can also cause the delay effect (see Goguel 1951). The apparent velocity of the low velocity layer (VA) could be derived by $VA = \frac{\text{Width of Delay}}{\text{Time of Delay}}$,

and then the true velocity of the layer $(VL) = \sqrt{VH.VA}$ where VH is the velocity surrounding the low velocity layer (ie, high velocity). Furthermore, the thickness of the layer (L) could be calculated from the formula

$$\text{Delay (sec)} = \frac{2L.\ VH}{VL\ \sqrt{(VH)_2 - (VL)_2}}$$

After calculating the true velocity and the thickness of the low velocity layer, program LAUFZEIT was used to match a depth-velocity structure for the

Girvan, Loch Doon and Colmonell line (fig 4.8a,b,c). The input to the program is estimated depth-velocity values and the output is time-distance values. The program is simply a ray-tracing technique with horizontal layering (ie, no lateral velocity changes are accommodated). The same velocity structure could be fitted for both the Girvan and Loch Doon lines, with the low velocity zone narrower on the latter. Although the results match reasonably well with the T-X graphs, certain limitations are to be considered. Firstly, lateral variation in the velocity structure is well expected in the study area (see fig 4.2), secondly, according to this model, no arrivals are expected in the shadow zone produced by the low velocity layer (see fig 4.7c); whereas, on the Girvan and Colmonell lines many recordings were obtained along the slope of the low velocity segment. Normal field procedures provide only a limited number of points on the time-distance curve; consequently a small shadow zone could very easily be missed. However, sites situated in the shadow-zone field with the minimum spacing that could be achieved in the field, have proved that first arrivals could be recorded along this area and subsequently this model could be questioned on this basis.

Nevertheless, two P-wave arrivals on some delayed seismograms could be explained on the basis of fig 4.7c, where undelayed arrivals could overtake the delayed ones. These seismograms are at 37 km range on the Loch Doon line (fig 11 appendix 2) and 40 km and 43 km on the Girvan line (fig 10 appendix 2).

The depth of the low velocity zone controls the range at which it affects the measurements at the surface. The occurence of the delay at 35 km on both the Girvan and Loch Doon lines supports this model, but having it at shorter range (22 km) on the Colmonell line may be explained by the low velocity zone shallow-

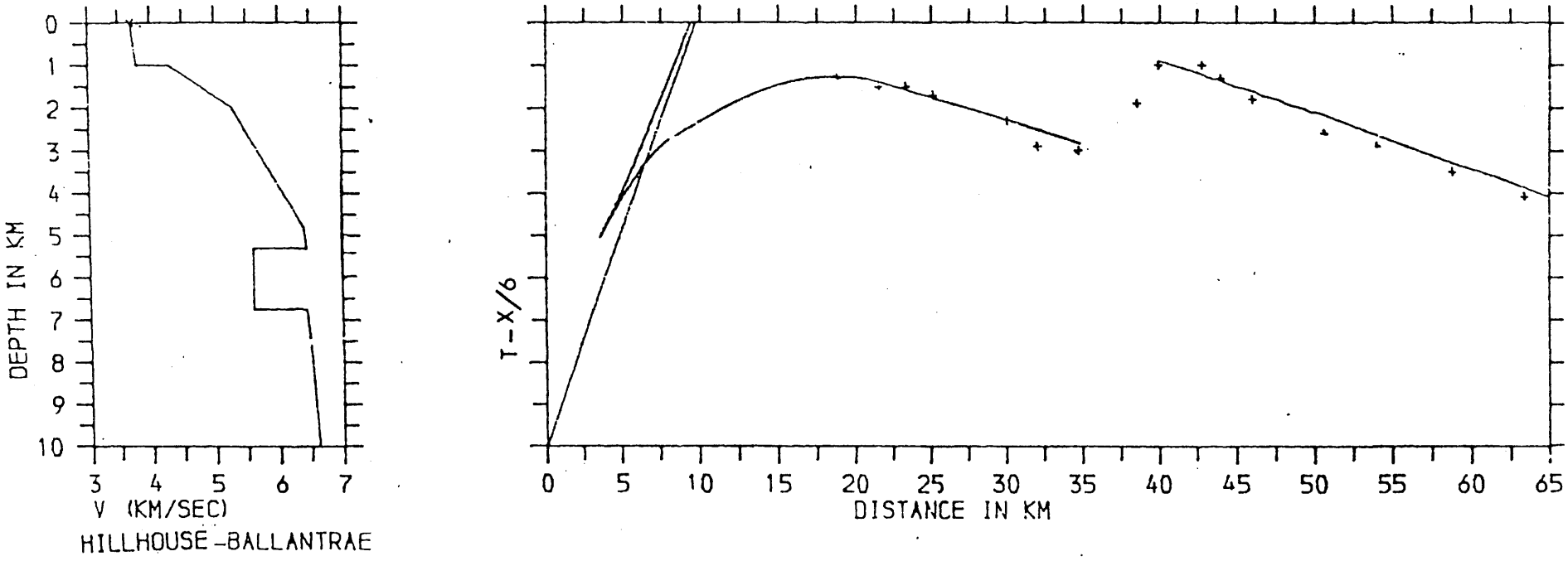

Fig 4.8a Girvan line-velocity structure calculated with no lateral changes.

Observed + Calculated —

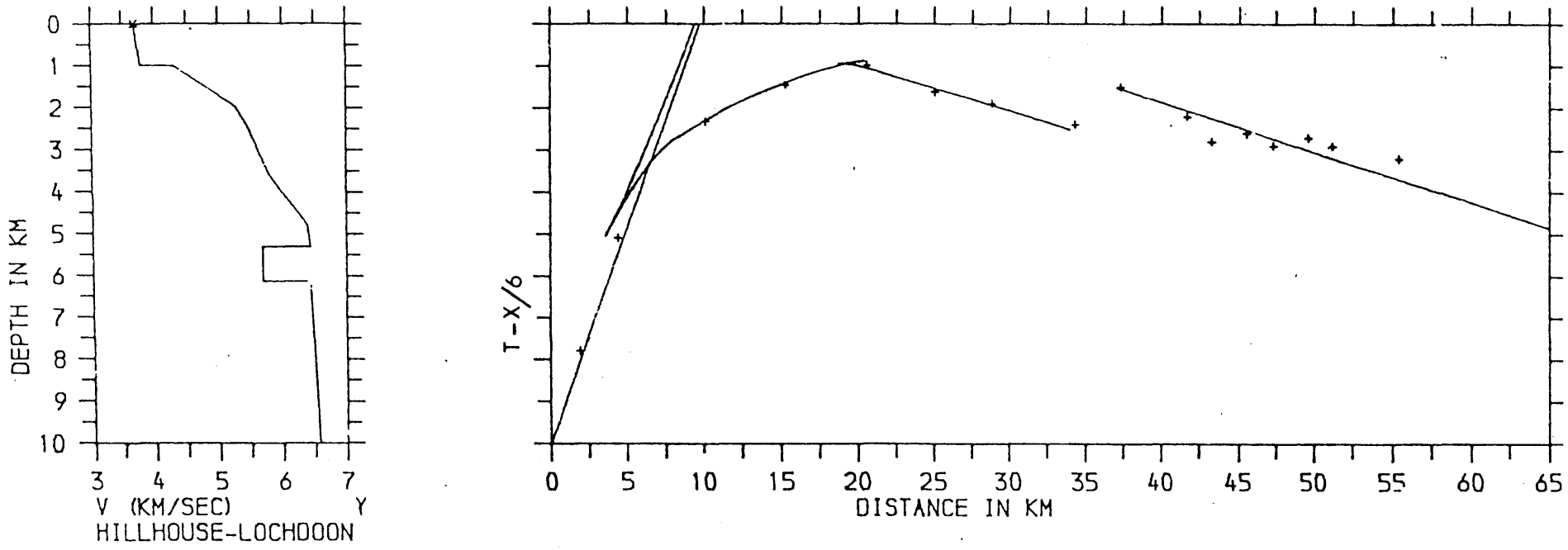

Fig 4.8b Loch Doon line-velocity structure calculated with no lateral changes.

Observed + Calculated —

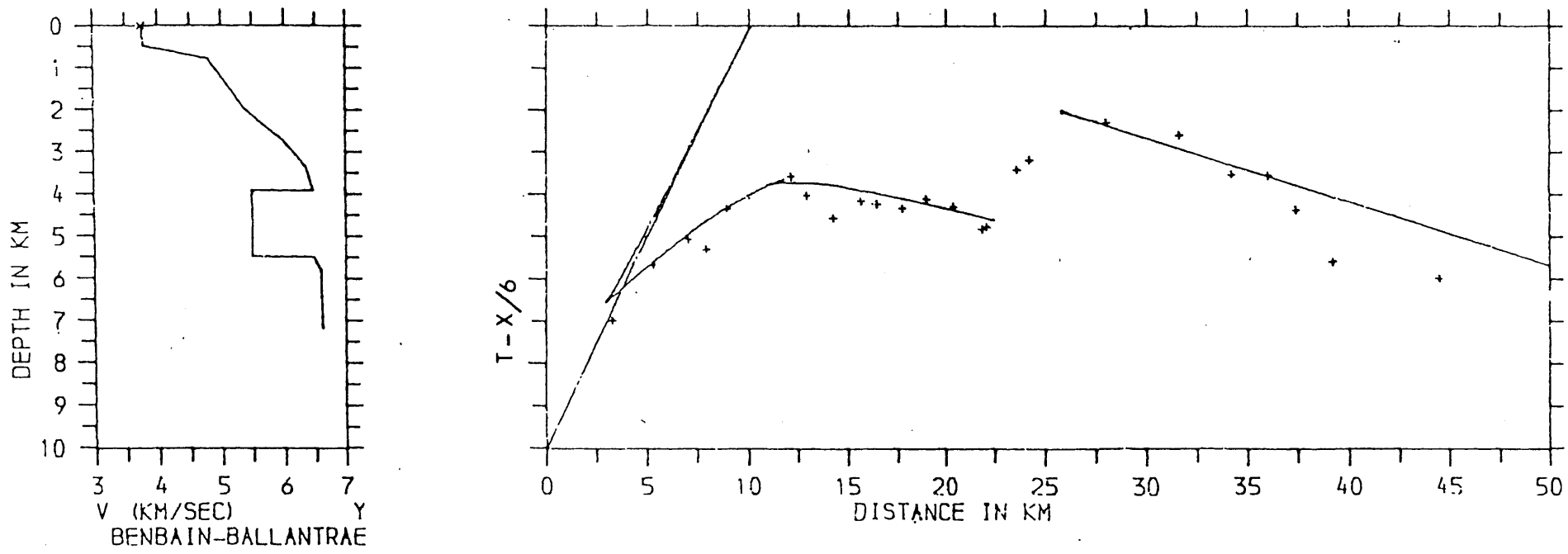

Fig 4.8c Colmonell line-velocity structure calculated with no lateral changes.

Observed + Calculated —

ing eastwards.

4.5 The Reversal of the Girvan line (Portobello-Troon Line)

The unavailability of productive quarries in the south of the study area obstructed the reversal of any of the recorded seismic profiles. At a late stage in this study, use was made of an offshore shot fired by the Royal Navy (see chapter 2) to reverse the Girvan line. The reversal was important to sort out the following:

1. The nature of the delay that took place on the Girvan line. Three possibilities were anticipated before the reversal, in relation to the delay models in section 4.4.

   A. If model 4.4.1 is the case, then an acceleration is expected after passing the Craighead station, crossing from the hanging wall to the footwall of the fault.

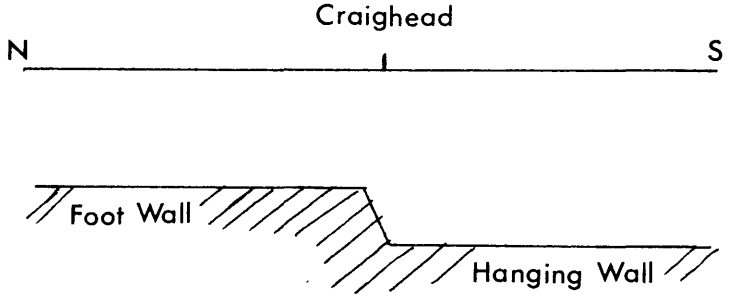

   B. A delay in either direction across a fractured zone is expected, if model 4.4.2 is true. Therefore, the area between Fauldribon and Byne Hill stations will be delayed if this line is reversed.

   C. A delay at about 35 km should occur according

to model 4.4.3, since this is the range for the delay when recording from Hillhouse quarry.

2. To identify the nature of the high apparent velocity (about 6·4 km/sec) which has been recorded at short ranges (13-20 km). A velocity of 6·0 km/sec has been recognised by Sola (1985) and Davidson (1985) at comparable ranges in the central and southern Midland Valley. Therefore, the 6·4 km/sec might be an updip on 6·0 km/sec, especially since LISPB suggested a rise in the basement southwards.

The T-X graph of the reversal line (fig 4.2c) shows an apparent velocity of 6·0 km/sec across the Ballantrae ophiolite, with its points suffering delays and accelerations due to the rays travelling along low velocity (serpentinite) and high velocity (gabbroic) rocks. This fluctuation in the T-X points is not seen when recording across the ophiolite from Hillhouse quarry. It seems possible to explain this phenomena on the basis of the geological structure in the area, where the general picture of the formations is dipping southwards. Therefore, rays travelling northwards along the structure (fig 4.9) would be expected to spend more time in either low or high velocity formations, whereas those travelling southwards (from Hillhouse quarry) would have compensation in their travel times by crossing low and high velocities successively.

The distributed 6·0 km/sec segment suffers a big delay of 0·16 sec at the Fauldribon station and then an acceleration takes place, making a slope on the T-X graph quite parallel to the deceleration segment on the Girvan line (fig 4.2c). A conclusion can be drawn that the Fauldribon station is situated

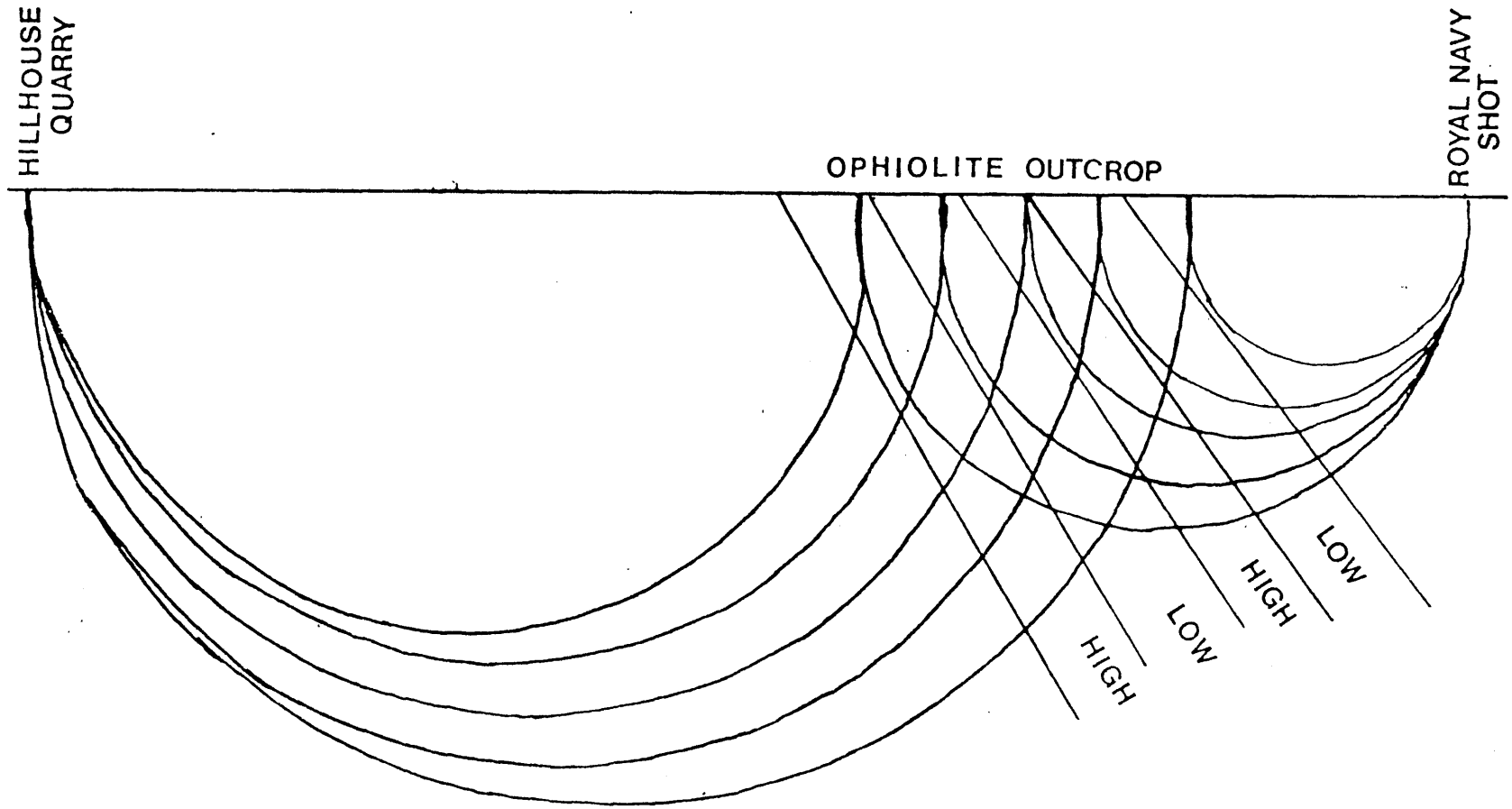

Fig 4.9 Simplified diagram showing seismic waves travelling along and across the geological structure of the Ballantrae ophiolite.

on a low velocity zone, justifying having the peak delay value from both directions in the same place. Further confirmation of this conclusion comes from the fan-shooting (fig 9 appendix 2) where the same station suffers a delay of 0·4 sec in reference to others.

Model 4.4.2 is therefore favoured for the delay and models 4.4.1 and 4.4.3 are disregarded. The delay on the Loch Doon line and Colmonell lines could be explained on the same basis, although reversing them is essential for final confirmation.

The parallel acceleration and deceleration mentioned above could be explained as updip (reversal line) and downdip (Girvan line) on the refractor, and the Craighead station is located on an anticlinal structure since it maintains the earliest reduced time from both directions. At 50 km range on the reversal line (Portobello-Troon), after passing the Craighead station, the 6·0 km/sec appears again to confirm that the 6·4 km/sec recorded at 20-50 km from Hillhouse quarry, is an updip velocity on a refractor which has a velocity between 6·0 and 6·4 km/sec. The 6·4 km/sec velocity takes over at 55 km from the Royal Navy shot, as that of LISPB (Bamford 1977) and parts of recent seismic profiles across the Midland Valley (Dr J Hall, personal communication).

4.6 Modelling by Ray Tracing

The velocity structure underneath the reversed Girvan line, Loch Doon line and Colmonell line is derived by applying the ray-tracing technique, using a computer program written by Cerveny and Psenick (1981). As different input of velocity-mesh along each line can produce similar travel times to the observed ones, tight geological and geophysical

controls are needed when applying the ray-tracing method.

Ray-tracing on the reversed Girvan line (fig 4.10) was controlled as follows:

1. Velocities of 3·7-3·8 km/sec for Carboniferous and Upper Old Red Sandstone were taken from the direct measurements of the Loch Doon line (see section 4.2.1). The thickness of this layer is estimated from published geological literature (see chapter 1).

2. Velocities of 5·0-5·5 km/sec for Lower Old Red Sandstone and Lower Palaeozoic sediments were mainly from direct measurements from the Royal Navy shot in the south (see section 4.2.4), laboratory measurements (see chapter 3), Sola (1985) and Davidson (1985). The thickness of this layer was adjusted to match with the second segments on the T-X graph of the Loch Doon and Colmonell lines, which share parts of the velocity-structure of this line.

3. Velocities for the Ballantrae ophiolite rocks are those derived in section 4.3 under the Lendalfoot array. A similar velocity gradient was applied to the basement along the line.

On the Loch Doon line (fig 4.11), the basement has the same velocity gradient as that of the previous line, and velocities for the Loch Doon granite are mainly from Christensen (1982).

The Colmonell line (fig 4.12) comes as a very important means to check on the velocity structure of the previous two lines, with its E-W azimuth

Numbers at the base of the diagram refer to seismometer stations shown on fig 2.15a.

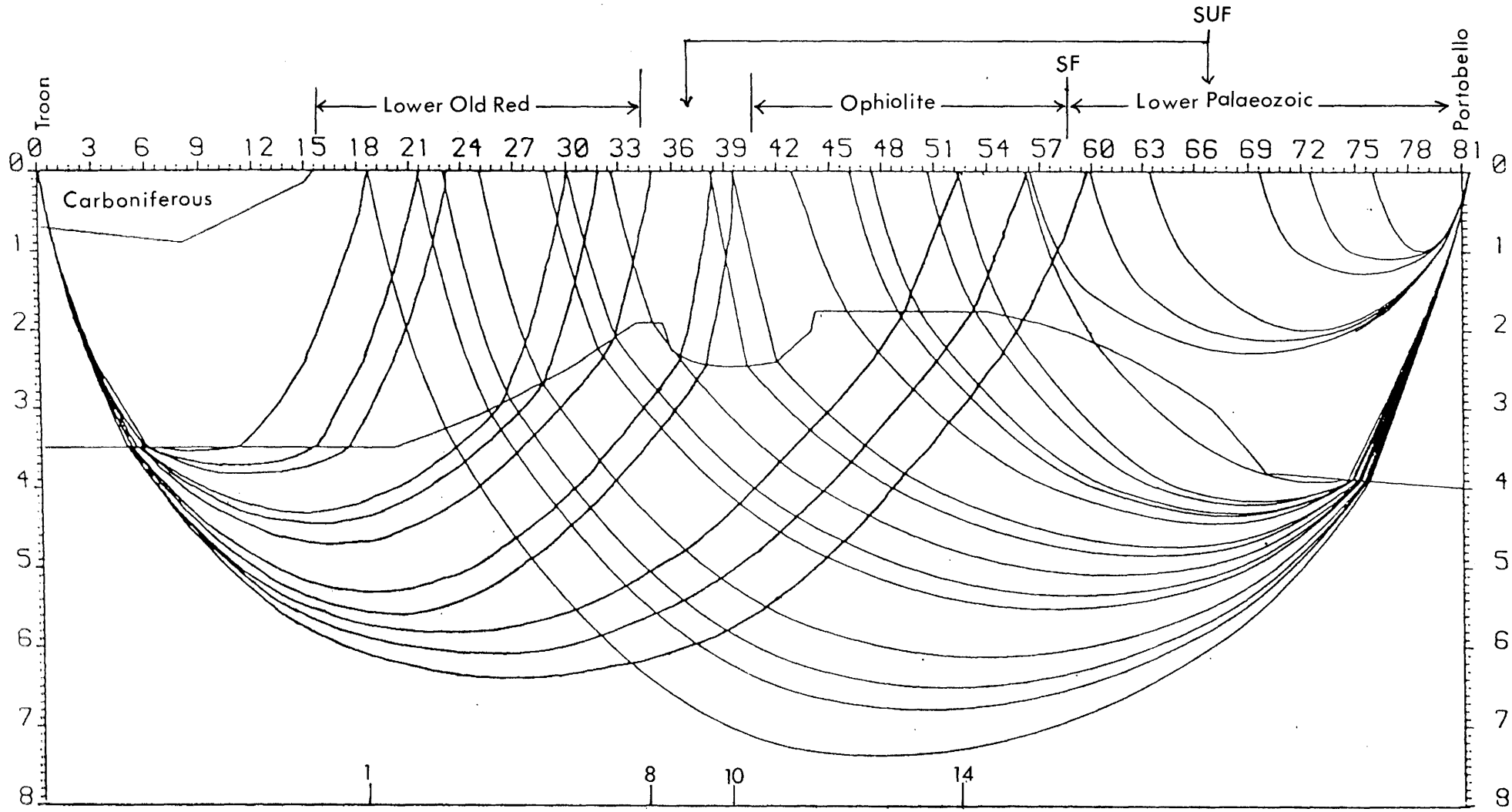

Fig 4.10a Ray-tracing on the Girvan line.

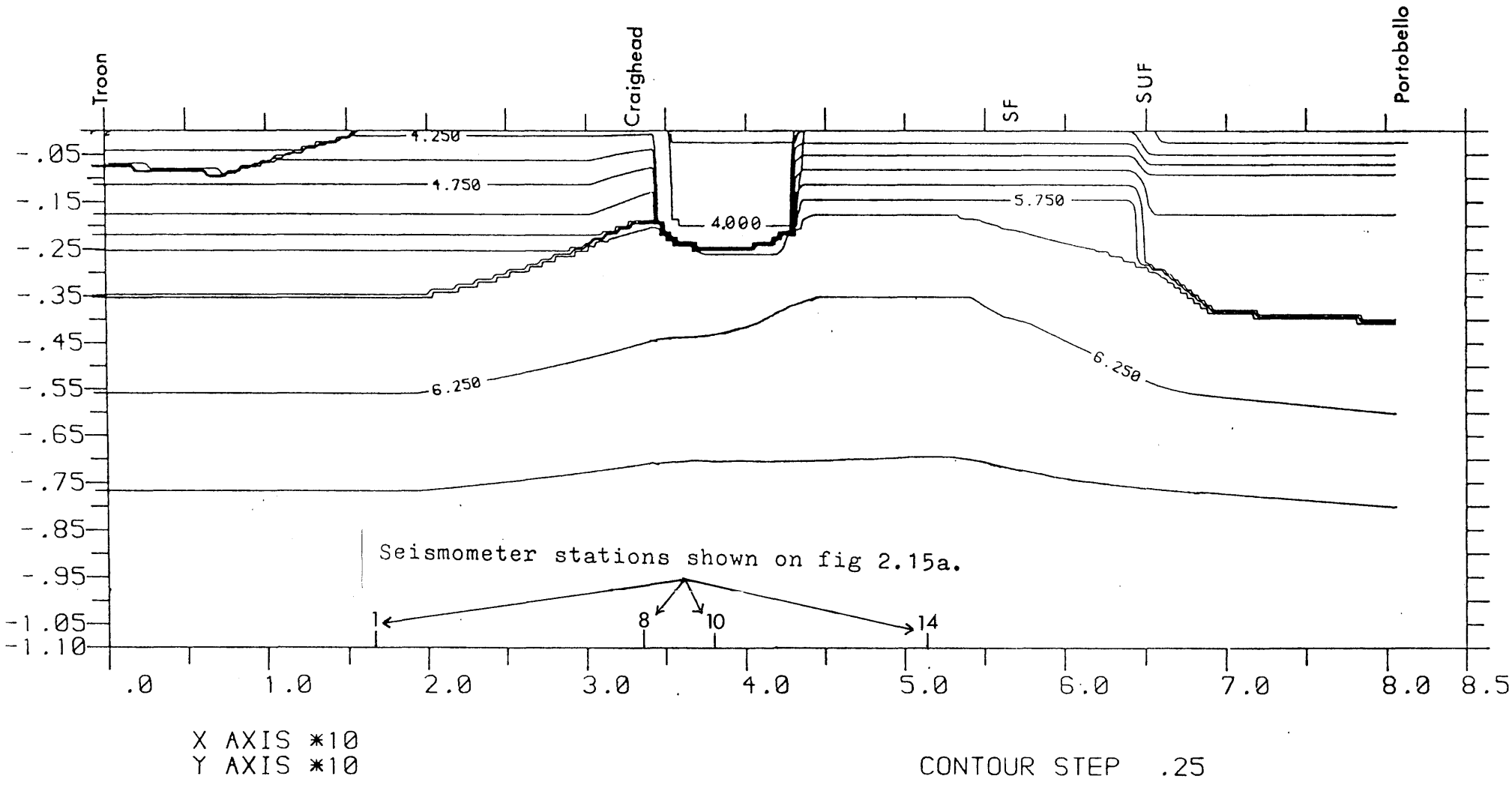

Fig 4.10b Velocity structure under the Girvan line.

Numbers at the base of the diagram refer to seismometer stations shown on fig 2.15a.

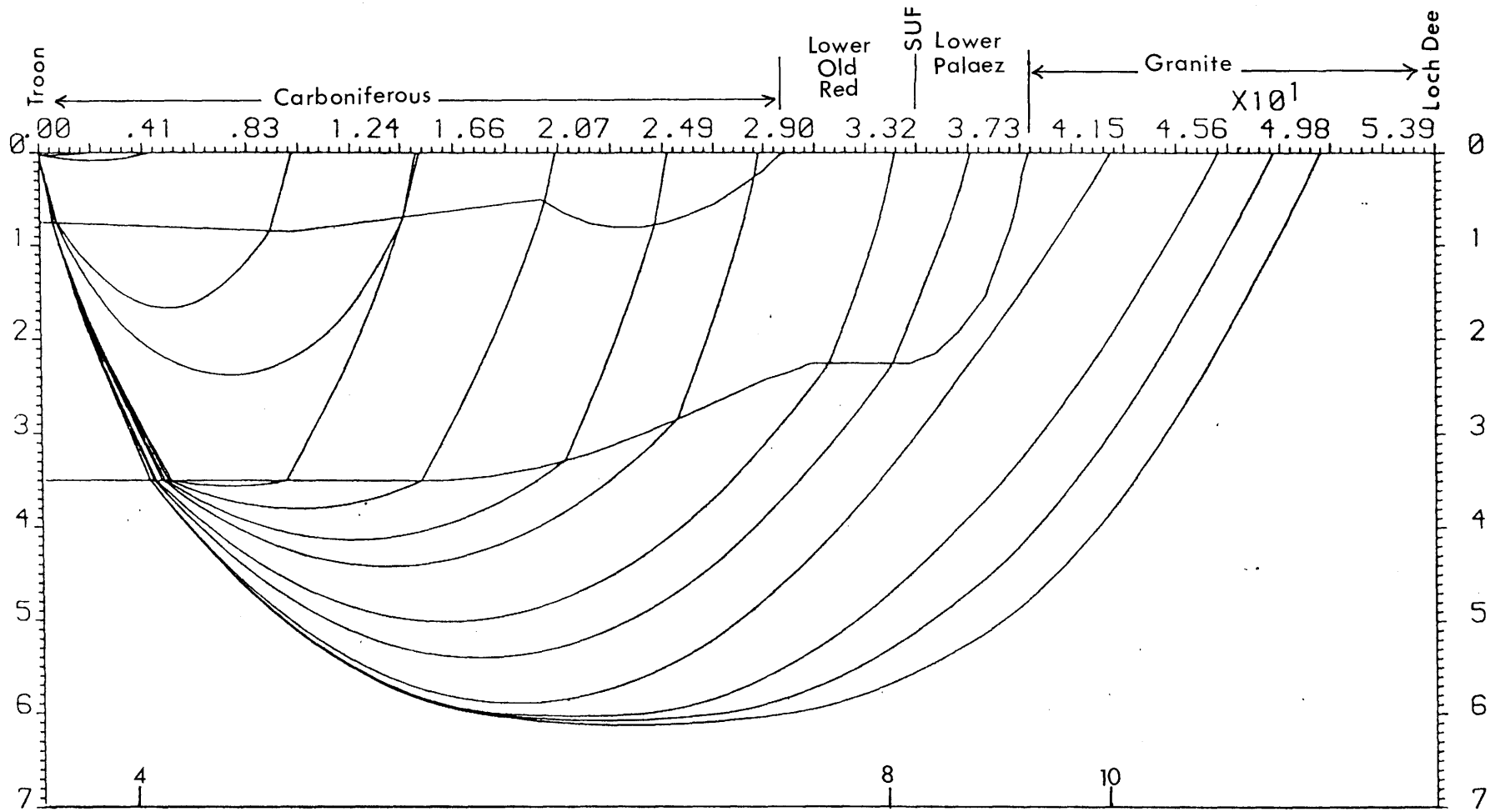

Fig 4.11a Ray-tracing on the Loch Doon line.

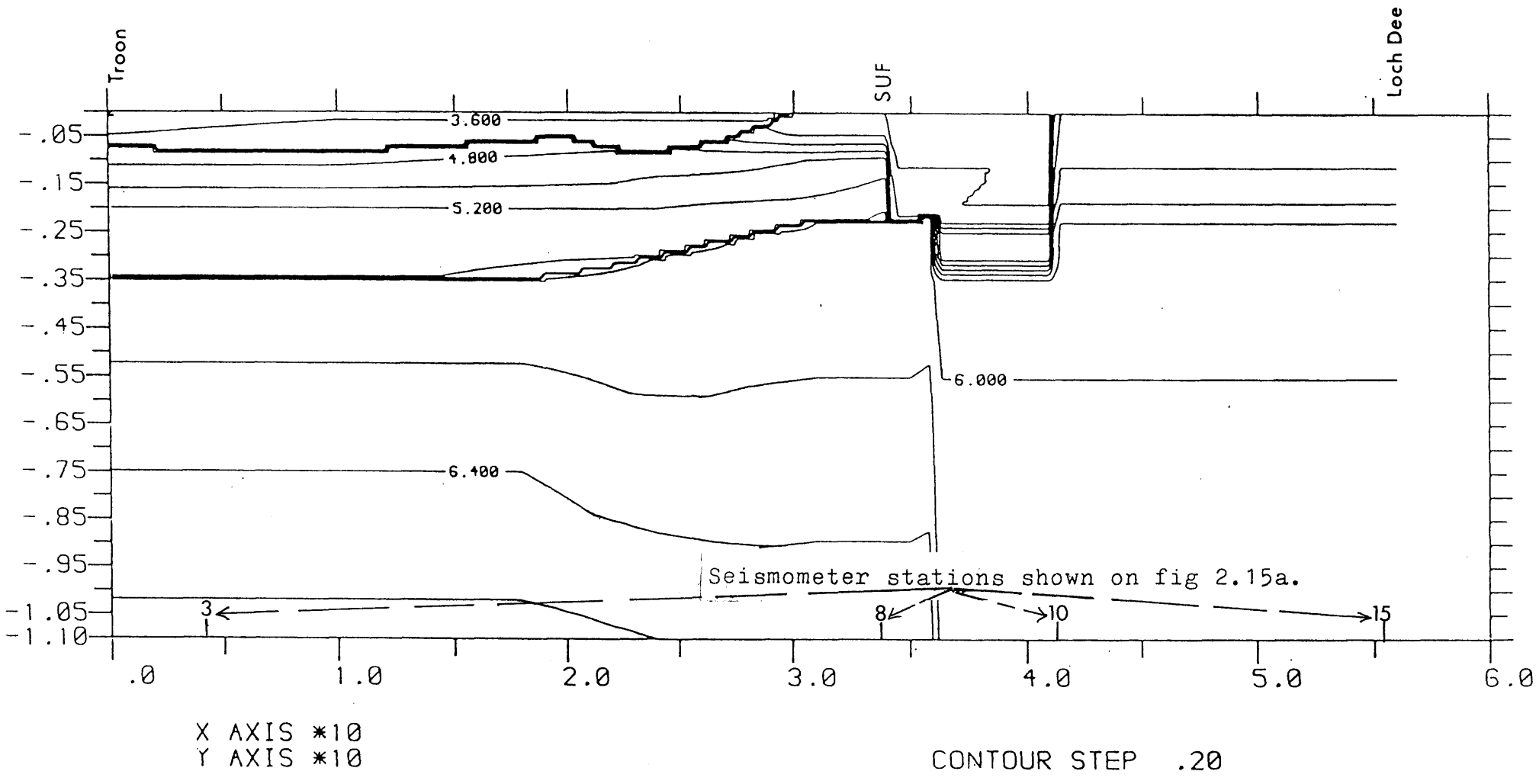

Fig 4.11b Velocity structure under the Loch Doon line.

Numbers at the base of the diagram refer to seismometer stations shown on fig 2.15a.

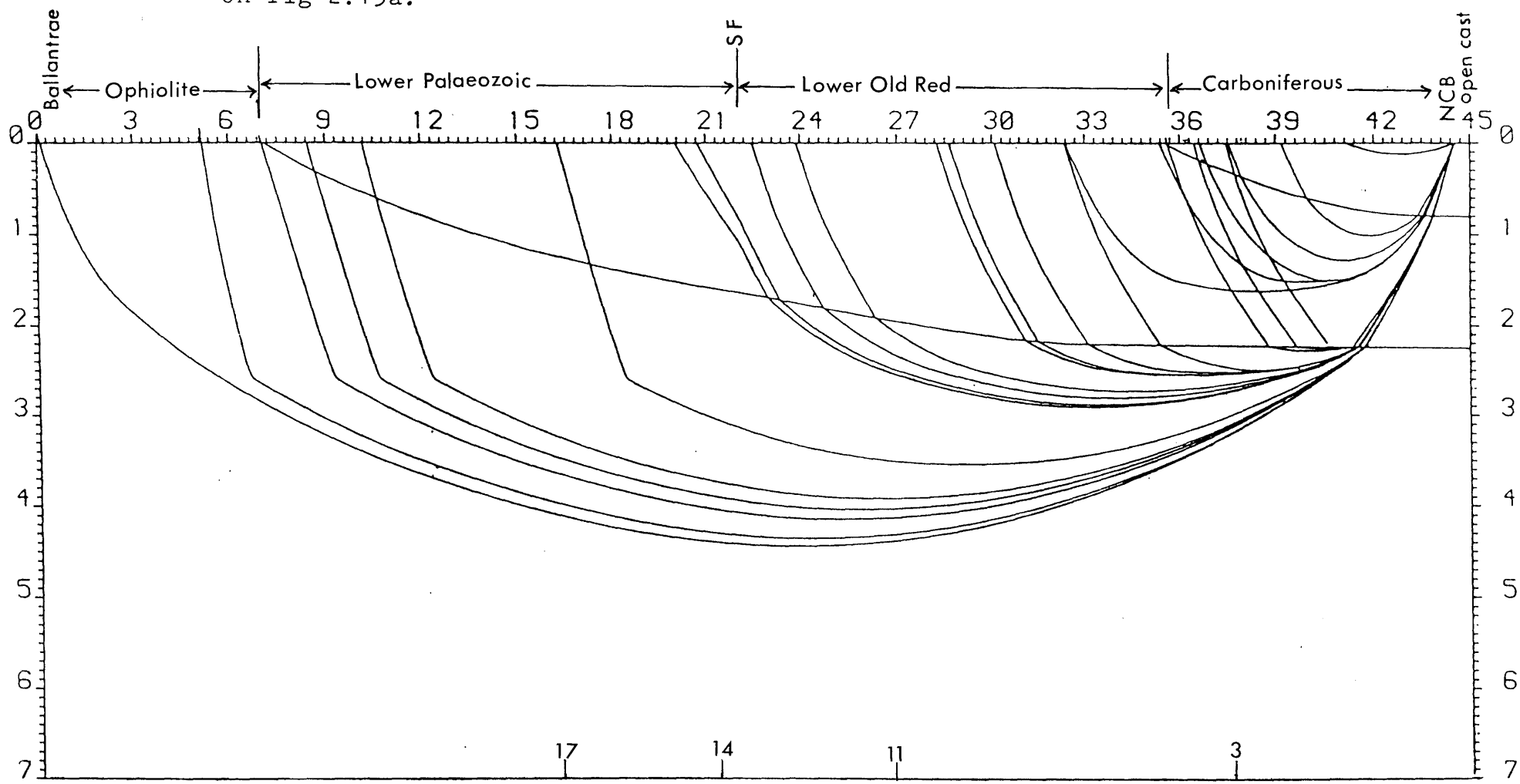

Fig 4.12a Ray-tracing on the Colmonell line.

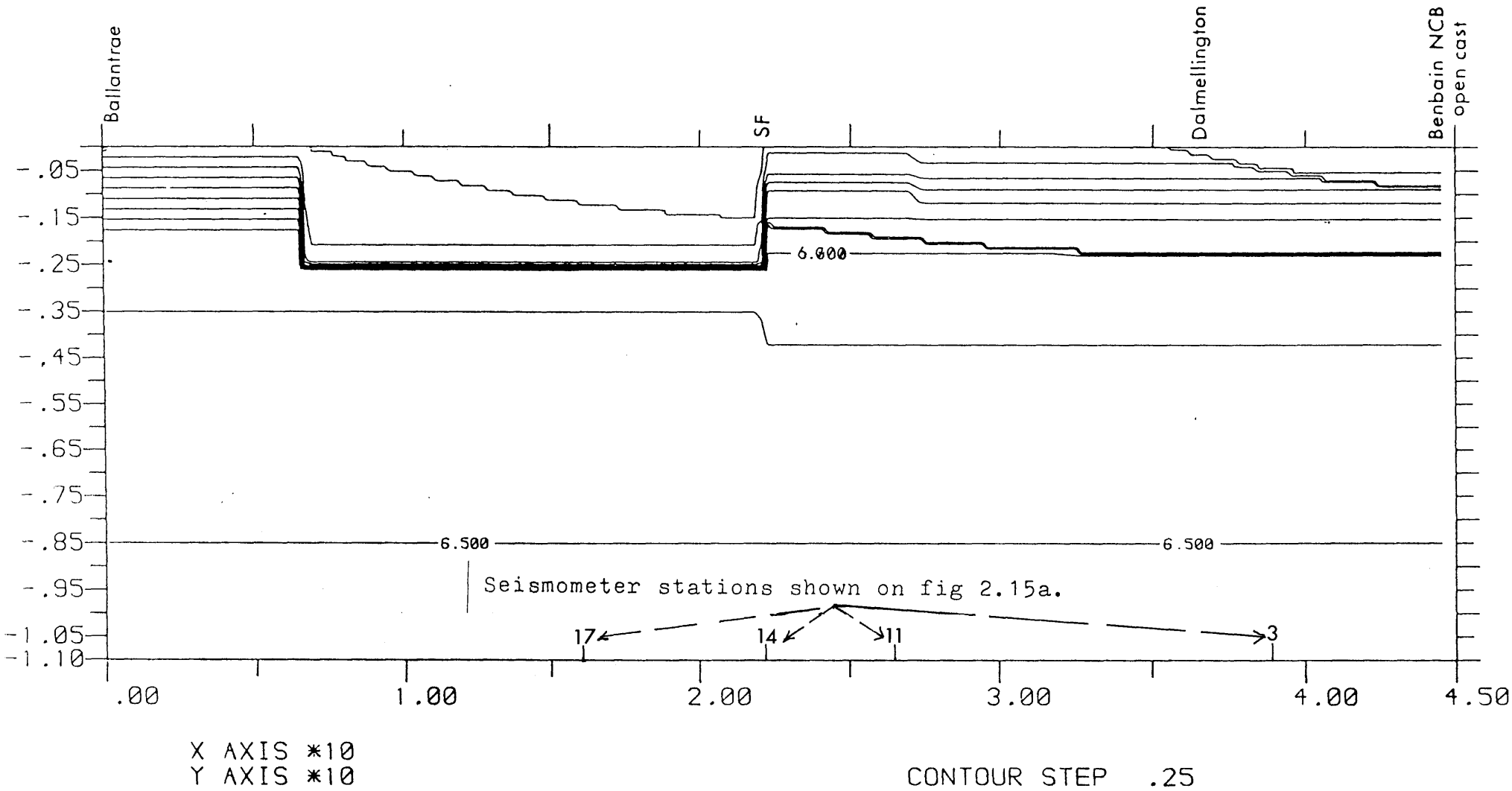

Fig 4.12b Velocity structure under the Colmonell line.

crossing both of them.

The low velocity zones that produce the delay on the three lines were introduced after ray-tracing for delay-free structure, and good matching with the undelayed observed travel times is achieved. The depth and width of the low velocity zones are then decided from the delay-free output. The three models are very similar and incorporated three layers:

Layer 1	Carboniferous sediments/ Upper Old Red Sandstone	of velocity 3·7-4·0 km/sec
Layer 2	Lower Old Red Sandstone/ Lower Palaeozoic	of velocity 5·0-5·5 km/sec
Layer 3	Crystalline Basement	of velocity 6·0-6·4 km/sec

The Reversed Line

The basement on this line is deepest under Hillhouse quarry; 3·5 km. Davidson (1985) estimated a similar depth in the same area. The basement shallows southwards to have its shallowest point under the Craighead inlier, where it deepens again rapidly to outcrop as the Ballantrae ophiolite. The boundary at 1·75 km under the ophiolite outcrop (fig 4.10a) is taken to delimit the start of a 6·0 km/sec velocity. This boundary extends at the same depth south of the Stinchar Fault, then dips steeply southwards after crossing the Southern Uplands Fault. The control on the angle of the dip is poor, but the slope is needed to match the travel times on the first segment from the Royal Navy shot and to be in agreement with the thickening of the Lower Palaeozoic sediments suggested

by the Galloway line, which ends 30 km NE of this shot, 5 km short of the Southern Uplands Fault. A similar gradient could be achieved for the basement along the line and the observed and calculated travel times are shown in fig 4.13.

Loch Doon Line

The basement under Hillhouse quarry is at 3·5 km as in the previous line, and it starts to shallow near Patna reaching a depth of 2·2 km at the Southern Uplands Fault. The same depth and velocity gradient of the basement extend underneath the Northern Belt till the boundary of the Loch Doon granite, where lower velocities take over. The low velocity zone affects the Lower Palaeozoic rocks of the Northern Belt as well as the northern limit of the Loch Doon granite. Figure 4.14 shows the calculated and observed travel times on this line.

Colmonell Line

The basement on this line is at 2·2 km depth under the Benbain NCB open-cast, NE of Dalmellington. This depth continues westwards, crossing the Loch Doon line, and then it shallows to outcrop as the Ballantrae ophiolite. The low velocity zone is wider on this line and it is within the boundary of Lower Palaeozoic rocks as well as the basement. Figure 4.15 shows the ray-tracing results on this line.

4.7 Conclusions

1. A velocity of 5·77 km/sec is obtained for Lower Palaeozoic rocks of the Southern Uplands from a

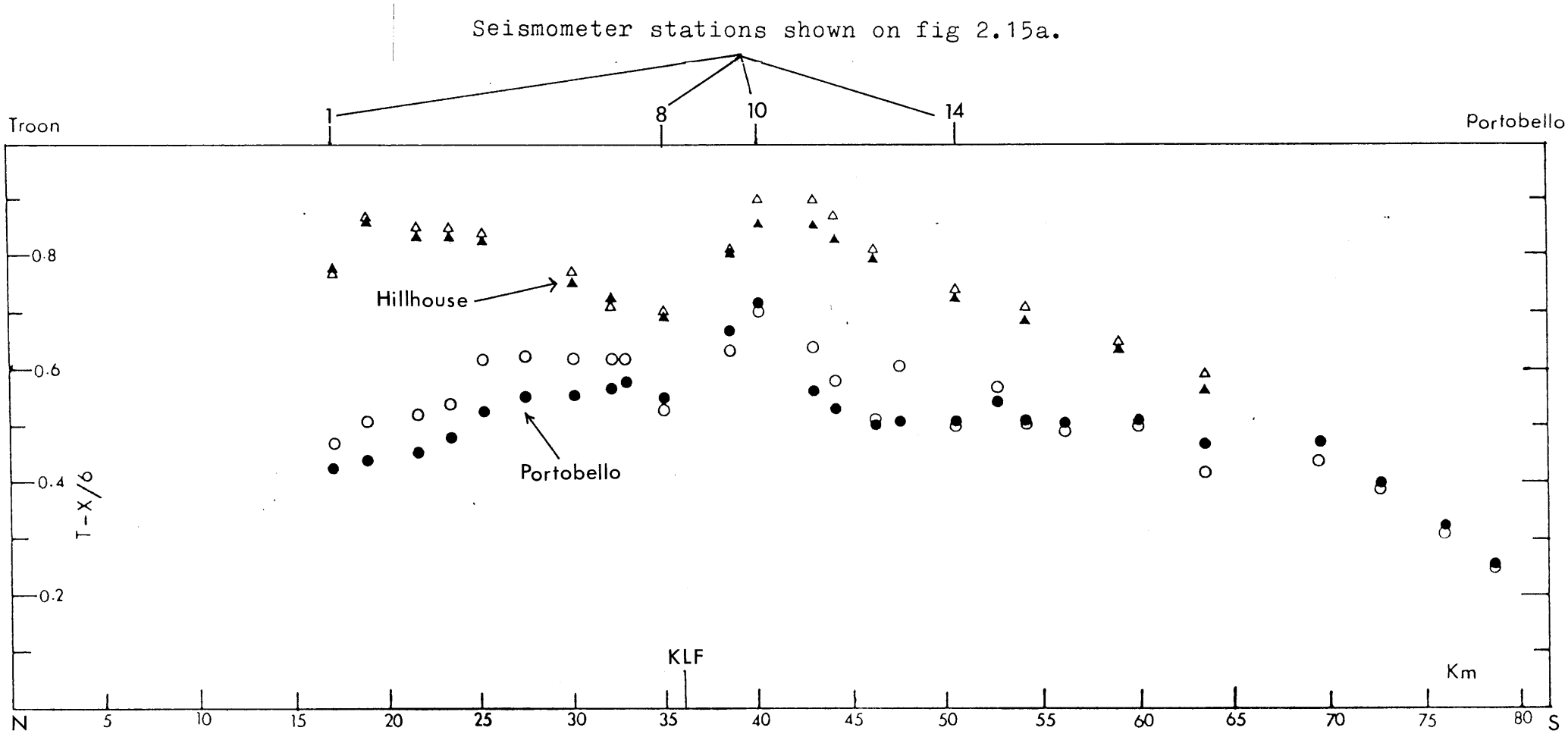

Fig 4.13 Reduced time-distance graph of the Girvan line showing observed & calculated values.

open symboles:observed, solid symboles:calculated

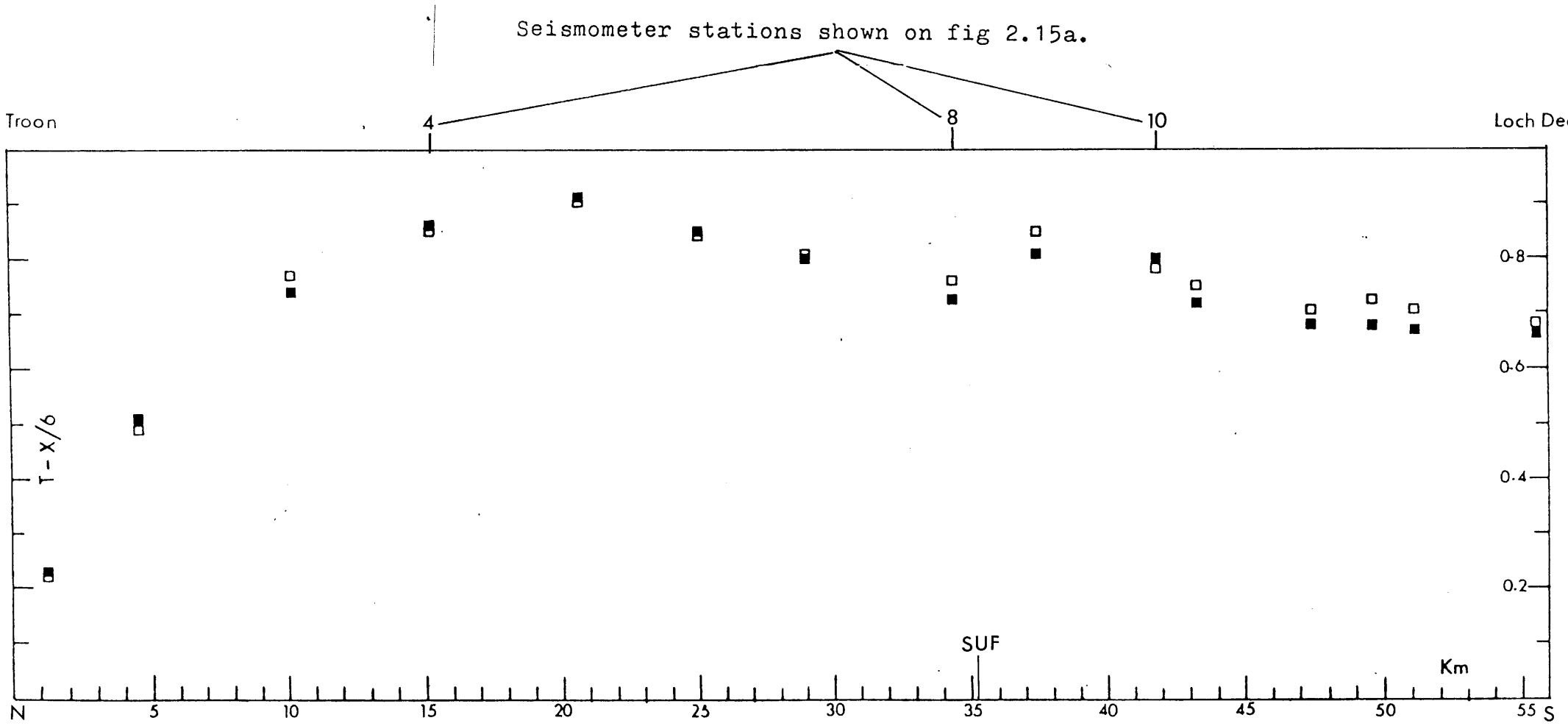

Fig 4.14 Reduced time-distance graph of the Loch Doon line showing observed□& calculated■values.

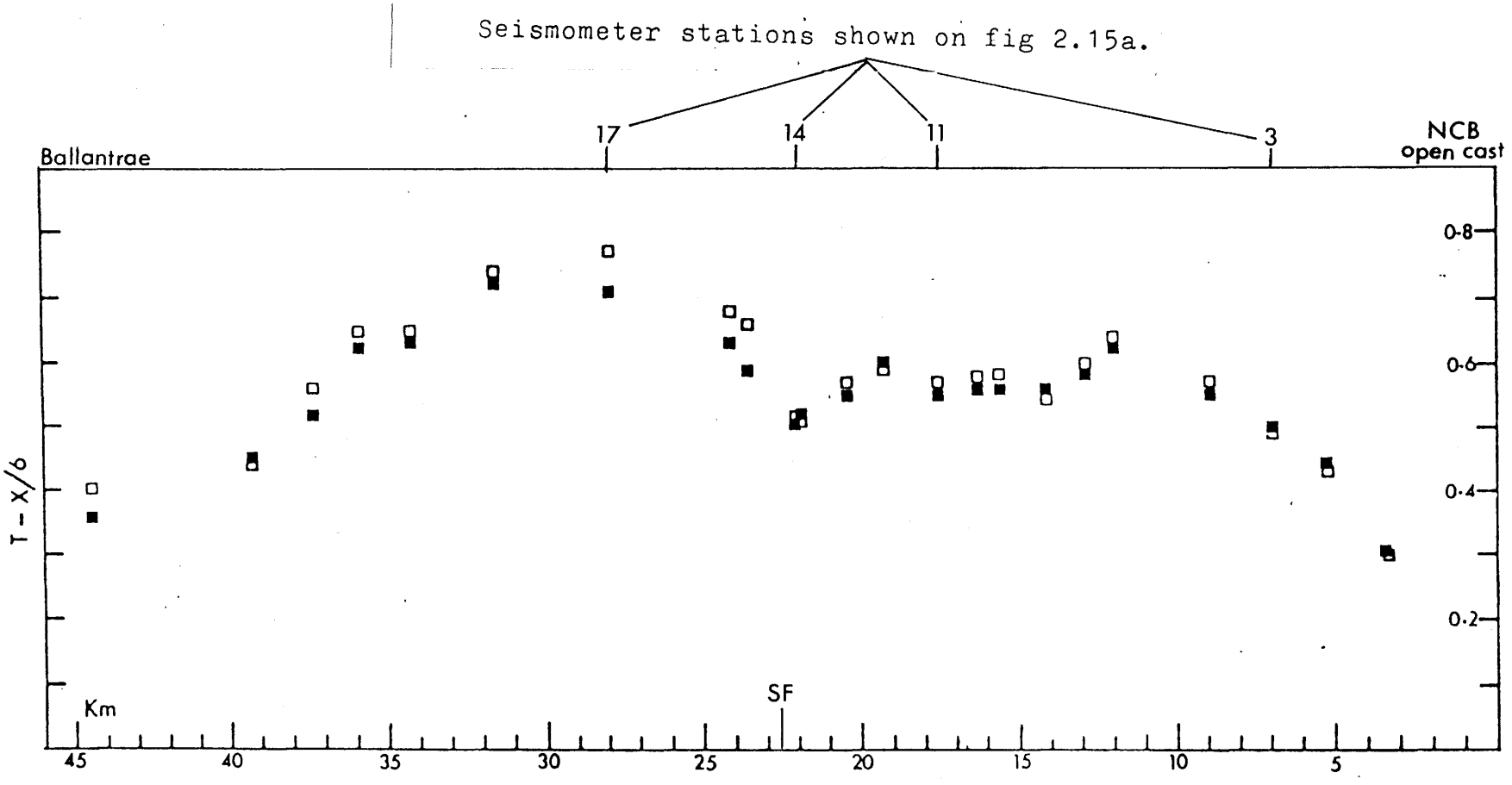

Fig 4.15 Reduced time-distance graph of the Colmonell line showing observed□& calculated■values.

seismic refraction line which runs across the strike from Burrowhead to 5 km short of the Southern Uplands Fault.

2. An average surface velocity of 4·21 km/sec could be assigned to the Ballantrae ophiolite, increasing continiously with depth, reaching 6·0 km/sec at 1·75 km depth and 6·21 km/sec at about 2·5 km depth.

3. The high recorded apparent velocities presented in chapter 2 are a structure on a basement with velocity gradient similar to that of the Ballantrae ophiolite. It is shallowest under the Craighead inlier in the Midland Valley and dips steeply southwards in the Rhinns of Galloway in the Southern Uplands, whereas it crosses the Southern Uplands Fault with the same depth (2·2 km) near Dalmellington.

4. Rocks with a velocity of about 4·0 km/sec occur at the fault zones of Kerse Loch Fault, the Stinchar Fault and the Southern Uplands Fault. Any rays passing through these low velocity rocks will be delayed in reference to other rays.

CHAPTER FIVE

Geological Constraints and Conclusions

5.1 Introduction

The interpretation of seismic data in geological terms is the objective and end product of seismic work. The analysis of velocity data constitutes and important interpretation problem. As with other interpretation problems, some interpretations can be ruled out because they imply impossible or highly improbable situations.

There is little doubt that crystalline continental basement underlies the weakly deformed Palaeozoic rocks of the Midland Valley. If the Southern Uplands is a Lower Palaeozoic accretionary prism, then it would have been underlain by oceanic crust at the time of its formation. The nature of the present basement to the Southern Uplands has been questioned ever since Powell (1970, 1971) suggested that it is underlain by rocks with the magnetic properties of continental crust (see chapter 1). This opinion was considerably strengthened by the discovery of xenoliths of gneissose rocks in Carboniferous vents sited on the Irish equivalent of the accretionary prism (Strogen 1974), and by the discovery of xenoliths in vents of the same age in the Southern Uplands (Upton et al 1983, 1984). Hall et al (1983, 1984) found evidence from seismic experiments for crust of continental affinity at 1-5 km below the present surface in the Southern Uplands (see chapter 1). This basement is indistinguishable seismologically from the crust of the Midland Valley, and Davidson et al (1984) interpreted it as quartzo-feldspathic gneiss.

He traced its continuity from the Midland Valley across the Southern Uplands Fault to a short distance into the northern margin of the Southern Uplands.

The basement underneath the Midland Valley is not necessarily homogeneous (Aftalion et al 1984) and the same could be said about the Southern Uplands. The Ballantrae ophiolite on the boundary between the Midland Valley and the Southern Uplands constitutes the basement for the Lower Palaeozoic succession in the Girvan District. Fig 5.1 represents the derived geological and geophysical interpretations by the ray-tracing technique. Unfortunately, the data sets available in this thesis provide no conclusive results about the thickness of the Ballantrae ophiolite and the basement below it is still questionable.

Assimilation of the mass of data to arrive at the most plausible geological picture in the south-western part of the Midland Valley, is the prime target of this chapter.

5.2 Low Velocity Rocks

Rocks in the area of investigation that are likely to have a velocity of about 4·20 km/sec at 2 km depth, producing the delay discussed in section 4.4 can be:-

1. Carboniferous sediments (see 4.2.1).
2. Serpentinite (see chapter 3).
3. Fractured or sheared rocks.

The absence of Carboniferous strata from the delay zones of the Loch Doon line (Southern

Carboniferous thickness is taken from previous geological work. Boundary between Lower Old Red Sandstone and Lower Palaeozoic is predicted from surface geology and is indistinguishable at depth. Dotted area indicates low velocity zone. Boundary between Lower Palaeozoic sediments and basement is derived from ray-tracing technique. Boundaries of the ophiolite with the surrounding sediments are predicted from surface geology; dashed indicating unknown dip.

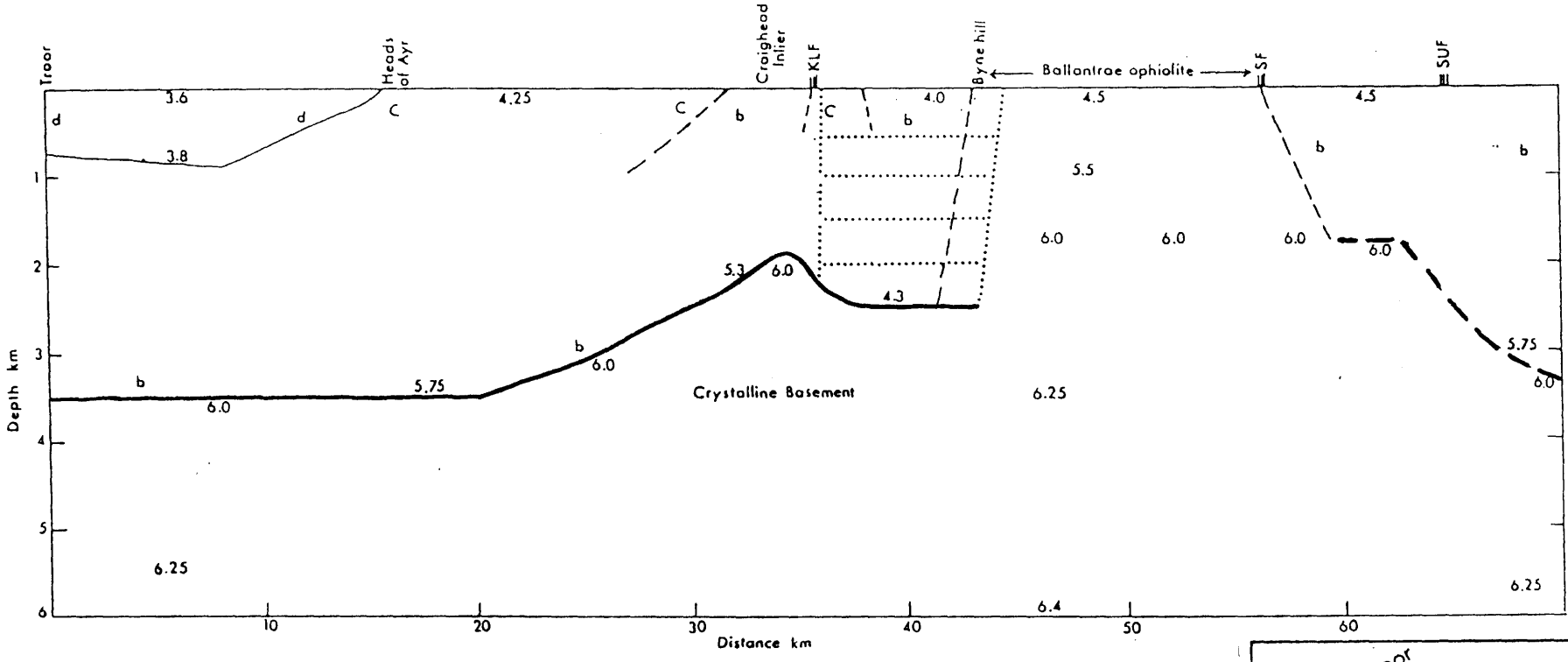

Fig 5.1a Upper crustal structure on the Girvan line.

b:Lower Palaeozoic, c:Lower Old Red Sandstone, d:Carboniferous, KLF:Kerse Loch Fault, SUF:Southern Uplands Fault, SF:Stinchar Fault.

Carboniferous thickness is taken from previous geological work. Boundary between Lower Old Red Sandstone and Lower Palaeozoic is predicted from surface geology and is indistinguishable at depth. Dotted area indicates low velocity zone. Boundary of the Loch Doon granite is taken from gravity modelling.

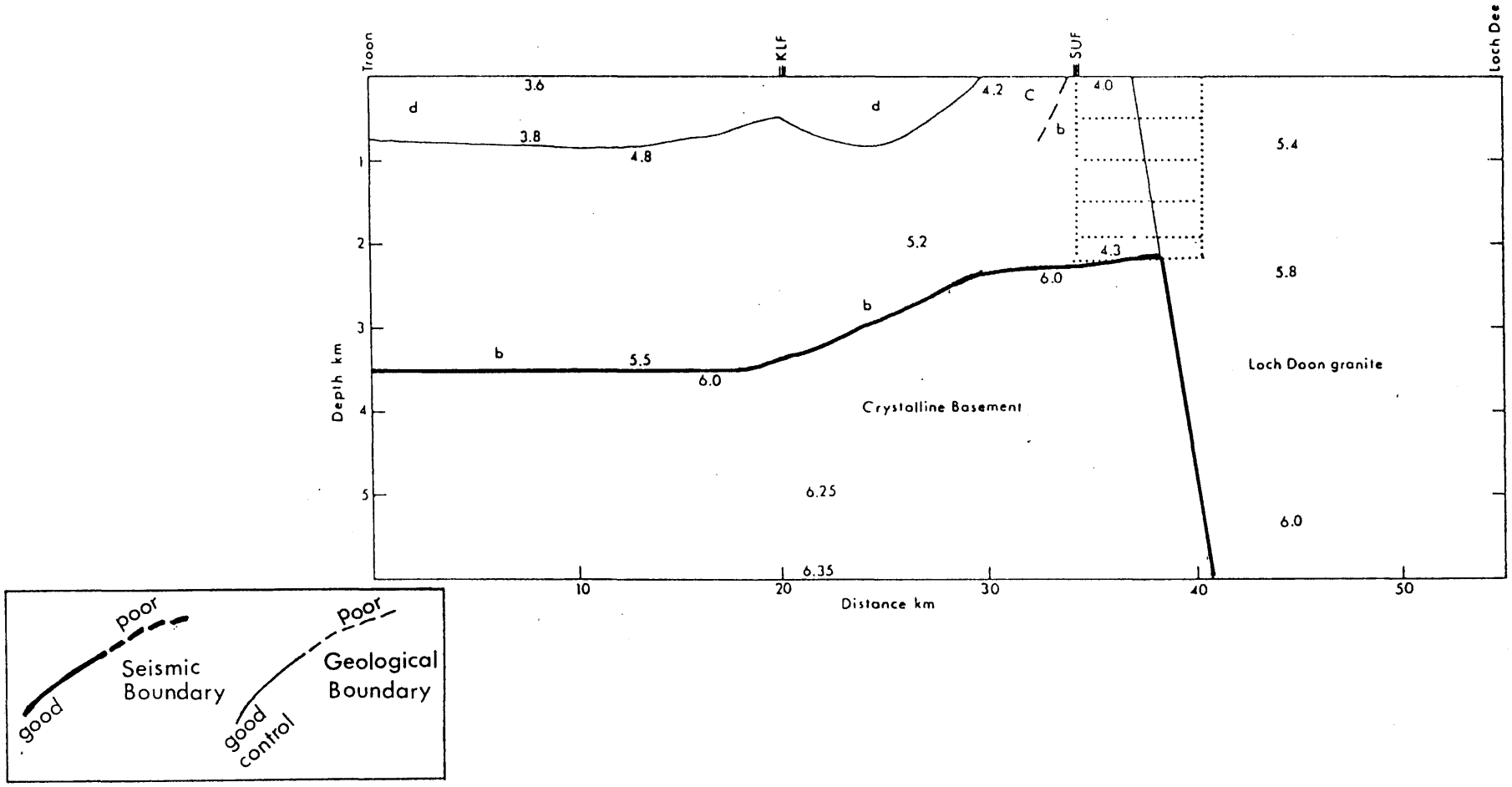

Fig 5.1b Upper crustal structure on the Loch Doon Line.

Carboniferous thickness is taken from previous geological work. Boundary between Lower Old Red Sandstone and Lower Palaeozoic is predicted from surface geology and is indistinguishable at depth. Dotted area indicates low velocity zone.

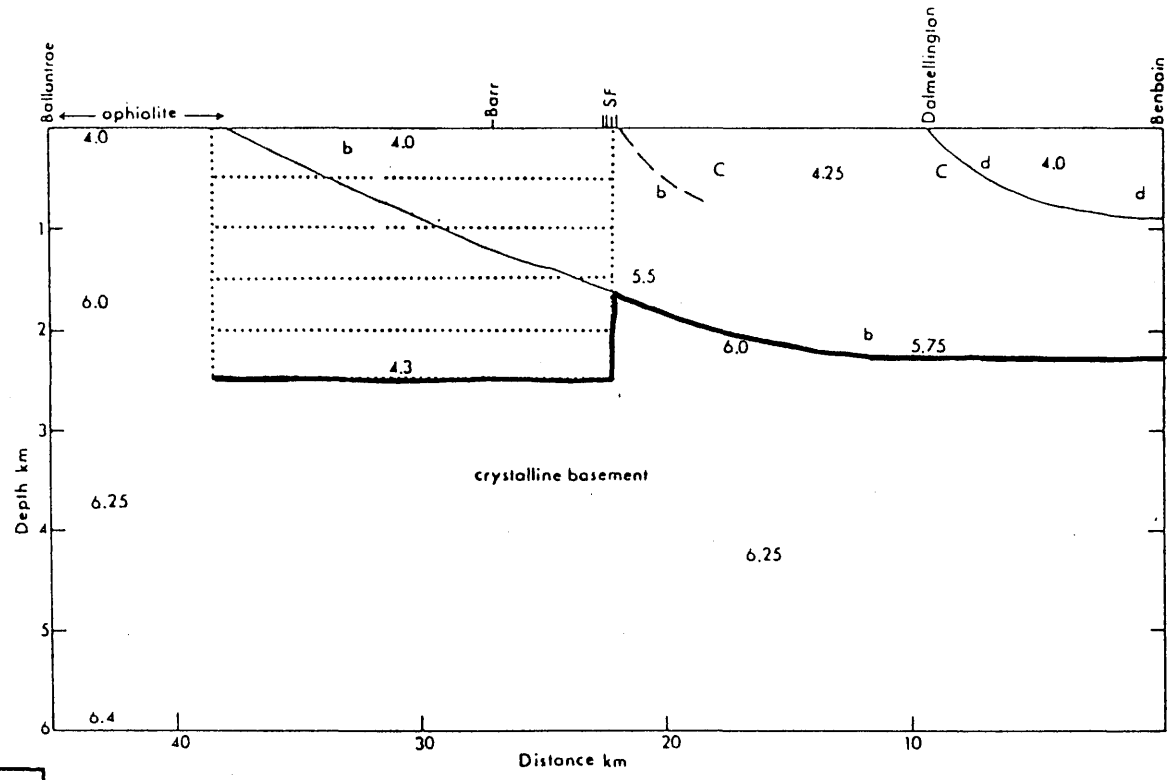

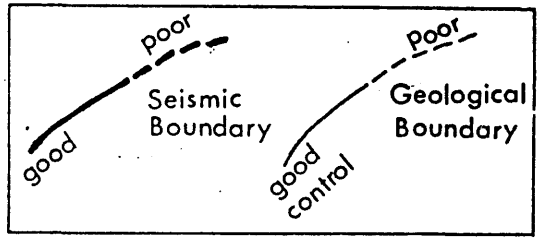

Fig 5.1c Upper crustal structure on the Colmonell line

Uplands Fault), Colmonell line (Stinchar Fault) and the Girvan line (Kerse Loch Fault), rules out the first possibility. Serpentinite and the wide range of its velocities (see table 3.4) might produce such seismic delay. It is abundant in the study area and constitutes the commonest detrital mineral in the Lower Palaeozoic components (Williams 1962). As a result of the subduction of oceanic crust, both the continent or island arc and the ophiolites attached to it are underlain by a subduction zone. The subducting plate will take water down into the mantle in water-bearing metamorphic minerals such as zeolites and amphiboles. On being subducted, these minerals will be heated and will release water, which will convert some of the peridotite in the overlying mantle into serpentinite. The serpentinisation of peridotite increases the volume and makes it lighter, so that it tends to rise. This process contributes to the uplift of the overlying crust and mantle (Gass 1982). According to this, the delay localities delimited in chapter 4 are expected to have serpentinite cumulates near the surface. The magnetic anomalies associated with the Southern Uplands Fault, Kerse Loch Fault and the Stinchar Fault (fig 5.2) support this possibility.

Another explanation for low velocity rocks might be fault zones. These are zones of numerous discrete displacement planes on all scales. The dislocation does not occur simply along a single plane, it is a response to:-

1. Many separate stress/strain fields along irregular primary fault plane surfaces, producing high and low stress fields (fig 5.3a).
2. Dislocation propagation along any single plane. As the dislocation propagates, it can meet positions where it is easier (less resistance/

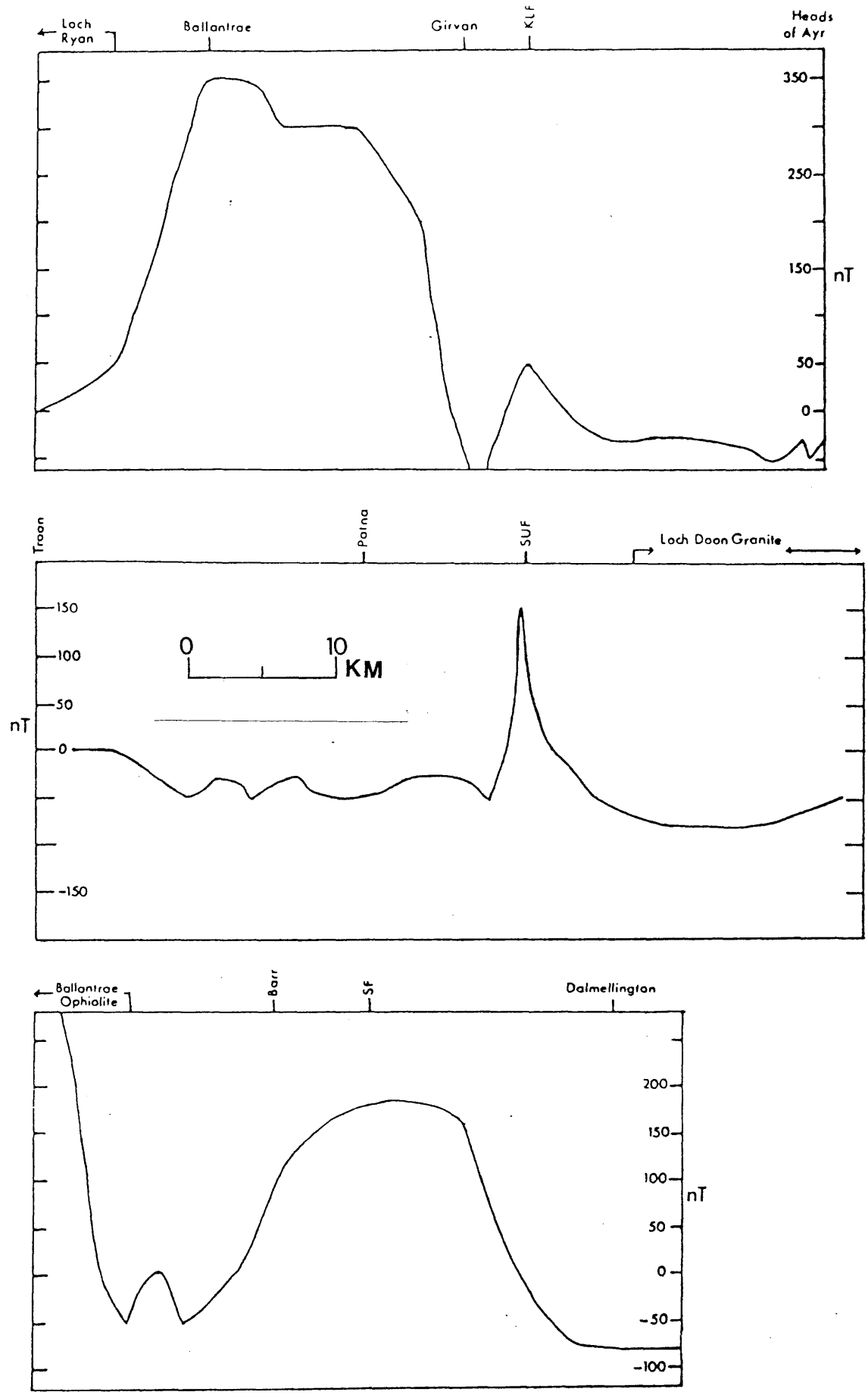

Fig 5.2 Magnetic anomalies across the Kerse Loch ,Southern Uplands and Stinchar Faults in the study area.

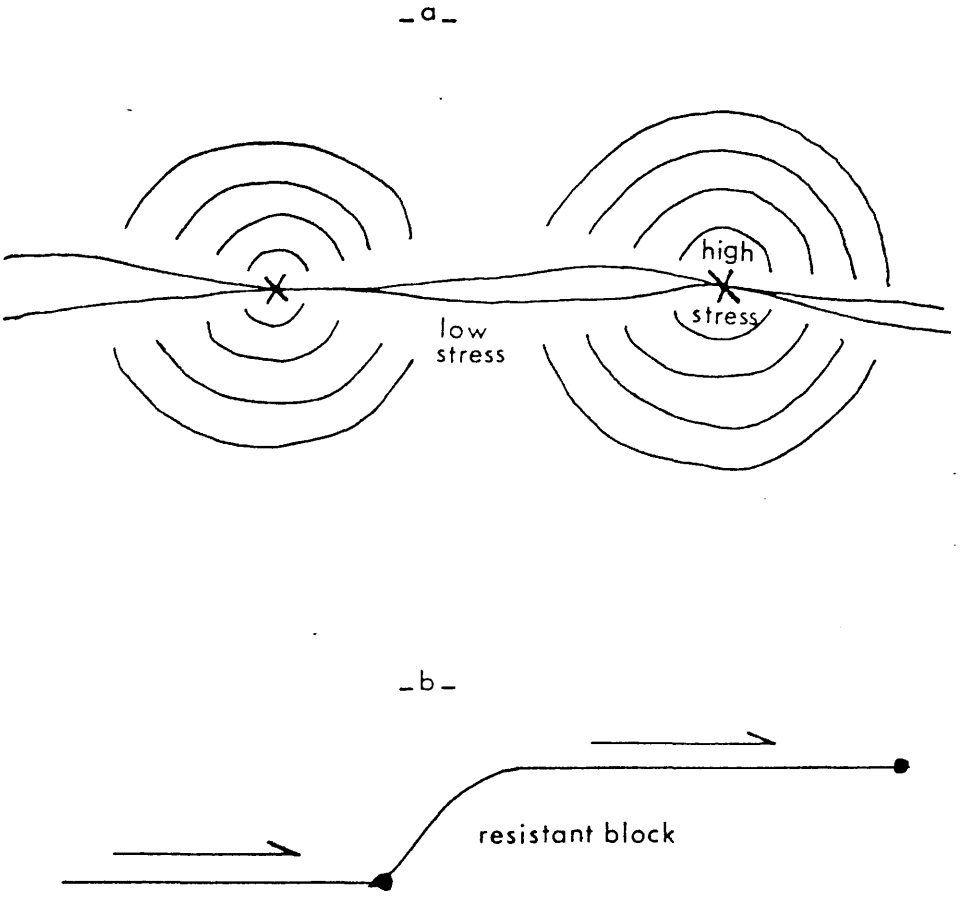

Fig 5.3 Illustration of fault plane development.

a)Irregular fault planes meeting at high stress areas.

b)Migration of dislocation along less sesistant areas.

less lowest energy required) to continue by migrating to another horizon (fig 5.3b).

Such slicing and dislocation is expected to reduce the velocity of propagation of seismic waves and to absorb most of its energy; therefore, it may sometimes be located by amplitude effects (note low amplitude first arrivals on fig 12 appendix 2).

Davidson (1985) indicated that there is good evidence that in some areas (in the Lesmahagow Inlier and the Southern Uplands Fault near Biggar), there has been no significant vertical movement of the basement in response to large vertical movements in overlying active faults. As the delay affects the basement and extends beyond the boundaries of the sedimentary cover, serpentinite is a favoured possibility.

5.3 The Basement

Geological evidence concerning the nature of the crystalline rocks below the Midland Valley has come from the study of inclusions in volcanic rocks (Upton et al 1976). Upton et al 1984, have indicated that foliated pyroxene granulite forms a significant component of the lower crust together with stratiform bodies of metacumulates which vary from gabbroic to anorthositic in composition. They interpreted the upper crust as being mainly foliated quartzo-feldspathic rocks with some unfoliated plutonic rocks; granites, trondhjemites, tonalites and kinzigites. It is unlikely, however, that the xenolith material would be representative of a wide range region, particularly since closely-spaced vents may yield very different rock types. The LISPB experiment shows a Lewisian-like basement extending

from northern Scotland and the central Highlands at a depth of 6-15 km, and it rises to a depth of 6 km beneath the Midland Valley. This basement was interpreted by Smith & Bott (1975) as being composed of granulite facies.

On geophysical evidence, Powell (1971) interpreted the Southern Uplands to be underlain by granulites. Oliver and McKerrow (1984) accepted the conclusion of Hall et al (1983) that there are crystalline rocks at shallow depth in the Southern Uplands, but they argued against its continental affinity. They suggested that the rocks are greenschist facies metagreywackes, part of an accretionary wedge occupying nearly all the present crustal pile. The similarity in the velocity structure (fig 5.4) between the Colmonell line (SW of the Midland Valley) and SUSP (along the Northern Belt of the Southern Uplands), suggest a unique basement across the Southern Uplands Fault. The continuity of the basement across the Southern Uplands Fault on the Loch Doon line, comes as further support for the conclusions of Hall et al (1983, 1984a).

It is impossible to differentiate the rock type from P-wave velocity (Vp) only. Since S-wave velocities (Vs) do not depend solely on Vp, and there is quite a marked variation in Vp/Vs ratios among the mineral groups, a knowledge of Vs can be a useful indicator of rock type (Hall 1978b). Poisson's Ratio (σ) is directly calculable from Vp/Vs and is unusually low in quartz and exceptionally high in some of the hydrous minerals, particularly serpentine. No S-waves could be clearly picked on all the recorded profiles except the Colmonell line, where clear arrivals of S-waves on six seismograms give a velocity of 3· $\pm$ 0· km/sec, from a refractor equivalent to that having a P-wave velocity of 6·28 $\pm$ 0·03 km/sec. A brief analysis of this shear wave velocity function is given in appendix 4.

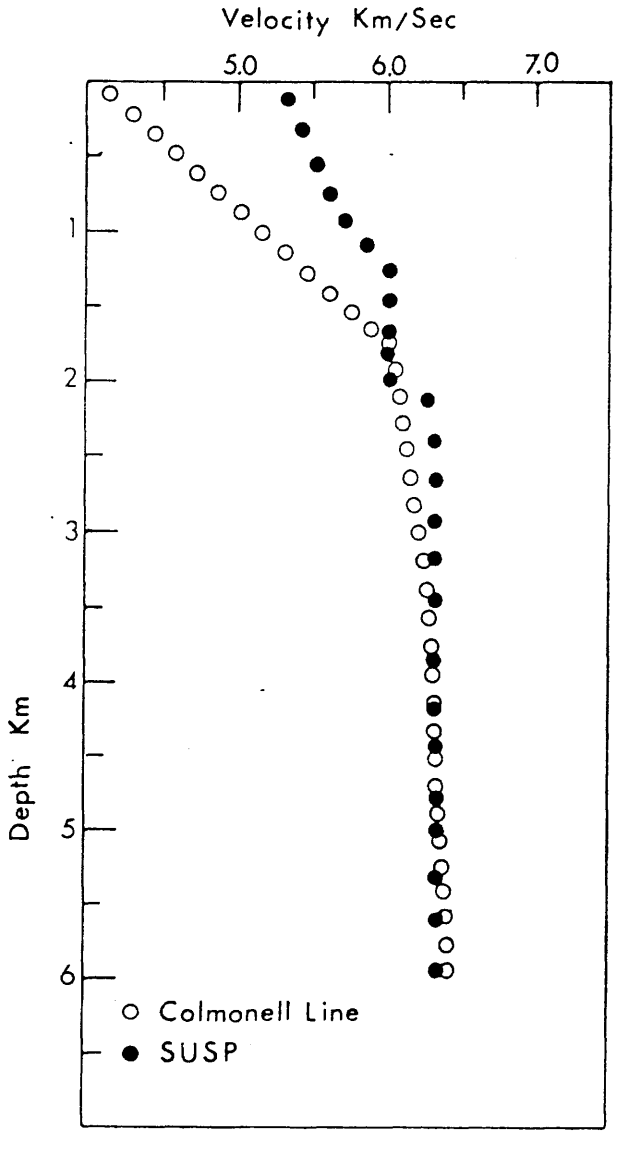

Fig 5.4 Comparison between the velocity structure of the Colmoell and SUSP lines.

The Poisson's Ratio is then calculated to be 0·31±0.03.

$$\sigma = \frac{1}{2} \left(1 - \frac{1}{(Vp/Vs)_2 - 1}\right)$$

This is significantly higher than that of LISPB (0·25) and might indicate inhomogenity in the basement from E to W across the Midland Valley. Such high values of (σ) are expected for rocks bearing basic minerals, such as gabbro, serpentinite, dolerite, etc (see Christensen 1972 and Hall 1978b). A region in which the crust is gravitationally dominated by basic igneous intrusions runs from Arran southwards, suggested by Hipkin and Hussain (1983). They emphasised that these are not localised to obvious Tertiary centres, but occupy a north-south tract of land about 50 km wide. The eastern boundary reaches as far inland as the Loch Doon and Cairnsmore of Fleet granites. Two-dimensional gravity modelling along the Colmonell line, which runs almost vertical to the high gravity structure, is shown in fig 5.5. A basement that outcrops as the Ballantrae ophiolite, with a density of 2·85 could be fitted under the sedimentary cover (Carboniferous, Lower Old Red Sandstone and Lower Palaeozoic) which have thicknesses comparable to those of the seismic model (see fig 4.12a). This density is appropriate for the gabbroic components of the Ballantrae ophiolite. The gravity-modelling is in agreement with the seismic interpretation of a basement that has a velocity gradient indistinguishable from that of the ophiolite. The presence of ophiolitic debris in the Heads of Ayr vent (Whyte 1961) and suspected by McLean (1966) on gravity basis, as forming the basement there, may come as further support.

A conclusion could be drawn that either the upper crust is thin, giving greater thickness of a basic lower crust of the Midland Valley (Upton 1984),

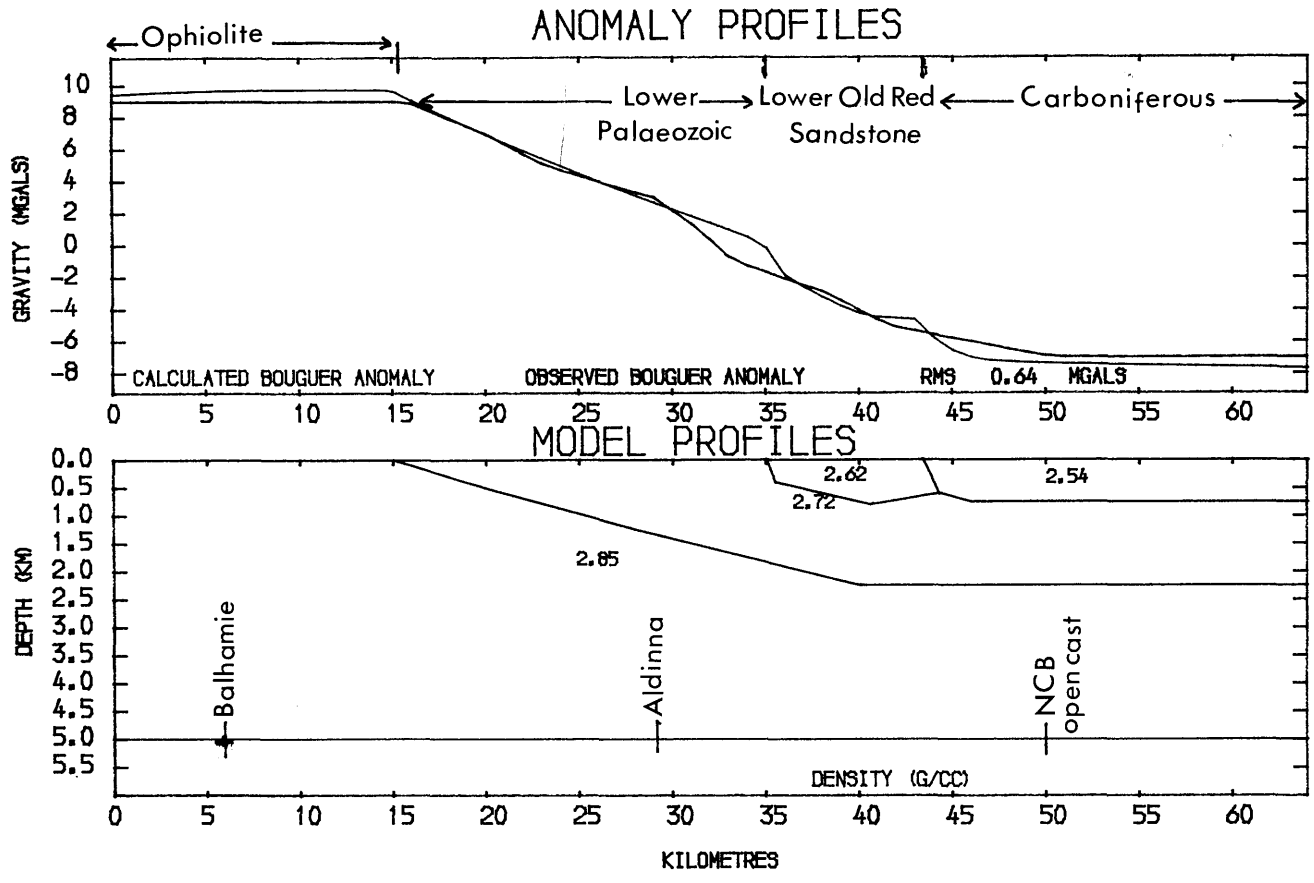

Fig 5.5 Two-dimensional gravity modelling along the Colmonell line.

or the gabbroic components of the Ballantrae ophiolite extend underneath the surrounding sediments.

5.4 Suggestions for Future Work

1. Laboratory-velocity measurements at higher pressures on the greywacke samples (discussed in chapter 3), to better define velocities at depth.

2. Davidson's (1985) seismic refraction line (Troon-Biggar, across the Lesmahagow Inlier) shows a thicker basement of quartzo-feldspathic gneiss, therefore, a line that runs from Troon, across the Mauchline basin to the Southern Uplands (i.e. inbetween the Loch Doon line and Davidson's line), might impose more constraints on the inhomogenity in the basement.

REFERENCES

ADESANYA, O. 1982. Seismic velocities of the upper crust of the Southern Uplands. Univ. Glasgow Ph.D. thesis (unpubl).

AFTALION, M., VAN BREEMEN, O. and BOWES, D.R. 1984. Age constraints on basement of the Midland Valley of Scotland. Trans. R. Soc. Edinburgh Earth Sci. Vol. 75 Part 2, 53-64.

AGGER, H.E. and CARPENTER, E.W. 1964-65. A crustal study in the vicinity of the Eskdalemuir Seismological Array Station. Geophys. J. R. astron. Soc. 9, 69-83.

ALI, M. 1983. Study of shear wave velocities in the Lewisian Metamorphic Complex of NW Scotland. Univ. Glasgow Ph.D. thesis (unpubl).

ALLSOP, M. JENNIFER. 1974. Geophysical surveys at the Spilmersford Borehole, East Lothian, Scotland. Bul. Geol. Surv. G.B., 45, 63-73.

ANDERSON, O.L. and LIEBERMANN, R.C. 1968. Sound velocities in rocks and minerals: experimental methods, extrapolations to very high pressures, and results. In Mason, W.P. (ed) Physical Acoustics IVB, New York, 329-472.

ASSUMPCAO, M. and BAMFORD, D. 1978. LISPB-V. Studies of crustal shear waves. Geophys. J.R. astron. Soc., 54, 61-73.

BACON, M. 1978. Hewlett-Packard 9810 program for converting Decca Main Chain Fixes to Geographical Co-ordinates. NERC, Institute of Geophysical Science, Continental Shelf Division, Report No. HP7.

BALSILLIE, D. The Ballantrae Igneous Complex, south Ayrshire. Geol. Mag., 69, 107-131.

BAMFORD, D. 1979. Seismic constraints on the deep geology of the Caledonides of northern Britain. In Harris, A.L., Holland, C.H.& Leake, B.E. (eds). The Caledonides of the British Isles - reviewed, spec. publ. Geol. Soc. London, 8, 93-96.

BAMFORD, D., FABER, S., JACOB, B., KAMINSKI, W., NUNN, K., PRODEHL, C., FUCHS, K., KING, R. and WILLMORE, P. 1976. A lithospheric seismic profile in Britain - I, preliminary results. Geophys. J.R. astron. Soc. 44, 145-160.

BAMFORD, D., NUNN, K., PRODEHL, C. and JACOB, B. 1977. LISPB III - Upper Crustal structure of northern Britain. J. Geol. Soc. 133, 481-488.

BAMFORD, D., NUNN, K., PRODEHL, C. and JACOB, B. 1978. LISPB - IV. Crustal structure of northern Britain. Geophys. J.R. astron. Soc. 54, 43-60.

BIRCH, F. 1960. The velocity of compressional waves in rocks to 10 kbars, 1 J. Geophys. Res., 65, 1083-1102.

BIRCH, F. 1961. The velocity of compressional waves in rocks to 10 kbars, 2. J. Geophys. Res., 66, 2199-2222.

BLACKMAN, R.B. and TUKEY, J.W. 1958. The measurement of power spectra. Dover, New York.

BLUCK, B.J. 1978a. The Ballantrae Complex. In Bowes, D.R. & Leake, B.E. (eds). Crustal evolution in north-western Britain and adjacent regions. Spec. Issue. Geol. J. 10, 151-162.

BLUCK, B.J. 1978. The Old Red Sandstone of the Midland Valley of Scotland. In Bowes, D.R. & Leake, B. E. (eds). Crustal evolution in norther-western Britain and adjacent regions. Spec. Issue. Geol. J. 10, 249-278.

BLUCK, B.J. 1983. Role of the Midland Valley of Scotland in the Caledonian orogeny. Trans. R. Soc. Edinburgh, Earth Sci., 74, 119-136.

BLUCK, B.J. 1984. Pre-Carboniferous history of the Midland Valley of Scotland. Trans. R. Soc. Edinburgh, Earth Sci., 75, 275-295.

BLUCK, B.J., HALLIDAY, A.N., AFTALION, M. and MACINTYRE, R.M. 1980. Age and origin of Ballantrae ophiolite and its significance to the Caledonian orogeny and Ordovician time scale. Geology - 8, 492-495.

BOTT, M.H.P. and MASSON-SMITH, D. 1960. A gravity survey of the Criffell granodiorite and New Red Sandstone deposits near Dumfries. Proc. Yorks. Geol. Soc. 32, 317-332.

BOTT, M.H.P., LONG. R.E., GREEN, A.S.P., LEWIS, A.H.J., SINHA, M.C. and STEVENSON, D.L. 1985. Crustal structure south of the Iapetus structure beneath northern England. Nature 34, 724-727.

COCKS, L.R.M. and TOGHILL, P. 1973. The biostratigraphy of the Silurian rocks of the Girvan district, Scotland. J. Geol. Soc. London, 129, 209-243.

CHRISTENSEN, N.I. 1965. Compressional wave velocities in metamorphic rocks at pressures to 10 kbars. J. Geophys. Res., 70, 6147-6164.

CHRISTENSEN, N.I. 1966. Elasticity of ultrabasic rocks. J. Geophys. Res. 71, 5921-5931.

CHRISTENSEN, N.I. 1972. The abundance of serpentinites in the oceanic crust. J. of Geology. 80, 709-719.

CHRISTENSEN, N.I. 1978. Ophiolites seismic velocities and oceanic crustal structure. Tectonophysics, 47, 131-157.

CHRISTENSEN, N.I. 1982. Seismic Velocities. Handbook of physical properties of rocks. Volume II, 1-229, Robert S. Carmichael. CRC Press, Inc. Boca Raton, Florida.

CHRISTENSEN, N.I. and SALISBURY, M.H. 1972. Sea floor spreading, progressive alteration of layer 2 basalts and associated changes in seismic velocities. Earth Planet, Sci. Lett, 15, 367-372.

CHRISTENSEN, N.I. and SALISBURY, M.H. 1982. Lateral heterogeneity in the seismic structure of the oceanic crust inferred from velocity studies in the Bay of Islands ophiolite, Newfoundland. Geophys. J.R. astron. Soc., 68, 675-688.

CHURCH, W.R. and GAYER, R.A. 1973. The Ballantrae Ophiolite. Geol. Mag., 110, 497-510.

CRAIG, G.Y. 1983. Geology of Scotland. Second Edition. Scottish Academic Press, Edinburgh.

DAVIDSON, K.A.S. 1986.* Seismological studies of upper crustal structure of the southern Midland Valley of Scotland. Univ. Glasgow Ph.D. thesis (unpubl).

* Referred to as "Davidson 1985" in text.

DAVIDSON, K.A.S., SOLA, M., POWELL, D.W. and HALL, J. 1984. Geophysical model for the Midland Valley of Scotland. Trans. R. Soc. Edinburgh. Earth Sci. 75, 175-181.

DEWEY, J.F. 1969. Evolution of the Appalachian/ Caledonian orogen. Nature, 222, 124-129.

DEWEY, J.F. 1971. A model for the Lower Palaeozoic evolution of the southern margin of the Early Caledonides of Scotland and Ireland. Scott. J. Geol., 7, 219-240.

DEWEY, J.F. 1974. Continental margins and ophiolite obduction: Appalachian Caledonian System. In Burk, C.A. & Drake C.L. (eds). Geology of Continental margins, Springer, New York, 933-950.

DOBRIN, M.B. 1976. Introduction to geophysical prospecting. Third Edition, Editors McGraw-HILL, Book Company.

EL-BATROUK, S.I. 1975. Geophysical investigation on Loch Doon granite south-west Scotland. Univ. Glasgow Ph.D. thesis (unpubl).

EL-ISA, Z.H.M. 1977. Seismic studies of local events received at three arrays in southern central Scotland. Univ. Glasgow Ph.D. thesis (unpubl).

EYLES, V.A., SIMPSON, J.B. and MACGREGOR, A.G. 1949. Geology of central Ayrshire. Mem. geol. Surv. U.K.

FLOYD, J. 1975. The Ordovician rocks of west Nithsdale. Univ. St. Andrews Ph.D. thesis (unpubl).

FLOYD, J. 1982. Stratigraphy of a flysch succession: the Ordovician of W. Nithsdale, SW Scotland. Trans. R. Soc. Edinburgh. Earth Sci., 73, 1-9.

FRESHNEY, E.C. 1961. The cementstone group of the west Midland Valley of Scotland. Univ. Glasgow Ph.D. thesis (unpubl).

GARDINER, C.I. and REYNOLDS, S.H. 1931. The Loch Doon granite area, Galloway. Quat. J. Geol. Soc. London, 88, 1-34.

GASS, I.G. 1982. Ophiolites. Scientific American, 247, 108-117.

GEIKIE, A. 1897. The ancient volcanoes of Great Britain. 2. Vols. London.

GOGUEL, J.M. 1951. Seismic refraction with variable velocity. Geophysics, 16, 81-101.

GRAMPIN, S. 1970. A method for the location of near seismic events using travel times along ray paths. Geophys. J. 21, 535-539.

GRANT, F.S. and WEST, G.F. 1965. Interpretation theory in applied Geophysics. Editors McGraw-Hill, Inc.

GUNN, P.J. 1973. Location of the Proto-Atlantic suture in the British Isles. Nature, 242, 111-112.

HALL, J. 1970. The correlation of seismic velocities with formations in the southwest of Scotland. Geophys. Prospect. 18, 134-148.

HALL, J. 1978a. Seismic refraction studies in Firth of Clyde. In McLean, A.C. and Deegan, C.E. (eds). The solid geology of Clyde Sheet (55°N/6°W). Rep. Inst. Geol. Sci., 78/79, 43-48.

HALL, J. 1978b. Crustal structure of the eastern North Atlantic seaboard, in Crustal evolution in north-western Britain and adjacent regions, Bowes, D.R. and Leake, B.E. (eds), Geol. J. Spec. Issue, 20, 23-38.

HALL, J. 1978. "LUST" - a seismic refraction survey of the Lewisian basement complex in NW Scotland. J. Geol. Soc. London, 135, 555-565.

HALL, J. 1980. Crustal structure of the Caledonides in Britain. Proc. of the 17th Assembly of the ESC Budapest, 1980, 501-505.

HALL, J. and AL-HADDAD, F.M. 1979. Variation of effective seismic velocities of minerals with pressure and its use in velocity production. Geophys. J.R. astron. Soc., 57, 107-118.

HALL, J. and SIMMONS, G. 1979. Seismic velocities of Lewisian metamorphic rocks at pressures to 8 kbar: relationship to crustal layering in North Britain. Geophys. J.R. astron. Soc., 58, 337-347.

HALL, J., POWELL, D.W., WARNER, M.R., EL-ISA, Z.H.M., ADESANYA, O. and BLUCK, B.J. 1983. Seismological evidence for shallow crystalline basement in the Southern Uplands of Scotland. Nature, 305, 418-420.

HALL, J., POWELL, D.W., WARNER, M.R., EL-ISA, Z.H.M., ADESANYA, O. and BLUCK, B.J. 1984a. Seismological evidence for shallow crystalline basement in the Southern Uplands of Scotland. Nature, 309, 89-90.

HALL, J., BREWER, J.A., MATHEWS, D.H. and WARNER, M.R. 1984. Crustal structure across the Caledonides from the "WINCH" seismic reflection profile: influences on the evolution of the Midland Valley of Scotland. Trans. R. Soc. Edinburgh, Earth Sci.,75, 97-109.

HAMILTON, P.J., BLUCK, B.J. and HALLIDAY, A.N. 1984. Sm-Nd ages from the Ballantrae Complex, SW. Scotland. Trans. R. Soc. Edinburgh, Earth Sci., 75,183-187.

HIPKIN, R.G. and HUSSAIN, A. 1983. Regional gravity anomalies. 1 Northern Britain. Rep. Inst. Geol. Sci., 82/10.

HOLMES, A. 1930. Petrographic methods and calculations.

HOLUB, F.V., KLAPOVA, H., BLUCK, B.J. and BOWES, D.R. 1984. Petrology and geochemistry of post-obduction dykes of the Ballantrae Complex, SW Scotland. Trans. R. Soc. Edinburgh, Earth Sci., 75, 211-223.

HUGHES, D.H. and MAURETTE, C. 1956. Variation of elastic wave velocities in granites with pressure and temperature. Geophys, 21, 277-284.

HUTTON, V.R.S., INGHAM, M.R. and MBIPOM, E.W. 1980. An electrical model of the crust and upper mantle in Scotland. Nature, 287, 30-33.

JACOB, A.W.B. 1969. Crustal phase velocities observed at the Eskdalemuir Seismic Array. Geophys. J.R. astr. Soc., 18, 189-197.

JONES, A.G. and HUTTON, R. 1979. A multi-station magnetotelluric study in southern Scotland - I. Fieldwork, data analysis and results. Geophys. J.R. astr. Soc., 56, 329-349.

JONES, A.G. and HUTTON, R. 1979. A multi-station magnetotelluric study in southern Scotland - II. Monte-Carlo inversion of the data and its geophysical and tectonic implications. Geophys. J.R. astr. Soc., 56, 351-368.

JONES, H.J. and MORRISON, J.A. 1954. Cross-correlation filtering. Geophys, 19, 660-683.

KANASEWICH, E.R. 1981. Time sequence analysis in geophysics. The Univ. of Alberta Press (eds) 3rd. edition.

KELLING, G. 1961. The stratigraphy and structure of the Ordovician rocks of the Rhinns of Galloway. Quat. J. Geol. Soc. London, 117, 37-75.

LAGIOS, E. and HIPKIN, R.G. 1979. The Tweeddale granite- a newly discovered batholith in the Southern Uplands. Nature, 280, 672-675.

LAMBERT, R. and MCKERROW, W.S. 1976. The Grampian orogeny. Scott. J. Geol., 12, 271-292.

LEGGETT, J.K. 1980. The sedimentological evolution of a Lower Palaeozoic accretionary fore-arc in the Southern Uplands of Scotland. Sedimentology,27, 401-417.

LEGGETT, J.K., MCKERROW, W.S., MORRIS, J.H., OLIVER, G.J.H. and PHILLIPS, W.E.A. 1979. The north-western margin of the Iapetus Ocean. In Harris, A.L., Holland, C.H. & Leake, B.E. (eds). The Caledonides of the British Isles reviewed. Geol. Soc. London Spec. Publ., 8, 499-511.

LEWIS, A.D. and BLOXAM, T.W. 1977. Petrotectonic environments of the Girvan-Ballantrae lavas from rare-earth element distribution. Scott. J. Geol., 13, 211-222.

LONGMAN, C.D. 1980. Age and affinity of granitic detritus in Lower Palaeozoic conglomerates, SW. Scotland: implications for Caledonian evolution. Univ. Glasgow Ph.D. thesis (unpubl).

LONGMAN, C.D., BLUCK, B.J. and BREEMEN, V. 1979. Ordovician conglomerates and the evolution of the Midland Valley. Nature, 280, 578-581.

LOVELL, J.P.B. 1983. Permian and Triassic. In Geology of Scotland, 325-338. Edited by G.Y. Craig 1983.

MACGREGOR, A.G. 1960. Divisions of the Carboniferous on Geological Survey (Scottish) maps. Bull. Geol. Surv. G.B.16, 127-130.

MCKERROW, W.S., LEGGETT, J.K. and EALES, M.H. 1977. Imbricate thrust model of the Southern Uplands of Scotland. Nature, 263, 304-306.

MCLEAN, A.C. 1961. A gravity survey of the Sanquhar Coalfield. Proc. R. Soc. Edinburgh, 68, 112-127.

MCLEAN, A.C. 1961b. Density measurements of rocks in SW. Scotland. Proc. R. Soc. Edinburgh, 68, 103-111.

MCLEAN, A.C. 1966. A gravity survey in Ayrshire and its geological interpretation. Trans. R. Soc. Edinburgh, 66, 239-283.

MCLEAN, A.C. and DEEGAN, C.E. 1978. The solid geology of the Clyde Sheet (55°N/6°W. Rep. Inst. Geol. Sci. 78/9.

MCLEAN, A.C. and QURESHI, I.R. 1966. Regional gravity anomalies in the Western Midland Valley of Scotland. Trans. R. Soc. Edinburgh, 56, 267-283.

MECHIE, J. 1980. Program to calculate Time-Term Anisotropy. Dept. of Geological Sciences, Univ. of Birmingham.

MOSELEY, F. 1977. Caledonian plate tectonics and the place of the English Lake District. Bull. Geol. Soc. Amer., 88, 764-768.

MYKURA, W. 1983. Old Red Sandstone. In Craig, G.Y., (edt). Geology of Scotland (2nd edn). 205-242.

NICHOLS, J., WARREN, N., LUYENDYK, B.P., SPUDICH, P. 1980. Seismic velocity structure of the ophiolite at Point Sal, Southern California, determined from laboratory measurements. Geophys. J.R. astr. Soc., 63, 165-185.

PEACH, B.N. and HORNE, J. 1899. The Silurian rocks of Britain. 1 Scotland Mem. Geol. Surv. U.K.

PETERSON, J.J., FOX, P.J. and SCHREIBER, E. 1974. Newfoundland ophiolites and the geology of the oceanic layer. Nature, 247, 194-196.

POWELL, D.W. 1956. Gravity and magnetic anomalies in North Wales. Q.J. Geol. Soc. London., 61, 375-397.

POWELL, D.W. 1970. Magnetised rocks within the Lewisian of W. Scotland and under the Southern Uplands. Scott. J. Geol., 6, 297-301.

POWELL, D.W. 1971. A model for the Lower Palaeozoic evolution of the southern margin of the early Caledonides of Scotland and Ireland. Scott. J. Geol., 7, 369-372.

POWELL, D.W. 1978a. Gravity and magnetic anomalies attributable to basement sources under northern Britain. In Bowes, D.R. and Leake, B.E. (eds). Crustal evolution in north-western Britain and adjacent regions. Geol.J. Spec. Issue, 10, 107-114.

POWELL, D.W. 1978. Gravity and magnetic anomaly interpretation of the Girvan-Ballantrae district. Geol. J. Spec. Issue, 10, 177-182.

PRINGLE, J. 1935. British Regional Geology: The South of Scotland. (Geol. Surv. 1).

RICHEY, J.E., ANDERSON, E.M. and MACGREGOR, A.G. 1930. The geology of north Ayrshire. Mem. geol. Surv. U.K.

ROBINSON, E.A. 1966. Fortran II programs for filtering and spectral analysis of single channel time series. Geophys. Pros., 14.

SALISBURY, M.H. and CHRISTENSEN, N.I. 1978. The seismic velocity structure of a traverse through the Bay of Islands ophiolite complex, Newfoundland, an exposure of ocean crust and upper mantle. J. Geophys. Res., 83, 805-816.

SCHNEIDER, W.A. and BACKUS, M.M. 1969. Dynamic correlation analysis. Geophysics, 32, 33-51.

SMELLIE, J.L. 1984. Metamorphism of the Ballantrae igneous complex: A preliminary survey. Rep. Br. Geol. Surv., 16, 13-17.

SMITH, M.K. 1958. A review of methods of filtering seismic data. Geophysics, 23, 44-57.

SMITH, P.J. and BOTT, M.H.P. 1975. Structure of the crust beneath the Caledonian Foreland and Caledonian belt of the North Scottish shelf region. Geophys. J.R. astr. Soc., 40, 187-205.

SOLA, M.A. 1985. The seismic structure under the central Midland Valley from refraction measurements. Univ. Glasgow Ph.D. thesis, (unpubl).

STROGEN, P. 1974. The sub-Palaeozoic basement in central Ireland. Nature, 250, 562-563.

SUMMERS, T.P. A seismic study of crustal structure in the region of the Western Isles of Scotland. Univ. Durham Ph.D. thesis, (unpubl).

TERRELL, G.W. 1914. A petrographic sketch of the Carrick Hills, Ayrshire. Trans. geol. Soc. Glasg., 15, 64-83.

UPTON, B.G.J., ASPEN, P., GRAHAM, A. and CHAPMAN, N.A. 1976. Pre-Palaeozoic basement of the Scottish Midland Valley. Nature, 260, 517-518.

UPTON, B.G.J., ASPEN, P. and CHAPMAN, N.A. 1983. The upper mantle and deep crust beneath the British Isles: Evidence from inclusions in volcanic rocks, J. Geol. Soc. London, 140, 105-122.

UPTON, B.G.J., ASPEN, P. and HUNTER, R.H. 1984. Xenoliths and their implications for the deep geology of the Midland Valley of Scotland and adjacent regions. Trans, Roy. Soc. Edinburgh. Earth Sci., 75, 65-70.

WALTON, E.K. 1983. Lower Palaeozoic - stratigraphy. In Craig, G.Y. (edt). Geology of Scotland, 105-160.

WARNER, M.R., HIPKIN, R.G. and BROWITT, C.W.A. 1982. Southern Uplands Seismic Refraction Profile - preliminary results. Geophys. J.R. astr. Soc., 69, 279.

WARREN, R.D. 1981. Signal processing techniques applied to seismic refraction data. Univ. Durham M.Sc. thesis (unpubl).

WHYTE, F. 1961. The Heads of Ayr vent. Trans. Geol. Soc. Glasgow, 25, 72-97.

WILLIAMS, A. 1962. The Barr and Lower Ardmillan Series (Caradoc) of the Girvan District, South-West Ayrshire. Mem. geol. Soc. London, 3.

WILLIAMS, A. 1972. Distribution of brachiopod assemblages in relation to Ordovician Palaeontology. In Hughes, N.F. (edt). Organisms and continents through time. Special pap. Palaeontol., 12, 241-269.

WILLMORE, P.L. 1973. Crustal structure in the region of the British Isles. Tectonophysics, 20, 341-357.

WILLMORE, P.L. and BANCROFT, A.M. 1960. The time-term approach to refraction seismology. Geophys. J.R. astr. Soc., 3, 419-432.

WILSON, J.T. 1966. Did the Atlantic close and then re-open? Nature, 211, 676-681.

WYLLIE, M.R.J., GREGORY, A.R. and GARDNER, L.W. 1956. Elastic wave velocities in heterogeneous and porous media. Geophysics, 21, 41-70.

APPENDIX 1

List of P-wave travel times.

Shot-points and site co-ordinates. Distances are in kilometres, and travel times are given in total and reduced (in seconds) with a reduction velocity of 6·0 km/sec.

APPENDIX 1. TABLE 1.

LAND SHOTS - LENDALFOOT ARRAY 1979

Millenderdale Shot Grid Reference:- 217·850/590·600

	Station	Grid Reference		Distance (km)	Time (sec)	T-X/6 (sec)
1	Lendalfoot	213·600	590·760	4·253	0·970	0·261
2	Cundry Mains	215·220	590·920	2·649	-	-
3	Knockbain	216·080	589·870	2·432	0·410	0·005
4	Breaker Hill	217·750	589·050	1·553	0·322	0·063
5	Bargain Hill	219·000	588·410	2·474	0·475	0·063
6	Millenderdale	217·830	590·850	0·112	0·035	0·016
7	Currarie	216·590	591·210	1·400	0·303	0·070
8	Letterpin	219·350	592·110	2·128	-	-

Knockormal Shot Grid Reference:- 214·500/588·530

	Station	Grid Reference	Distance (km)	Time (sec)	T-X/6 (sec)
1	Lendalfoot	As Above	2·405	0·555	0·154
2	Cundry Mains	"	2·496	-	-
3	Knockbain	"	2·072	0·485	0·14
4	Breaker Hill	"	3·291	0·626	0·078
5	Bargain Hill	"	4·502	0·950	0·200

	Station	Grid Reference		Distance (km)	Time (sec)	T-X/6 (sec)
6	Millenderdale	As Before		3·856	-	-
7	Currarie	"		3·399	0·818	0·252
8	Letterpin	"		6·028	-	-
9	Pinbraid Bridge	214·500	588·530	0·244	0·120	0·079

Dinvin Shot Grid Reference:- 220·250/593·160

Station	Grid Reference	Distance (km)	Time (sec)	T-X/6 (sec)
Lendalfoot	As Before	7·070	1·530	0·352
Cundry Mains	"	5·506	-	-
Knockbain	"	5·312	-	-
Breaker Hill	"	4·811	0·959	0·157
Bargain Hill	"	4·912	0·960	0·141
Millenderdale	"	3·571	0·737	0·142
Currarie	"	4·147	-	-
Letterpin	"	1·383	0·338	0·108

Pinmore Shot Grid Reference:- 220·820/587·900

Station	Grid Reference	Distance (km)	Time (sec)	T-X/6 (sec)
Lendalfoot	As Before	7·766	-	-

Station	Grid Reference	Distance (km)	Time (sec)	T-X/6 (sec)
Cundry Mains	As Before	6·362	-	-
Knockbain	"	5·133	1·019	0·164
Breaker Hill	"	3·278	0·667	0·121
Bargain Hill	"	1·890	0·394	0·079
Millenderdale	"	4·109	0·805	0·120
Currarie	"	5·371	1·050	0·155
Letterpin	"	4·459	-	-

Craigconnachie Shot Grid Reference:- 223·700/586·200

Station	Grid Reference	Distance (km)	Time (sec)	T-X/6 (sec)
Lendalfoot	As Before	11·082	-	-
Cundry Mains	"	9·705	-	-
Knockbain	"	8·458	1·549	0·139
Breaker Hill	"	6·597	1·178	0·079
Bargain Hill	"	5·194	0·995	0·129
Millenderdale	"	7·420	-	-
Currarie	"	8·698	1·652	0·202
Letterpin	"	7·338	1·355	0·132

Cundry Mains Shot Grid Reference:- 215·150/590·790

Station	Grid Reference	Distance (km)	Time (sec)	T-X/6 (sec)
Lendalfoot	As Before	1·550	0·446	0·188
Cundry Mains	"	0·148	0·116	0·091
Knockbain	"	1·308	0·394	0·176
Breaker Hill	"	3·129	0·722	0·201
Bargain Hill	"	4·526	0·978	0·224
Millenderdale	"	2·596	0·676	0·243
Currarie	"	1·500	0·394	0·144
Letterpin	"	4·403	1·053	0·319
Pinbraid Bridge	As Before	2·512	0·626	0·207

APPENDIX 1. TABLE 2.

MARINE EXPLOSIVE SHOTS - LENDALFOOT ARRAY 1979

Wise Explosive (1). Grid Reference:- 211·019/589·841

	Station	Grid Reference	Distance (km)	Time (sec)	T-X/6 (sec)
1	Lendalfoot	As Before	2·740	0·760	0·303
2	Cundry Mains	"	4·537	1·069	0·346
3	Knockbain	"	5·061	1·133	0·289
4	Breaker Hill	"	6·777	1·416	0·286
5	Bargain Hill	"	8·108	1·657	0·306
6	Millenderdale	"	-	-	-
7	Currarie	"	5·737	1·320	0·364
8	Letterpin	"	8·634	1·814	0·375

Wise Explosive (2). Grid Reference:-201·118/605·150

Station	Grid Reference	Distance (km)	Time (sec)	T-X/6 (sec)
Lendalfoot	As Before	19·049	3·814	0·639
Cundry Mains	"	20·034	4·062	0·723
Knockbain	"	21·386	4·276	0·712
Breaker Hill	"	23·148	4·485	0·627
Bargain Hill	"	24·495	4·696	0·614

Station	Grid Reference	Distance (km)	Time (sec)	T-X/6 (sec)
Millenderdale	As Before	-	-	-
Currarie	"	20·826	4·145	0·674
Letterpin	"	22·415	4·407	0·671

Wise Explosive (3). Grid Reference:- 191·275/621·283

Station	Grid Reference	Distance (km)	Time (sec)	T-X/6 (sec)
Lendalfoot	As Before	37·816	6·974	0·671
Cundry Mains	"	38·669	7·189	0·744
Knockbain	"	40·026	7·357	0·686
Breaker Hill	"	41·712	7·536	0·584
Bargain Hill	"	43·004	7·732	0·565
Millenderdale	"	40.390	7·389	0·657
Currarie	"	39·309	7·143	0·591
Letterpin	"	40·488	7·398	0·650

Wise Explosive (4). Grid Reference:- 182·243/635·898

Station	Grid Reference	Distance (km)	Time (sec)	T-X/6 (sec)
Lendalfoot		54·961	9·273	0·113
Cundry Mains		55·772	9·469	0·174

Station	Grid Reference	Distance (km)	Time (sec)	T-X/6 (sec)
Knockbain		-	-	-
Breaker Hill		58·783	9·837	0·040
Bargain Hill		60·052	10·040	0·031
Millenderdale		57·409	9·761	0·193
Currarie		56·363	9·597	0·203
Letterpin		57·396	9·689	0·123

APPENDIX 1. TABLE 3.

AIRGUN SHOTS - LENDALFOOT ARRAY 1979

Airgun (224) Grid Reference:- 204·296/587·413

	Station	Grid Reference	Distance (km)	Time (sec)	T-X/6 (sec)
1	Lendalfoot	As Above	9·868	2·34	0·700
2	Cundry Mains	"	-	-	-
3	Knockbain	"	-	-	-
4	Breaker Hill	"	13·578	3·010	0·750
5	Bargain Hill	"	14·749	3·158	0·7
6	Millenderdale	"	-	-	-
7	Currarie	"	-	-	-
8	Letterpin	"	15·782	3·380	0·750

Airgun (228) Grid Reference:- 204·612/588·757

Station	Grid Reference	Distance (km)	Time (sec)	T-X/6 (sec)
Lendalfoot	As Above	9·190	2·030	0·500
Cundry Mains	"	-	-	-
Knockbain	"	-	-	-
Breaker Hill	"	13·159	2·710	0·520

Station	Grid Reference	Distance (km)	Time (sec)	T-X/6 (sec)
Bargain Hill	As Before	14·404	2·920	0·520
Millenderdale	"	-	-	-
Currarie	"	-	-	-
Letterpin	"	15.128	3.030	0.510

Airgun(238) Grid Reference:- 205.870/592·079

Station	Grid Reference	Distance (km)	Time (sec)	T-X/6 (sec)
Lendalfoot	As Above	7·831	1·850	0·540
Cundry Mains	"	9·410	2·180	0·610
Knockbain	"	10·452	2·350	0·610
Breaker Hill	"	12·259	2·650	0·610
Bargain Hill	"	13·647	2·880	0·610
Millenderdale	"	-	-	-
Currarie	"	-	-	-
Letterpin	"	13·497	2·840	0·590

Airgun (240) Grid Reference:- 206·192/592·839

Station	Grid Reference	Distance (km)	Time (sec)	T-X/6 (sec)
Lendalfoot	As Above	7·684	1·860	0·580
Cundry Mains	"	9·216	2·180	0·640

Station	Grid Reference	Distance (km)	Time (sec)	T-X/6 (sec)
Knockbain	As Before	10·327	2·370	0·65(
Breaker Hill	"	12·155	2·670	0·64(
Bargain Hill	"	13·564	2·890	0·63(
Millenderdale	"	-	-	-
Currarie	"	-	-	-
Letterpin	"	13·193	2·820	0·62(

Airgun (242) Grid Reference:- 206·501/593·598

Station	Grid Reference	Distance (km)	Time (sec)	T-X/6 (sec)
Lendalfoot	As Above	7·637	1·880	0·61(
Cundry Mains	"	9·108	2·170	0·65(
Knockbain	"	10·281	2·370	0·66(
Breaker Hill	"	12·070	2·650	0·64(
Bargain Hill	"	13·544	2·910	0·65(
Millenderdale	"	-	-	-
Currarie	"	-	-	-
Letterpin	"	12·950	2·800	0·64(

Airgun (248) Grid Reference:- 208·088/594·419

Station	Grid Reference	Distance (km)	Time (sec)	T-X/6 (sec)
Lendalfoot	As Above	6·600	1·700	0·600
Cundry Mains	"	7·923	1·980	0·660
Knockbain	"	9·188	2·210	0·680
Breaker Hill	"	11·024	2·500	0·660
Bargain Hill	"	12·463	2·720	0·640
Millenderdale	"	-	-	-
Currarie	"	-	-	-
Letterpin	"	11·506	2·560	0·640

Airgun (250) Grid Reference:- 208·725/594·105

Station	Grid Reference	Distance (km)	Time (sec)	T-X/6 (sec)
Lendalfoot	As Above	5·897	1·520	0·540
Cundry Mains	"	7·212	1·810	0·610
Knockbain	"	8·479	2·020	0·610
Breaker Hill	"	10·314	2·340	0·620
Bargain Hill	"	11·753	2·560	0·600
Millenderdale	"	-	-	-

Station	Grid Reference	Distance (km)	Time (sec)	T-X/6 (sec)
Currarie	As Before	-	-	-
Letterpin	"	10·821	2·400	0·600

Airgun (252) Grid Reference:- 209·244/593·827

Station	Grid Reference	Distance (km)	Time (sec)	T-X/6 (sec)
Lendalfoot	As Above	5·312	1·140	0·550
Cundry Mains	"	6·625	1·700	0·600
Knockbain	"	7·891	1·920	0·600
Breaker Hill	"	9·726	2·220	0·600
Bargain Hill	"	11·165	2·460	0·600
Millenderdale	"	-	-	-
Letterpin	"	10·262	2·311	0·600
Currarie	"	-	-	-

Airgun (256) Grid Reference:- 210·185/593·234

Station	Grid Reference	Distance (km)	Time (sec)	T-X/6 (sec)
Lendalfoot	As Above	4·223	1·180	0·480
Cundry Mains	"	5·544	1·460	0·540
Knockbain	"	-	-	-
Breaker Hill	"	8·639	2·000	0·560

Station	Grid Reference	Distance (km)	Time (sec)	T-X/6 (sec)
Bargain Hill	As Before	10·077	2·240	0·56C
Millenderdale	"	-	-	-
Currarie	"	-	-	-
Letterpin	"	9·271	2·100	0·55C

Airgun (262) Grid Reference:- 211·614/592·548

Station	Grid Reference	Distance (km)	Time (sec)	T-X/6 (sec)
Lendalfoot	As Above	2·670	0·830	0·380
Cundry Mains	"	3·939	1·140	0·480
Knockbain	"	-	-	-
Breaker Hill	"	7·035	1·680	0·510
Bargain Hill	"	8·473	1·920	0·510
Millenderdale	"	-	-	-
Currarie	"	-	-	-
Letterpin	"	7·759	1·800	0·510

Airgun (267) Grid Reference:- 212·357/591·966

Station	Grid Reference	Distance (km)	Time (sec)	T-X/6 (sec)
Lendalfoot	As Above	1·719	0·570	0·280
Cundry Mains	"	3·026	0·880	0·380

Station	Grid Reference	Distance (km)	Time (sec)	T-X/6 (sec)
Knockbain	As Before	4·264	1·100	0·390
Breaker Hill	"	6·102	1·470	0·450
Bargain Hill	"	7·540	1·710	0·450
Millenderdale	"	-	-	-
Currarie	"	-	-	-
Letterpin	"	7·005	1·620	0·450

Airgun (269) Grid Reference:- 211·970/591·662

Station	Grid Reference	Distance (km)	Time (sec)	T-X/6 (sec)
Lendalfoot	As Above	1·846	0·590	0·280
Cundry Mains	"	3·312	0·950	0·400
Knockbain	"	4·477	1·190	0·440
Breaker Hill	"	6·320	1·470	0·420
Bargain Hill	"	7·752	1·730	0·440
Millenderdale	"	-	-	-
Currarie	"	-	-	-
Letterpin	"	7·404	1·670	0·440

Airgun (276) Grid Reference:- 210·654/590·011

Station	Grid Reference	Distance (km)	Time (sec)	T-X/6 (sec)
Lendalfoot	As Above	3·024	0·860	0·360

Station	Grid Reference	Distance (km)	Time (sec)	T-X/6 (sec)
Cundry Mains	As Before	4·643	1·250	0·480
Knockbain	"	5·435	1·350	0·440
Breaker Hill	"	-	-	-
Bargain Hill	"	8·511	1·860	0·440
Millenderdale	"	-	-	-
Currarie	"	-	-	-
Letterpin	"	-	-	-

APPENDIX 1. TABLE 4.

CALEDONIAN SUTURE SEISMIC PROJECT 1982

RECORDED ACROSS THE SOUTHERN UPLANDS (GALLOWAY).

Shot (M 05) Grid Reference:- 269·508/529·731

Station	Grid Reference		Distance (km)	Time (sec)	T-X/6 (sec)
Low Glasnick	234·975	561·000	46·59	8·46	0·69
Eldrig	234·430	565·850	50·35	9·13	0·74
Closes	232·425	568·600	53·72	9·65	0·70
Drumloskie	230·360	571·955	57·58	10·38	0·78
Loch Dornal	228·950	576·605	61·98	11·12	0·79
Wood Park	227·540	579·810	65·34	11·65	0·76
Barmalloch	226·865	584·270	69·23	12·26	0·72

Shot (M 06) Grid Reference:- 265·076/528·005

Station	Grid Reference	Distance (km)	Time (sec)	T-X/6 (sec)
Low Glasnick	As Above	44·66	8·18	0·74
Eldrig	"	48·70	8·87	0·75
Closes	"	52·10	9·45	0·77
Drumloskie	"	56·01	10·14	0·80
Loch Dornal	"	60·56	10·91	0·82

Station	Grid Reference	Distance (km)	Time (sec)	T-X/6 (sec)
Wood Park	As Before	63·97	11·57	0·91
Barmalloch	"	68·01	12·16	0·82

Shot (M 07) Grid Reference:- 261·001/526·403

Station	Grid Reference	Distance (km)	Time (sec)	T-X/6 (sec)
Low Glasnick	As Above	43·29	7·98	0·76
Eldrig	"	47·56	8·70	0·77
Closes	"	50·96	9·29	0·80
Drumloskie	"	54·90	9·95	0·80
Loch Dornal	"	59·56	10·77	0·84
Wood Park	"	63·02	11·45	0·95
Barmalloch	"	67·19	12·03	0·83

Shot (M 08) Grid Reference:- 257·296/524·699

Station	Grid Reference	Distance (km)	Time (sec)	T-X/6 (sec)
Low Glasnick	As Above	42·61	7·80	0·70
Eldrig	"	47·08	8·56	0·71
Closes	"	50·46	9·14	0·73
Drumloskie	"	54·39	9·83	0·76

Station	Grid Reference	Distance (km)	Time (sec)	T-X/6 (sec)
Loch Dornal	As Before	59·14	10·65	0·79
Wood Park	"	62·63	11·26	0·82
Barmalloch	"	-	-	-

Shot (M 09) Grid Reference:- 253·639/523·220

Station	Grid Reference	Distance (km)	Time (sec)	T-X/6 (sec)
Low Glasnick	As Above	42·14	7·63	0·61
Eldrig	"	46·76	8·48	0·69
Closes	"	50·09	9·07	0·72
Drumloskie	"	54·01	9·52	0·52
Loch Dornal	"	58·82	10·57	0·77
Wood Park	"	62·32	11·17	0·78
Barmalloch	"	66·66	11·98	0·87

Shot (M 10) Grid Reference:- 249·499/521·592

Station	Grid Reference	Distance (km)	Time (sec)	T-X/6 (sec)
Low Glasnick	As Above	42·00	7·65	0·65
Eldrig	"	46·75	8·53	0·74
Closes	"	50·01	9·07	0·73

Station	Grid Reference	Distance (km)	Time (sec)	T-X/6 (sec)
Drumloskie	As Before	53·88	9·81	0·83
Loch Dornal	"	58·73	10·64	0·85
Wood Park	"	62·22	11·25	0·88
Barmalloch	"	66·64	12·00	0·89

Shot (M 11) Grid Reference:- 245·137/519·864

Station	Grid Reference	Distance (km)	Time (sec)	T-X/6 (sec)
Low Glasnick	As Above	42·37	7·71	0·65
Eldrig	"	47·22	8·54	0·67
Closes	"	50·37	9·09	0·69
Drumloskie	"	54·15	9·77	0·74
Loch Dornal	"	59·01	10·62	0·78
Wood Park	"	62·48	11·26	0·85
Barmalloch	"	66·95	12·01	0·85

Shot (M 12) Grid Reference:- 240·859/518·156

Station	Grid Reference	Distance (km)	Time (sec)	T-X/6 (sec)
Low Glasnick	As Above	43·25	7·77	0·56
Eldrig	"	48·13	8·64	0·62

Station	Grid Reference	Distance (km)	Time (sec)	T-X/6 (sec)
Closes	As Before	51·15	9·14	0·61
Drumloskie	"	54·81	9·82	0·70
Loch Dornal	"	59·65	10·67	0·73
Wood Park	"	63·08	11·25	0·74
Barmalloch	"	67·58	12·01	0·75

APPENDIX 1. TABLE 5.

HILLHOUSE QUARRY - BALLANTRAE

Hillhouse Quarry Grid Reference:- 235·175/634·010

	Station	Grid Reference		Distance (km)	Time (sec)	T-X/6 (sec)
1	Perryston Farm	229·800	617·780	17·097	3·620	0·771
2	Sportfield	230·100	615·965	18·745	3·990	0·866
3	Glenbay	228·140	613·680	21·513	4·430	0·845
4	Howmoor Cottage	227·940	611·897	23·266	4·730	0·852
5	Mochrum Wood	227·150	610·125	25·197	5·040	0·840
6	Knox Hill	223·715	606·308	29·979	5·770	0·774
7	Chapelton	223·500	604·300	31·922	6·030	0·710
8	Craighead Quarry	223·270	601·375	34·739	6·490	0·700
9	Brae	220·770	598·350	38·460	7·220	0·810
10	Fauldribon	220·150	597·100	39·851	7·540	0·898
11	Byne Hill	218·200	594·780	42·745	8·020	0·896
12	Balkeachy	218·258	593·385	44·007	8·200	0·866
13	Knocklaugh	216·700	591·800	46·076	8·490	0·811
14	Moak Hill	214·200	587·950	50·611	9·170	0·735
15	Knockdhu Bridge	213·365	584·585	54·023	9·710	0·706

	Station	Grid Reference		Distance (km)	Time (sec)	T-X/6 (sec)
16	High Kilphin	211·540	580·200	58·772	10·440	0·645
17	Shallochwreck	207·270	577·120	63·365	11·150	0·589

APPENDIX 1. TABLE 6.

HILLHOUSE QUARRY - LOCH DEE

Hillhouse Quarry Grid Reference:- 235·175/634·010

	Station	Grid Reference		Distance (km)	Time (sec)	T-X/6 (sec)
1	Hotel Backyard	234·940	632·110	1·194	0·540	0·221
2	Hobsland Farm	235·790	629·600	4·453	1·230	0·488
3	St. Quivox	237·480	624·175	10·102	2·450	0·766
4	Roodland Farm	239·360	619·345	15·223	3·390	0·853
5	S. Craig Quarry	243·260	615·090	20·575	4·330	0·901
6	Patna Forest	240·870	609·570	25·095	5·020	0·838
7	Red Burn Bridge	243·130	606·235	28·892	5·620	0·805
8	Knockdon Farm	243·550	600·710	34·337	6·480	0·757
9	Loch Braden	243·770	597·640	37·372	7·080	0·851
10	Craigfionn	245·662	593·580	41·768	7·740	0·779
11	Wee Craigfionn	245·625	592·100	43·193	7·950	0·751
12	Riders Rig	248·145	588·428	47·391	8·610	0·711
13	L. Craigtarson	247·608	585·960	49·632	9·000	0·728
14	Backhill Bush	247·985	584·355	51·281	9·260	0·713
15	McWhan Stone	249·155	580·310	55·490	9·930	0·682

APPENDIX 1. TABLE 7.

NCB OPEN SITE (BENBAIN) - BALLANTRAE

Benbain Shot Grid Reference:- 250·760/609·820

	Station	Grid Reference		Distance (km)	Time (sec)	T-X/6 (sec)
3	Dalcairnie Brdg	246·530	604·240	7·002	1·660	0·493
8	Newt. Stewart Rd	240·340	600·080	14·263	2·920	0·543
10	Garleffin	239·135	598·250	16·401	3·310	0·576
12	River Sticher	237·140	596·450	19·086	3·770	0·589
14	Aldinna	234·290	595·360	21·917	4·170	0·517

Benbain Shot Grid Reference:- 250·860/609·840

	Station	Grid Reference		Distance (km)	Time (sec)	T-X/6 (sec)
1	Pennyvenie	249·200	606·920	3·359	0·860	0·300
4	Auldcraighoch	245·305	604·175	7·934	1·790	0·468
6	Glenauchie	242·060	601·520	12·110	2·660	0·642

Benbain Shot Grid Reference:- 250·710/609·830

	Station	Grid Reference		Distance (km)	Time (sec)	T-X/6 (sec)
7	Loch Braden Rd	241·280	601·000	12·919	2·750	0·597
9	Tallaminnock	239·930	598·420	15·697	3·200	0·584

	Station	Grid Reference		Distance (km)	Time (sec)	T-X/6 (sec)
11	Forest Waterfall	238·480	597·000	17·725	3·520	0·566
13	Black Row	236·050	595·565	20·455	3·980	0·571
15	Knockeen	231·810	595·610	23·652	4·600	0·658
17	Barr	226·825	595·075	28·075	5·450	0·771

Benbain Shot Grid Reference:- 251.065/609.882

	Station	Grid Reference		Distance (km)	Time (sec)	T-X/6 (sec)
1	Pennyvenie	249·200	606·920	3·500	0·870	0·287
2	Craigengillan	247·460	605·953	5·332	1·320	0·431
14	Aldinna	234·290	595·360	22·188	4·220	0·522
16	Daljedburgh	230·810	596·470	24·293	4·730	0·681
18	Kirkland	224·570	592·520	31·677	6·020	0·741
19	Minuntion	222·285	591·270	34·274	6·360	0·648
20	Asselfoot	220·610	590·515	36·091	6·660	0·645
21	Aldons	219·670	589·530	37·415	6·800	0·564
22	Breaker Hill	217·750	589·050	39·292	6·990	0·441
23	Balhamie	213·500	586·000	44·514	7·820	0·401

Benbain Shot Grid Reference:- 250·720/609·790

Station	Grid Reference		Distance (km)	Time (sec)	T-X/6 (sec)
Forest Foot Path	244·225	603·600	8·972	2·060	0·565

APPENDIX 1. TABLE 8.

ROYAL NAVY SHOT (PORTOBELLO) - TROON

Marine Shot Grid Reference:- 194·725/564·030

Station	Grid Reference		Distance (km)	Time (sec)	T-X/6 (sec)
Perryston Farm	229·800	617·780	64·182	11·170	0·473
Sportfield	230·100	615·965	62·838	10·980	0·507
Glenbay	228·242	613·718	59·936	10·510	0·521
Howmoor Cottage	227·940	611·897	58·262	10·250	0·540
Mochrum Wood	227·150	610·125	56·357	10·010	0·617
Kirkoswald	224·432	607·280	52·470	9·370	0·625
Knox Hill	223·715	606·308	51·263	9·160	0·616
Chapelton	223·500	604·300	49·494	8·870	0·621
Drummuck	223·470	603·300	48·666	8·730	0·619
Cr'head Quarry	223·270	601·375	47·005	8·360	0·526
Brae	220·770	598·350	43·084	7·810	0·629
Fauldribon	220·150	597·100	41·714	7·650	0·698
Byne Hill	218·200	594·780	38·686	6·990	0·542
Balkeachy	217·870	593·090	37·151	6·770	0·578
Knocklaugh	216·700	591·800	35·413	6·410	0·508

Station	Grid Reference		Distance (km)	Time (sec)	T-X/6 (sec)
Currarie	215·807	590·530	33·863	6·250	0·606
Moak Hill	214·200	587·950	30·845	5·640	0·499
Balhamie	213·363	586·000	28·811	5·370	0·568
Knockdhu Bridge	213·365	584·585	27·748	5·130	0·505
North Garphar	211·280	582·902	25·104	4·670	0·486
Big Park	208·221	580·938	21·634	4·110	0·504
Shallochwreck	207·270	577·120	18·131	3·440	0·418
Portnauchtry	202·250	573·360	11·986	2·440	0·442
East Kirkbryde	200·410	570·760	8·810	1·860	0·392
Valleyfield	197·960	568·375	5·417	1·210	0·307
Portobello	196.100	566·380	2·723	0·700	0·246

APPENDIX 1. TABLE 9.

NCB OPEN CAST (DALLEAGLES) - WEST AYRSHIRE

Rough Hill Shot Grid Reference:- 259·500/611·300

Station	Grid Reference		Distance (km)	Time (sec)	T-X/6 (sec)
Perryston Farm	229·800	617·780	30·399	5·860	0·794
Sportfield	230·100	615·965	29·768	5·760	0·799
Glenbay	228·242	613·718	31·351	6·000	0·775
Howmoor Cottage	227·940	611·897	31·566	6·050	0·789
Mochrum Wood	227·150	610·125	32·371	6·130	0·735
Kirkoswald	224·432	607·280	35·298	6·490	0·607
Knox Hill	223·715	606·308	36·132	6·760	0·738
Chapelton	223·500	604·300	36·674	6·780	0·668
Drummuck	223·470	603·300	36·907	6·700	0·549
Craighead Quarry	223·270	601·375	37·565	6·780	0·519
Brae	220·770	598·350	40·838	7·250	0·444
Fauldribon	220·150	597·100	41·834	7·850	0·878
Byne Hill	218·200	594·780	44·481	7·840	0·426
Balkeachy	217·870	593·090	45·439	8·100	0·527
Knocklaugh	216·700	591·800	47·033	8·180	0·341

Station	Grid Reference		Distance (km)	Time (sec)	T-X/6 (sec)
Currarie	215·807	590·530	48·378	8·390	0·327
Moak Hill	214·200	587·950	50·964	8·720	0·226
Balhamie	213·363	586·000	52·619	8·960	0·190
Knockdhu Bridge	213·365	584·585	53·312	9·090	0·205

APPENDIX 1. TABLE 10.

CALEDONIAN SUTURE SEISMIC PROJECT 1982

Recorded across the Southern Uplands (Galloway)

Airgun Shot (14·56 0·58) Grid Reference:- 247·706/531·433

Station	Grid Reference		Distance (km)	Time (sec)	T-X/6 (sec)
Eldrig	565·850	234·430	36·89	6·62	0·47
Black Park	557·975	237·800	28·33	5·17	0·45
High Barness	554·000	238·790	24·26	4·44	0·40
Whauphill	549·940	240·120	20·00	3·69	0·36
Doon Hill	547·200	241·640	16·89	3·18	0·37
Moss Park	543·780	241·725	13·72	2·61	0·32

APPENDIX 2

Reduced time-distance graphs and record sections.

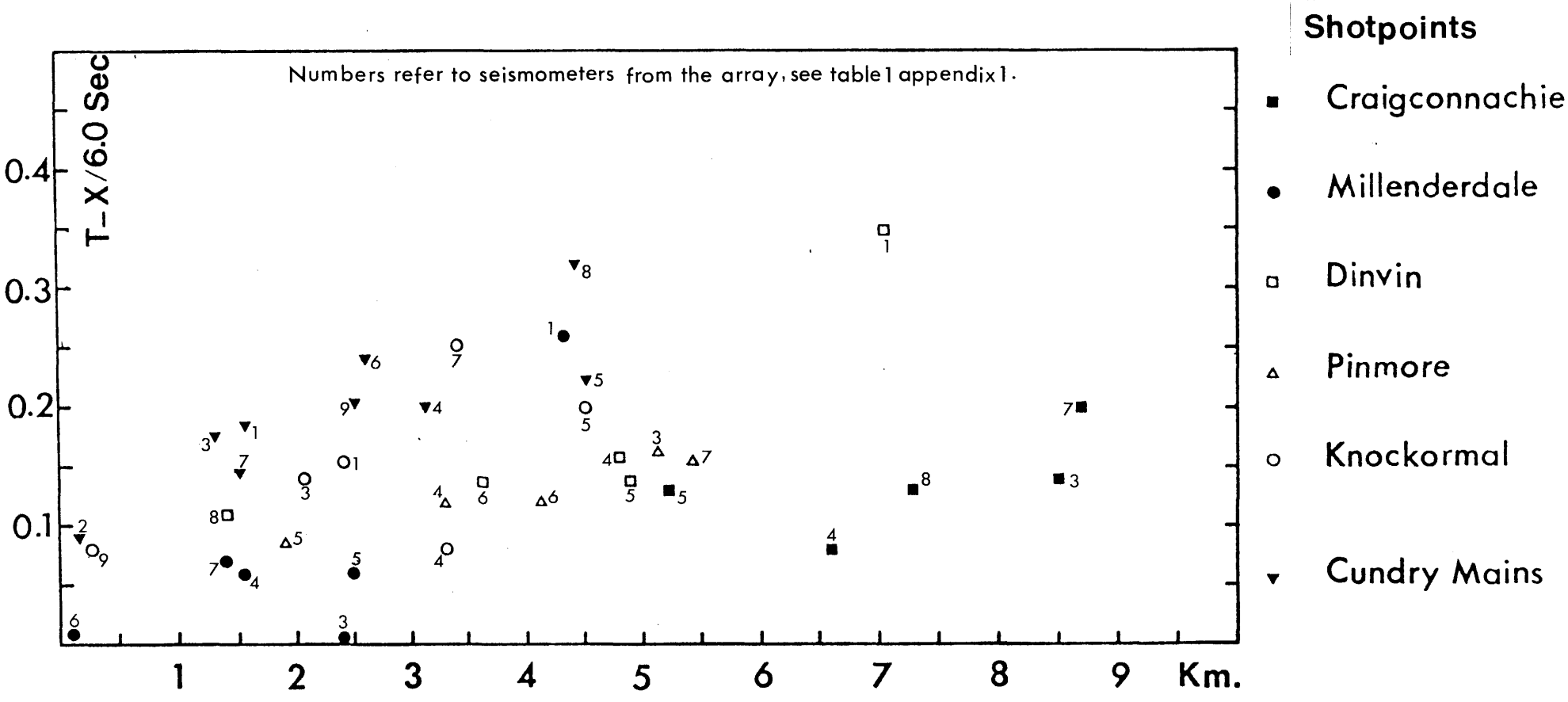

Fig 1. Reduced time-distance plot of first arrivals of land-shots recorded on the Lendalfoot Array.

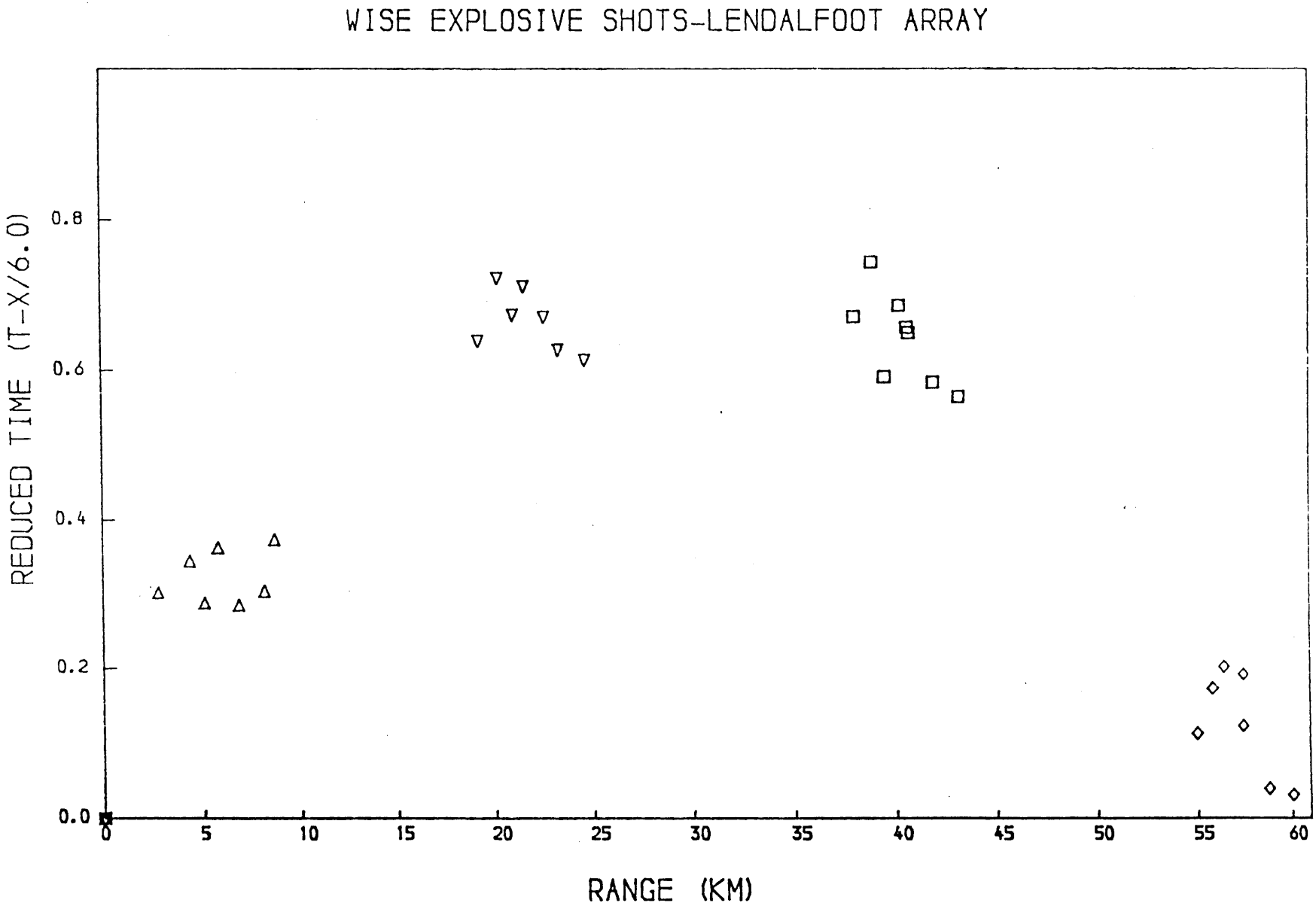

Fig 2. Reduced time-distance plot of first arrivals of WISE marine shots (1-4) recorded on the Lendalfoot Array.

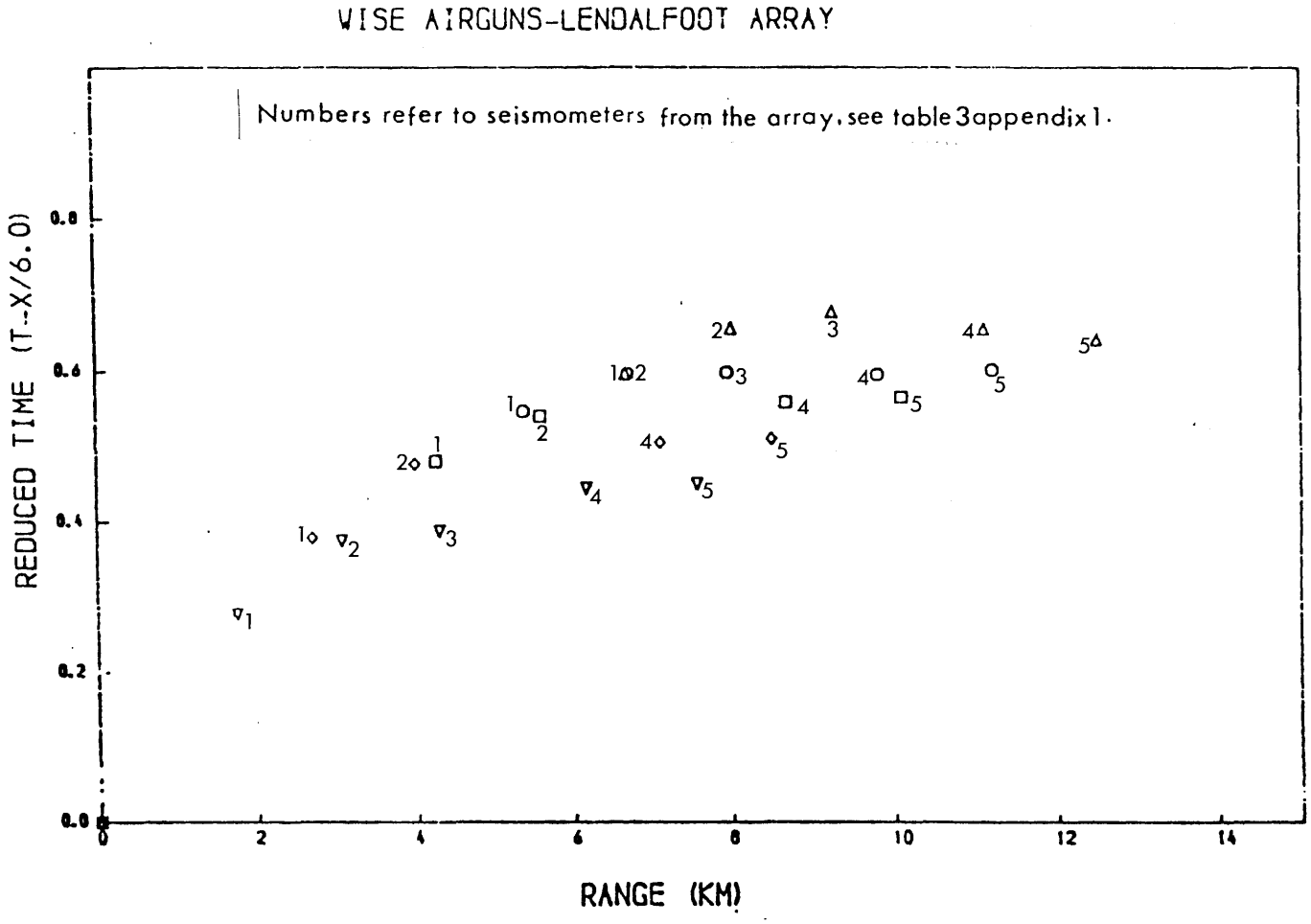

Fig 3. Reduced time-distance plot of first arrivals of five airgun shots recorded on the Lendalfoot Array.

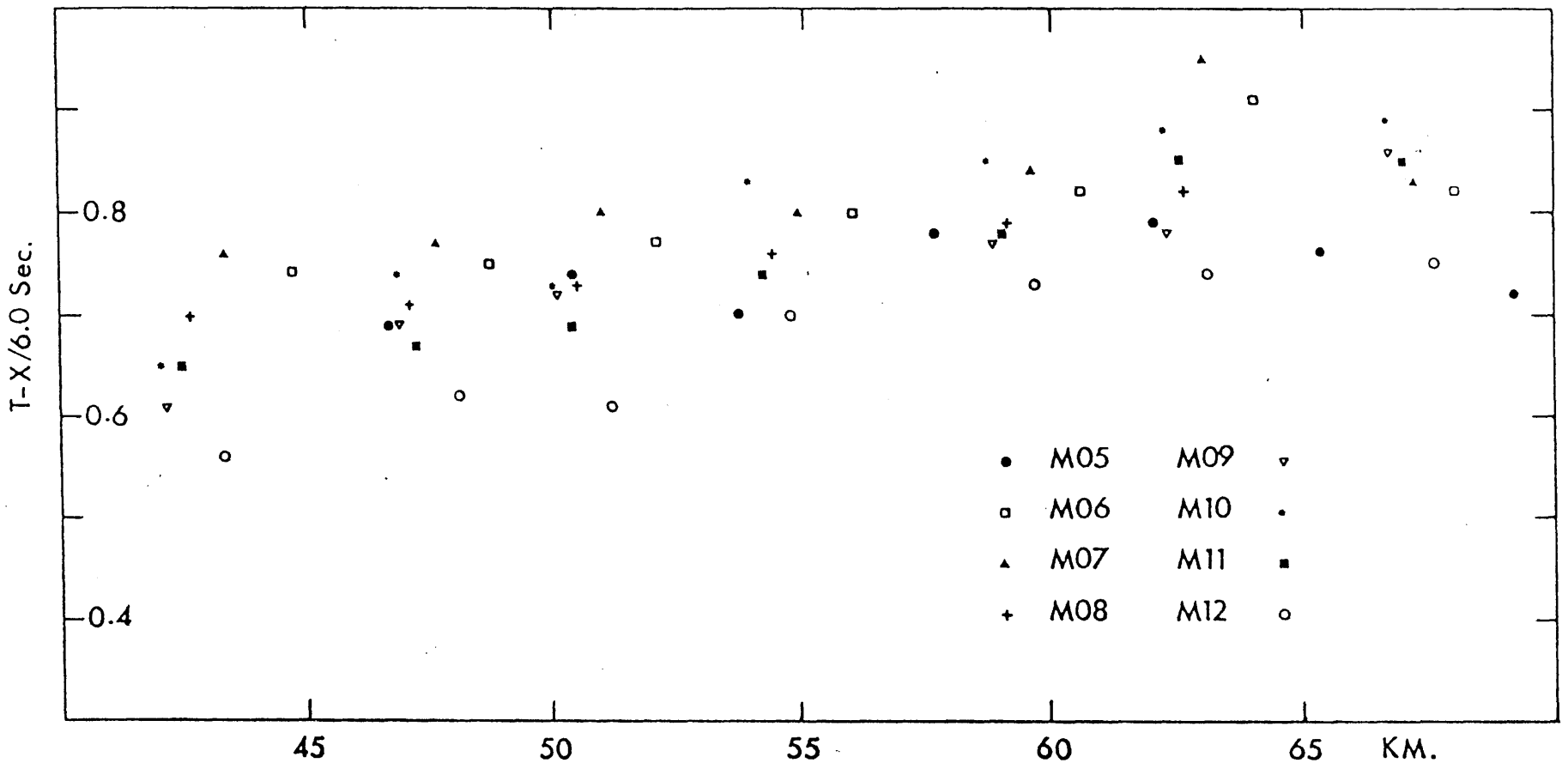

Fig 4. Reduced time-distance plot of first arrivals of marine explosive shots of the Caledonian Suture Seismic Project, recorded across the Galloway area.

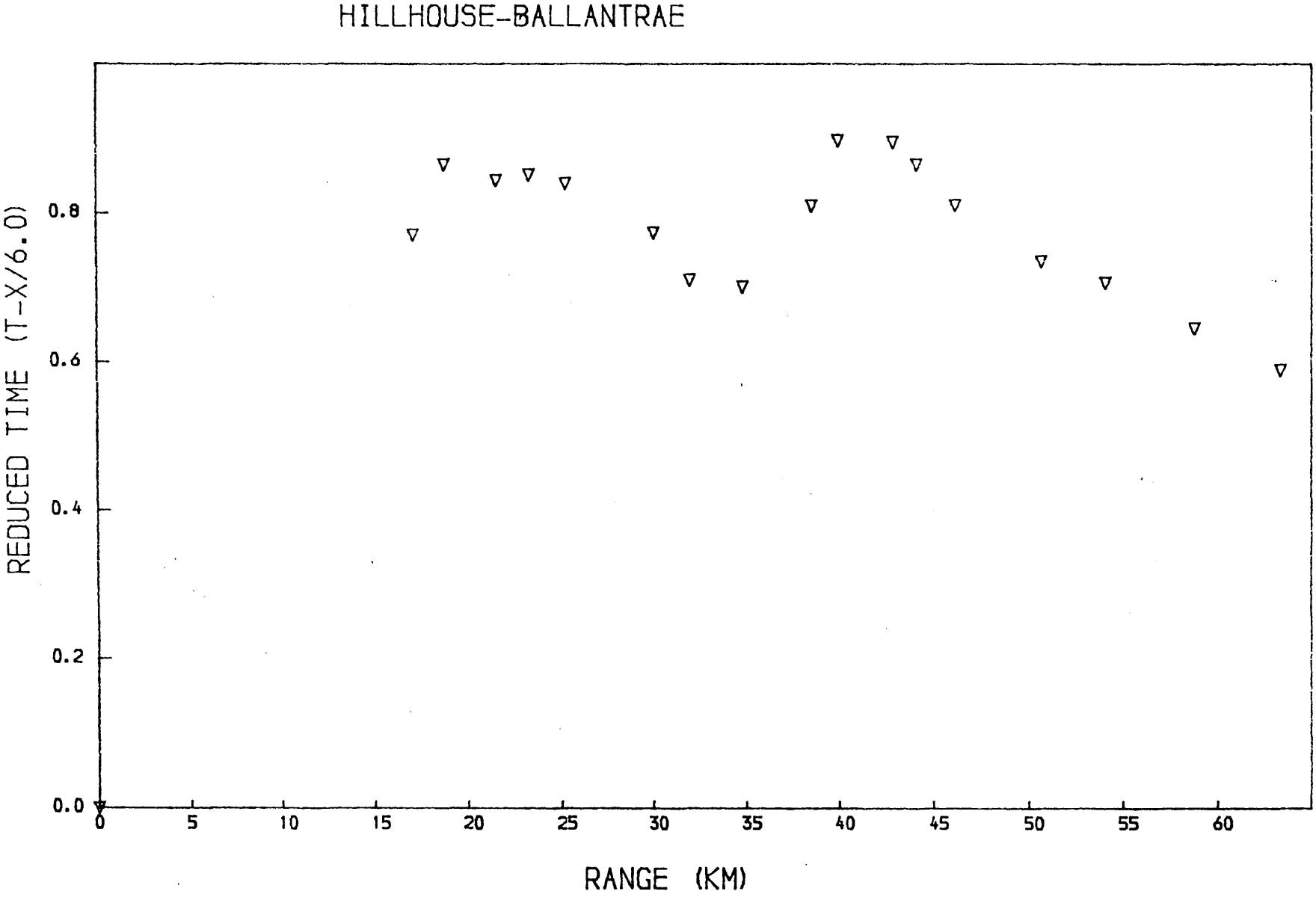

Fig 5. Reduced time-distance plot of first arrivals along the Girvan line, recording from Hillhouse Quarry.

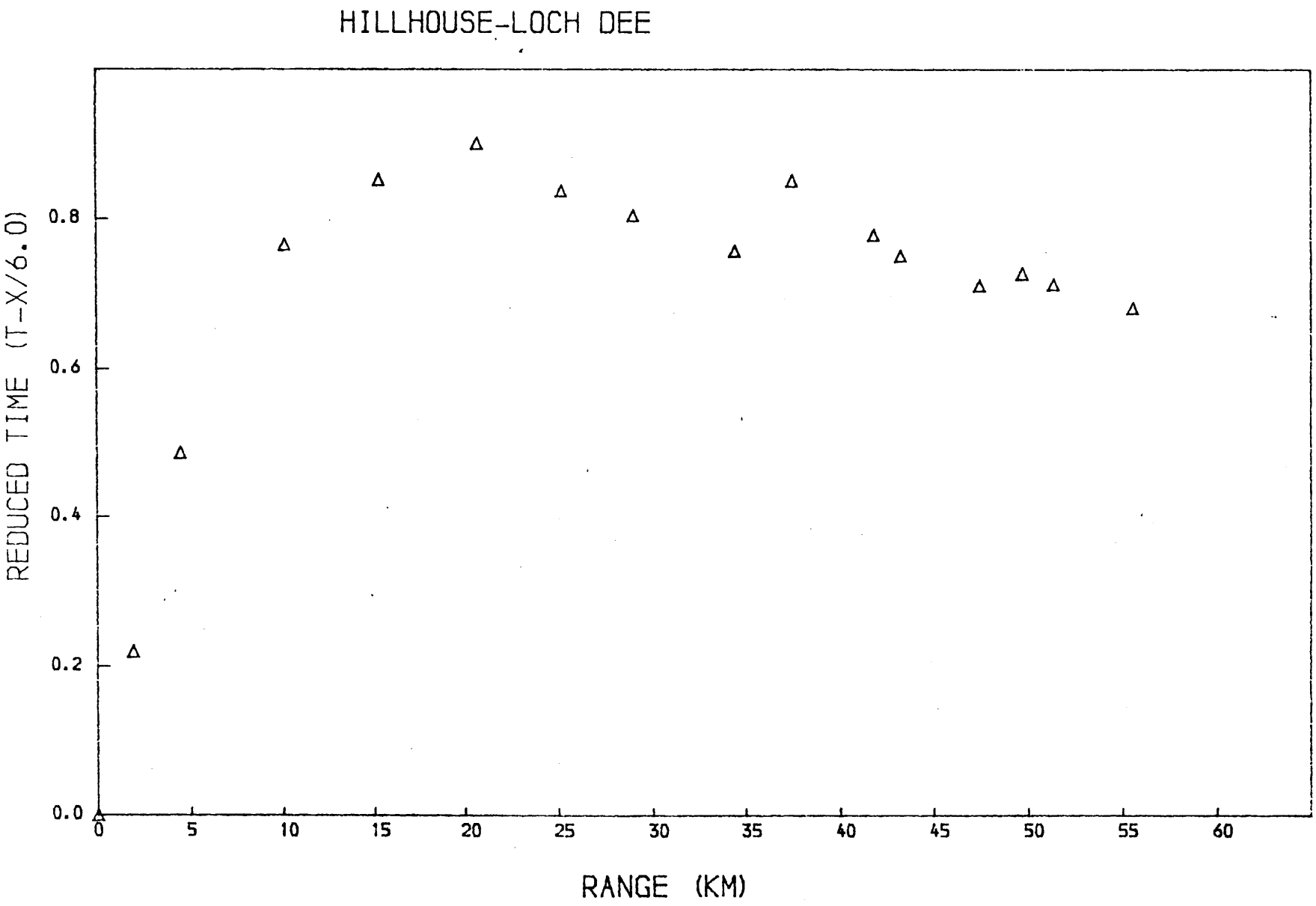

Fig 6. Reduced time-distance plot of first arrivals along the Loch Doon line, recording from Hillhouse Quarry.

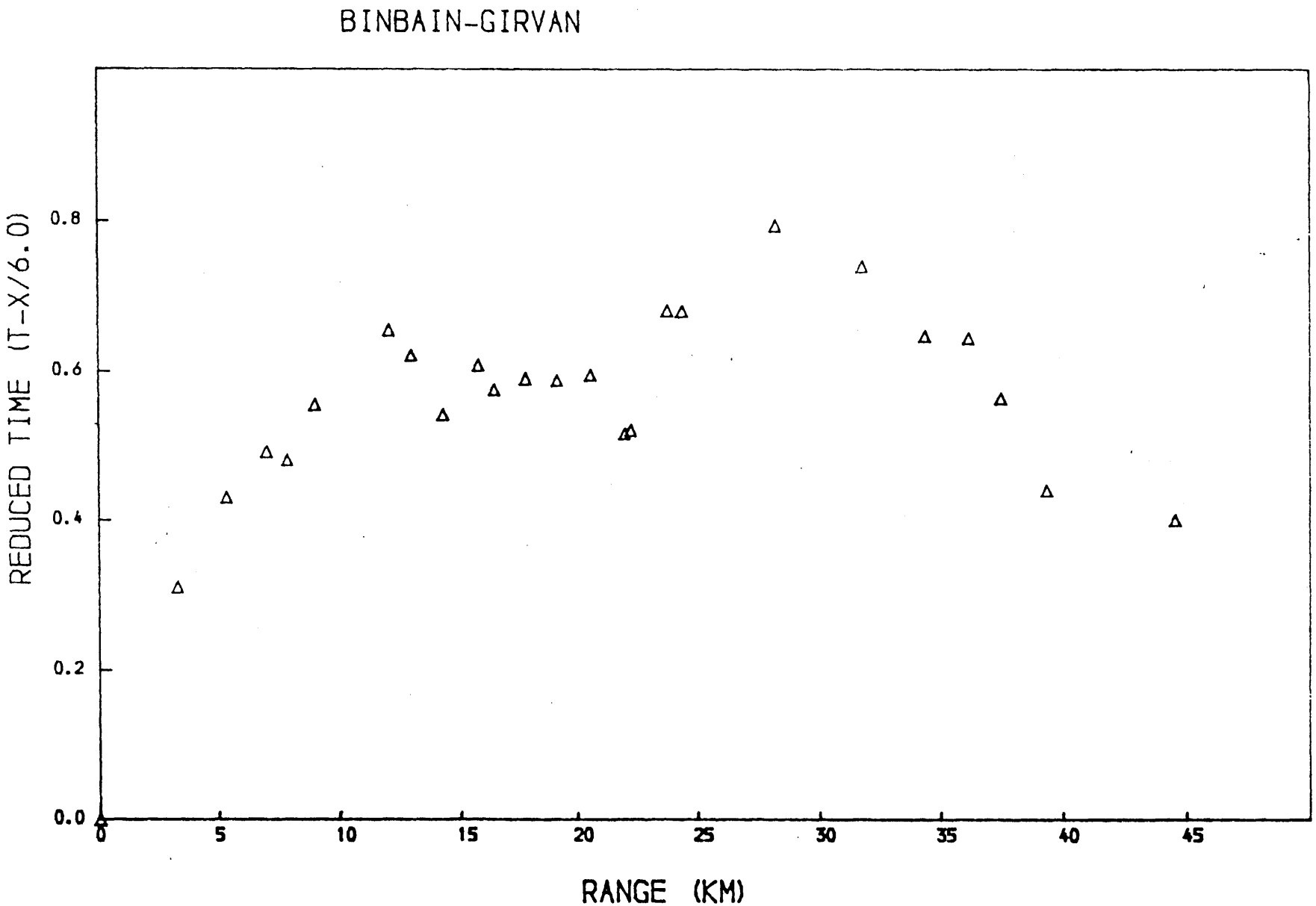

Fig 7. Reduced time-distance plot of first arrivals along the Colmonell line, recording from Benbain NCB open-cast.

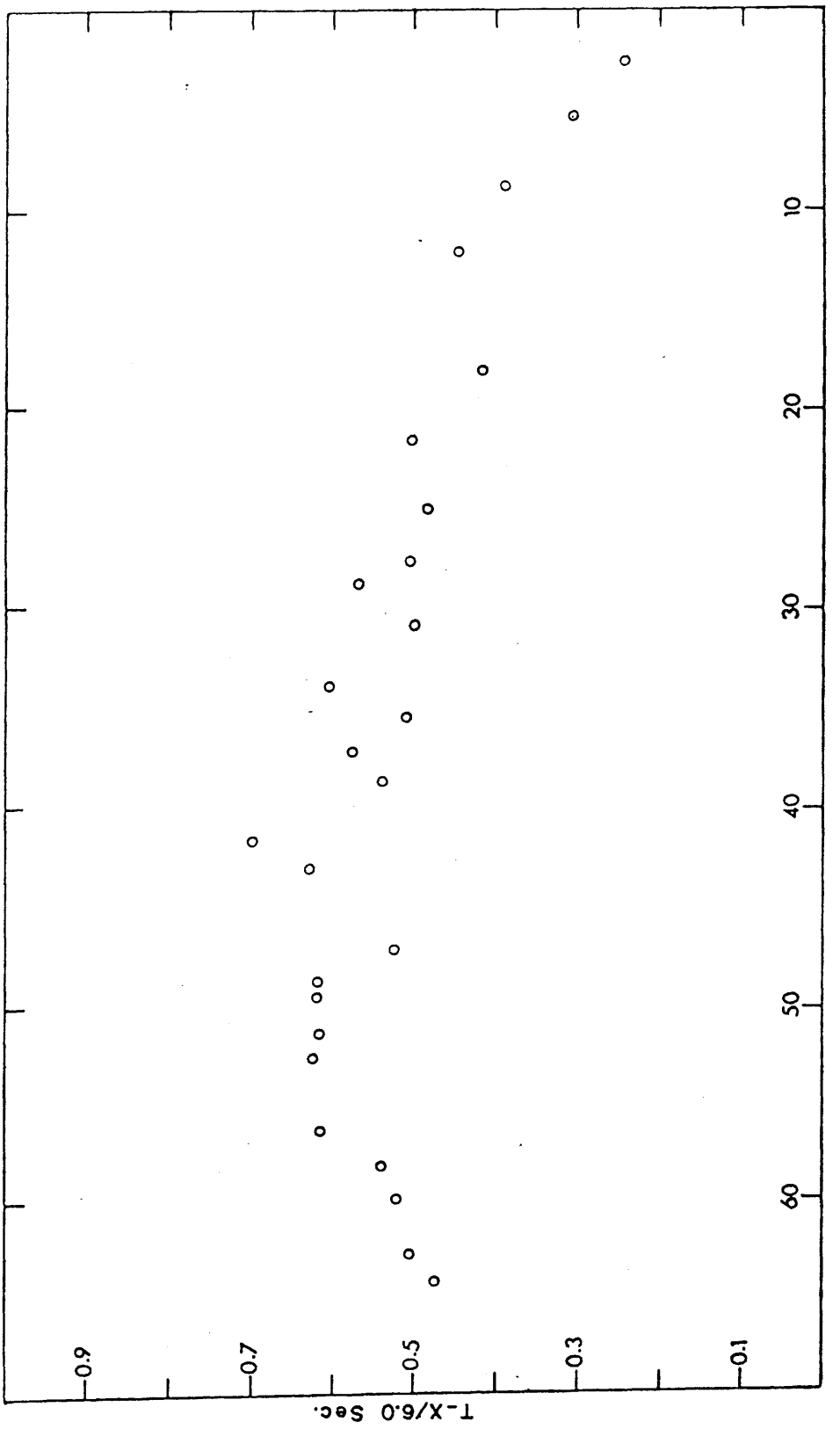

Fig 8. Reduced time-distance plot of first arrivals along the Girvan line, recording the Portobello Royal Navy shot.

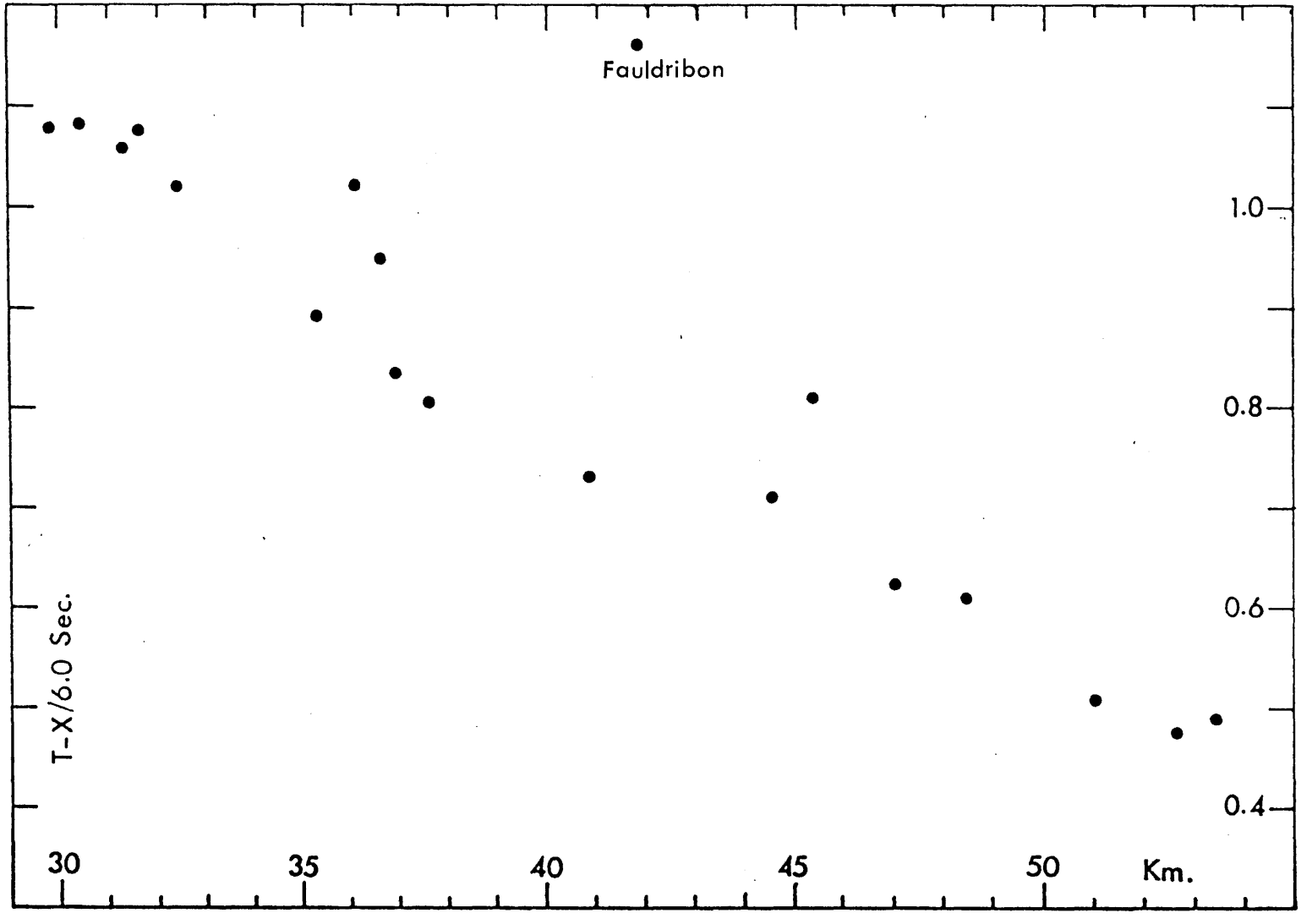

Fig 9. Reduced time-distance plot of first arrivals of Rough Hill NCB open-cast shot, recorded in fan-pattern on the Girvan line seismometers.

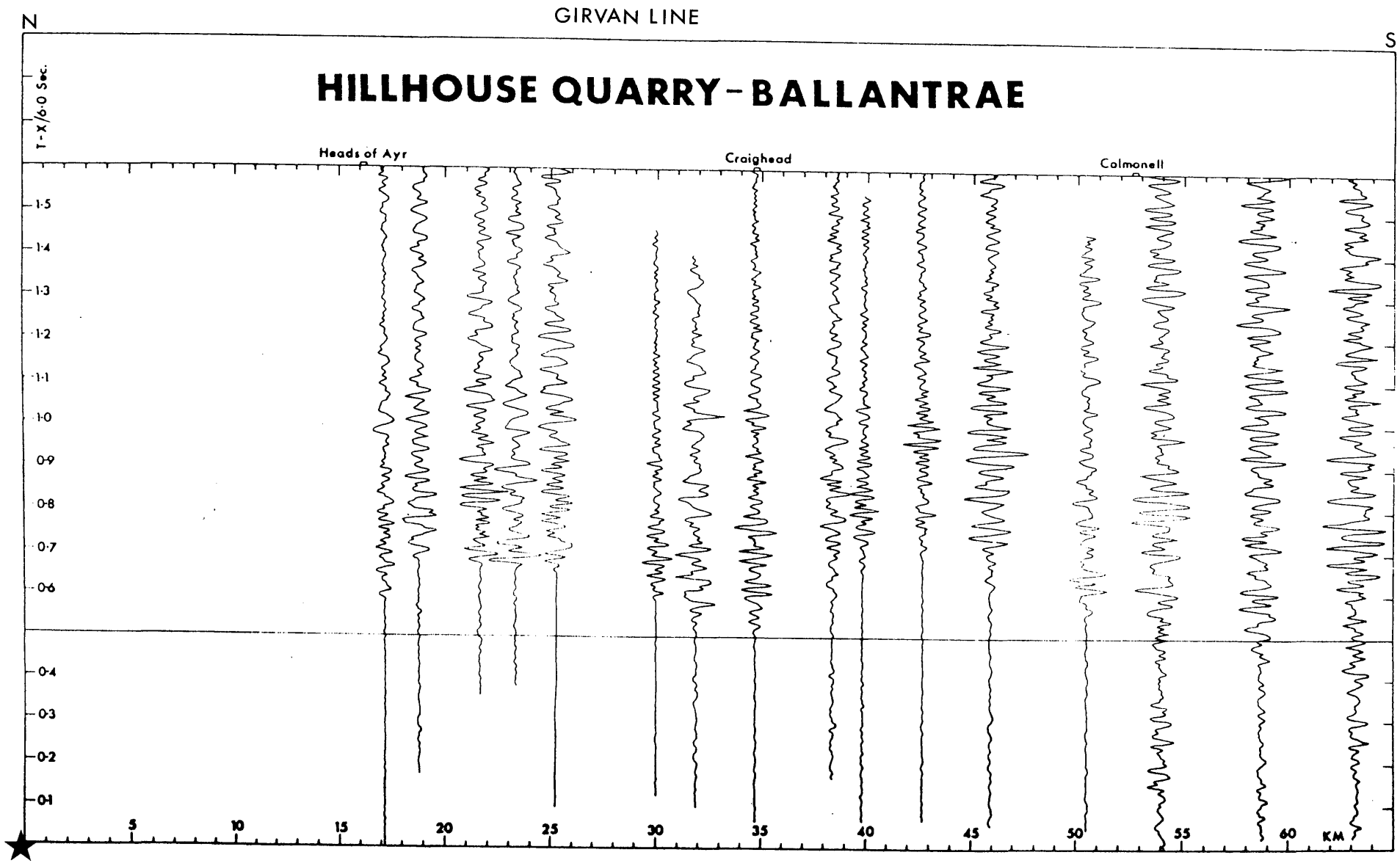

Fig 10. Reduced record section from Hillhouse Quarry, southwards to Ballantrae.

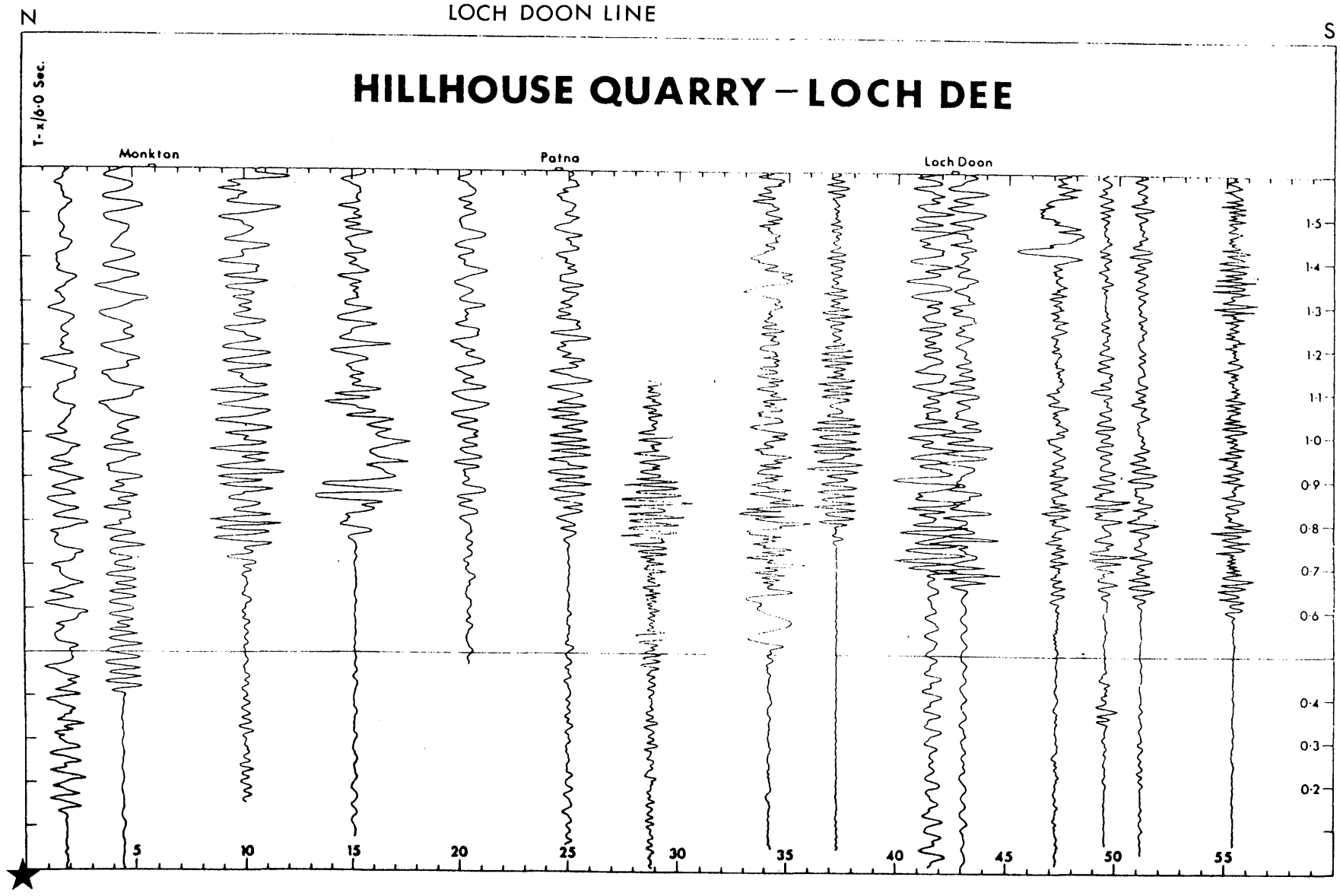

Fig 11. Reduced record section from Hillhouse Quarry, south-eastwards to Loch Dee.

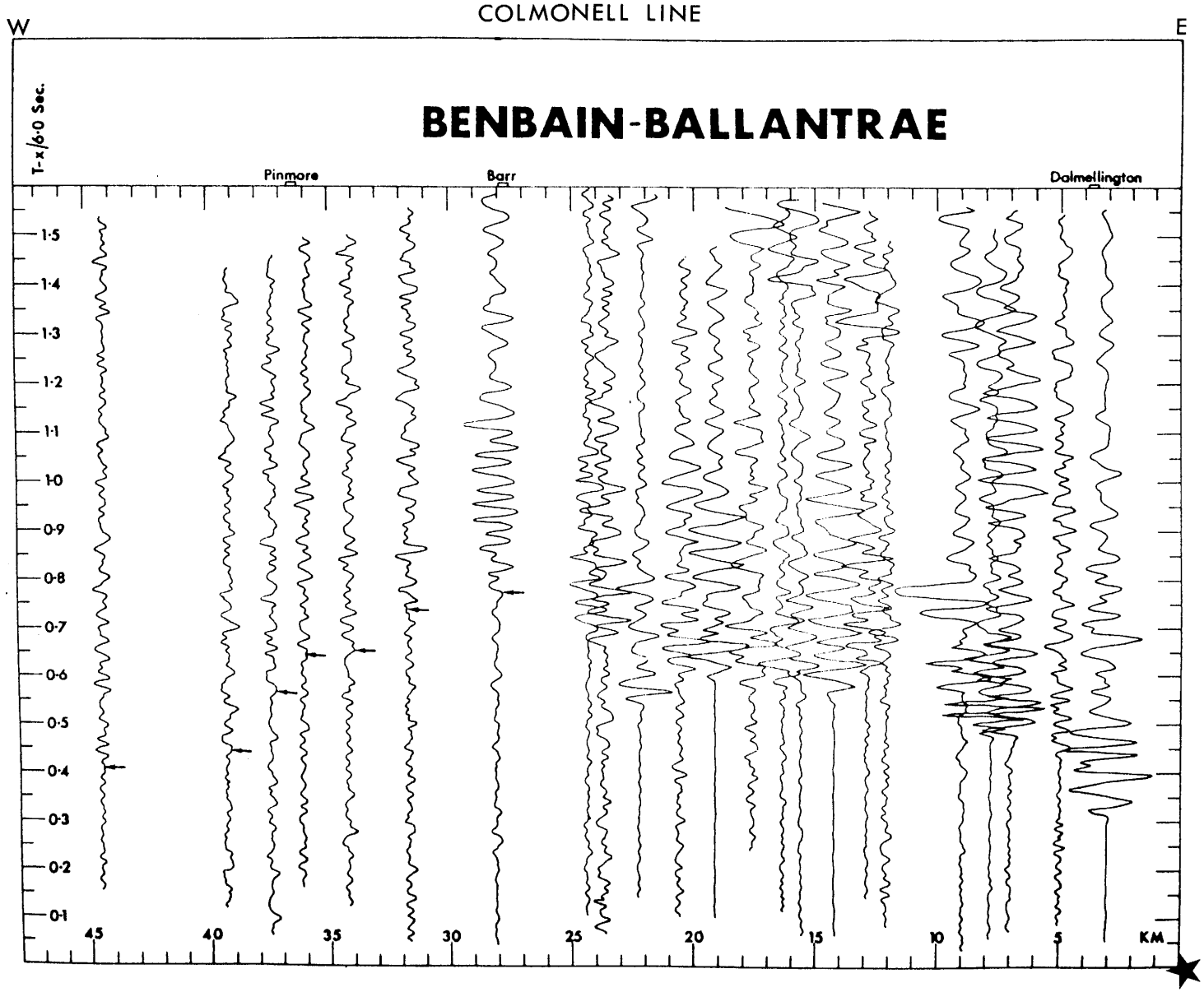

Fig 12. Reduced record section from Benbain NCB open-cast, westwards to Ballantrae.

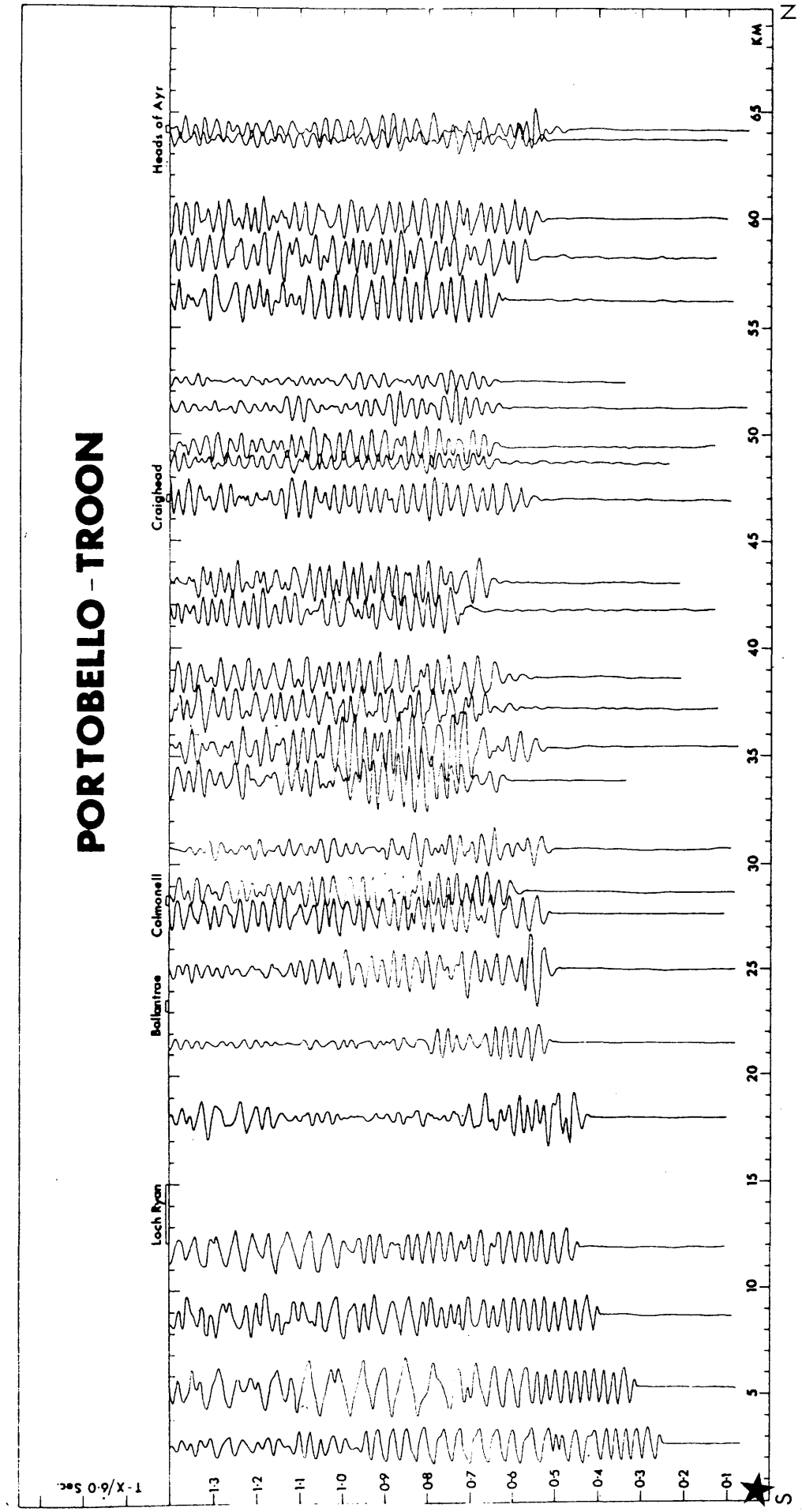

Fig 13. Reduced record section from Royal Navy shot at Portobello, northwards to the Heads of Ayr.

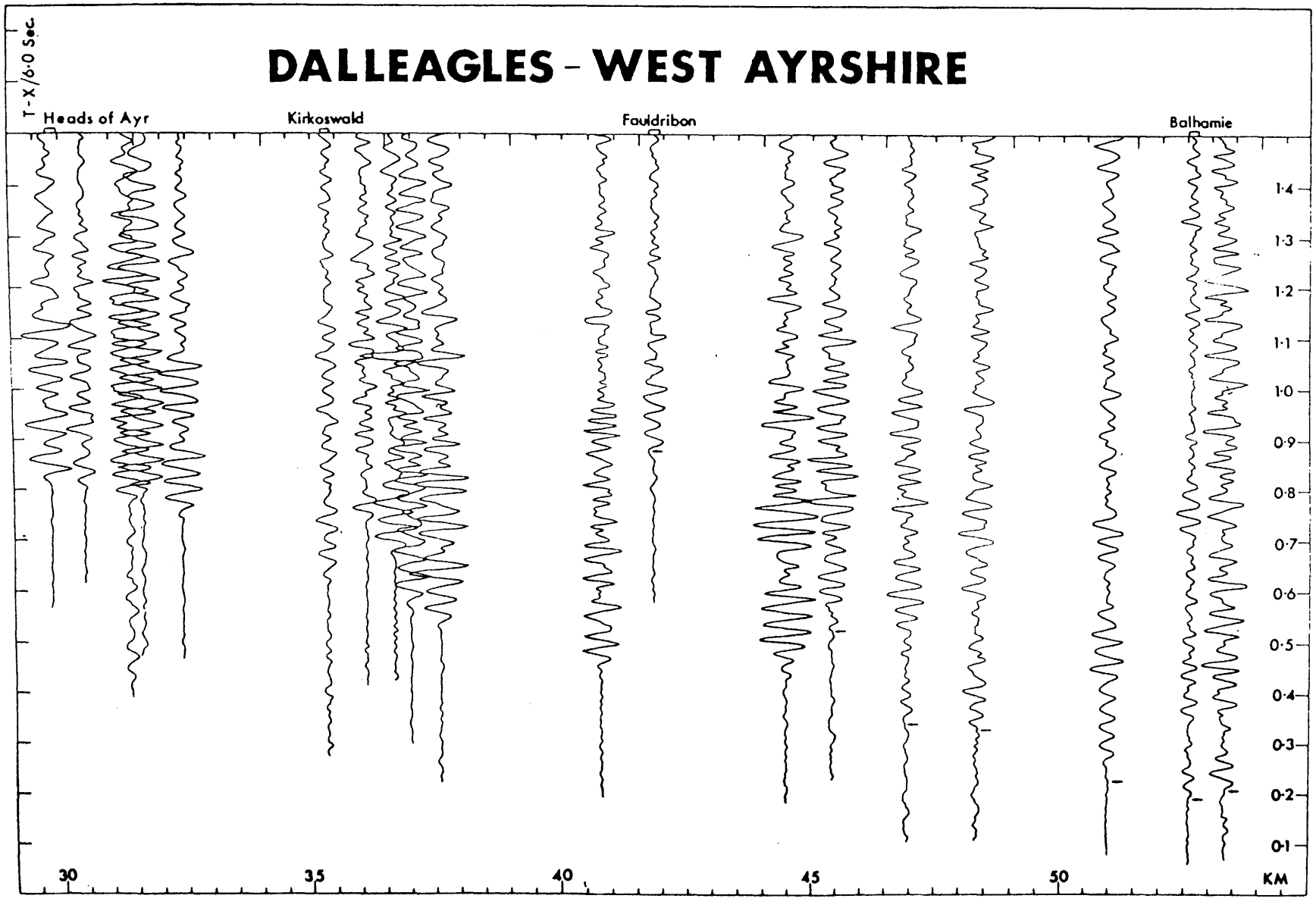

Fig 14. Reduced record section of fan-shooting from Rough Hill NCB open-cast, westwards to the coastline between the Heads of Ayr and Ballantrae.

APPENDIX 3A

P-wave velocities in the main rock components of the Ballantrae ophiolite, in relation to increasing confining pressure.

CH: Chert, D: Dolerite, FG: Foliated Gabbro, G: Gabbro, Gr: Granite, S: Serpentinite, SP.LV: Spilitic Lava.

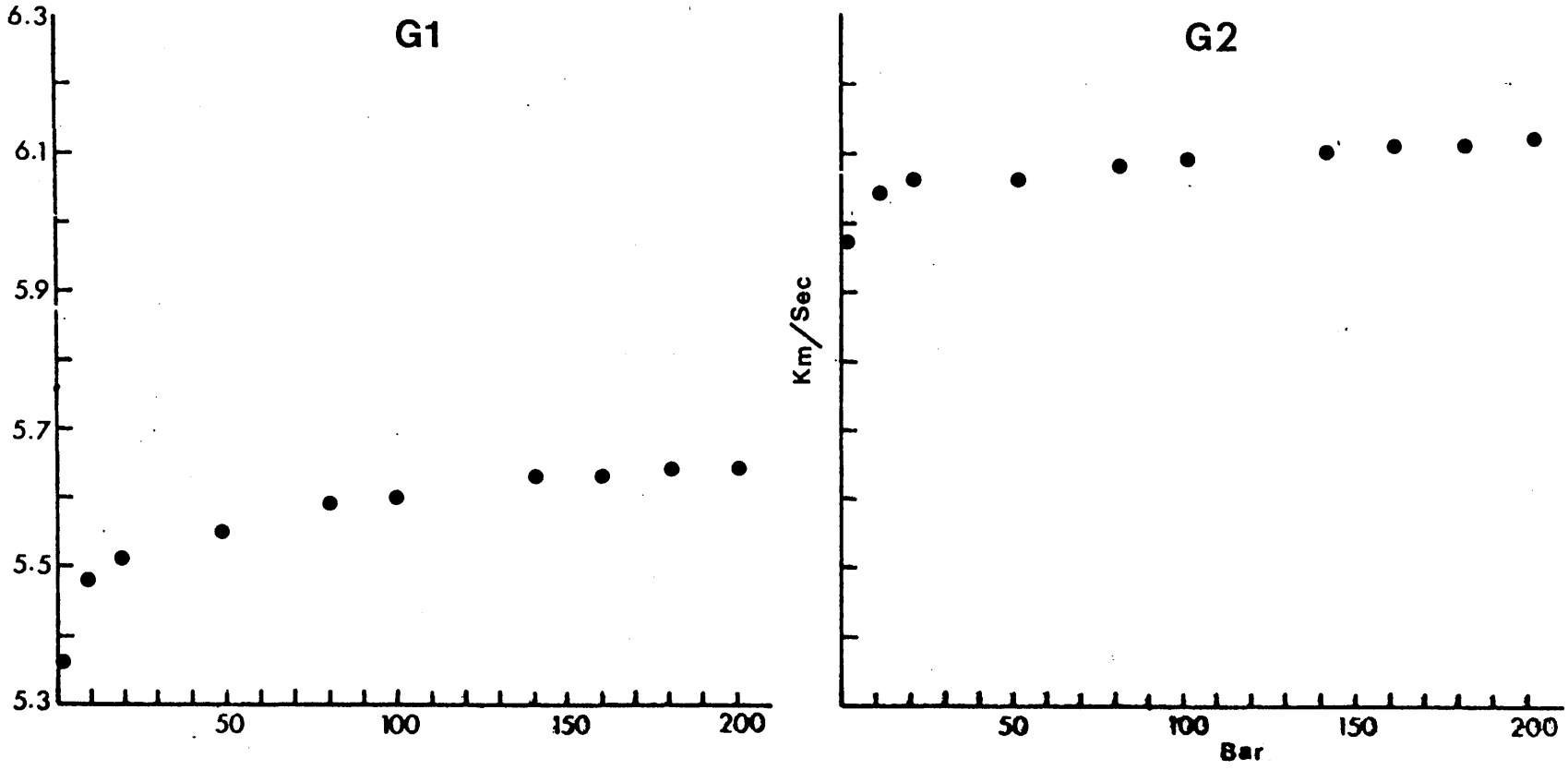
G1
G2
6.3
6.1
5.9
5.7
5.5
5.3
Km/Sec
50
100
150
200
Bar

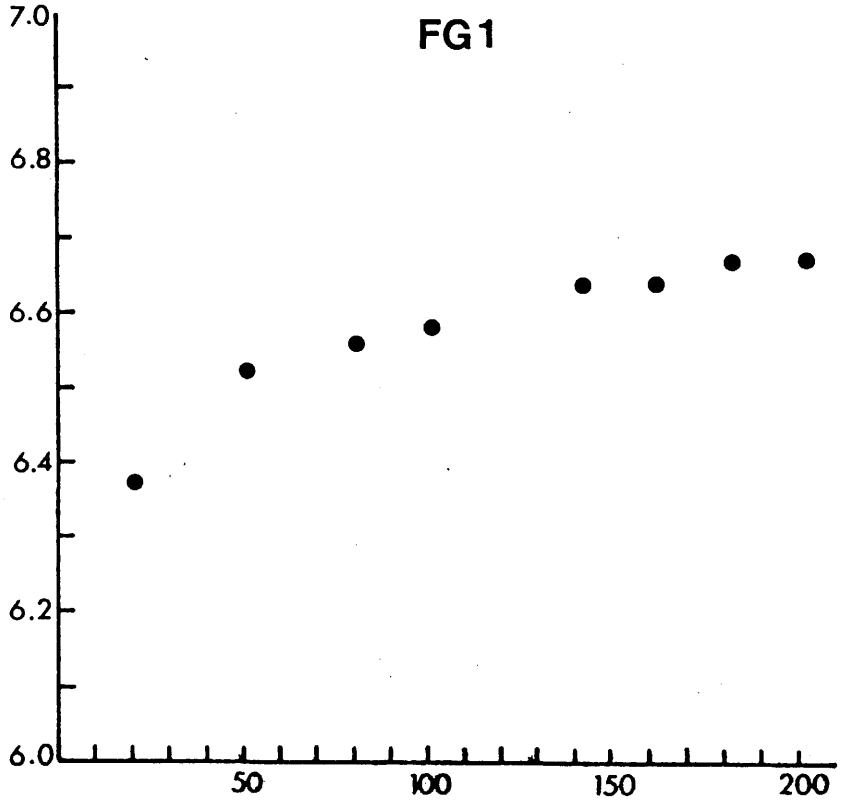
FG1
7.0
6.8
6.6
6.4
6.2
6.0
50
100
150
200

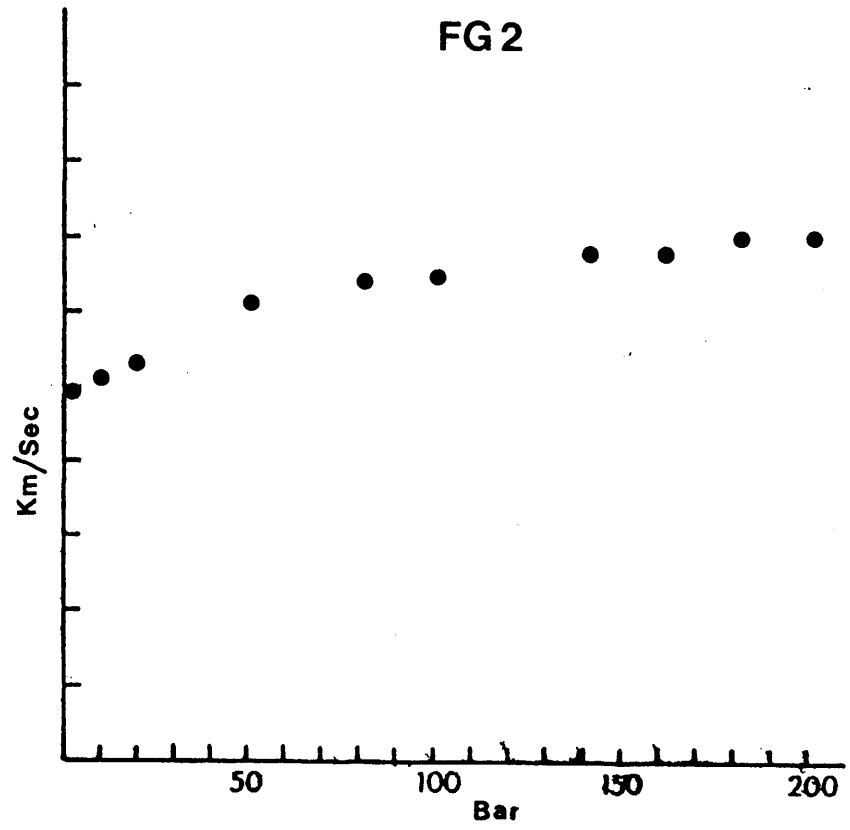
FG2
Km/Sec
50
100
150
200
Bar

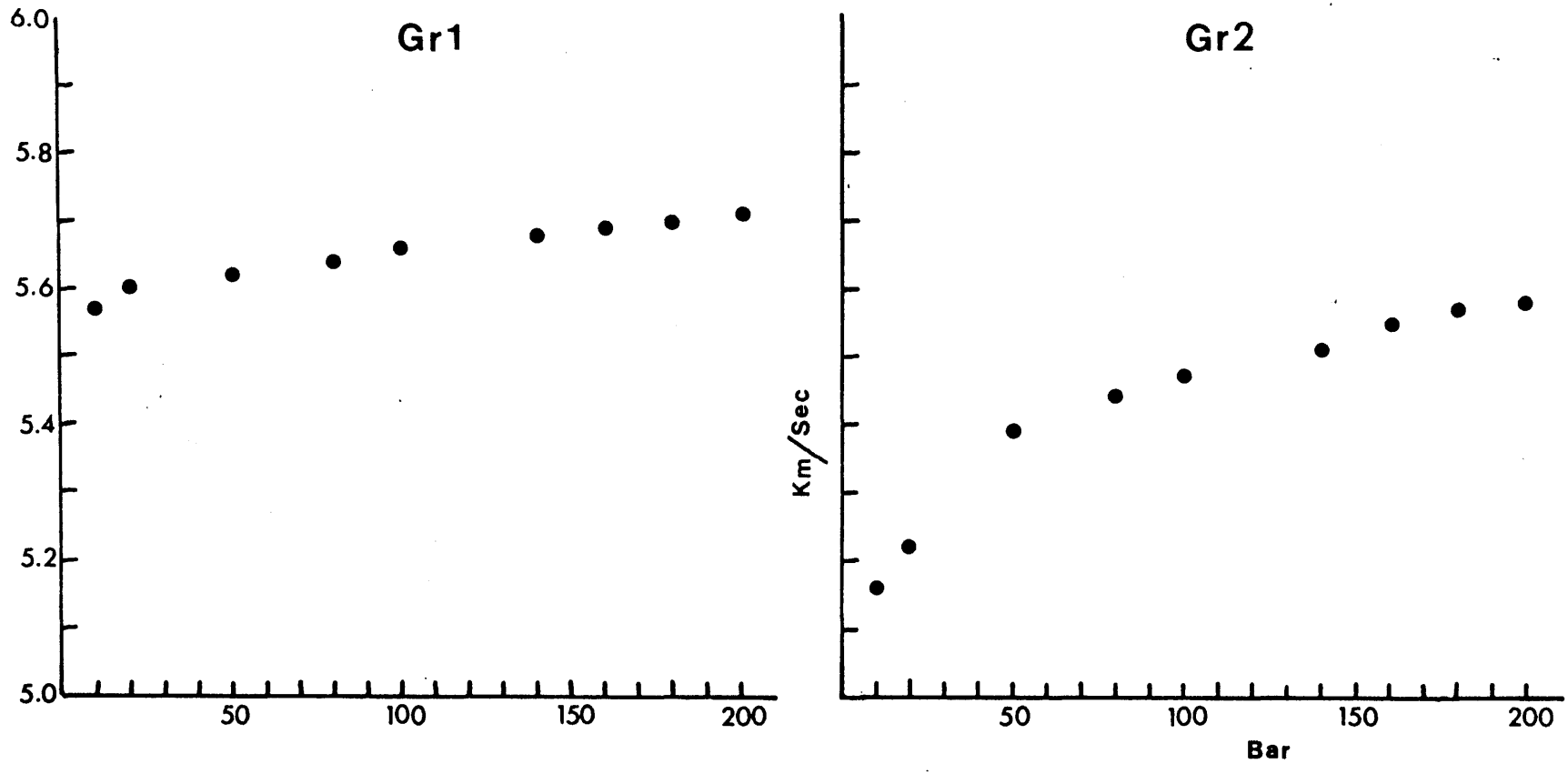
Gr1
Gr2
6.0
5.8
5.6
5.4
5.2
5.0
Km/Sec
50
100
150
200
Bar

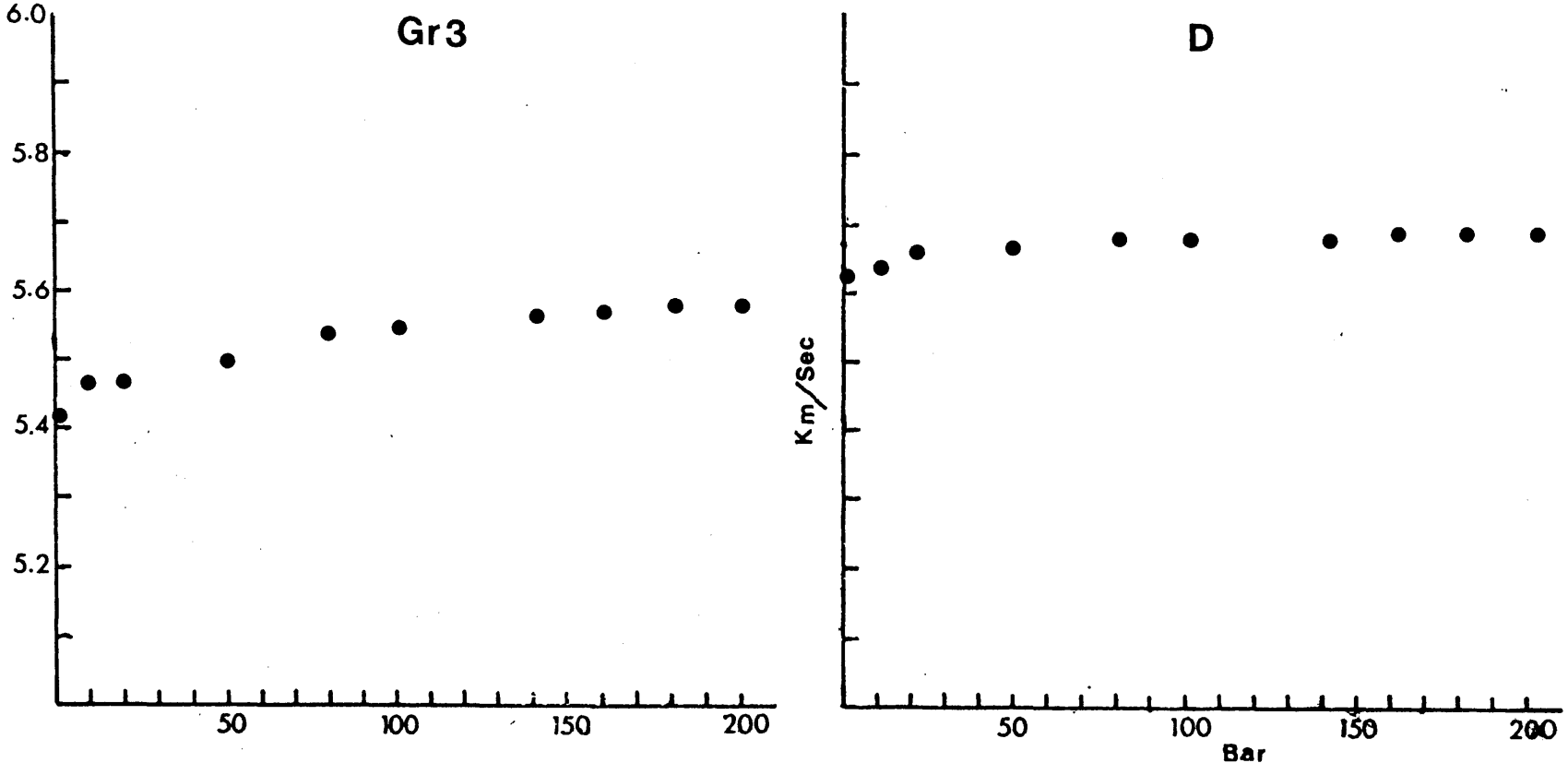
Gr3
D
6.0
5.8
5.6
5.4
5.2
Km/Sec
50
100
150
200
Bar

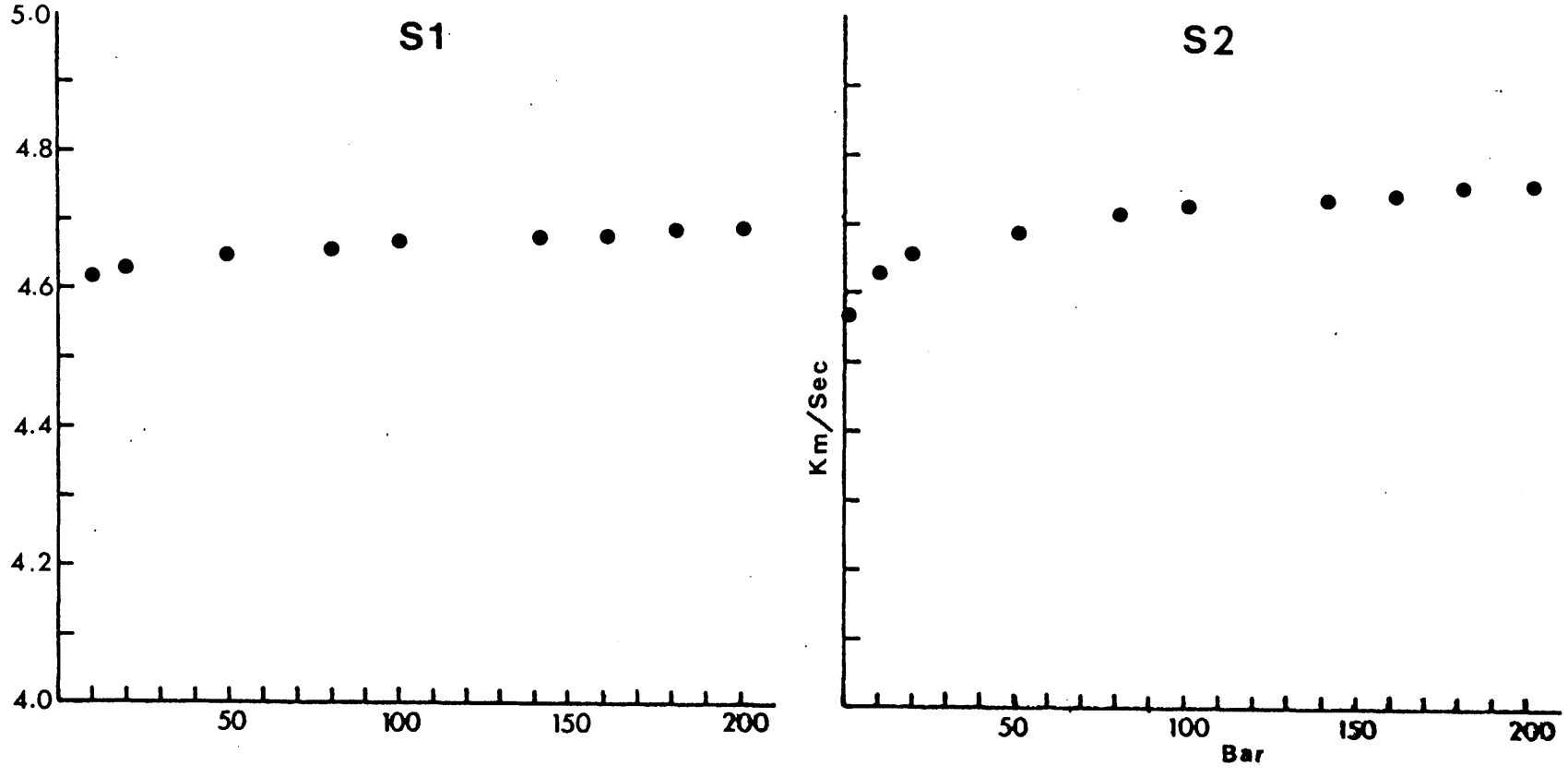
S1
S2
5.0
4.8
4.6
4.4
4.2
4.0
Km/Sec
50
100
150
200
Bar

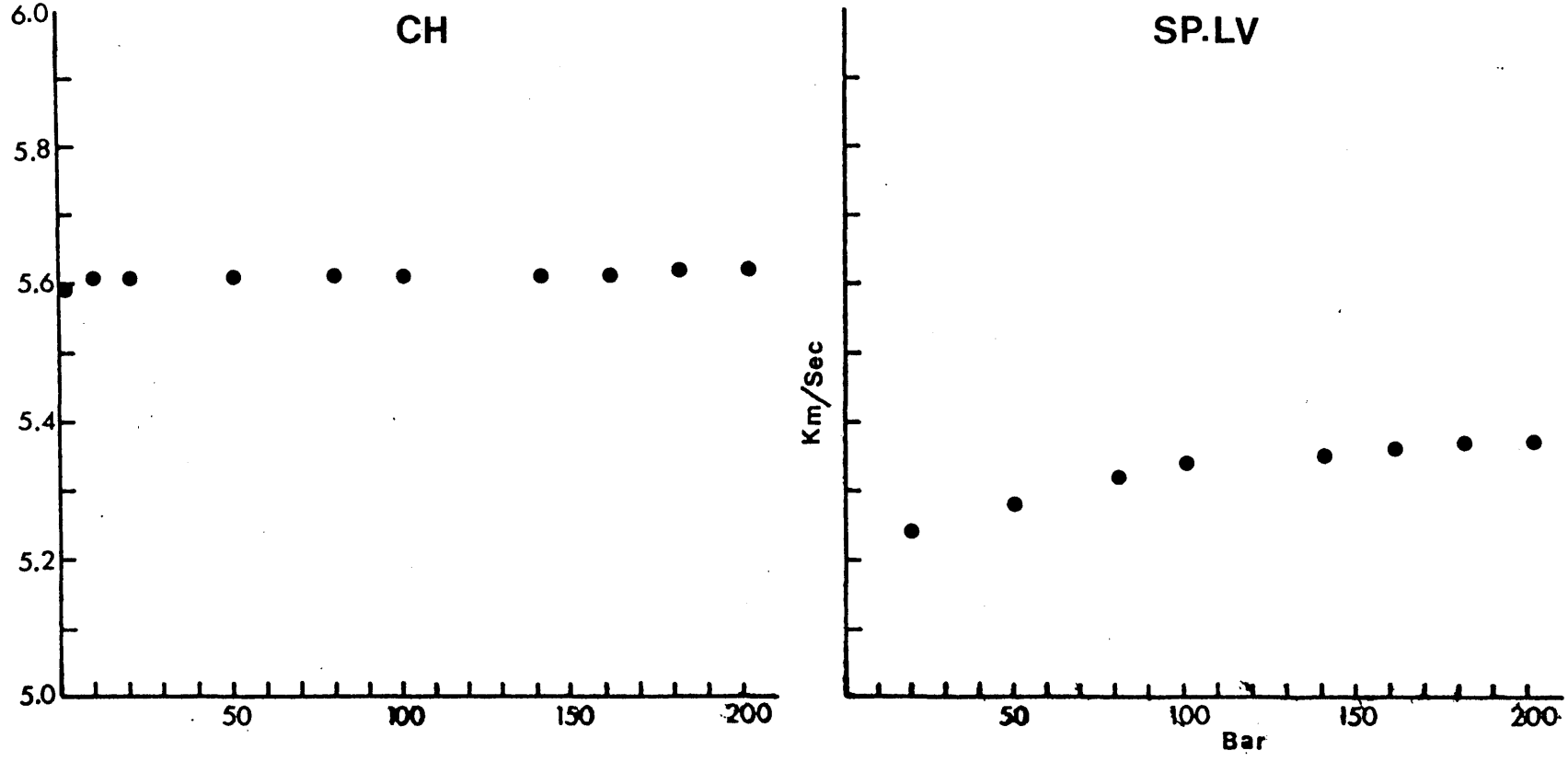
CH
SP.LV
6.0
5.8
5.6
5.4
5.2
5.0
Km/Sec
50
100
150
200
Bar

APPENDIX 3B

P-wave velocities in greywacke samples from the Northern Belt of the Southern Uplands, in relation to increasing confining pressure.

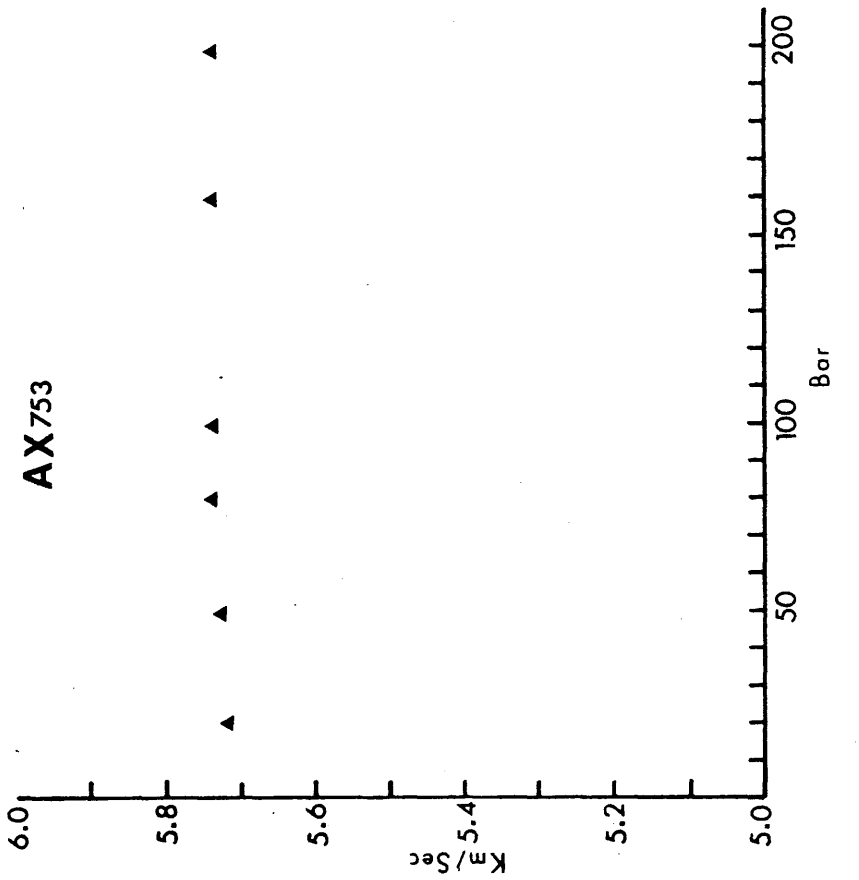
AX753
6.0
5.8
5.6
5.4
5.2
5.0
Km/Sec
50
100
150
200
Bar

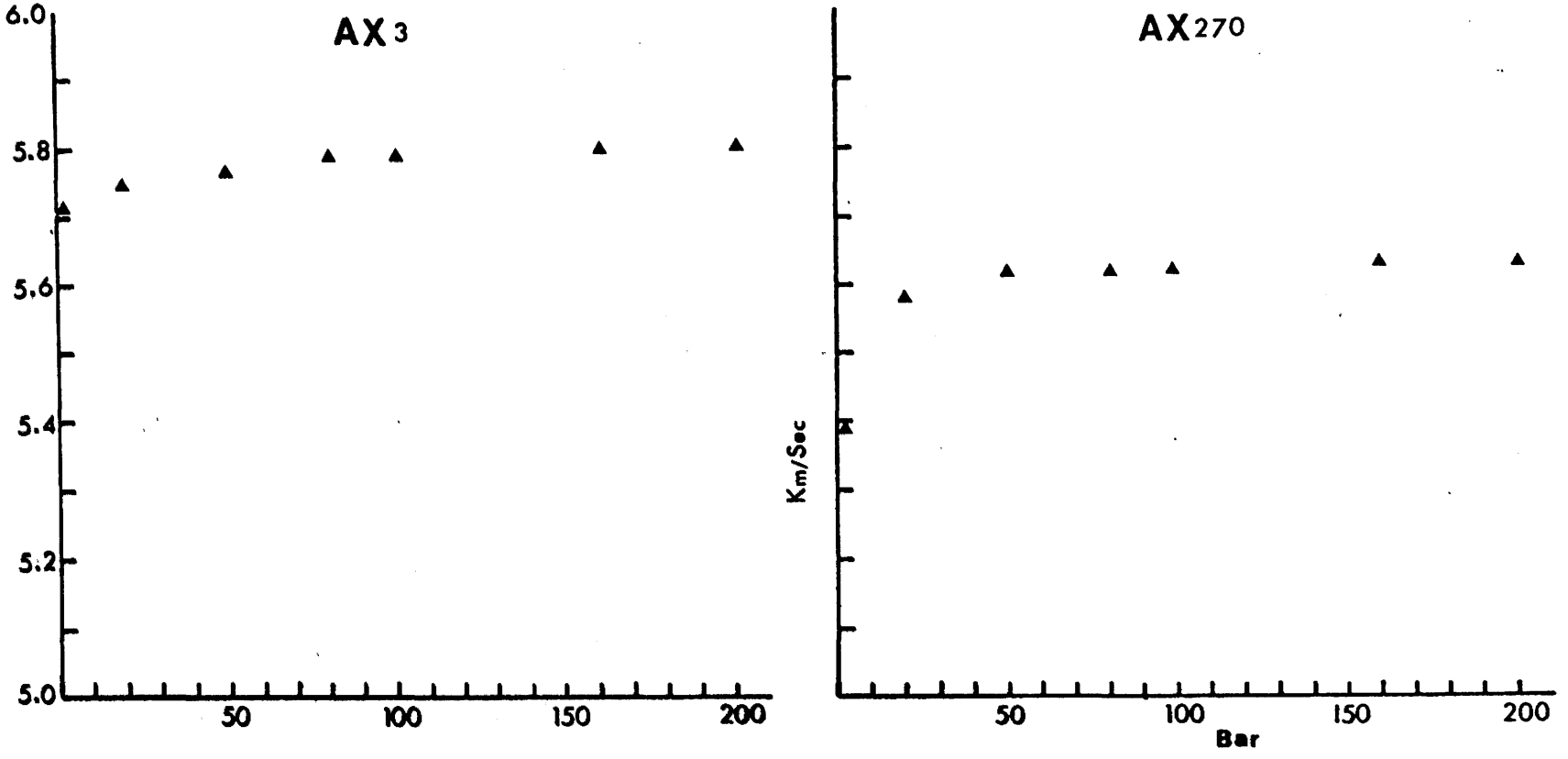
AX3
AX270
6.0
5.8
5.6
5.4
5.2
5.0
Km/Sec
50
100
150
200
Bar

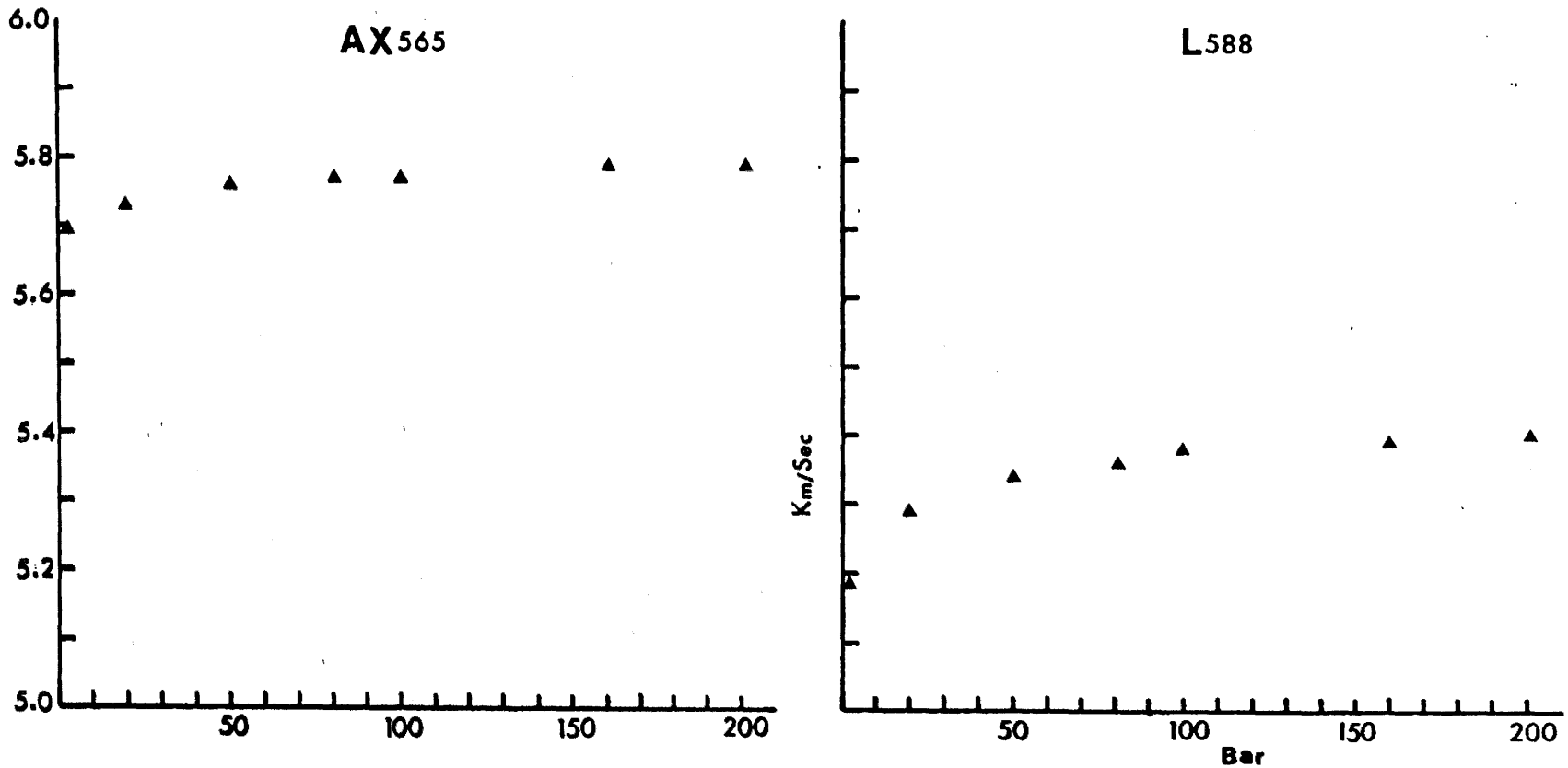
AX565
L588
6.0
5.8
5.6
5.4
5.2
5.0
Km/Sec
50
100
150
200
Bar

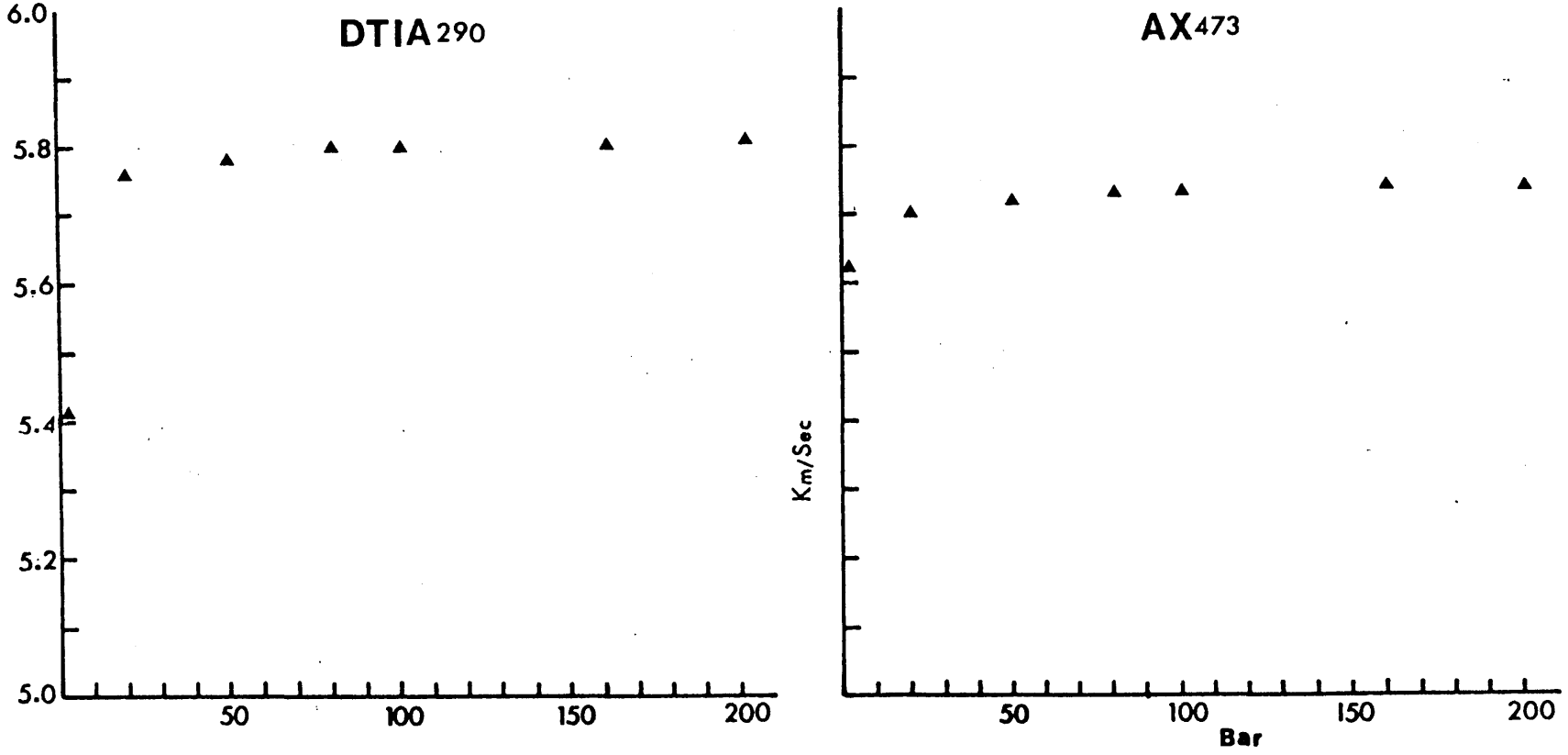
DTIA 290
AX 473
6.0
5.8
5.6
5.4
5.2
5.0
Km/Sec
50
100
150
200
Bar

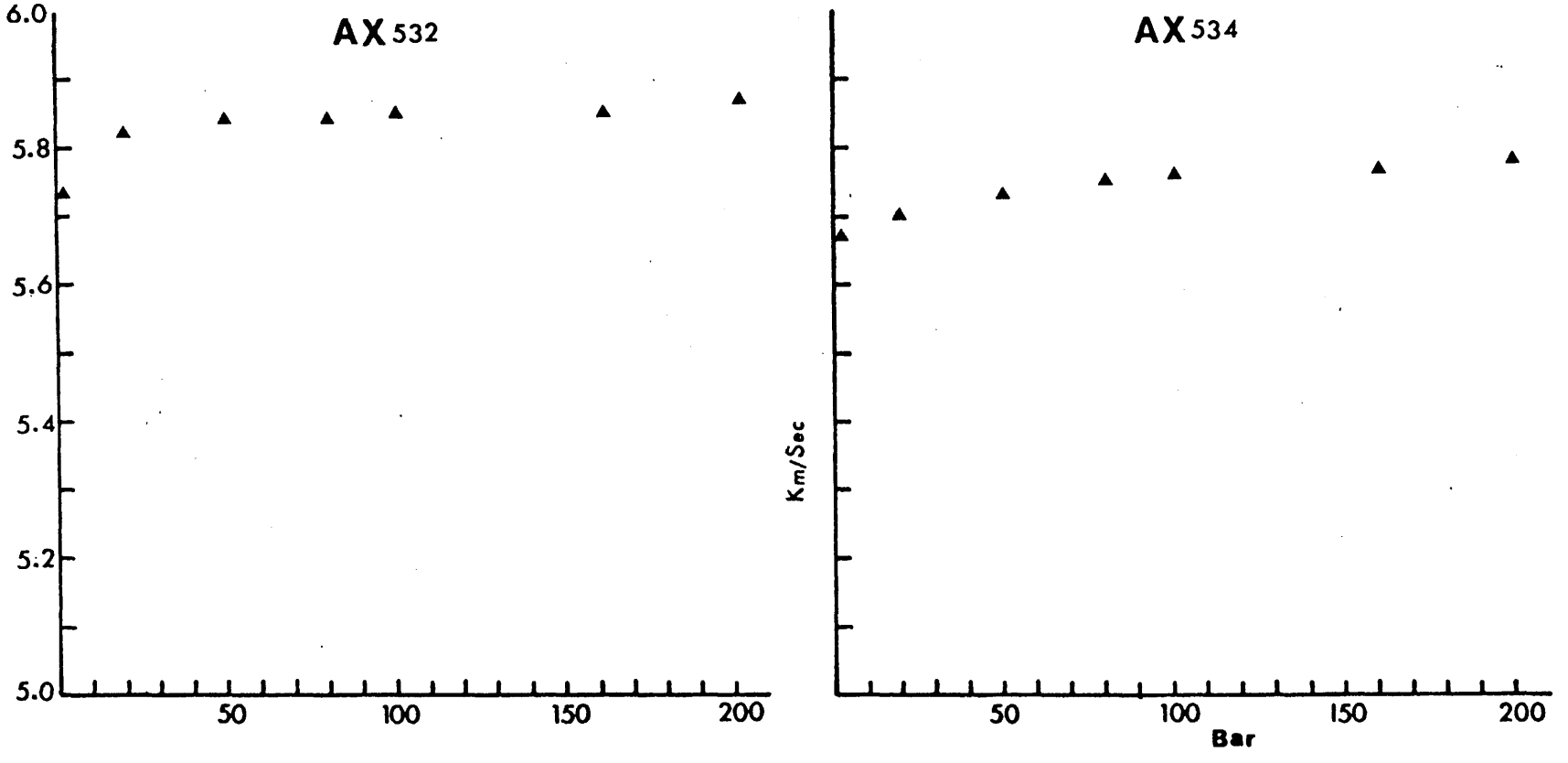
AX 532
AX 534
6.0
5.8
5.6
5.4
5.2
5.0
Km/Sec
50
100
150
200
Bar

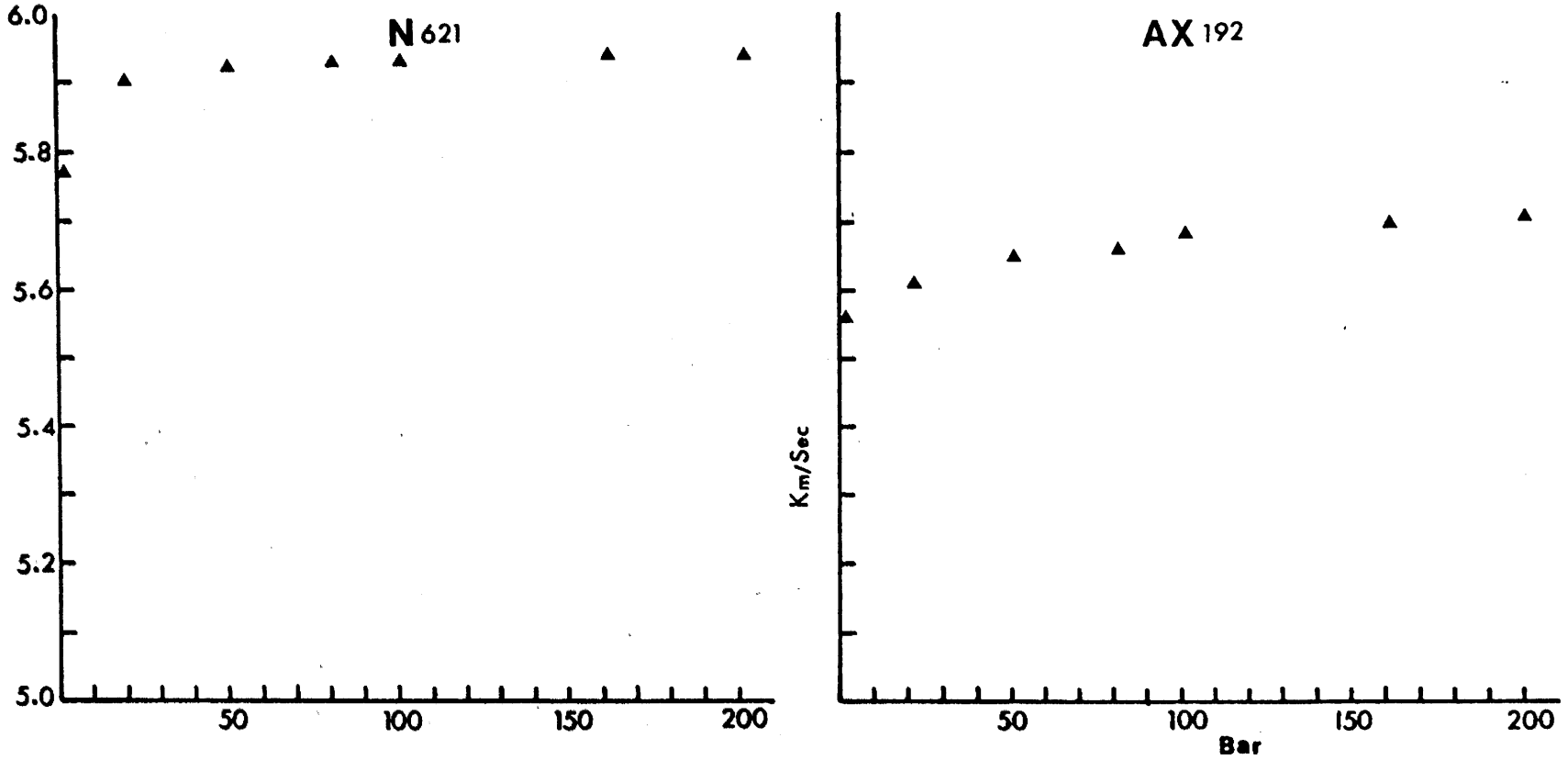
N 621
AX 192
6.0
5.8
5.6
5.4
5.2
5.0
Km/Sec
50
100
150
200
Bar

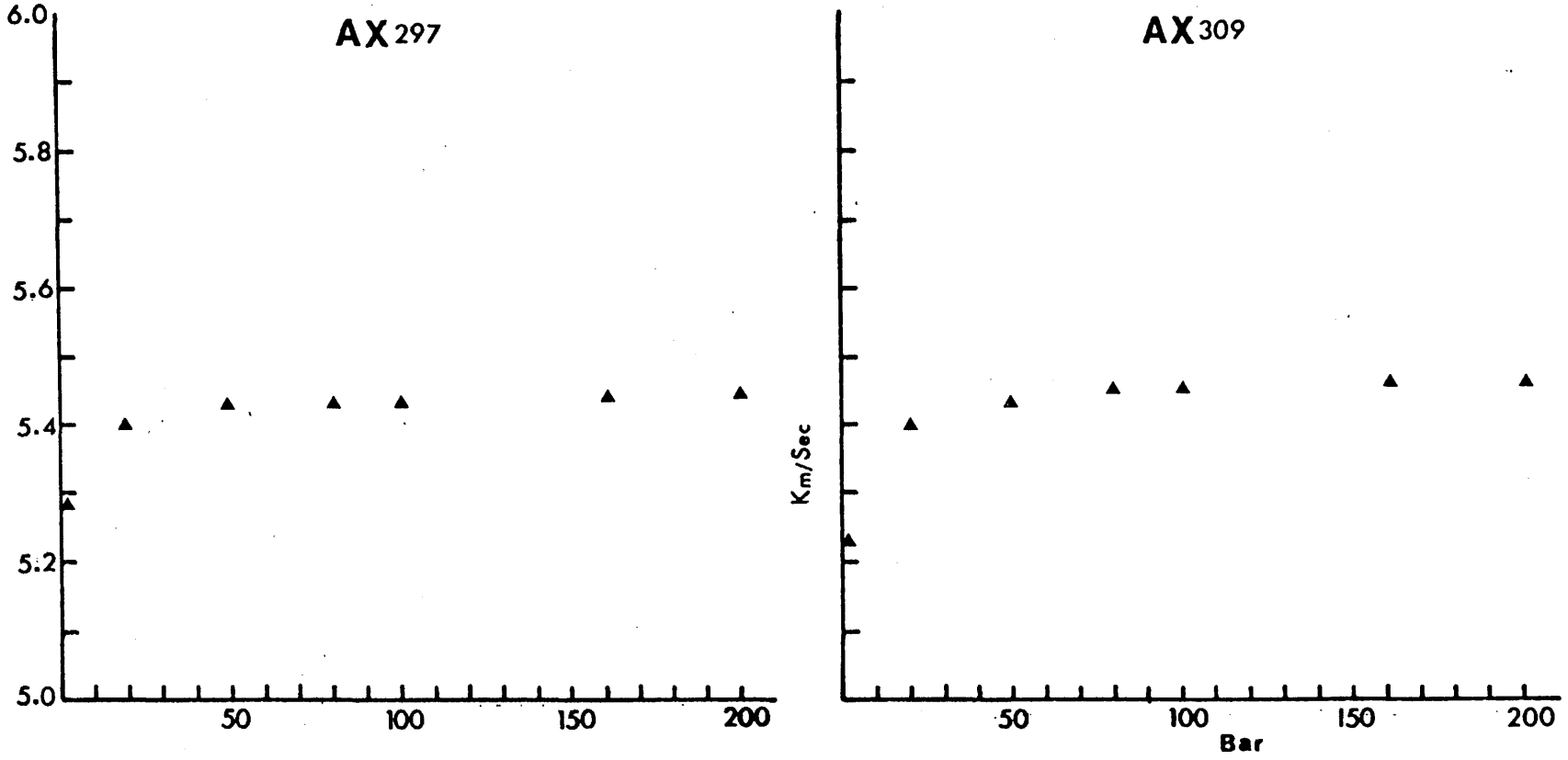
AX 297
AX 309
6.0
5.8
5.6
5.4
5.2
5.0
Km/Sec
50
100
150
200
Bar

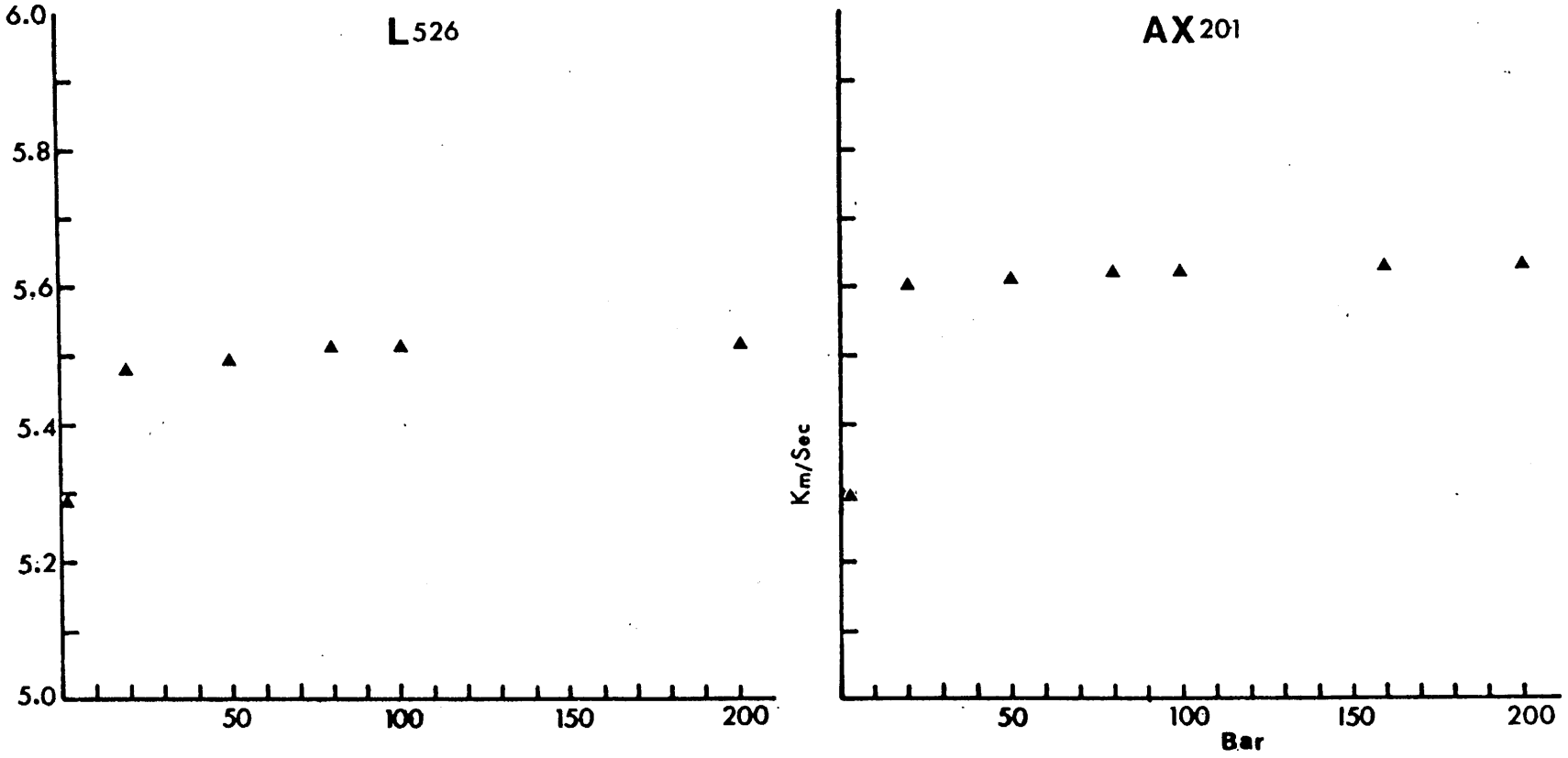
L526
AX201
6.0
5.8
5.6
5.4
5.2
5.0
Km/Sec
50
100
150
200
Bar

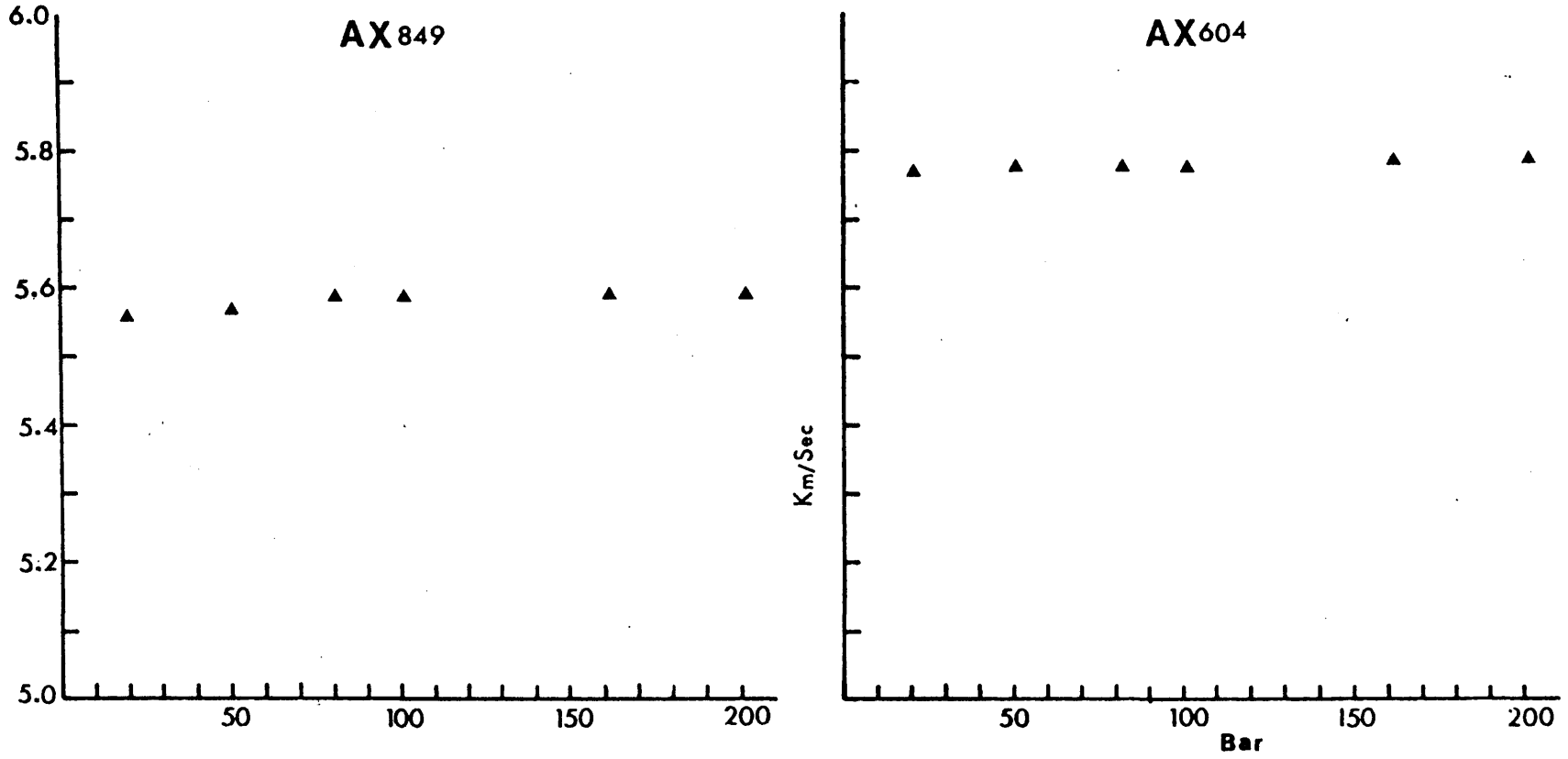
AX849
AX604
6.0
5.8
5.6
5.4
5.2
5.0
Km/Sec
50
100
150
200
Bar

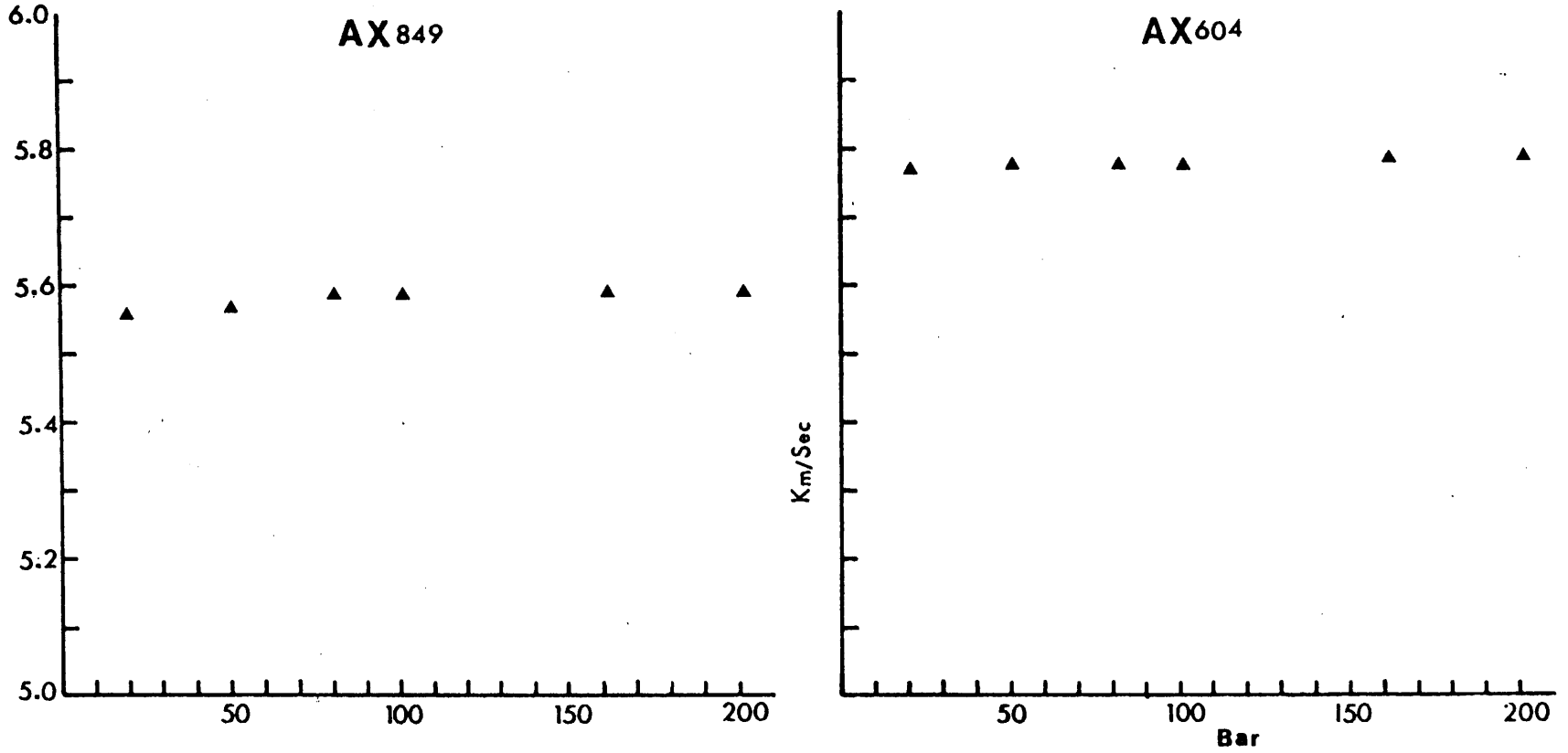
AX849
6.0
5.8
5.6
5.4
5.2
5.0
50
100
150
200
AX604
Km/Sec
50
100
150
200
Bar

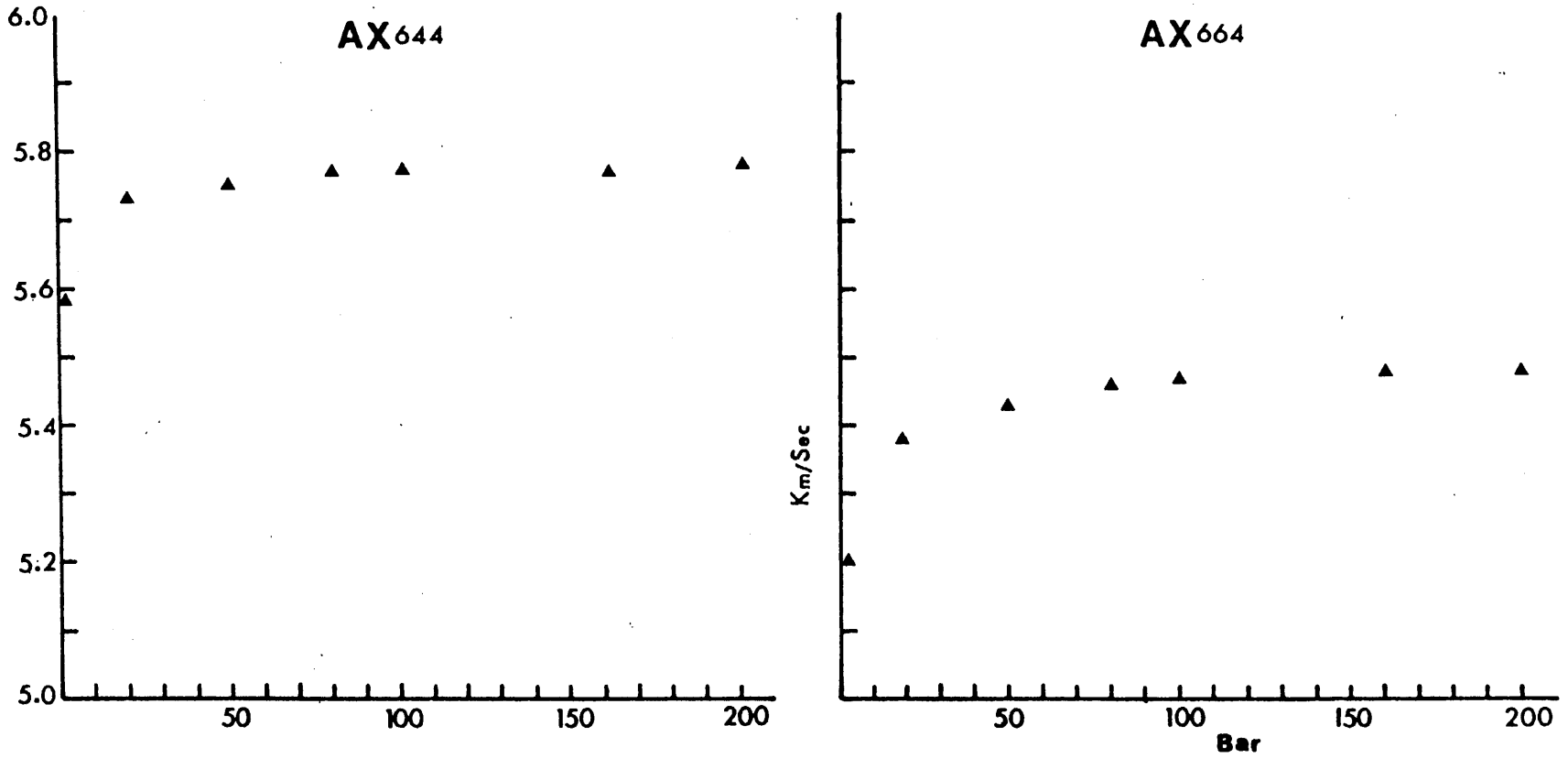
AX644
AX664
6.0
5.8
5.6
5.4
5.2
5.0
Km/Sec
50
100
150
200
Bar

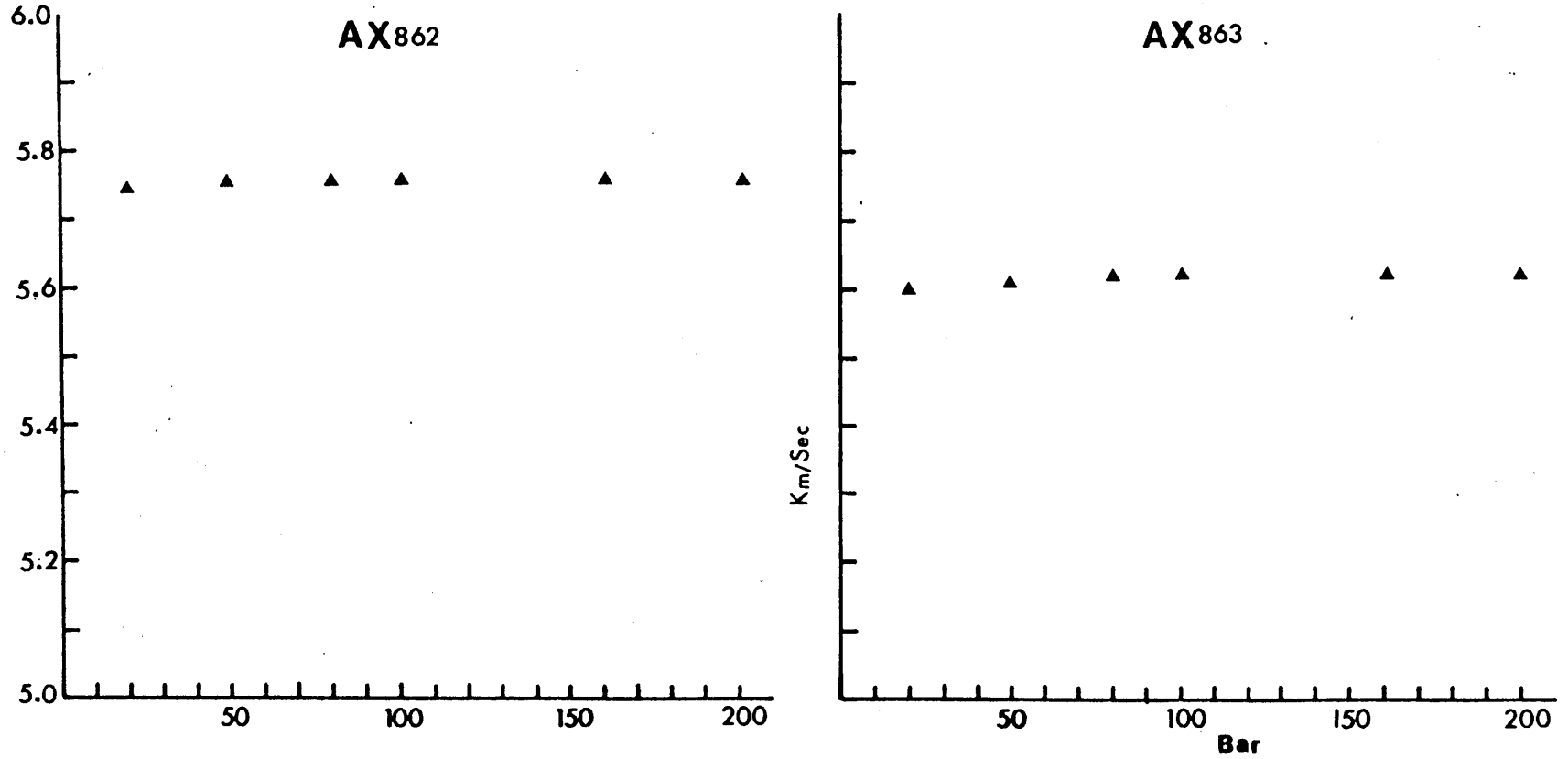
AX862
AX863
6.0
5.8
5.6
5.4
5.2
5.0
Km/Sec
50
100
150
200
Bar

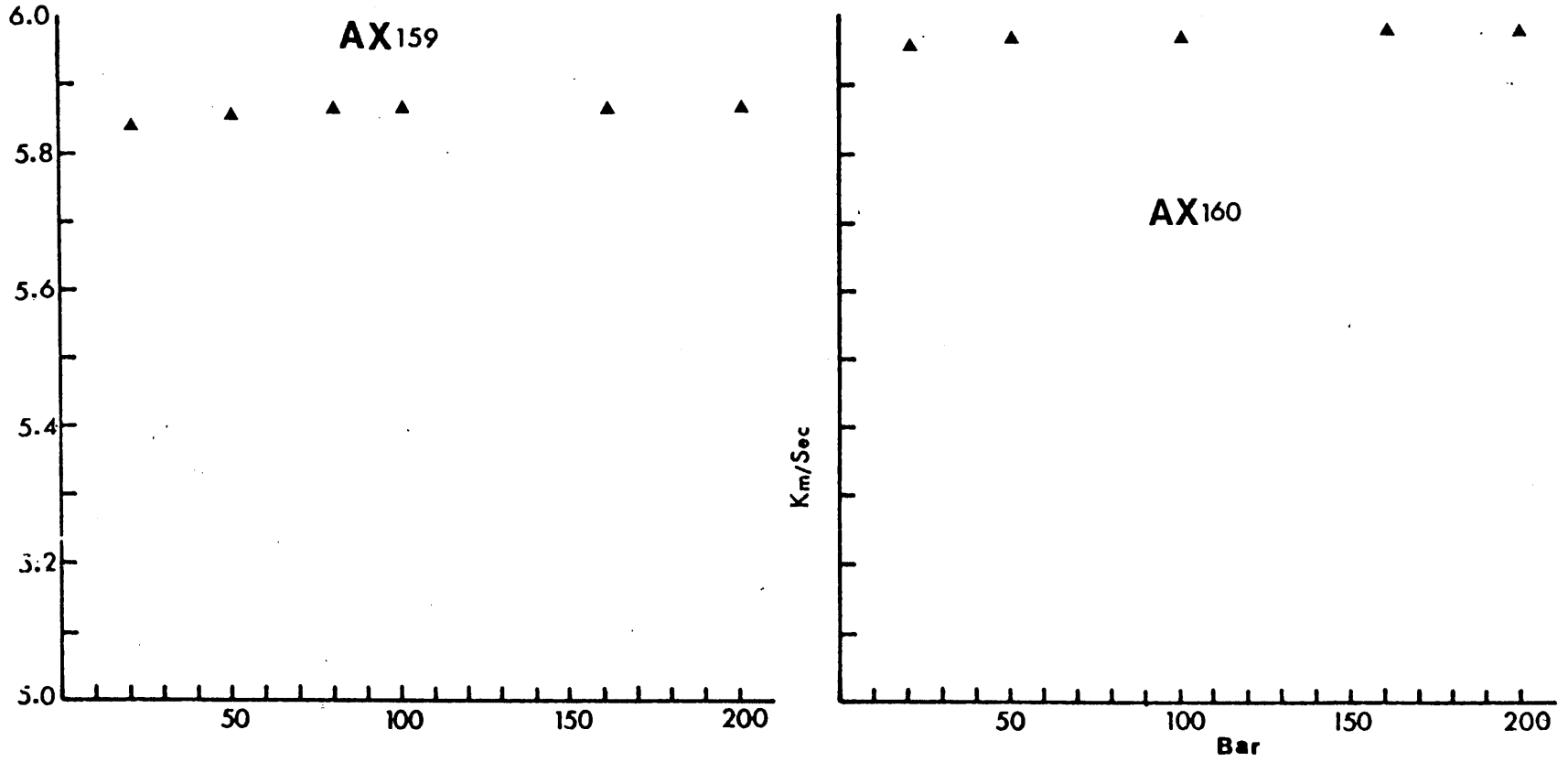
AX159
AX160
6.0
5.8
5.6
5.4
3.2
5.0
Km/Sec
50
100
150
200
Bar

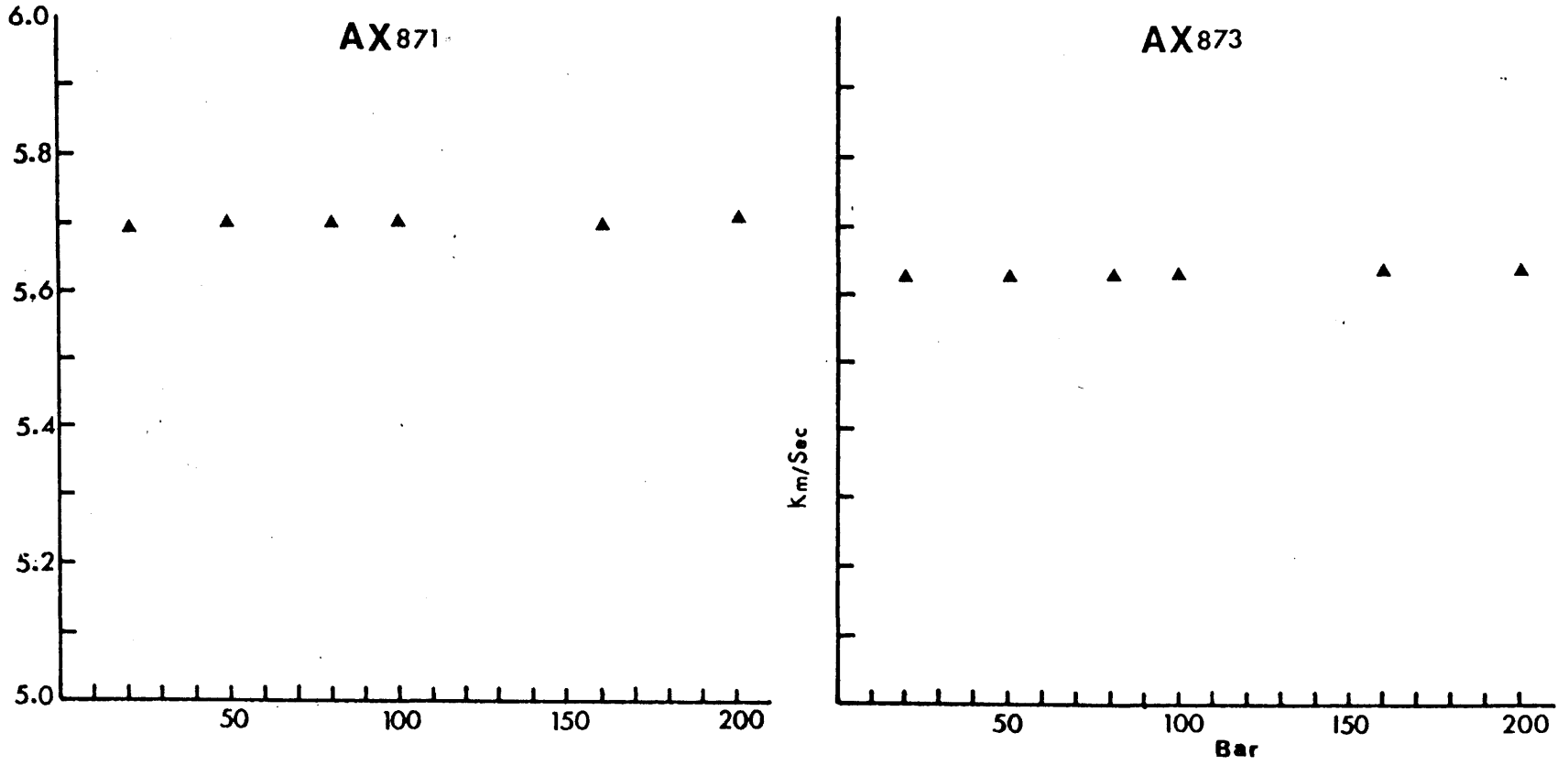
AX871
AX873
6.0
5.8
5.6
5.4
5.2
5.0
Km/Sec
50
100
150
200
Bar

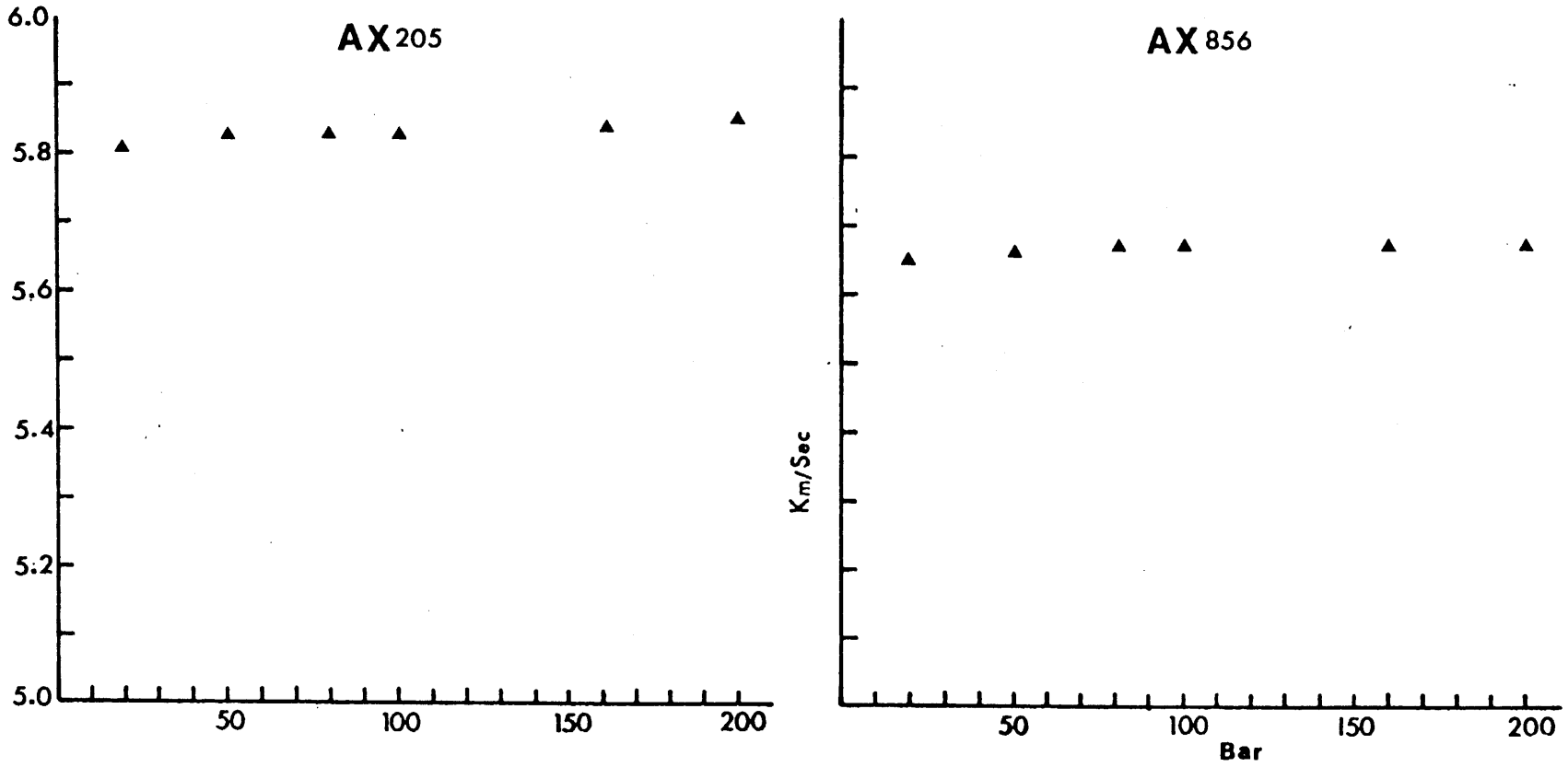
AX205
AX856
6.0
5.8
5.6
5.4
5.2
5.0
Km/Sec
50
100
150
200
Bar

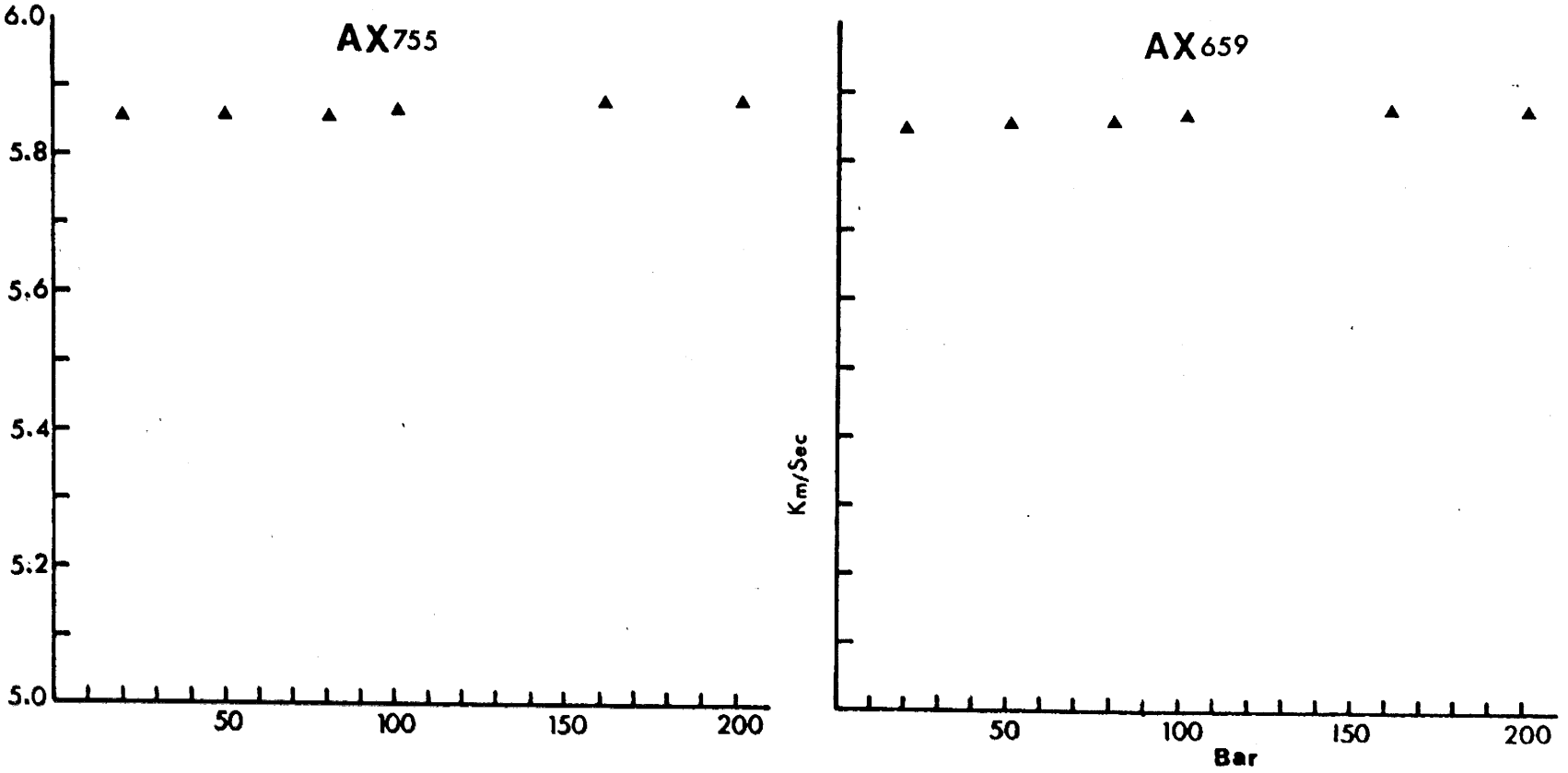
AX755
AX659
6.0
5.8
5.6
5.4
5.2
5.0
Km/Sec
50
100
150
200
Bar

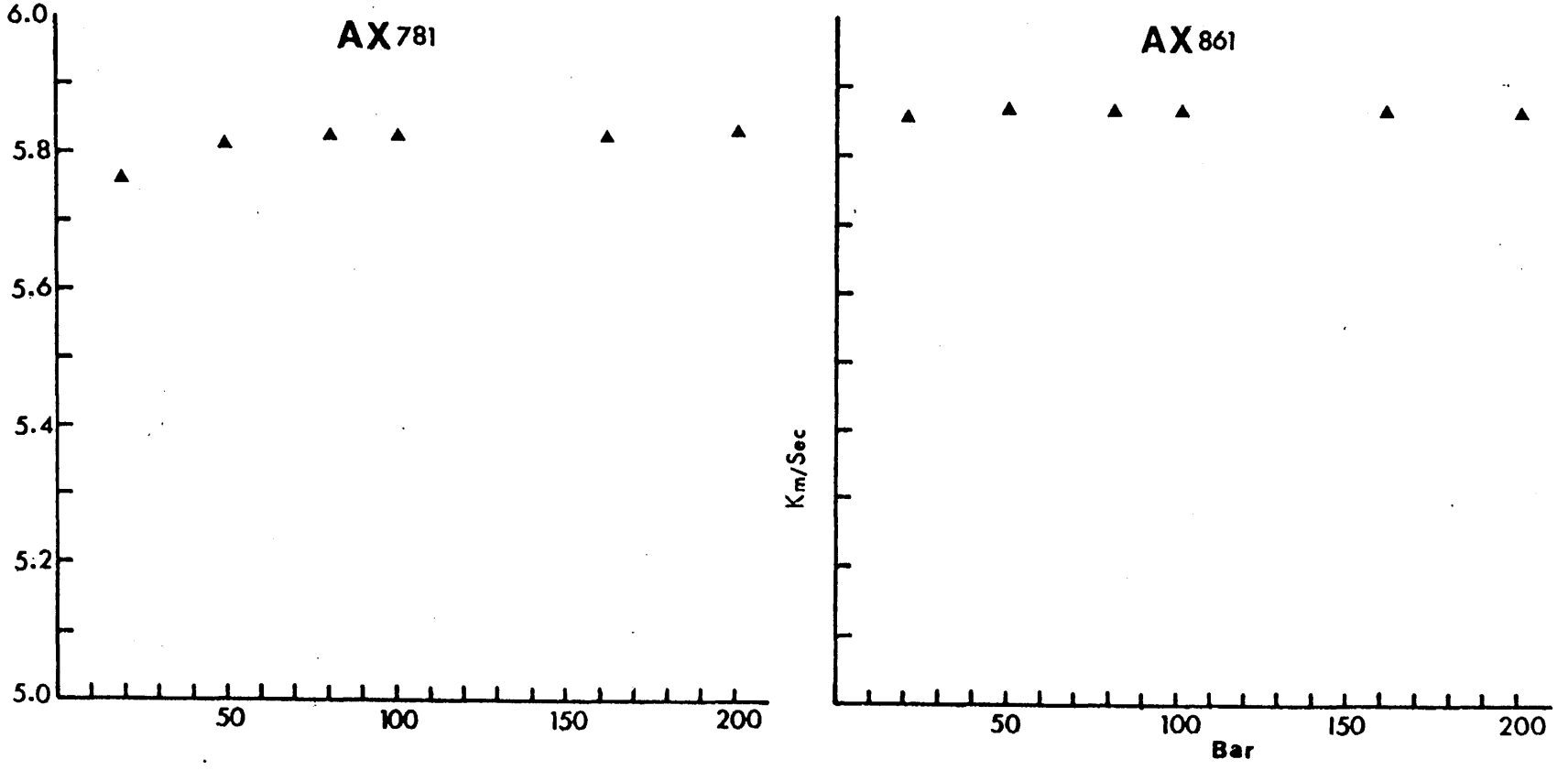
AX781
AX861
6.0
5.8
5.6
5.4
5.2
5.0
Km/Sec
50
100
150
200
Bar

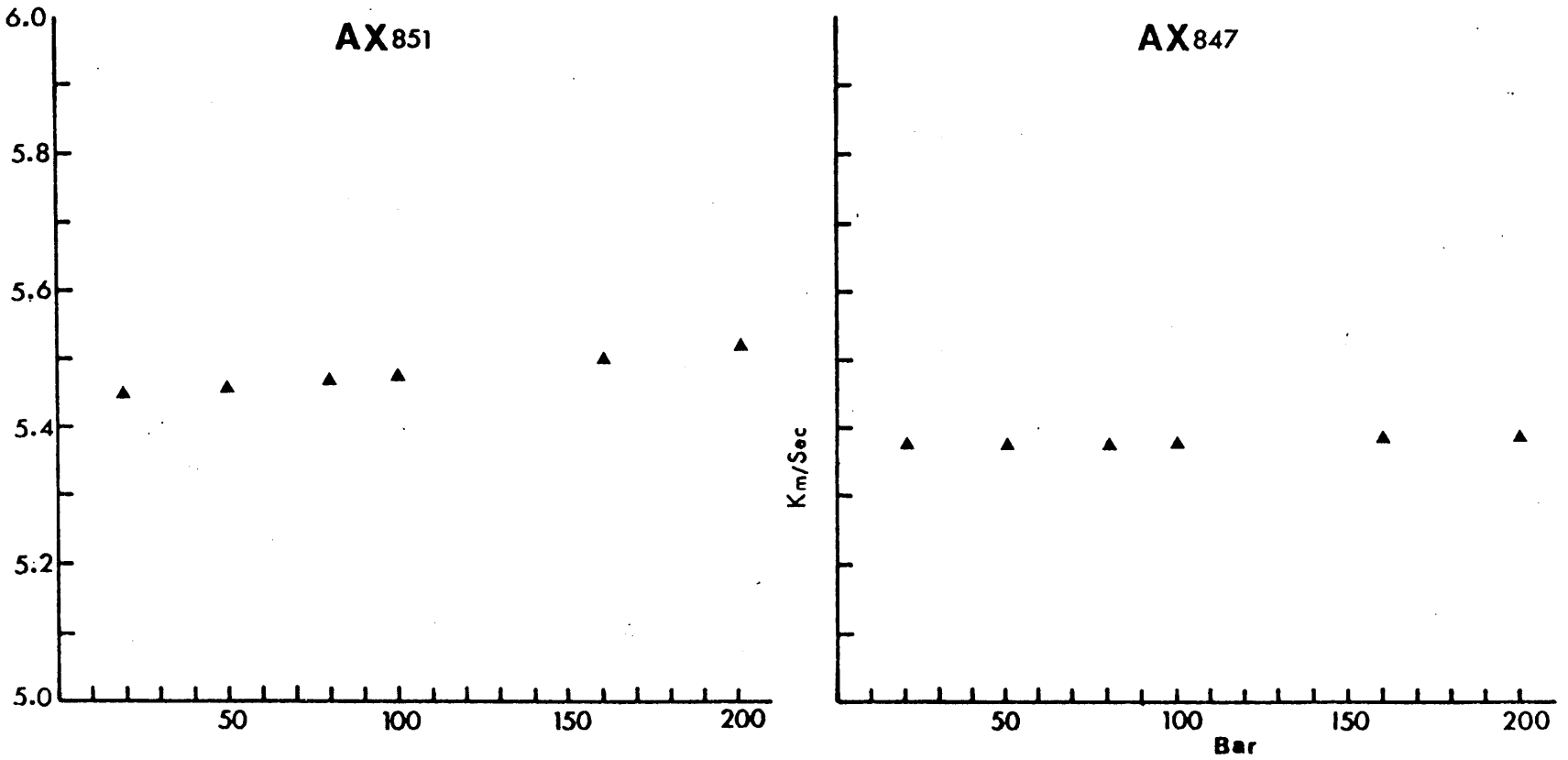
AX851
AX847
6.0
5.8
5.6
5.4
5.2
5.0
Km/Sec
50
100
150
200
Bar

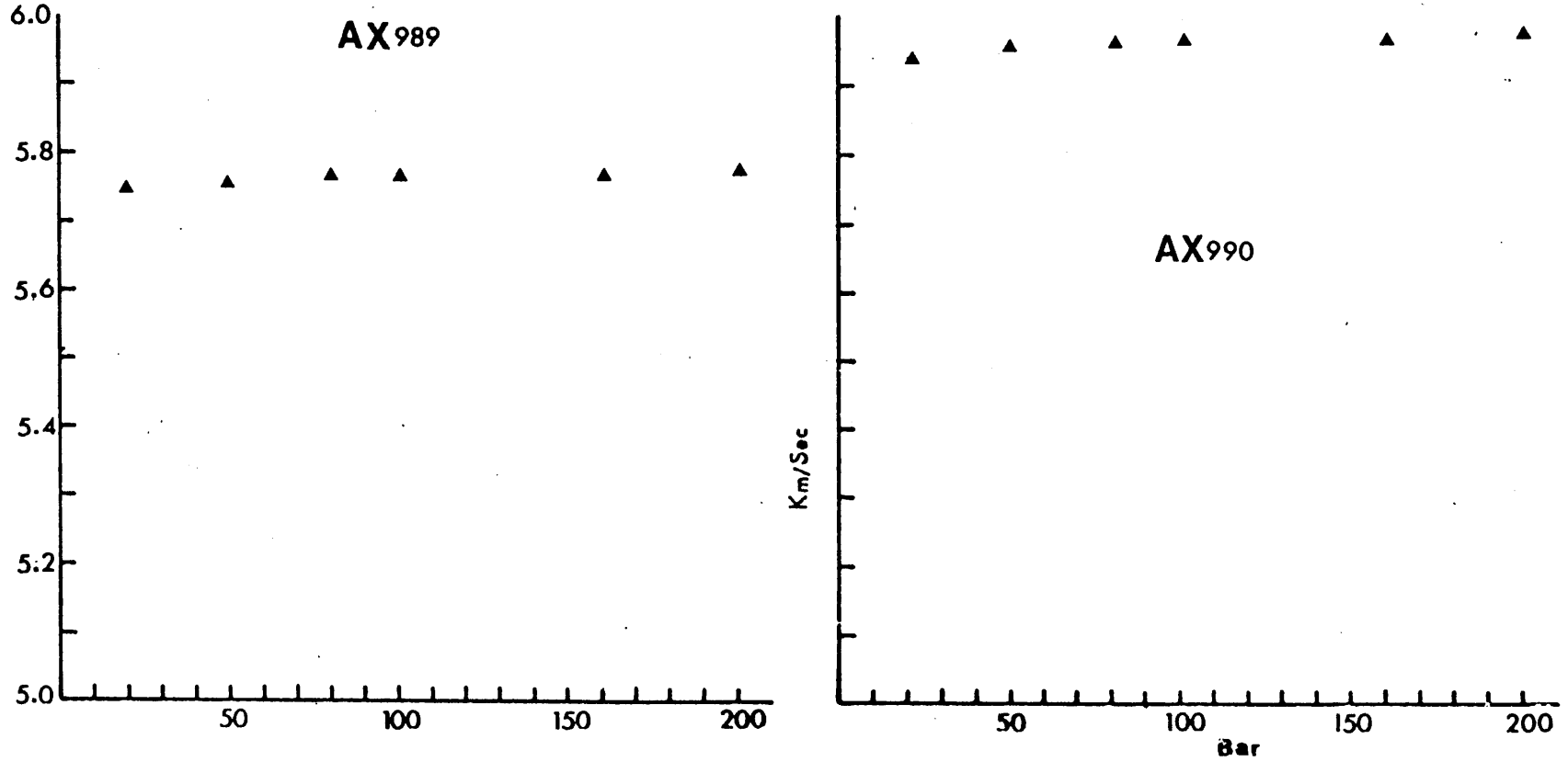
AX989
AX990
6.0
5.8
5.6
5.4
5.2
5.0
Km/Sec
50
100
150
200
Bar

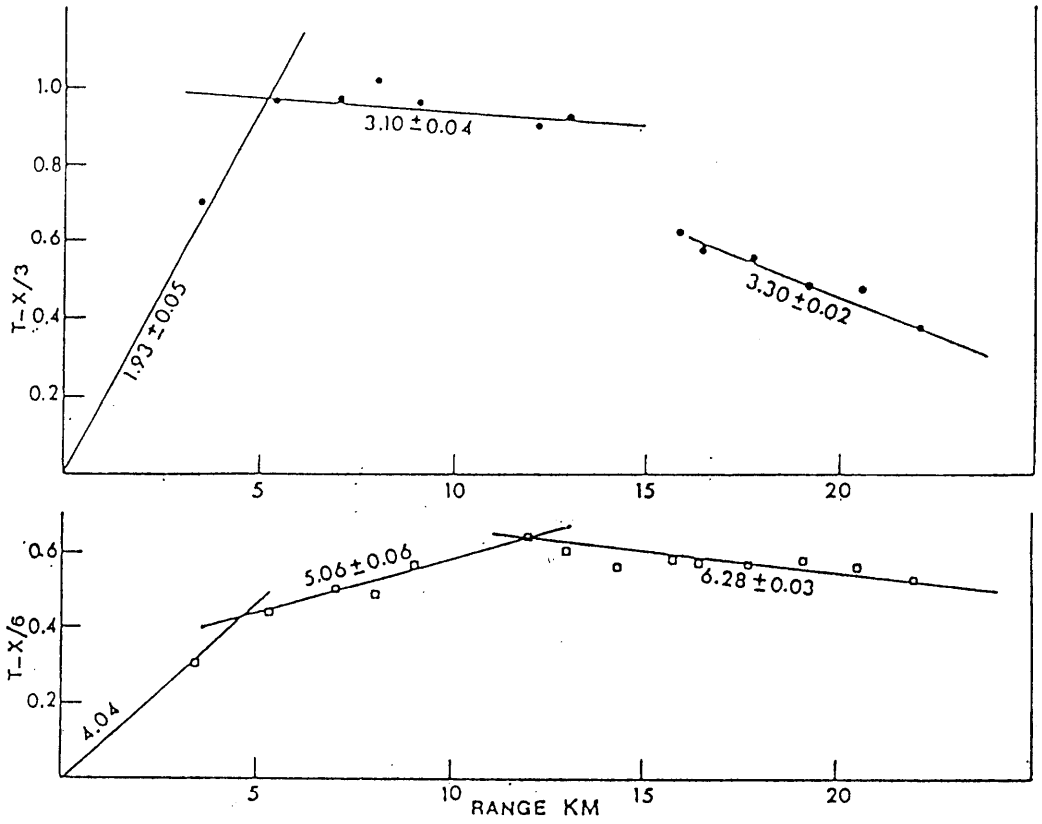

APPENDIX 4

Reduced time-distance plots of P and S waves recorded on the Colmonell line. The S waves are partly represented in fig 12 appendix 2. The error affecting the S-wave travel time is estimated to be ± 0·04 sec. This is due to:

1. Picking of onset time ± 0·04 sec.

2. Irregularities in playback paper speed ± 0·007 sec.

3. Uncertainty in locating the shot points and recording sites ± 0·006 sec.